VOLUME 101 NUMBER 2

THE ASTROPHYSICAL JOURNAL

AN INTERNATIONAL REVIEW OF SPECTROSCOPY AND ASTRONOMICAL PHYSICS

Founded in 1895 by GEORGE E. HALE *and* JAMES E. KEELER

MARCH 1945

THE UNIVERSITY OF CHICAGO PRESS
CHICAGO, ILLINOIS, U.S.A.

March 1945 Vol. 101, No. 2

THE ASTROPHYSICAL JOURNAL

AN INTERNATIONAL REVIEW OF SPECTROSCOPY AND ASTRONOMICAL PHYSICS

The Astrophysical Journal is published bimonthly by the University of Chicago at the University of Chicago Press, 5750 Ellis Avenue, Chicago, Illinois, during July, September, November, January, March, and May. ¶The subscription price is $10.00 a year; the price of single copies is $2.00. Orders for service of less than a full year will be charged at the single-copy rate. ¶Postage is prepaid by the publishers on all orders from the United States and its possessions, Argentina, Bolivia, Brazil, Chile, Colombia, Costa Rica, Cuba, Dominican Republic, Ecuador, Guatemala, Haiti, Republic of Honduras, Mexico, Morocco (Spanish Zone), Nicaragua, Panama, Paraguay, Peru, Rio de Oro, El Salvador, Spain (including Balearic Islands, Canary Islands, and the Spanish Offices in Northern Africa; Andorra), Spanish Guinea, Uruguay, and Venezuela. ¶Postage is charged extra as follows: for Canada and Newfoundland, 42 cents on annual subscriptions (total $10.42); on single copies, 7 cents (total $2.07); for all other countries in the Postal Union, 96 cents on annual subscriptions (total $10.96), on single copies 16 cents (total $2.16). ¶Patrons are requested to make all remittances payable to The University of Chicago Press, in United States currency or its equivalent by postal or express money orders or bank drafts.

The following are authorized agents:

For the British Empire, except North America, India, and Australasia: The Cambridge University Press, Bentley House, 200 Euston Road, London, N.W. 1, England. Prices of yearly subscriptions and of single copies may be had on application.

Claims for missing numbers should be made within the month following the regular month of publication. The publishers expect to supply missing numbers free only when losses have been sustained in transit, and when the reserve stock will permit.

Business correspondence should be addressed to The University of Chicago Press, Chicago 37, Illinois.

Communications for the editors and manuscripts should be addressed to: Otto Struve, Editor of THE ASTROPHYSICAL JOURNAL, Yerkes Observatory, Williams Bay, Wisconsin.

Line drawings and photographs should be made by the author, and all marginal notes such as co-ordinates, wave lengths, etc., should be included in the cuts. It will not be possible to set up such material in type.

One copy of the corrected galley proof should be returned as soon as possible to the editor, Yerkes Observatory, Williams Bay, Wisconsin. Authors should take notice that the manuscript will not be sent to them with the proof.

The cable address is "Observatory, Williamsbay, Wisconsin."

The articles in this journal are indexed in the *International Index to Periodicals*, New York, N.Y.

Applications for permission to quote from this journal should be addressed to The University of Chicago Press, and will be freely granted.

Entered as second-class matter, July 31, 1940, at the Post-Office at Chicago, Ill., under the act of March 3, 1879.
Acceptance for mailing at special rate of postage provided for in United States Postal Act of October 3, 1917, Section 1103, amended February 28, 1925.

[PRINTED IN U.S.A.]

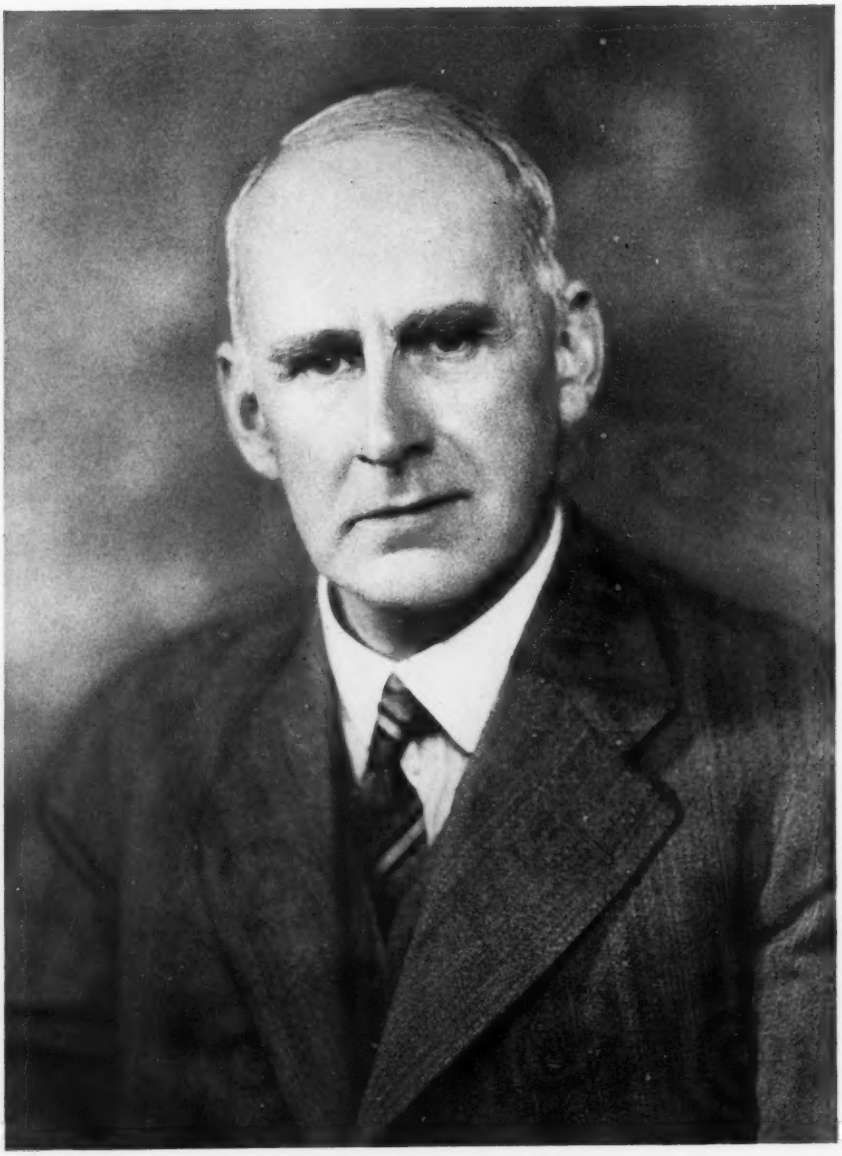

Lafayette, Ltd., London

ARTHUR STANLEY EDDINGTON

1882–1944

THE ASTROPHYSICAL JOURNAL

AN INTERNATIONAL REVIEW OF SPECTROSCOPY AND ASTRONOMICAL PHYSICS

VOLUME 101 MARCH 1945 NUMBER 2

ARTHUR STANLEY EDDINGTON
1882–1944

The death of Sir Arthur Eddington deprives astrophysics of its most distinguished representative. The history of its advance during the past generation and the story of his work are inseparable.

Those who have been responsible for filling the major posts in English science have been remarkably successful in picking the best men young and giving them the opportunities by which they could profit. Appointments as chief assistant at Greenwich have been so judiciously made that a large proportion of those who later took the leading parts in British astronomy have held this position. Rarely, if ever, was it offered to a younger man than when, in 1906, Eddington, at the age of twenty-four, began his astronomical career; and never was it offered more wisely.

The new assistant had been senior wrangler two years before, and he was fully equipped with that capacity to apply mathematical methods to practical problems which belongs to the great tradition of Cambridge. His first published paper (1907), on the systematic motions of the stars, is a fine example. It treated Kapteyn's two-drift hypothesis (then new) by methods elegant analytically and practical in numerical application. Several papers in the next few years dealt with other problems of stellar motion and distribution and culminated in his first book, *Stellar Movements*, in 1914. A group of papers on the dynamics of star clusters are related to these studies.

Meanwhile he showed his mettle in a very different field. The floating photographic zenith telescope, designed by Bryan Cookson, failed, at the start, to give results of the anticipated precision. The untimely death of its originator left these problems unsolved. Eddington took on this discouraging problem and found that, by changing the program of observation so that the star trails were observed only in a small central region of each plate, the trouble was eliminated. Thus rehabilitated, the instrument was started on a career of almost thirty years of successful operation (interrupted only by the present war). Outstanding small but systematic errors were attributed to local disturbances of refraction, dependent partly on the wind—a conclusion confirmed by the later observations.

In 1913 Eddington was elected, at the age of thirty-one, to the historic Plumian professorship at Cambridge, as Sir George Darwin's successor. Again the sound judgment of the electors was fully justified.

His interest in physical problems, which had already been shown in work on the envelopes of Morehouse's Comet, now became predominant; and his earlier work—excellent and varied as it had been—appears as little more than a prelude to that of the great

period which was inaugurated in 1916–1917 with his two papers on the radiative equilibrium of the stars. Here he pointed out, for the first time, the importance of radiation pressure in the internal equilibrium of a star and derived the equation for determining it which has ever since borne his name. He derived the equation of radiative equilibrium and showed that by a simple assumption it became integrable and led to the polytropic sphere with $n = 3$ (now usually described as "Eddington's model"). In the second of these papers he recognized that the ionization in the interior of a star must be so high that the mean molecular weight is small and that, in consequence, the luminosity of a star should be a rapidly increasing function of its mass.

It was not until 1924, however, that—guided partly by observational data—he realized that this highly ionized matter would behave practically like a perfect gas up to very high densities. With this obstacle disposed of and with the aid of Kramers' opacity formula, he made the second great step, in 1924, which led to the mass-luminosity relation in substantially its present form, disposed of the older theories of stellar evolution, and showed that only enormous masses of matter could shine and that the fundamental properties of atoms compelled such bodies to be luminous stars. A year later, by inventing the point-source model and calculating it by quadratures, he showed that the influence of the internal density-distribution upon the mass-luminosity relation was small.

Finally, in 1932, he pointed out that the luminosity for a given mass varied very considerably with the hydrogen content and permitted a determination of the latter. (Strömgren independently reached the same conclusions, publishing these a month earlier.)

This series of investigations forms one of the most original and fertile contributions by which astrophysics has yet benefited. All but the last were collected and summarized in his *Internal Constitution of the Stars*. This volume has every claim to be regarded as a masterpiece of the first rank.

The importance, novelty, and convincing character of its results justify high praise—but its distinctive merit is the unrivaled elegance and lucidity of the presentation. Many good scientific books are compilations—more or less well edited—of separate original papers; but here Eddington has followed Austin Dobson's exhortation:

> See that thy form demand
> The labour of the file.

The book is itself a work of art. The short introductory chapters on the thermodynamics of radiation and the quantum theory provide the student with all he needs and no more, and so skilfully that the novice will not realize what struggles he has been spared. From beginning to end, the presentation is integrated—the product of a great teacher as well as a great investigator.

Every student of physical science might well be required to read, mark, and inwardly digest the admirable discussion[1] of the relative functions of mathematical rigor and physical insight, which ends: "Whereas, for the mathematician, insight is one of the tools and proof the finished product, for the physicist proof is one of the tools, and insight the finished product."

Other related investigations of Eddington's are given place in the volume. His discussion of the pulsation theory of Cepheid variables has formed the basis of all later work. His treatment of the "reflection" effect in eclipsing variables (along with Milne's contribution made at the same time) is still the last word on the subject. The highly original chapter on diffuse matter in space initiated the interpretation of interstellar lines.

Perhaps the most remarkable characteristic of the book is how well it holds up after nearly twenty years. For some topics, such as the source of stellar energy, the physical basis for a valid theory was not then available. For others, such as the equilibrium of stellar atmospheres and the behavior of absorption lines, so much progress has been

[1] Pp. 102–103 (1926 ed.).

made that a modern treatment would be very different—though here Eddington contributed approximate solutions which are still very useful.

But the main discussion is still required reading for the advanced student, and his teachers do not have to put him seriously on his guard lest he accept outdated concepts. Eddington's physical insight was amazingly sound.

This book marks the culmination of the second phase of his career, and his later contributions in the field were largely amplifications of special points.

He had long been deeply interested in relativistic theory and had published two standard works—one technical, the other more popular. In the third phase of his activity he became more and more deeply convinced that the primary properties of matter and of its ultimate constituents—especially those which are represented by the dimensionless constants which occur in nature—were neither arbitrary nor independent but had simple, and often integral, values, which could be predicted by abstract epistemological reasoning from very general considerations—and that other constants, such as that which relates the apparent velocity of recession of a nebula to its distance, were similarly predictable.

Upon these investigations the present reviewer is not qualified to speak, save to note that, for the most part, they appear to be still *sub judice*, while his disagreement with the ordinary formulation of relativistic degeneracy appears to have been shared with no one else.

A quite different side of his interests is represented by the Gifford Lectures on "The Nature of the Physical World," one of the most notable contributions of our times to the discussion of the relation between the realm of "pointer-readings" and that of values.

No summary of his work would be complete without mention of his gift of epigrammatic wit. Everyone knows the "hotter place"; fewer, perhaps, know his imaginary Scottish professor of "geloelogy," who had a comprehensive knowledge of this hypothetical science of humor and could infallibly classify any kind of joke—without ever having *seen* one!

Less familiar, because buried in a British Association report from which the writer is obliged to quote from memory, is: "When an investigator has developed a formula which gives a complete representation of the phenomena within a certain range, he may be prone to a certain satisfaction. Would not he be wiser if he should say 'Foiled again! I can find out no more about Nature along this line.' " At times he turned the joke upon himself. In a cloakroom at the Stockholm meeting of the International Astronomical Union in 1938, he said: "I always hang my hat on peg 137"—suiting the action to the word!

Few people cared less for formal distinction. A very vivid memory from the same meeting is of the delegates gathering at their hotel before a formal banquet, at which courtesy demanded the wearing of decorations, and of Eddington in the crowd, with an ancient raincoat, buttoned tightly at the neck—to hide the Order of Merit!

He came of a family of quiet people—long and sincerely devoted to the principles of the Society of Friends—and, apart from the honors brought him by his work, his life was uneventful. He never married; his widowed mother and his sister (who survives him) made for him a home perfectly adapted to his temperament and his work.

After a short illness, the gravity of which did not reveal itself until near the end, he died, on November 21, 1944, leaving a name which will endure in the annals of science and warm memories among a host of friends.

HENRY NORRIS RUSSELL

PRINCETON UNIVERSITY OBSERVATORY

A PRELIMINARY REPORT ON CHROMOSPHERIC SPICULES OF EXTREMELY SHORT LIFETIME

WALTER ORR ROBERTS
Harvard College Observatory, Fremont Pass Station, Climax, Colorado
Received November 30, 1944

ABSTRACT

Small spikes of chromospheric material, observed in *Hα* with the coronagraph and quartz-polaroid monochromator, are described. These spicules, seen in polar regions of the sun, have very brief lifetimes, amounting on the average to 4 or 5 minutes. The typical spicule is low in brightness and has a height at maximum of less than 15 seconds of arc. At least in polar regions, they appear to be present in greater or smaller numbers at all times. The spicules are apparently distributed at random in the polar regions studied. The behavior of the spikes, while well typed, exhibits considerable variation. Possible association with polar coronal "plumes" and with "rice grains" of the disk is discussed.

For many years solar observers have been aware of the irregular appearance of the chromosphere of the sun when viewed under the best observing conditions. Frequent reference has been made to Secchi's observations of the "vertical flames" of the chromosphere in polar regions of the sun.[1] In discussing Lick Observatory eclipse photographs Menzel has called attention[2] to the "spike" prominences of the chromosphere and to the fact that "the difference between the chromosphere and the prominences is merely one of degree." The irregularities of the chromosphere are evident in the eclipse photographs reproduced by Menzel and, still more strikingly, in the photographs taken by Marriott, of Swarthmore College, at the eclipse of October, 1930. In the latter, small vertical polar prominences are clearly visible in some sections of the solar limb.

During the fall of 1943 I noticed that small chromospheric spike prominences were clearly discernible in photographs of the polar regions of the sun which I was taking with the Lyot-type coronagraph of the Harvard College Observatory located at Climax, Colorado. I was amazed at the extremely brief lifetimes and the great frequency of occurrence which visual observations of these spicules indicated. Consequently, I decided, toward the end of the year, to undertake a further investigation of this interesting phenomenon. On December 12, 1943, under the very best conditions of atmospheric steadiness and purity, I obtained a motion-picture film centered near the position angle of the north pole of solar rotation. The 35-mm film was exposed at a rate of one picture per minute through an interference polarization monochromator designed and built by Dr. John W. Evans[3] and similar to that used by Pettit for prominence observations.[4] Exposures were about 2 seconds on a 103 *Hα* sensitization film produced especially by Eastman Kodak Company. With a red-glass filter and the special film, the over-all transmission band utilized was about 4 A wide, centered on 6563 A of *Hα*.

From this first film and from subsequent visual and photographic observations I have ascertained, at least roughly, the behavior of the typical polar chromospheric spicule. The typical spicule shows first as a barely detectable lump on the solar limb. The lump rapidly enlarges and brightens to a maximum intensity that is still relatively faint for prominences in general. Within a minute or two of first appearance the lump elongates to maximum height, after which there is no detectable motion but simply a relatively gradual fading-out. Average proportions for a spicule at maximum extension are approximately 3″ or 4″ × 10″, though strong observational selection undoubtedly favors the recording of the large spicules and the overlooking of the small ones. Average total lifetimes are

[1] E.g., Abetti, *The Sun*, p. 134, 1938.

[2] *Pub. Lick Obs.*, **17**, 287 ff., 1931.

[3] *Pub. A.S.P.*, **52**, 305, 1940.

[4] *Pub. A.S.P.*, **53**, 171, 1941.

PLATE V

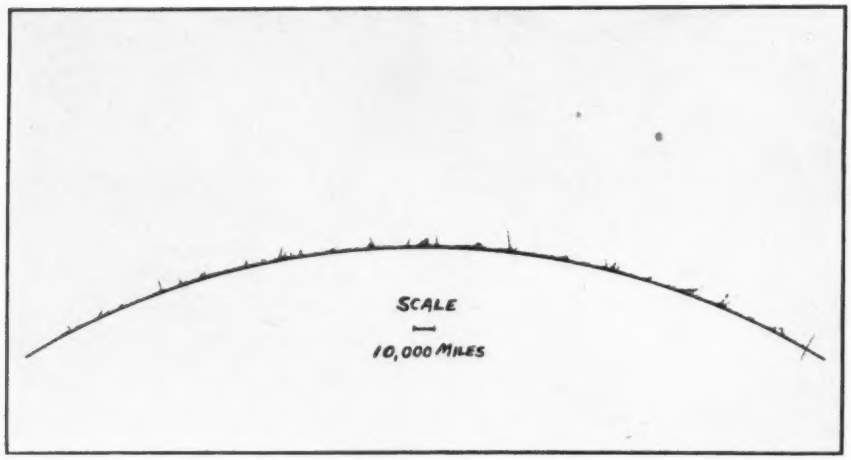

DRAWING SHOWING GENERAL CHARACTER OF THE POLAR REGIONS OF THE SUN

This sketch of the chromosphere was made from visual observations in $H\alpha$ with best seeing conditions and sky purity. The finer details shown have not yet been successfully photographed.

PLATE VI

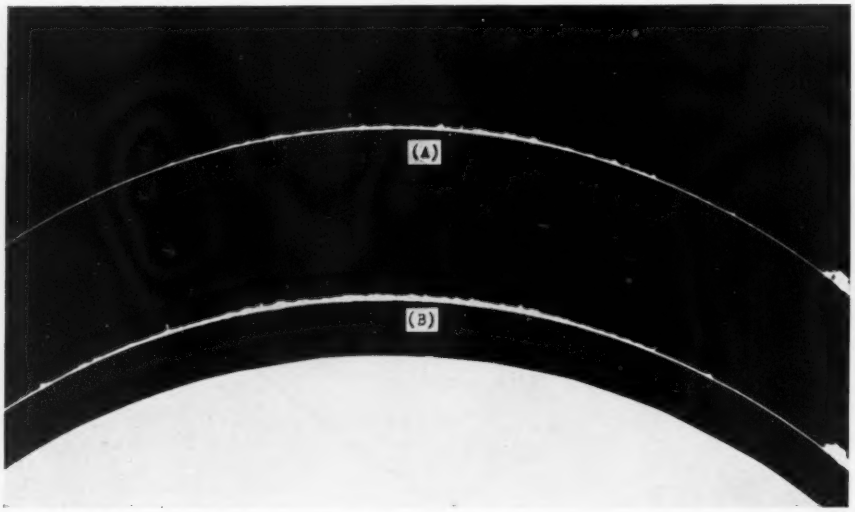

PHOTOGRAPHS OF CHROMOSPHERIC SPICULES NEAR NORTH POLE OF SUN ON FEBRUARY 3, 1944

The time interval between *A* and *B* is approximately 8 minutes. All spicules of *A* have disappeared by the time of *B*, and a new set shows on *B*.

about 4–5 minutes. Spicules much smaller than the typical one exist, and perhaps the frequency of occurrence for the smaller ones is even greater than for those I have called typical.

At a given moment of time I have observed visually more than 25 of the spicules within a 60° arc centered on the solar pole. Only the larger ones show on even the best photographs. On no occasion of satisfactory seeing and atmospheric purity have I failed to find the spicules present in considerable numbers in both polar regions. The intensity of the spikes is very low, on the average, and a great number of them exists at the very threshold of visibility. It is doubtful that they would be visible in apparatus not possessing relatively high resolution and high image-to-background contrast. Thus it is not surprising that the spicules have not attracted greater attention previously. Also it is unlikely that

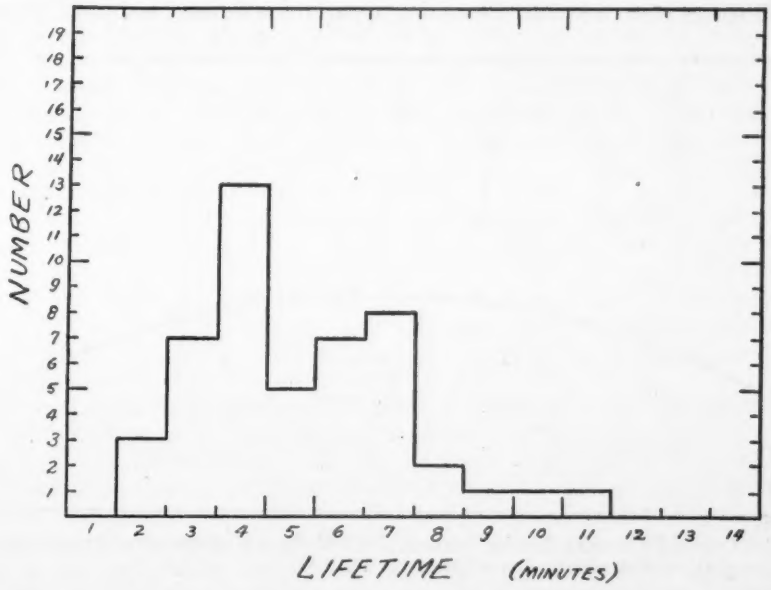

FIG. 1.—Histogram showing the frequency distribution of the lifetimes of spicules. Strong observational selection undoubtedly favors the inclusion in the measurements of spicules of long lifetime. The double maximum is probably not significant.

observers would be attracted to them in preference to the more striking prominences usually in evidence in other portions of the sun's disk. To study the spicules in detail from drawings is almost impossible, in spite of the advantages of visual observation, because of their intricacy and their rapid changes and because they are frequently obliterated momentarily by atmospheric unsteadiness. The drawing in Plate V depicts the general character of the spicules as seen during brief intervals of outstanding seeing steadiness. The drawing displays resemblance to eclipse photographs but does not quite show the fineness of detail drawn by Secchi from spectroscopic observations. In Plate VI, direct photographs of the spicules are shown. These photographs were taken under unusually favorable observational conditions. Comparison of the two parts of Plate VI shows that in the 8-minute interval between the two photographs, *A* and *B*, all the spicules visible in the first have disappeared and those in the second are new.

I have partially analyzed the film obtained on December 12, 1943; but for more complete studies I shall need improved measuring equipment. Preliminary results from the

first 50 frames of this motion picture, taken at the rate of one picture per minute, disclosed the formation of just over 50 distinct spicules. The 48 which could be measured with improvised apparatus displayed the frequency distribution of lifetimes given in Figure 1. These tabulated lifetimes represent simply the difference in number between the frame on which the spicule was first seen and the one on which it was last seen. The results are rough because of the difficulty of ascertaining the frame of first and last appearances with variable picture quality and too long an interval between pictures. The double maximum in the frequency distribution need not be regarded as significant in view of the grossness of the measurements and the small number of spicules involved. The drop in frequency for the shorter lifetimes may possibly be simply the result of observational selection. I have secured other films of the spicules at the more suitable rate of 6 frames per minute, and these should reveal more accurately the lifetime and behavior of the small spikes when adequate measuring apparatus is devised and constructed.

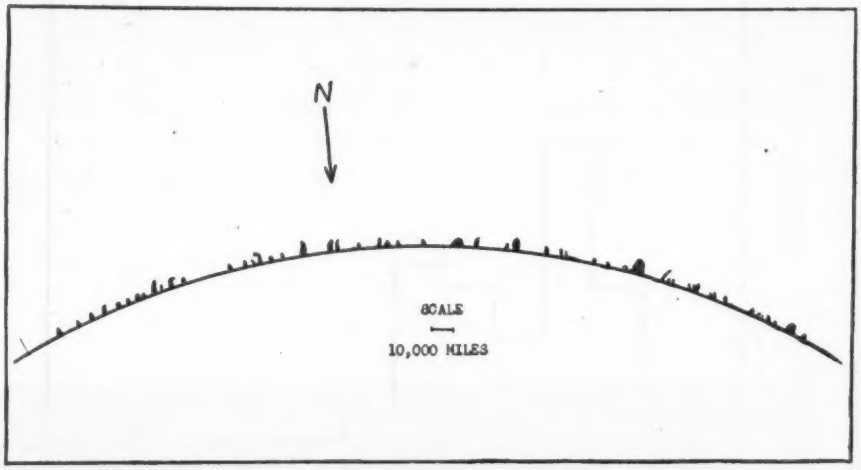

FIG. 2.—Composite drawing showing location, size, and shape of all the spicules measured in the first fifty frames of the motion-picture film of December 12, 1943.

The diagram in Figure 2 exhibits the distribution along the limb of the spicules detected in the first 50 frames of the December 12 film. No significant clustering exists; no large number of spicules came from any particular point of the arc, nor was any significant part of the arc devoid of the small spikes. No significant relationship to the position angle of the pole appears to exist.

Plates V and VI and Figure 2 also display to some extent the variation in behavior of the spikelets, one from another. Considerable range in size and shape exists. The size and length of life seem from rough comparison to be correlated strongly. The largest spicule in Figure 2 possessed the 11-minute lifetime, and some of the smallest as short as 2-minute lifetimes. This correlation serves further to accentuate the observational selection favoring observation of the larger and longer-lived spicules.

I have also made numerous visual observations of the small-scale chromospheric structure in the low latitudes of the sun. In most cases the spicules, if present, appear to have a more complex structure at low latitudes than at high. The inclinations to the vertical seem systematically greater, and the curvatures of the spikes themselves seem to be greater. Typical spicules definitely appear in low latitudes at times and apparently most conspicuously when the activity of larger prominences is at a minimum. I have taken motion-picture films to check this observation, but these will be too difficult to examine

without improved measuring apparatus. At present the data are too meager to say more than that the typical spicule structure is generally most pronounced in polar latitudes.

An interesting feature of the spicules—as, indeed, of all prominences—is the extreme sharpness of the boundaries of the emitting gases. In all cases the edges of prominences, from the faintest spicules to the brightest surges and the largest eruptives, appear perfectly sharp with no evident diffusion or haziness at the borders. This is definitely not an effect of the use of high-contrast photographic records, since not only are many of my films developed to a gamma well under 1 but also the effect is most noticeable by visual observation. To the very limit of resolution of the coronagraph (about 1″) the boundaries appear clear and distinct, and even the internal structure of the larger prominences seems invariably to be a complex interlacing of perfectly sharp filaments and knots of prominence gas.

There appears to be no mention elsewhere of measurements of the lifetimes or frequencies of spicules. Hale has referred[5] to "spike" prominences, but the phenomenon to which he was referring is evidently of a somewhat different nature, being very bright and related closely to a sunspot group. Hale's observation probably relates to a prominence of the "sunspot" classification (Class III) according to Pettit.[6] The small chromospheric spicules are not mentioned by Pettit in his prominence classification scheme,[6] nor does reference to them appear in the works of McMath and his collaborators or in the publications available here of Lyot or Waldmeier.

Measures of the dimensions of the spicules and the number visible at a given moment were made, previous to my observations, by Mohler,[7] of the McMath-Hulbert Observatory, from the excellent eclipse plates of Marriott exposed at the Swarthmore eclipse expedition of October, 1930. Mohler found from the eclipse plates average dimensions of about $2'' \times 11''$ for the spicules, in close agreement with my independent measures. Mohler estimated from the number visible along the limb that the disk of the sun should possess approximately 2×10^6 such spicules.

Of course, it is difficult to decide when a given prominence is to be classified as a spicule. Especially is this true at lower solar latitudes where the extreme simplicity of behavior of the spicules is not preserved uniformly. Undoubtedly all gradations of intermediate behavior between spicules and other prominences are possible. Still, the spicules seem to fall well enough into a pattern of behavior sufficiently typed and sufficiently distinguishable to be regarded as a characteristic phenomenon of the solar poles, at least at this phase of the solar cycle, much as the well-known coronal plumes are considered a phenomenon characteristic of the corona in the polar latitudes of the sun near minimum activity. And it is inviting to consider possible physical associations between the two.

The spicules and their constant rapid changes provide additional evidence of large-scale turbulence in the chromosphere. The velocity of motion of a typical spicule is apparently of the order of 30 km/sec radially outward from the sun's center. It must be remembered, however, that this "typical" spicule is possibly one of the less frequent and larger spicules because of observational selection. Spicules possess characteristics very close to those now ascribed to solar granulations,[8] namely, diameters of 1″–2″ and lifetimes of about 3 minutes. The recent interest in granulations stimulated by the work of Plaskett[9] and ten Bruggencate[10] impresses one with the importance of the possibility of associating spicules with the granulations. However, the expected velocity of outflow

[5] *Pub. A.S.P.*, **38**, 99, 1926.

[6] *Mt. W. Contr.*, No. 679; *Ap. J.*, **98**, 309, 1943.

[7] Private communication of unpublished results from Dr. Mohler.

[8] R. O. Redman, *M.N.*, **104**, 99, 1944.

[9] *M.N.*, **96**, 402, 1936.

[10] Ten Bruggencate and Grotrian, *Zs. f. Ap.*, **12**, 323, 1936; ten Bruggencate, Grotrian, and von der Pahlen, *Zs. f. Ap.*, **16**, 51, 1938; ten Bruggencate, *Zs. f. Ap.*, **16**, 374.

from granulations is about 1 km/sec, only one-thirtieth that estimated for the spicules. Further measures of the spicules and attempts to measure Doppler displacements in the granules should be made in order to determine whether this discrepancy is real. Still further, if direct photography of the polar coronal plumes and spicules can establish a link between the two, it may be reasonable to consider that the spicules associate granulations with the polar corona.

It is also reasonable to hope that a more detailed investigation of spicules may contribute to an understanding of the process of supply of material to the corona and regular prominences. The spicules are the only solar feature thus far discerned which seems observationally to indicate a continuous outflow of material through the chromosphere to the coronal regions. Indeed, it may prove that the spicules and the somewhat similar small-scale, low-latitude prominence structure are all that there is to the chromosphere and that actually the only difference between the chromosphere and the prominences is, as Menzel suggests, one of degree. In this case, the meaning of the "height of the chromosphere" becomes vague and the comparison of different measures extremely uncertain. In any event, the spicules are certainly further evidence of large-scale turbulence at the sun's surface; and, as such, they may provide, after careful study, valuable observational information regarding problems of disk-prominence-coronal interactions in general.

I wish to express my gratitude to Mrs. Roberts and to Miss Dorothy Emery for assistance in observing, recording, and measuring these spicules, and to Lt. Comdr. Donald H. Menzel for assistance and guidance in development of the coronagraph. To the Climax Molybdenum Company, on whose property our observatory is located, I wish to extend thanks for services performed in connection with the establishment of the coronagraphic station.

McCORMICK PHOTOVISUAL SEQUENCES

C. A. WIRTANEN AND A. N. VYSSOTSKY

Leander McCormick Observatory

Received December 30, 1941

ABSTRACT

A network of 329 photovisual magnitude sequences covering the sky from +75° to −15° is presented in Table 2. Each sequence contains, on the average, 13 stars ranging from 6^m3 to 10^m5. Although the accuracy of the individual magnitudes is not high (p.e. = $\pm 0^m075$), an attempt has been made to determine them in a fairly fundamental manner, so that the system would be as uniform and as close to the IPv as possible. Comparisons are given with various other catalogues of photovisual and visual magnitudes.

The various proper-motion programs of the Leander McCormick Observatory require a knowledge of the photovisual magnitudes of the stars observed. It is not necessary that these magnitudes be of high individual accuracy, but it is of great importance that they be rigorously related to a fundamental system of magnitudes, such as the IPv system. In the first and second proper-motion catalogues of this observatory, the magnitudes are very close to the IPv system; this was achieved by methods described elsewhere.[1,2] For the current and future proper-motion programs, however, it seemed wiser to undertake the task on a broader basis, so that photovisual magnitudes of stars down to the twelfth or thirteenth magnitude may be obtained readily when needed.

OBSERVATIONS

Previously, photovisual magnitudes have been observed here with the 26-inch visual refractor. For this new program, however, the 10-inch Cooke camera is used exclusively. The attachment to the IPv system has been effected by direct comparison with standard magnitudes at the pole. In order to avoid long exposures when these comparisons are made, we have divided the program into two parts. First, many magnitude sequences evenly distributed over the sky have been compared with a standard sequence at the pole; these sequences include stars from the sixth to the tenth magnitudes. Second, with these sequences as second-order standards, the magnitudes of stars down to the thirteenth photovisual are obtained from long-exposure photographs taken with an objective grating. In this scheme each sequence serves chiefly to provide the zero point for the final magnitudes, and the grating constants largely determine the scale.

The first part of the project has now been completed, and the results are presented herewith. The observations have extended over a number of years. One reason for this was that other observatory programs were more pressing; a more important reason, however, was that it was thought best to exercise extreme care in the choice of nights suitable for photometric work. The discussion of the results has also been delayed, because for the last two years, one of the authors (Wirtanen) has been engaged in war work.

The distribution of the sequences was determined primarily by the size of the field of the 10-inch camera. In order to provide one sequence for each 8 × 10 plate, we have spaced them at every 8.5° of right ascension in each declination zone, these zones being 10° apart. For the southernmost zone we chose −15°, since its altitude on the meridian is not very different from the altitude of the north pole at the latitude of the McCormick Observatory. Table 1 (see end of article) lists the sequences, designating them according

[1] *Pub. McCormick Obs.*, Vol. 7, 1937.

[2] E. R. Dyer, Jr., "On the System of Magnitudes in the Second McCormick Proper-Motion Catalogue." To be published.

to their declination zone and their serial number in that zone. The approximate right ascension of each sequence is also given. We did not originally plan to observe any sequences north of declination +75°, since the polar cap had been included in the Mount Wilson Observatory program[3] and was also well covered at Potsdam.[4] However, eleven additional sequences were later obtained at +82° in order to provide a direct comparison of our magnitudes with those of the polar cap catalogues.

All observations have been made at the altitude of the north pole within 4 minutes of the precise time when the observed region reached that altitude. A 3-minute exposure on the pole (or region) was immediately followed by an exposure of precisely the same duration on the region (or pole). Great care was exercised in the choice of nights with steady transparency, only 68 nights having been utilized for this program in the course of almost five years. To insure that the two exposures were made under similar instrumental conditions and to avoid difficulties arising from the order of the exposure, a kit was designed for the plateholder such that only one-half of a 5 × 7 plate was exposed through a filter in the center of the field, the other half remaining completely covered; after the

TABLE 3

BD	McC	MtW	MtW−McC	BD	McC	MtW	MtW−McC
+88°112	6^m32	6^m37	$+0^m05$	+88°142	9^m52	9^m41	-0^m11
89. 13	7.06	7.09	+ .03	89. 18	9.56	9.61	+ .05
88. 64	7.57	7.58	+ .01	89. 38	9.76	9.75	− .01
88. 9	8.13	8.14	+ .01	89. 12	9.83	9.82	− .01
88. 2	8.16	8.13	− .03	89. 35	9.87	9.85	− .02
89. 28	8.73	8.68	− .05	89. 7	10.04	9.99	− .05
88.131	8.93	8.98	+ .05	88.141	10.11	10.10	− .01
89. 21	9.04	.....	.....	89. 6	10.34	10.31	− .03
89. 3	9.06	9.07	+ .01	89. 29	10.37	10.40	+ .03
89. 9	9.24	9.22	− .02	89. 33	10.39	10.42	+ .03
89. 2	9.26	9.15	− .11	89. 36	10.41	10.39	− .02
88. 10	9.39	9.29	− .10	89. 31	10.46	10.45	−0.01
88. 20	9.49	9.39	−0.10				

first exposure the plate was turned through 180° and the second exposure obtained. Thus at no time was the plate left in the camera directly exposed to the air. An inspection of residuals disclosed no dependence on the order of exposure. Eastman I-G plates and Wratten No. 12 filter were used.

In Table 2 (see end of article) there are 329 sequences containing 4378 stars, which range in magnitude from 6^m3 to 10^m5. The magnitudes in 305 sequences are based on one polar comparison; for the remaining 24 sequences duplicate comparisons were made for the sake of determining the accidental errors. The plates were measured with the thermoelectric microphotometer and reduced in the usual manner. The standard North Polar Sequence[5] was supplemented with stars measured by Ross;[6] but it was found that a constant correction of $+0^m05$ brings Ross's magnitudes into improved agreement with the IPv system. Table 3 lists the stars chosen for the standard sequence at the north pole, together with the magnitudes as they were used. For comparison, in the same table are given the magnitudes from the Mount Wilson polar cap catalogue[7] which appeared after our measures were completed.

[3] *Trans. I.A.U.*, **5**, 164, 1935.

[4] *Pub. Ap. Obs. Potsdam*, **26**, No. 2, 1927.

[5] *Trans. I.A.U.*, **1**, 71, 1922.

[6] *Ap. J.*, **84**, 241, 1936.

[7] Seares, Ross, and Joyner, *Magnitudes and Colors of Stars North of +80°* ("Carnegie Inst. Publications," No. 532), 1941.

ACCIDENTAL ERRORS

An evaluation of the accidental errors of the McC magnitudes may be made either by repeating the observations of a number of our sequences on different nights or by comparing our final magnitudes with the magnitudes of the same stars given in other catalogues. Both methods have been used.

Twenty-four regions were compared twice with the standard polar sequence. The average zero-point difference for these duplicate comparisons has been found to be $\pm 0^m.111$; the probable error of one plate due to the zero-point error corresponding to this average difference is equal to $\pm 0^m.067$. Correcting the observed magnitudes for the zero-point difference of the particular pair of plates, we find that the probable error of one magnitude due to other accidental causes is equal to $\pm 0^m.047$. Thus the total probable error of one magnitude as derived from duplicate exposures is equal to $\pm 0^m.082$, and the probable error of this determination is $\pm 0^m.007$. We have also investigated the question of whether, possibly, a comparison made when the sequence is at the polar altitude in the east differs systematically from a similar comparison in the west. Fourteen of the twenty-four pairs just referred to were taken for this purpose. The difference was found to be negligible (-0.01 ± 0.02).

Eleven sequences obtained around the parallel of $+82°$ provided 136 stars in common with the Mount Wilson polar cap catalogue.[7] Assuming that the probable error of one magnitude in that catalogue is negligible compared with the error of our magnitudes, we obtain for the zero-point error of the McC magnitudes the value of $\pm 0^m.047$ and for the accidental probable error, $\pm 0^m.045$, which gives for the total error of one McC magnitude in the $+82°$ zone the value of $\pm 0^m.065$, and the probable error of this determination is $\pm 0^m.008$.

Finally, the magnitudes of 531 stars in the zones from $-15°$ to $+45°$ and between magnitudes $6^m.7$ and $8^m.2$ were compared with magnitudes of the same stars found in the Harvard mimeograph catalogue.[8] Assuming that, for most of these stars, the Harvard magnitude was derived from one visual catalogue, we take for the probable error of one Harvard magnitude the value ± 0.063.[9] Under this assumption, the total probable error of one McC magnitude comes out equal to ± 0.076.

Combining the three values obtained, we conclude that the probable error of one McC magnitude is not far from ± 0.075. It is possibly somewhat larger for the faintest and for the brightest stars.

COMPARISON WITH OTHER CATALOGUES

As stated above, the purpose of this work is to establish a network of photovisual sequences on a well-defined uniform system. In the attempt to assure this, a standard sequence at the north pole was chosen which represented the IPv system as closely as possible, and all the comparisons with it were made at the same altitude as the pole. Thus the zero point and the scale of our system of magnitudes should primarily depend on the chosen standard sequence (Table 3). Naturally, the color system is determined largely by the properties of the 10-inch objective and by the color filter and brand of plates used.

Nonetheless, it is very difficult to determine to what extent the system thus established is actually a uniform system, in other words, how stable the zero point and the scale are. Some information, however, can be obtained by establishing the relations between our magnitudes and some other sets of visual or photovisual magnitudes. For this purpose we have used four catalogues: the Mount Wilson polar cap catalogue,[7] the

[8] C. Payne-Gaposchkin, *Visual Magnitudes of Bright Stars Reduced to the Harvard Photovisual System* ("Harvard Obs. Mimeograms," Ser. III, Nos. 1 and 2), 1938.

[9] C. Payne-Gaposchkin, *Harvard Ann.*, **89**, 192, 1938.

Potsdam polar cap catalogue,[4] the Harvard Mimeograph Catalogue,[8] and the Potsdam Durchmusterung.[10]

Mount Wilson Polar Cap Catalogue (*MtW*).—This catalogue became available after most of our observations had been completed. It was then decided to make a number of direct comparisons between our magnitudes and those given by Seares, Ross, and Joyner. For this purpose eleven regions with 136 stars in common with their catalogue were observed and measured in precisely the same manner as the rest of our sequences. These additional regions were all chosen in the zone between +81° and +84° declination.

Our first concern is with the color system of our magnitudes. Table 4 gives the mean differences (MtW − McC) for eight color groups, the colors being those given in the

TABLE 4

MTW−MCC

Color Index	Mean Diff.	n	Color Index	Mean Diff.	n
− +0.19.....	−0^{m}04	27	+0.80 − +0.99....	−0^{m}03	17
+0.20 − + .39.....	− .04	19	+1.00 − +1.19....	− .03	21
+ .40 − + .59.....	− .12	14	+1.20 − +1.39....	− .10	12
+0.60 − +0.79.....	−0.06	4	+1.40 −	−0.10	15

Probable error of one difference = ±0^{m}06

TABLE 5

MTW−MCC

Mean Mag.	Mean Diff.	n	Mean Mag.	Mean Diff.	n
7.0.....	−0^{m}05	11	9.0.....	−0^{m}05	22
7.5.....	− .07	20	9.5.....	− .04	23
8.0.....	− .06	17	10.0.....	−0.01:	21
8.5.....	−0.07	22			

Probable error of one difference = ±0^{m}06

MtW catalogue. The last column in this and the following tables indicates the number of stars used in forming each mean difference. It is seen that there is no great change in the zero-point difference as we go from the white to the red stars, with the exception, perhaps, of the last two groups. A formal solution of these differences by the method of least squares gives $\Delta c = -0.03 \pm 0.02$ per magnitude for the value of the color coefficient and for the zero-point difference at color index zero, $\Delta z = -0^m04 \pm 0^m02$. As only one filter and only one brand of plates were used throughout, we may conclude that this evaluation of the color equation holds for all our sequences. However, since the coefficient is not much larger than its probable error, we have neglected it in our further discussion.

We may now investigate the scale and zero point of our magnitudes. The results of the comparison (Table 5) indicate no scale difference between the two catalogues. The zero-point difference of $-0^m05 \pm 0^m005$ is determined with greater accuracy than in the preceding paragraph.

It should be noted here that only one regression-curve was used (the regression of

[10] *Pub. Ap. Obs. Potsdam*, **17**, 1907.

MtW on McC) when comparing these two catalogues, since the precision of the MtW magnitudes is much higher than that of ours. However, in the comparisons with other catalogues the mean of both regression-curves has always been used.

The origin of the zero-point difference between the MtW and the McC magnitudes in the zone around +82° declination is not easy to explain, as it obviously does not follow from the deviations of the adopted magnitudes of the standard sequence (Table 3) from the magnitudes given for the same stars in the MtW catalogue.

Potsdam Polar Cap Catalogue (PDP).—The same eleven McCormick regions in the +82° zone as were used in the MtW comparison were also used for a comparison with the Potsdam photometrische Durchmusterung der polar Zone.[4] Preliminary to a comparison of McC magnitudes with PDP, the magnitudes of the latter were reduced to the IPv system.[11] The results of the comparison $PDP_1 - McC$ are given in Table 6. If we disregard the last group, which is affected by selection, the average zero-point difference ($PDP_1 - McC$) is equal to $-0.02 \pm .007$. This value is somewhat smaller than the zero-point difference (MtW−McC) found from the same eleven regions.

TABLE 6

$PDP_1 - McC$

Mean Mag.	Mean Diff.	n	Mean Mag.	Mean Diff.	n
7.0	-0^m01	10	9.0	-0^m03	22
7.5	− .01	20	9.5	− .03	23
8.0	− .03	17	10.0	+0.05:	21
8.5	−0.03	21			

Probable error of one difference = $\pm 0^m09$

Harvard Mimeograph Catalogue (HPvP) and Potsdam Durchmusterung (PD).—When one compares magnitudes in widely separated portions of the sky, a dependence of the zero point on both R.A. and Decl. is to be expected.[12] That this is so has been amply demonstrated by Seares, Ross, and Joyner,[7] who have found variations of the zero point in several catalogues even within the narrow ranges of the polar cap. All that we can do at present is to indicate differences of zero point, depending on R.A. and Decl. between our magnitudes and some other catalogues, without any prejudice as to which catalogue is really affected by systematic errors.

For these comparisons we chose the Harvard Mimeograph Catalogue and the Potsdam Durchmusterung. These two catalogues cover large areas and have many stars in common with those in our regions. While HPvP contains many stars as faint as 9^m5, PD does not reach much beyond 7^m5. The two catalogues are not independent, the PD magnitudes having been incorporated into the Mimeograph Catalogue north of the equator. For these reasons we have treated the comparison with the HPvP more extensively and have used the comparison with PD in order to have some supplementary information.

As the relation between the HPvP and the IPv color systems has been well established in the polar cap, we have reduced all magnitudes of the Harvard catalogue to the IPv, using the reduction formula given by C. Payne-Gaposchkin.[8] In what follows, the designation "HPvI" refers to the Harvard magnitudes thus reduced to IPv. Subsequent grouping of differences (HPvI−McC) according to the spectral class indicated that no further color correction is necessary.

There are 1206 stars in our sequences found also in the Harvard catalogue. There are

[11] F. H. Seares, *Systematic Corrections to Magnitudes* ("Mount Wilson Contr." No. 472), 1933.

[12] O. Bergstrand, *Trans. I.A.U.*, **5**, 157, 1936.

thus enough stars to divide them into six magnitude groups and treat each declination zone separately. The results of the comparison are summarized in Table 7, in which the differences are given in the sense (HPvI−McC). The table shows that the zero-point difference varies from group to group in a steady systematic manner, with the exception of the first magnitude group, in which the variation is rather erratic. For comparison in the last two lines we repeat the differences (MtW−McC) and (PDP_1−McC) for the polar cap zone.

A similar comparison of Potsdam Durchmusterung with McC for three magnitude groups and eight declination zones reveals great similarity in the general run of the differences (PD−McC) and (HPvI−McC). This might possibly be interpreted as an in-

TABLE 7

HPvI−McC

Zone	Magnitude											
	6.5		7.0		7.5		8.0		8.5		9.0	
	Mean Diff.	n	Mean Diff.	n	Mean Diff.	n	Mean Diff.	n	Mean Diff.	n	Mean Diff.	n
−15°	−0m03	15	+0m07	28	+0m08	26	+0m04	27	−0m01	12	−0m02	40
− 5	− .00	19	+ .03	35	− .00	30	+ .01	23	+ .01	18	− .09	30
+ 5	+ .11	10	+ .06	30	+ .10	14	+ .07	25	− .03	29	− .10	30
+15	+ .09	24	+ .08	37	+ .07	40	+ .14	30	+ .02	18	− .01	18
+25	− .06	12	+ .06	38	+ .04	24	+ .06	24	+ .01	20	− .08	8
+35	+ .03	13	+ .06	22	+ .07	30	+ .01	22	− .06	9	− .13	10
+45	− .01	12	+ .05	23	+ .04	28	− .00	30	+ .01	12	− .02	12
+55	+ .06	12	+ .07	20	+ .01	17	+ .00	18	− .15	8	− .21	10
+65	+ .00	9	+ .04	12	− .01	24	− .03	14	− .08	6	− .11	4
+75, +82	+0.02	8	− .07	19	− .06	24	− .06	26	− .05	13	− .16	13
MtW−McC	.....	....	− .05	11	− .07	20	− .06	17	− .07	22	− .05	22
PDP_1−McC	.....	....	−0.01	10	−0.01	20	−0.03	17	−0.03	21	−0.03	22

Probable error of one difference (HPvI−McC) = ±0m10

dication that the McC magnitudes are affected by systematic errors, while the other two catalogues are free from them. Several considerations, however, should be kept in mind before a definite opinion on this point is reached.

First of all, HPvI and PD magnitudes are not independent, since the PD magnitudes were incorporated in the Harvard Mimeograph Catalogue. Second, one cannot dismiss the possibility of zero-point variations depending on declination in a large catalogue based on visual observations. The zero point in the Potsdam Durchmusterung is determined by the 144 standard stars (*Fundamentalsterne*), and the various Harvard visual catalogues observed at Cambridge depend on the zero point defined by the 100 circumpolar stars. In neither case were all standards used during one night or for a given series of observations. On the other hand, all McC observations were made at the altitude of the pole, and one and the same standard sequence (with a few insignificant exceptions) was used throughout.

A possible source of variation of the McC zero point might be the necessity of comparing stellar images photographed at the pole, where the guiding is very good, with the

images obtained on a region of low declination, where the guiding is unavoidably somewhat inferior. To clear up this point the differences (HPvI−McC) formed from zones −5°, +5°, and +15° were divided into two groups, the first group containing 77 regions in which a slight but perceptible elongation of the images was visible, and the second with 87 regions in which the images were perfectly round. No appreciable difference in the zero point of the two groups is evident (+0.03±0.01). Thus at present it seems to be advisable to suspend judgment as to the source of the observed variations of the zero-point differences listed in Table 7.

We may now investigate the dependence of the zero-point differences (HPvI−McC) on right ascension. As the differences in Table 7 appear to be fairly stable in the zones from −15° to +45° for the magnitude groups 7^m0, 7^m5, and in the zones from −15° to +25° for the magnitude group 8^m0, only these zones and groups have been used for regrouping according to R.A. Eight groups, each of 3 hours width, have been formed, and the results are given in Table 8. As is seen from this table, there is a pronounced dependence of the zero-point difference on R.A., as it varies from $+0^m06\pm^m01$ at 3^h to $-0^m06\pm^m01$ at 12^h. It would be important if some other material were available for

TABLE 8

HPvI−McC

R.A.	Mean Diff.	n	R.A.	Mean Diff.	n
23^h– 1^h	$+0^m01$	65	11^h–13^h	-0^m06	60
2 – 4	+ .06	63	14 –16	− .04	54
5 – 7	+ .02	65	17 –19	+ .03	76
8 –10	−0.05	68	20 –22	+0.01	80

Probable error of one difference = $\pm0^m10$

further investigation as to whether a R.A. term in the McC magnitudes is really present. However, the Potsdam Durchmusterung will not supply us with any additional information, inasmuch as C. Payne-Gaposchkin,[13] having reached the conclusion that PD was free from a R.A. term, eliminated this term from various Harvard visual catalogues by comparing them with PD. Similarly, Yerkes Actinometry[14] was reduced by means of PD standards and consequently cannot be regarded as independent of either PD or HPvP.

The Potsdam observers[10] were the first ones to suggest that a possible R.A. term in HA 24 might be a consequence of a faulty procedure in correcting the observations for atmospheric extinction. They were at loss, however, to explain why, if this were so, there would be no declination term in the same catalogue. C. Payne-Gaposchkin[13] after an investigation of Harvard catalogues accepted the tentative explanation proposed by Potsdam. However, this does not seem to be satisfactory to the present authors, for there are several other catalogues which are affected by variations not easily explainable by seasonal variations in the atmospheric extinction. There is the notable case of Bailey's magnitudes of northern stars (HA 46) observed at Cambridge and reduced in precisely the same manner as those of Pickering (HA 44–45). As was shown by C. Payne-Gaposchkin,[13] Bailey's magnitudes show a R.A. term with respect to the latter. Again, the very arrangement of the McC observational procedure should tend to obliterate any seasonal error in our magnitudes, for regions as far apart as 6–8 hours of R.A. were frequently observed during one and the same evening.

[13] *Harvard Ann.*, **89**, 63, 1932.

[14] *Ap. J.*, **36**, 169, 1912.

Further comparisons which reveal the existence of R.A. terms are given in Table 9. The second column gives the differences MtW−PDP derived by Seares, Ross, and Joyner.[7] These are well established because of the great number of stars in common (note that the probable errors at the foot of the table now refer to the tabulated mean differences rather than to the untabulated individual differences as in previous tables). The fifth column contains a comparison of magnitudes in the Harvard Standard Regions "C" as observed by S. Gaposchkin[15] with those observed by C. Payne-Gaposchkin and H. Leavitt.[16] It is of interest that the magnitudes of S. Gaposchkin show the same variation from HPvI as do the McC magnitudes (Table 8). In the eighth column the differences between the Potsdam Durchmusterung and the HPvP magnitudes in Harvard Stand-

TABLE 9

MtW−PDP*			HPvI−SG†			PD−HPvP‡		
R.A.	Diff.	n	R.A.	Diff.	n	R.A.	Diff.	n
0h– 3h.....	+0m02	140	1.....	+0m04	16	1h0.....	+0m01:	2
4 – 7.....	− .02	135	3.....	+ .03	13	3.6.....	+ .03	9
8 –11.....	− .05	157	5.....	+ .04	17	6.0.....	+ .06	7
12 –15.....	− .01	156	7.....	− .02	12	8.3.....	+ .02	10
16 –19.....	+ .02	154	9.....	− .03	14	11.6.....	− .01	11
20 –23.....	+0.02	143	11.....	− .06	12	14.4.....	− .03	13
			13.....	− .07	14	17.1.....	− .01	9
			15.....	− .04	13	19.6.....	− .01	7
			17.....	+ .02	15	22.8.....	−0.01	9
			19.....	+ .06	12			
			21.....	+ .05	17			
			23.....	+0.03	16			
Approximate p.e. of one item....	±0m006			±0m02			±0m02	

* See Table 38, Mount Wilson Polar Cap Catalogue.

† SG denotes the magnitudes of S. Gaposchkin, reduced to the IPv system by means of the relation HPvI − SG = +0m026–0.16 (CI − 0m60). The differences were smoothed by taking means of three consecutive values.

‡ This includes stars in Harvard Standard Regions, "A," "B," and "C" common with Potsdam Durchmusterung; the differences are smoothed by taking means of three consecutive values; a constant zero-point difference of 0m30 has been removed.

ard "A," "B," and "C" regions[16] are given. With various degrees of certainty, these comparisons establish variations of zero point with R.A. in several catalogues. The underlying causes of these remain obscure at present. It does not appear to have been previously suggested, however, that variations of zero point may possibly occur in visual observations at a result of variations of the average color of standard stars in different parts of the sky, when the color perception of the observer deviates considerably from the IPv color system. A more extensive treatment of this question is outside the scope of this paper.

Miss Dorothy R. Watson prepared the tables for photo-offset reproduction and assisted in the computations for the other tables.

[15] *Harvard Ann.*, **108**, 1, 1939.

[16] *Harvard Ann.*, **89**, 3, 1931.

TABLE 1

Seq.	B.D.	Seq.	B.D.	Seq.	B.D.	Seq.	B.D.	Seq.	B.D.
o	h	o	h	o	h	o	h	o	h
+75.1	23.8	+55.24	22.7	+35.20	12.9	+25.38	22.7	+ 5.9	4.6
75.2	1.9	55.25	23.4	35.21	13.5	25.39	23.3	5.10	5.0
75.3	4.1			35.22	14.3			5.11	5.6
75.4	6.3	+45.1	23.9	35.23	14.9	+15.1	23.9	5.12	6.1
75.5	8.6	45.2	0.6	35.24	15.6	15.2	0.4	5.13	6.7
75.6	10.9	45.3	1.5	35.25	16.3	15.3	1.0	5.14	7.2
75.7	13.0	45.4	2.2	35.26	17.0	15.4	1.6	5.15	7.8
75.8	15.2	45.5	3.0	35.27	17.7	15.5	2.2	5.16	8.3
75.9	17.4	45.6	3.7	35.28	18.4	15.6	2.9	5.17	9.0
75.10	19.6	45.7	4.6	35.29	19.0	15.7	3.4	5.18	9.6
75.11	21.8	45.8	5.4	35.30	19.7	15.8	4.0	5.19	10.0
		45.9	6.1	35.31	20.3	15.9	4.5	5.20	10.6
+65.1	0.0	45.10	6.9	35.32	21.1	15.10	5.1	5.21	11.2
65.2	1.3	45.11	7.6	35.33	21.8	15.11	5.7	5.22	11.8
65.3	2.5	45.12	8.5	35.34	22.5	15.12	6.4	5.23	12.3
65.4	3.8	45.13	9.3	35.35	23.2	15.13	6.9	5.24	12.9
65.5	5.1	45.14	10.0			15.14	7.4	5.25	13.5
65.6	6.5	45.15	10.9	+25.1	23.9	15.15	8.1	5.26	14.0
65.7	7.8	45.16	11.7	25.2	0.6	15.16	8.6	5.27	14.7
65.8	9.2	45.17	12.4	25.3	1.2	15.17	9.2	5.28	15.2
65.9	10.5	45.18	13.2	25.4	1.7	15.18	9.8	5.29	15.7
65.10	11.9	45.19	14.0	25.5	2.5	15.19	10.3	5.30	16.3
65.11	13.2	45.20	14.8	25.6	3.0	15.20	10.9	5.31	16.8
65.12	14.6	45.21	15.6	25.7	3.5	15.21	11.5	5.32	17.4
65.13	16.0	45.22	16.4	25.8	4.2	15.22	12.2	5.33	17.9
65.14	17.3	45.23	17.2	25.9	4.8	15.23	12.7	5.34	18.6
65.15	18.6	45.24	17.8	25.10	5.4	15.24	13.3	5.35	19.1
65.16	20.0	45.25	18.7	25.11	6.0	15.25	13.9	5.36	19.7
65.17	21.3	45.26	19.5	25.12	6.6	15.26	14.4	5.37	20.3
65.18	22.6	45.27	20.3	25.13	7.3	15.27	15.0	5.38	20.8
		45.28	21.0	25.14	7.9	15.28	15.7	5.39	21.4
+55.1	0.0	45.29	21.9	25.15	8.5	15.29	16.3	5.40	22.1
55.2	0.9	45.30	22.6	25.16	9.2	15.30	16.8	5.41	22.5
55.3	1.9	45.31	23.4	25.17	9.7	15.31	17.4	5.42	23.2
55.4	2.8			25.18	10.4	15.32	18.0	5.43	23.7
55.5	3.8	+35.1	23.9	25.19	11.0	15.33	18.5		
55.6	4.7	35.2	0.5	25.20	11.6	15.34	19.1	-5.1	22.0
55.7	5.7	35.3	1.2	25.21	12.2	15.35	19.8	5.2	22.6
55.8	6.7	35.4	2.0	25.22	12.9	15.36	20.5	5.3	23.2
55.9	7.7	35.5	2.6	25.23	13.5	15.37	21.0	5.4	23.7
55.10	8.7	35.6	3.2	25.24	14.1	15.38	21.5	5.5	23.9
55.11	9.6	35.7	4.0	25.25	14.7	15.39	22.1	5.6	0.5
55.12	10.6	35.8	4.7	25.26	15.3	15.40	22.6	5.7	1.1
55.13	11.7	35.9	5.3	25.27	15.9	15.41	23.2	5.8	1.7
55.14	12.7	35.10	6.0	25.28	16.5	15.42	23.9	5.9	2.2
55.15	13.6	35.11	6.6	25.29	17.1			5.10	2.8
55.16	14.7	35.12	7.4	25.30	17.7	+ 5.1	23.9	5.11	3.3
55.17	15.7	35.13	7.9	25.31	18.3	5.2	0.5	5.12	3.9
55.18	16.6	35.14	8.7	25.32	19.1	5.3	1.0	5.13	4.5
55.19	17.6	35.15	9.2	25.33	19.6	5.4	1.7	5.14	5.0
55.20	18.5	35.16	10.2	25.34	20.2	5.5	2.2	5.15	5.6
55.21	19.6	35.17	10.8	25.35	20.9	5.6	2.7	5.16	6.1
55.22	20.6	35.18	11.5	25.36	21.5	5.7	3.4	5.17	6.7
55.23	21.6	35.19	12.2	25.37	22.1	5.8	3.8	5.18	7.3

TABLE 1 -- Continued

Seq.	B.D.	Seq.	B.D.	Seq.	B.D.	Seq.	B.D.	Seq.	B.D.
o	h	o	h	o	h	o	h	o	h
- 5.19	7.8	- 5.33	15.8	-15.3	1.1	-15.17	9.2	-15.30	16.8
5.20	8.4	5.34	16.3	15.4	1.7	15.18	9.8	15.31	17.5
5.21	8.9	5.35	16.9	15.5	2.3	15.19	10.4	15.32	18.0
5.22	9.5	5.36	17.5	15.6	2.8	15.20	11.0	15.33	18.6
5.23	10.1	5.37	18.1	15.7	3.4	15.21	11.6	15.34	19.2
5.24	10.6	5.38	18.6	15.8	4.0	15.22	12.2	15.35	19.7
5.25	11.2	5.39	19.1	15.9	4.6	15.23	12.7	15.36	20.3
5.26	11.8	5.40	19.8	15.10	5.2	15.24	13.3	15.37	20.9
5.27	12.4	5.41	20.3	15.11	5.7	15.25	13.9	15.38	21.5
5.28	12.9	5.42	20.9	15.12	6.3	15.26	14.5	15.39	22.1
5.29	13.4	5.43	21.5	15.13	6.9	15.27	15.1	15.40	22.7
5.30	14.1			15.14	7.5	15.28	15.6	15.41	23.3
5.31	14.6	-15.1	23.9	15.15	8.1	15.29	16.2	15.42	23.9
5.32	15.2	15.2	0.5	15.16	8.6				

TABLE 2

BD	Mag.	BD	Mag.	BD	Mag.	BD	Mag.
+75.1°		+75.2°		+75.3°		+75.4°	
+74° 1051	7.58	+74° 91	6.83	+75° 173	6.59	+75° 258	7.82
75 901	7.74	74 87	6.86	74 195	7.21	74 281	7.90
73 1068	7.78	75 83	7.34	75 182	8.06	75 264	8.07
74 1039	8.21	74 95	7.95	74 205	8.55	74 293	8.35
75 906	8.35	75 93	8.81	74 196	8.65	75 262	8.81
74 1042	8.45	74 88	9.12	75 167	8.69	75 268	9.14
75 904	8.50	74 90	9.33	75 175	8.93	75 260	9.16
75 896	8.58	74 89	9.74	74 207	8.98	74 295	9.35
75 907	8.62	75 85	10.02	75 174	9.35	74 285	9.54
75 1	8.65	75 87	10.31	75 178	9.38	75 255	9.83
74 1059	8.73			74 201	9.46	75 256	9.95
75 905	9.10			74 203	9.51	74 291	10.08
74 1046	9.16			74 198	9.52	74 296	10.23
74 1057	9.32			75 180	9.58	75 254	10.30
74 1052	9.67			75 172	10.04		
+75.5°		+75.6°		+75.7°		+75.8°	
+74° 379	7.31	+76° 411	7.15	+76° 470	7.06	+74° 609	6.77
74 382	8.25	75 438	7.63	75 500	8.10	75 547	6.86
75 359	8.28	75 409	8.05	75 501	8.33	75 561	7.63
75 352	8.36	75 429	8.27	75 489	8.41	76 557	7.98
74 381	8.41	74 452	8.28	74 516	8.87	75 560	8.15
75 350	8.76	74 448	8.68	75 490	8.89	75 550	9.11
74 374	8.77	74 446	8.75	75 498	9.04	75 558	9.25
75 353	8.98	75 434	8.82	76 478	9.20	75 559	9.51
74 383	8.89	74 453	9.02	76 479	9.31	75 554	9.62
75 357	9.13	74 450	9.57	75 496	9.43	75 563	9.81
75 347	9.22	75 432	9.99	75 491	9.77	74 608	10.06
75 351	9.38	75 433	10.04	75 493	9.99	75 555	10.33
75 348	9.45	75 436	10.05				
75 356	10.17	75 435	10.18				
		74 451	10.31				
+75.9°		+75.10°		+75.11°		+65.1°	
+74° 717	6.75	+74° 831	6.97	+74° 946	6.25	+64° 3	6.98
75 616	7.45	74 829	7.62	74 926	8.05	64 1894	7.16
74 710	7.55	74 830	7.74	74 938	9.00	64 1887	7.50
74 720	7.91	75 702	8.08	74 939	9.12	64 5	7.85
74 713	8.27	74 839	8.32	75 797	9.20	64 15	8.02
74 708	8.31	74 828	8.45	74 932	9.38	63 5	8.14
75 637	8.68	74 823	8.55	74 929	9.44	63 15	8.39
75 635	8.90	75 701	8.69	74 945	9.52	63 2088	8.63
74 721	9.35	74 835	9.11			63 2108	8.67
75 626	9.36	74 837	9.34			64 1900	8.79
74 722	9.38	74 841	9.68			64 1	9.27
74 709	9.48	74 833	9.77			64 4	9.30
74 711	9.53	74 827	9.77			63 2098	9.75
74 707	9.92	75 706	9.77			64 1896	10.21
		74 840	9.95				

TABLE 2 -- Continued

BD	Mag.	BD	Mag.	BD	Mag.	BD	Mag.
+65.2°		**+65.3°**		**+65.4°**		**+65.5°**	
+64 168	6.59	+64 351	7.55	+65 373	7.44	+64 523	7.53
64 150	7.57	63 343	7.75	64 424	7.81	65 464	7.95
64 144	7.86	64 354	7.81	65 394	7.99	66 399	8.01
63 186	8.28	64 346	8.73	64 429	8.18	64 505	8.26
63 199	8.73	64 340	9.05	65 381	8.26	66 391	8.36
63 191	8.78	63 354	9.37	65 392	9.05	64 516	8.91
63 168	9.12	64 352	9.55	65 382	9.08	65 474	8.98
63 183	9.12	63 357	9.66	65 390	9.50	64 509	9.09
63 192	9.28	64 353	9.74	64 416	9.52	65 470	9.35
64 154	9.29	64 342	10.05	64 420	9.73	65 472	9.48
64 161	9.30			64 425	10.07	65 469	9.58
63 170	9.36			64 417	10.14	64 521	9.59
64 172	9.68			64 418	10.14	64 528	9.70
64 158	9.83			64 422	10.32	65 471	10.07
64 159	10.22						
+65.6°		**+65.7°**		**+65.8°**		**+65.9°**	
+65 537	7.47	+65 606	7.08	+65 703	7.82	+64 810	6.31
64 600	7.84	65 599	7.30	65 711	8.32	65 803	6.42
65 547	8.10	66 537	7.39	64 735	8.58	65 798	7.84
64 596	8.12	65 607	7.62	64 736	8.77	65 797	8.09
65 541	8.80	64 661	8.78	65 705	9.17	65 791	8.09
65 543	8.87	65 610	9.08	64 728	9.49	64 807	8.35
64 599	9.13	65 612	9.14	65 710	9.73	65 801	8.55
64 598	9.31	64 670	9.26	65 717	9.84	65 788	8.71
64 597	9.40	65 601	9.39	65 713	9.88	65 799	8.90
65 536	9.54	65 608	9.71	66 607	9.93	65 800	9.18
64 594	9.80	65 604	9.76	65 706	9.96	65 789	9.26
65 542	10.07	65 605	9.86			65 796	9.38
		65 602	10.12			64 799	9.47
		64 663	10.27				
+65.10°		**+65.11°**		**+65.12°**		**+65.13°**	
+66 737	6.36	+64 951	6.88	+66 855	6.76	+65 1087	6.62
65 863	7.17	64 946	7.36	65 1011	7.39	65 1095	6.87
65 874	7.42	66 800	7.42	64 1018	7.61	65 1098	6.93
64 877	8.28	65 932	7.81	64 1017	7.62	65 1093	7.32
64 881	8.42	65 925	8.67	66 861	8.02	65 1094	8.57
65 867	8.55	65 927	8.72	66 856	8.16	64 1104	8.87
65 873	8.77	66 801	8.74	65 1012	8.34	64 1110	9.21
66 744	9.05	65 926	8.94	65 1000	8.65	64 1095	9.28
64 875	9.30	65 923	9.29	65 999	8.95	64 1105	9.38
64 872	9.40	65 931	9.39	65 1004	9.32	65 1086	9.42
64 879	9.42	65 920	9.76	65 998	9.50	64 1106	9.45
65 864	9.54	65 924	9.91	66 859	10.04	64 1102	9.46
		66 803	10.25	66 860	10.11	64 1094	9.68
				65 1003	10.14	64 1099	10.22

TABLE 2 -- Continued

BD	Mag.	BD	Mag.	BD	Mag.	BD	Mag.
	+65.14		+65.15		+65.16		+65.17
+64 1191	7.41	+65 1276	6.55	+63 1593	6.44	+63 1707	6.53
63 1343	7.42	64 1289	7.36	64 1407	6.61	64 1536	7.30
64 1196	8.39	64 1276	8.49	64 1398	7.07	63 1720	7.49
64 1198	8.63	64 1290	8.57	64 1415	7.55	64 1535	7.66
64 1184	8.69	65 1277	8.91	64 1417	7.89	64 1528	8.03
64 1190	8.72	65 1279	9.22	64 1406	7.97	64 1548	8.06
64 1192	8.92	64 1286	9.36	64 1414	8.31	64 1546	8.11
64 1202	9.17	64 1292	9.67	63 1583	8.40	64 1538	8.14
63 1352	9.17	64 1287	9.71	64 1411	9.03	63 1741	8.26
64 1197	9.53	64 1280	10.04	64 1402	9.27	63 1732	8.59
64 1195	9.73	64 1281	10.04	64 1410	9.74	64 1542	8.66
64 1194	9.77	64 1285	10.29	64 1403	9.95	63 1730	9.12
63 1346	10.08			64 1401	9.98	64 1532	9.47
64 1201	10.38			64 1409	10.06	63 1726	9.59
64 1193	10.38			64 1408	10.33	63 1739	10.25
	+65.18		+55.1		+55.2		+55.3
+64 1704	6.74	+54 3109	6.86	+55 229	6.44	+54 453	6.32
64 1717	6.82	54 1	7.71	53 211	6.61	53 440	7.53
64 1701	7.33	53 3267	7.73	54 187	6.83	54 444	7.67
63 1882	7.49	53 3280	7.78	54 215	7.64	53 451	7.95
64 1713	7.58	54 3081	8.02	55 236	8.00	54 452	8.02
64 1702	7.87	54 8	8.06	54 207	8.69	53 453	8.33
64 1698	8.53	53 3289	8.26	54 203	8.73	54 457	8.49
64 1699	8.94	54 3104	8.51	54 200	8.92	54 448	8.58
64 1716	9.18	54 3107	9.01	54 204	9.00	54 438	8.78
64 1705	9.28	54 3097	9.02	54 210	9.37	54 449	9.13
64 1709	9.50	54 3110	9.31	54 213	9.38	53 447	9.27
64 1706	9.50	53 3281	9.43	55 228	9.50	54 450	9.40
64 1703	9.53	54 3108	9.52	54 196	9.82	54 459	9.47
64 1714	10.30	54 3095	9.82	54 201	9.90	54 439	9.66
		54 3106	10.33	55 239	10.11	54 432	9.92
		54 3111	10.33	54 212	10.30	54 434	10.01
	+55.4		+55.5		+55.6		+55.7
+54 629	7.43	+54 734	6.38	+55 945	6.72	+55 1036	6.31
54 621	8.06	55 839	7.19	55 952	7.42	55 1022	7.54
55 740	8.43	55 844	7.72	54 831	7.86	55 1033	7.98
54 630	8.77	55 846	8.34	55 938	8.88	55 1024	8.61
54 623	9.13	55 845	8.61	55 944	9.15	54 966	8.64
55 737	9.23	54 733	8.72	55 939	9.16	55 1037	8.82
54 626	9.68	55 840	8.73	55 946	9.32	54 966	8.87
54 625	9.74	54 735	8.94	55 940	9.33	55 1034	9.23
54 632	9.79	55 838	9.10	55 942	9.67	55 1023	9.40
54 631	10.01	54 736	9.43	55 947	9.75	55 1029	9.58
55 732	10.07	54 731	9.43	54 842	9.85	55 1035	9.65
55 739	10.03	54 729	9.48	55 948	9.94	54 956	9.69
		54 738	9.62	55 943	10.11	55 1039	9.86
		54 725	9.69	55 949	10.25	55 1026	10.37

TABLE 2 -- Continued

BD	Mag.	BD	Mag.	BD	Mag.	BD	Mag.
+55.8		**+55.9**		**+55.10**		**+55.11**	
+55 1155	6.62	+55 1228	6.36	+55 1297	7.38	+55 1345	6.31
54 1083	7.68	54 1188	6.87	55 1301	7.94	54 1329	7.38
55 1137	7.93	55 1226	6.93	54 1264	8.03	54 1330	8.31
55 1138	7.94	55 1230	7.00	55 1299	8.57	55 1349	8.56
54 1077	7.96	55 1223	7.52	54 1254	8.86	56 1399	8.89
56 1164	8.08	55 1235	8.06	54 1258	8.87	56 1402	9.05
55 1132	8.32	55 1240	8.27	54 1261	9.09	55 1347	9.17
55 1131	8.42	55 1234	8.92	54 1262	9.37	55 1351	9.53
55 1136	9.02	55 1237	9.01	55 1294	9.51	56 1408	9.56
54 1092	9.07	54 1186	9.08	55 1295	9.74	56 1409	9.57
55 1141	9.12	55 1233	9.24	55 1296	9.77	56 1410	9.73
55 1145	9.37	55 1236	9.50	55 1298	9.81	55 1350	9.75
54 1085	9.54	55 1229	9.76	55 1300	10.45	55 1346	9.96
		55 1232	9.90			56 1407	10.04
		54 1183	10.09			56 1401	10.13
+55.12		**+55.13**		**+55.14**		**+55.15**	
+55 1408	8.06	+55 1481	6.74	+55 1564	6.82	+56 1677	7.24
56 1482	8.13	54 1468	8.37	55 1556	7.22	56 1682	7.46
56 1474	8.68	55 1494	8.52	55 1555	8.67	55 1630	7.99
55 1416	8.93	54 1461	8.60	55 1554	9.00	54 1614	8.24
55 1410	8.98	54 1473	8.65	54 1548	9.01	55 1624	9.24
55 1414	9.07	55 1485	8.72	54 1546	9.16	56 1689	9.72
55 1417	9.08	55 1493	8.95	54 1550	9.28	56 1681	9.77
55 1404	9.49	55 1496	8.98	55 1549	9.39	54 1617	9.77
55 1409	9.59	54 1474	9.04	54 1551	9.47	55 1629	10.11
55 1413	9.68	55 1490	9.36	54 1545	9.60	55 1632	10.16
55 1402	9.80	55 1488	9.88	55 1551	9.84	56 1686	10.22
55 1406	9.86			55 1550	10.09	55 1628	10.38
55 1405	10.14			55 1552	10.11		
55 1411	10.24						
+55.16		**+55.17**		**+55.18**		**+55.19**	
+54 1708	7.05	+55 1775	7.55	+55 1876	6.88	+54 1911	6.63
54 1700	7.64	55 1783	8.39	55 1873	8.12	55 1960	7.01
55 1704	7.74	56 1828	8.52	54 1834	8.58	54 1889	7.24
55 1713	8.16	55 1769	8.68	55 1864	8.66	55 1961	7.40
55 1706	8.85	55 1768	8.77	54 1827	8.77	55 1971	9.09
55 1708	8.91	55 1773	8.88	54 1828	8.89	55 1953	9.18
55 1710	9.03	54 1772	9.36	53 1885	9.17	54 1901	9.36
54 1701	9.26	55 1770	9.41	53 1887	9.25	54 1906	9.43
55 1707	9.37	55 1781	9.45	54 1837	9.44	55 1957	9.74
55 1712	9.43	55 1771	9.45	54 1830	9.46	55 1970	9.75
54 1709	9.44	55 1774	9.57	54 1829	9.48	54 1903	9.78
54 1706	9.48			54 1826	9.54	53 1965	9.87
55 1709	9.49			54 1823	9.67	54 1900	10.00
54 1704	9.68			54 1824	9.72		
				54 1825	9.80		

TABLE 2 -- Continued

BD	Mag.	BD	Mag.	BD	Mag.	BD	Mag.
+55.20		**+55.21**		**+55.22**		**+55.23**	
+55 2099	7.45	+55 2245	6.63	+55 2444	6.33	+54 2590	7.52
55 2094	7.58	54 2223	6.84	53 2435	6.88	55 2612	7.76
54 2020	7.66	54 2187	7.35	54 2408	6.96	54 2597	7.87
55 2089	7.95	53 2282	7.91	54 2374	7.03	53 2655	7.96
55 2098	7.98	54 2185	8.16	54 2396	7.32	54 2583	8.19
54 2024	8.32	54 2212	8.21	53 2471	8.01	54 2607	8.30
54 2011	8.52	54 2197	8.76	53 2466	8.02	54 2585	8.62
55 2096	8.83	55 2234	9.03	54 2397	8.42	54 2593	9.01
54 2018	8.89	54 2198	9.16	53 2456	8.99	54 2587	9.18
55 2092	9.18	55 2249	9.17	54 2380	9.31	54 2611	9.21
54 2015	9.20	54 2202	9.22	54 2379	9.32	55 2617	9.30
55 2101	9.81	54 2192	9.52	53 2458	9.37	55 2614	9.66
55 2095	9.84	54 2191	9.61	55 2440	9.63	54 2588	9.89
		54 2210	9.82	54 2383	9.64	54 2589	10.25
		54 2204	10.02	54 2381	9.92		
+55.24		**+55.25**		**+45.1**		**+45.2**	
+54 2856	6.72	+55 2990	7.21	+44 4538	6.47	+45 209	7.18
55 2797	6.84	54 3006	7.67	44 4550	6.77	45 199	7.54
53 2963	7.31	54 2970	7.96	43 4607	7.69	45 187	7.54
54 2867	7.52	54 2991	8.16	43 4629	7.92	44 162	7.58
55 2800	8.38	53 3190	8.28	43 4627	8.47	45 190	7.83
54 2865	8.53	54 3003	8.58	43 4592	8.48	44 169	7.83
54 2846	8.77	54 2992	8.59	43 4622	8.87	45 202	8.32
54 2875	8.83	55 2981	8.62	43 4608	9.10	45 192	8.88
55 2814	8.99	55 2987	8.86	44 4546	9.57	44 166	9.03
54 2871	9.12	55 2992	9.19	43 4599	9.63	45 208	9.06
54 2854	9.24	55 2976	9.32	44 4537	9.72	44 170	9.22
54 2873	9.61	54 2981	9.55	44 4547	10.00	45 193	9.45
54 2866	9.65	54 3001	9.67	44 4542	10.04	45 201	9.86
54 2870	9.95			43 4603	10.04	45 205	9.88
				44 4544	10.16	44 171	10.11
						44 172	10.32
+45.3		**+45.4**		**+45.5**		**+45.6**	
+43 337	7.97	+43 474	6.79	+45 716	7.21	+45 836	7.77
44 347	8.07	44 483	7.17	45 706	7.22	44 816	7.97
44 350	8.44	45 600	7.34	44 634	7.36	45 833	8.17
43 323	8.51	45 605	7.36	45 710	7.44	45 858	8.64
43 336	8.66	45 608	7.78	44 630	8.02	45 856	8.87
44 335	9.32	44 456	7.86	45 721	8.21	44 827	8.92
44 327	9.44	44 458	8.58	44 636	8.85	44 813	9.01
44 342	9.54	44 473	8.68	44 635	9.22	44 828	9.12
43 330	9.73	44 469	8.87	45 711	9.23	44 818	9.18
43 326	9.77	45 598	8.88	44 627	9.39	44 822	9.22
44 343	9.84	45 604	9.02	45 713	9.44	45 844	9.47
44 344	10.02	45 585	9.28	44 629	9.62	44 819	9.52
43 335	10.06	44 450	9.33	45 712	9.70	44 809	9.62
43 329	10.10	45 587	9.63	45 714	9.70		
		45 588	9.88	44 632	9.94		
		45 597	10.23	45 715	10.34		

TABLE 2 -- Continued

BD	Mag.	BD	Mag.	BD	Mag.	BD	Mag.
+45.7		**+45.8**		**+45.9**		**+45.10**	
+45 987	7.64	+44 1247	7.15	+46 1122	6.65	+45 1383	7.83
44 1013	7.68	44 1232	7.57	45 1281	7.71	45 1387	7.96
43 1047	7.82	45 1131	7.85	44 1399	8.13	44 1573	8.51
44 1036	8.23	45 1132	7.89	46 1123	8.29	45 1379	8.67
44 1016	8.96	45 1134	8.39	45 1270	8.54	46 1224	8.80
44 1012	9.06	45 1145	8.43	45 1264	8.67	45 1388	8.99
44 1034	9.16	45 1144	8.54	45 1278	8.96	45 1382	9.15
44 1021	9.32	44 1239	8.63	45 1284	9.00	45 1381	9.16
44 1018	9.42	45 1133	8.73	44 1410	9.03	44 1578	9.33
44 1025	9.53	45 1136	8.86	45 1277	9.05	45 1380	9.41
44 1014	9.57	45 1143	9.16	45 1272	9.36	45 1386	9.42
43 1048	9.58	45 1135	9.24	44 1404	9.67	45 1390	9.48
44 1015	9.77	45 1129	9.45	45 1283	9.84	45 1392	9.59
44 1008	9.81	44 1237	9.51	44 1409	9.89	45 1391	9.62
44 1017	9.94	44 1238	9.62	45 1275	10.17	45 1377	9.85
		44 1245	10.02	45 1280	10.25	44 1583	10.07
+45.11		**+45.12**		**+45.13**		**+45.14**	
+46 1323	6.31	+45 1601	7.77	+45 1726	7.41	+45 1814	7.40
46 1320	7.07	45 1620	7.88	45 1717	7.91	45 1798	7.68
46 1327	7.43	44 1769	8.42	46 1506	8.06	45 1811	8.12
45 1496	8.11	45 1614	8.77	45 1731	8.76	45 1819	8.40
44 1679	8.14	45 1613	8.96	45 1719	8.91	45 1802	8.44
45 1493	8.36	45 1612	9.40	45 1723	9.12	46 1600	9.55
45 1484	8.58	45 1623	9.52	45 1718	9.43	44 1955	9.61
45 1486	9.06	44 1765	9.63	45 1716	9.46	45 1803	9.80
45 1485	9.28	46 1416	9.65	45 1727	9.66	45 1807	10.01
45 1488	9.36	45 1603	9.70	45 1720	10.06	44 1957	10.40
45 1491	9.50	45 1622	9.85	45 1732	10.06	46 1591	10.43
45 1482	9.58	45 1610	9.86	45 1725	10.19		
45 1499	9.65	45 1602	10.08				
45 1483	9.88						
45 1490	10.14						
45 1494	10.31						
+45.15		**+45.16**		**+45.17**		**+45.18**	
+45 1879	6.94	+45 1961	7.74	+45 2038	6.68	+44 2265	6.42
45 1892	7.29	44 2132	7.95	44 2205	7.13	44 2264	8.53
44 2039	7.61	45 1968	8.43	46 1791	7.62	45 2105	8.73
46 1685	8.56	44 2126	8.53	44 2202	7.90	45 2104	8.73
45 1883	8.62	45 1963	9.33	45 2052	8.57	46 1861	8.77
46 1682	8.79	44 2136	9.41	44 2196	9.07	45 2096	8.82
45 1890	9.14	45 1964	9.49	45 2048	9.20	45 2100	9.38
46 1691	9.33	46 1745	9.67	45 2050	9.41	45 2094	9.42
45 1880	9.42			45 2044	9.64	44 2261	9.46
45 1877	9.50			44 2199	9.70	45 2101	9.68
45 1875	9.53			45 2040	9.73	44 2258	9.84
45 1876	9.69			45 2041	9.82		
45 1882	9.78			44 2206	10.17		
45 1884	9.78						
45 1886	9.91						

TABLE 2 -- Continued

BD	Mag.	BD	Mag.	BD	Mag.	BD	Mag.
+45.19		**+45.20**		**+45.21**		**+45.22**	
+46 1922	6.31	+45 2229	7.71	+44 2493	6.74	+45 2400	6.95
45 2154	8.07	45 2233	7.90	44 2501	7.09	45 2408	7.12
45 2148	8.52	46 1999	8.04	45 2318	7.43	43 2611	7.57
46 1934	8.91	45 2228	8.05	45 2329	7.72	44 2585	7.69
46 1927	9.21	44 2399	8.52	45 2317	8.09	44 2572	8.66
45 2157	9.43	45 2225	8.52	45 2323	8.12	45 2399	9.06
45 2159	9.56	46 2000	8.89	44 2499	8.15	44 2578	9.07
45 2155	9.62	46 1998	9.18	45 2325	8.26	45 2416	9.11
44 2323	9.82	45 2235	9.41	44 2498	8.66	44 2581	9.41
46 1926	9.88	45 2230	9.48	45 2321	9.03	44 2574	9.47
45 2151	10.04	45 2226	9.92	45 2322	9.21	45 2406	9.64
46 1929	10.09	45 2236	10.01	45 2326	9.24	44 2576	9.68
44 2331	10.20	45 2231	10.30	45 2315	10.22	45 2403	9.83
46 1932	10.32					44 2580	9.90
+45.23		**+45.24**		**+45.25**		**+45.26**	
+45 2504	6.47	+45 2626	6.86	+46 2551	6.38	+45 2929	7.26
43 2702	7.14	44 2780	7.17	45 2777	6.68	45 2920	7.56
45 2509	7.54	44 2777	7.86	44 3003	7.16	45 2927	7.99
44 2659	7.82	45 2621	8.08	45 2764	7.46	45 2936	8.11
45 2511	7.84	44 2800	8.13	45 2769	7.69	44 3193	8.21
44 2691	8.66	44 2773	8.63	45 2774	7.89	44 3170	8.33
45 2502	9.01	45 2617	8.82	44 2983	8.11	44 3178	8.36
44 2670	9.04	45 2618	8.89	45 2765	8.46	44 3179	8.38
45 2506	9.23	46 2383	9.03	45 2779	8.48	44 3169	8.92
44 2663	9.51	45 2608	9.51	45 2780	9.29	44 3183	8.95
44 2678	9.52	45 2610	9.61	44 2997	9.39	45 2928	9.46
44 2669	9.67	45 2613	9.67	44 2989	9.48	44 3181	9.69
45 2503	9.75	45 2609	9.72	45 2768	9.76	44 3197	9.78
		44 2775	9.78	44 3004	9.76	44 3188	10.34
		44 2782	9.78	45 2770	9.88		
		45 2611	9.90				
+45.27		**+45.28**		**+45.29**		**+45.30**	
+44 3429	6.97	+44 3679	6.58	+44 4044	6.32	+43 4298	6.98
44 3439	7.53	44 3718	6.85	44 4041	6.59	44 4197	7.07
44 3457	7.55	45 3438	6.93	45 3741	6.98	43 4288	7.22
44 3427	7.72	44 3741	7.38	44 3985	7.71	44 4232	8.24
44 3426	7.77	44 3710	7.47	45 3722	8.03	44 4217	8.74
44 3434	8.38	44 3711	7.54	45 3721	8.27	44 4224	8.86
44 3436	8.90	43 3822	7.63	44 3980	8.38	43 4299	9.10
44 3441	8.90	43 3842	7.80	45 3740	8.66	44 4219	9.16
44 3443	9.01	44 3717	8.45	45 3730	9.17	43 4310	9.40
43 3581	9.12	44 3693	8.72	44 3989	9.38	43 4306	9.48
44 3461	9.15	43 3823	9.01	45 3743	9.58	44 4214	9.54
44 3432	9.16	44 3691	9.21	44 4009	9.73	44 4215	9.80
43 3579	9.34	44 3704	9.46	45 3738	10.03	44 4216	9.84
44 3442	9.74	44 3715	9.47			43 4290	9.87
44 3444	9.78	44 3716	9.51				
44 3456	9.91	43 3814	10.09				

TABLE 2 -- Continued

BD	Mag.	BD	Mag.	BD	Mag.	BD	Mag.
+45.31		**+35.1**		**+35.2**		**+35.3**	
+43 4481	6.69	+34 5039	6.54	+34 79	7.41	+33 228	6.80
43 4489	6.89	35 5159	7.50	35 121	7.78	35 260	7.43
45 4252	7.03	34 5052	7.90	34 108	7.98	33 205	7.56
44 4454	8.24	33 4805	8.76	35 109	8.28	34 231	7.61
43 4484	8.31	34 5042	8.76	34 81	8.28	34 243	7.73
44 4440	8.32	34 5046	8.83	34 98	8.49	35 270	7.84
43 4486	8.35	34 5037	8.84	35 129	8.97	35 265	8.12
44 4432	8.64	33 4804	9.12	34 96	9.26	34 230	8.43
44 4435	9.06	34 5055	9.33	34 87	9.28	35 269	9.04
44 4438	10.16	34 5056	9.38	34 105	9.42	34 236	9.07
43 4483	10.42	33 4812	9.46	35 123	9.63	34 232	9.17
		35 5161	9.56	35 124	9.81	35 256	9.22
		35 5142	9.60			35 268	9.23
		34 5053	9.66				
		34 5040	9.84				
+35.4		**+35.5**		**+35.6**		**+35.7**	
+34 376	7.44	+34 504	7.03	+35 697	7.07	+34 829	7.47
34 379	8.18	34 510	7.52	34 645	8.56	36 829	7.65
35 416	8.38	35 550	7.69	34 623	8.69	35 807	7.69
34 375	9.02	35 531	8.30	34 639	8.75	35 796	7.90
35 418	9.08	35 544	8.81	35 674	8.98	35 809	7.95
34 382	9.12	34 488	8.93	34 637	9.04	34 807	8.46
34 390	9.20	35 541	9.52	34 640	9.05	35 806	8.70
34 391	9.27	34 499	9.56	35 681	9.24	34 817	8.99
34 380	9.52	34 503	9.59	34 636	9.29	34 804	9.12
34 373	9.66	35 547	9.62	35 676	9.59	34 827	9.31
34 384	9.68	35 542	9.65	35 673	9.66	35 793	9.38
34 386	10.20	34 495	9.74	34 627	9.80	34 819	9.69
		35 545	9.87	34 624	9.85	35 805	9.72
		34 496	10.05	34 638	10.27	35 802	9.78
		34 507	10.19			35 804	9.89
						34 823	10.03
+35.8		**+35.9**		**+35.10**		**+35.11**	
+35 914	6.67	+34 1083	6.28	+36 1364	7.02	+35 1495	7.22
34 916	7.76	34 1064	7.01	35 1339	7.18	33 1414	7.94
34 904	7.95	34 1069	7.59	34 1272	7.44	34 1462	8.23
33 907	8.45	34 1077	7.83	34 1266	7.87	35 1491	8.54
33 901	8.48	34 1080	8.11	35 1362	8.35	34 1442	8.72
34 917	8.51	34 1065	8.19	35 1341	8.43	35 1489	8.95
34 911	9.09	34 1088	8.38	34 1260	8.51	35 1496	8.98
35 907	9.55	34 1063	8.83	35 1358	8.83	35 1487	9.10
34 909	9.56	34 1066	8.83	35 1337	9.07	34 1470	9.15
34 905	9.81	34 1079	8.99	35 1360	9.08	34 1458	9.27
34 912	10.07	34 1081	9.45	34 1287	9.15	34 1465	9.35
34 907	10.13	34 1075	9.52	34 1276	9.23	35 1492	9.49
34 906	10.16	34 1073	9.54	34 1281	9.34	35 1488	9.55
		34 1078	9.64	35 1338	9.38	34 1444	9.78
		34 1070	9.94	34 1288	9.54	34 1456	9.85
		34 1071	10.12	35 1350	9.73	34 1457	9.95

TABLE 2 -- Continued

BD	Mag.	BD	Mag.	BD	Mag.	BD	Mag.
+35.12		**+35.13**		**+35.14**		**+35.15**	
+35 1635	7.13	+35 1767	6.62	+35 1905	7.18	+34 2000	7.58
35 1624	7.22	36 1752	7.36	35 1880	7.62	35 2022	7.90
34 1614	7.46	34 1753	7.59	35 1886	7.84	35 2005	8.81
35 1623	7.88	35 1754	8.07	35 1904	7.87	35 2019	9.44
36 1645	7.95	36 1745	8.54	35 1892	8.21	35 2009	9.47
35 1621	8.41	35 1741	8.62	35 1894	8.24	35 2016	9.54
35 1652	8.50	34 1757	8.88	35 1883	8.61	35 2002	9.59
35 1641	8.88	35 1744	8.93	35 1881	8.74	35 2004	9.70
35 1649	8.99	34 1741	9.14	35 1895	9.04	35 2014	9.81
35 1628	9.09	35 1749	9.41	35 1890	9.25	36 1965	9.82
35 1637	9.13	35 1743	9.44	35 1902	10.22	36 1971	9.93
35 1622	9.19	35 1761	9.55			35 2020	10.22
35 1632	9.21	34 1731	9.90				
35 1646	9.52	35 1762	9.95				
35 1629	9.62	35 1740	9.98				
35 1636	10.06	35 1742	10.08				
+35.16		**+35.17**		**+35.18**		**+35.19**	
+34 2124	6.92	+34 2176	8.40	+34 2230	7.25	+35 2333	7.13
35 2130	7.01	35 2196	8.47	35 2272	7.99	35 2334	8.63
34 2122	7.02	35 2198	9.18	34 2245	8.52	35 2331	8.96
35 2122	7.23	35 2201	9.42	35 2274	8.72	36 2257	8.98
35 2136	8.66	35 2194	9.56	34 2239	8.92	36 2254	9.04
35 2123	9.11	35 2199	9.64	35 2264	9.02	35 2337	9.08
35 2128	9.42	35 2202	9.73	34 2252	9.21	35 2332	9.20
36 2058	9.67	36 2134	9.83	35 2277	9.35	36 2258	9.54
36 2055	10.03	35 2193	9.84			36 2259	9.62
35 2121	10.27	35 2195	10.02			34 2307	9.65
34 2108	10.44					35 2336	9.90
35 2126	10.45					36 2261	9.92
						35 2330	10.43
+35.20		**+35.21**		**+35.22**		**+35.23**	
+35 2391	7.73	+35 2474	6.28	+36 2478	8.25	+35 2644	6.94
35 2392	7.87	35 2480	7.38	35 2561	8.73	35 2637	7.68
35 2387	8.11	34 2444	7.82	34 2515	9.03	35 2649	7.75
34 2377	8.59	35 2466	7.91	35 2548	9.57	35 2631	8.12
36 2321	9.30	36 2406	7.97	35 2552	9.84	34 2599	8.38
35 2396	9.54	35 2478	8.06	35 2549	9.87	35 2634	8.51
35 2389	9.59	35 2471	8.38	35 2555	9.92	35 2648	8.75
36 2328	9.63	36 2405	8.51	35 2544	10.11	36 2565	8.93
36 2325	10.14	35 2469	8.86	36 2489	10.25	34 2597	9.43
35 2388	10.20	36 2393	8.95	35 2546	10.29	36 2568	9.55
		35 2472	9.01	35 2554	10.36	35 2638	9.56
		35 2483	9.24	35 2550	10.37	34 2589	9.61
		35 2476	9.54			35 2640	9.62
		36 2401	9.83			34 2587	9.71
		35 2473	10.33			36 2567	9.76
						35 2641	10.12

TABLE 2 -- Continued

BD	Mag.	BD	Mag.	BD	Mag.	BD	Mag.
+35.24		**+35.25**		**+35.26**		**+35.27**	
+34 2674	7.79	+35 2828	6.32	+34 2889	6.59	+35 3059	6.46
35 2719	8.33	35 2810	7.06	35 2922	6.64	34 3050	6.49
34 2688	8.77	33 2742	7.12	35 2917	7.26	34 3035	7.41
34 2686	9.24	35 2823	7.38	34 2888	7.71	35 3042	7.82
34 2682	9.26	34 2776	7.63	35 2904	7.80	34 3049	8.00
35 2726	9.38	35 2824	8.10	35 2905	8.07	34 3019	8.00
35 2720	9.73	34 2799	8.33	35 2908	8.53	35 3068	8.04
		33 2739	8.37	35 2901	8.66	34 3024	8.09
		34 2787	8.71	35 2899	8.75	34 3031	8.14
		34 2786	8.97	35 2902	9.02	34 3036	8.81
		34 2768	9.11	34 2883	9.11	34 3032	9.05
		34 2771	9.32	36 2821	9.14	35 3057	9.08
		34 2784	9.56	35 2898	9.16	34 3028	9.43
		34 2775	9.83	36 2822	9.23	34 3042	9.45
				35 2900	9.65	34 3048	9.52
				35 2910	9.96		
+35.28		**+35.29**		**+35.30**		**+35.31**	
+35 3240	7.16	+35 3501	6.53	+34 3727	6.32	+34 3995	6.85
34 3238	7.38	34 3431	7.11	35 3826	6.92	35 4140	7.30
33 3124	7.42	34 3399	7.51	34 3708	7.81	35 4090	8.05
34 3239	7.56	35 3460	7.92	34 3749	7.93	35 4130	8.11
34 3226	8.23	34 3423	8.25	35 3839	8.01	35 4119	8.13
35 3255	8.32	34 3415	8.37	34 3706	8.16	35 4102	8.22
35 3266	8.58	34 3410	8.47	35 3799	8.41	35 3086	8.26
34 3211	8.83	35 3472	8.76	35 3825	8.47	35 4105	8.35
34 3207	8.88	34 3425	8.90	34 3756	8.64	35 4087	8.41
34 3223	8.98	34 3426	9.06	34 3720	8.66	35 4104	8.91
34 3222	9.08	34 3403	9.09	35 3830	8.86	35 4098	9.13
34 3225	9.13	35 3478	9.21	34 3733	8.91	35 4092	9.18
34 3210	9.24	35 3482	9.46	34 3710	8.94	34 3990	9.20
34 3219	9.71	34 3428	9.75	34 3725	8.97	35 4125	9.22
34 3217	9.90	35 3475	9.77	34 3754	9.05	35 4085	9.44
34 3209	9.92	35 3468	9.94	34 3742	9.22	34 4028	9.53
+35.32		**+35.33**		**+35.34**		**+35.35**	
+35 4435	6.62	+34 4566	6.99	+34 4728	6.36	+34 4899	6.33
34 4267	7.13	34 4563	7.11	34 4729	6.56	34 4883	6.77
35 4431	7.44	33 4371	7.38	34 4714	7.45	34 4875	7.87
34 4336	7.48	33 4384	7.92	33 4523	8.11	33 4674	7.94
34 4277	7.63	33 4379	8.05	33 4524	8.19	34 4878	8.43
34 4313	7.69	34 4567	8.23	33 4529	8.21	34 4887	8.51
35 4402	7.70	34 4573	8.35	34 4731	8.52	34 4873	8.63
34 4335	7.71	34 4557	8.44	35 4837	8.68	33 4676	8.98
35 4419	7.97	33 4385	8.77	34 4730	8.72	34 4886	9.18
34 4303	8.09	34 4571	8.82	33 4531	8.86	33 4673	9.27
34 4332	8.13	34 4559	9.01	34 4707	9.14	34 4884	9.42
35 4390	8.32	34 4551	9.11	34 4726	9.48	34 4867	9.47
34 4285	8.41	34 4562	9.15	33 4542	9.68	33 4668	9.55
34 4294	8.51	33 4387	9.40	34 4711	9.73	33 4677	9.71
34 4326	8.77	34 4570	9.54	33 4535	10.26	34 4871	9.93
34 4312	8.86	34 4556	9.61			34 4889	9.97

TABLE 2 -- Continued

BD	Mag.	BD	Mag.	BD	Mag.	BD	Mag.
+25.1		**+25.2**		**+25.3**		**+25.4**	
+23 4853	6.91	+25 118	7.05	+24 198	7.62	+25 319	7.44
25 5042	6.92	24 123	7.24	25 211	7.78	25 317	7.73
24 4885	7.59	25 112	8.01	24 200	8.38	25 311	8.08
25 5055	8.42	24 104	8.94	25 210	8.43	25 328	8.17
25 5051	9.19	25 97	9.15	24 205	8.56	25 307	8.59
24 4871	9.31	24 107	9.16	25 212	8.57	25 314	8.64
24 4866	9.38	24 99	9.36	24 204	8.87	24 267	8.92
23 4834	9.42	25 111	9.42	23 175	9.13	25 316	9.09
24 4872	9.44	25 104	9.62	25 216	9.22	25 308	9.20
24 4878	9.45	24 105	9.92	24 203	9.36	24 274	9.32
24 4868	9.49	24 117	9.92	25 207	9.41	24 273	9.35
24 4873	9.75	24 108	9.92	24 201	9.59	24 277	9.47
24 4880	9.85	24 116	9.94	24 199	9.74	24 281	9.67
24 4869	9.88			24 196	9.79	24 278	9.71
24 4877	9.92			24 202	9.89		
24 4874	10.17						
+25.5		**+25.6**		**+25.7**		**+25.8**	
+25 441	6.49	+24 441	7.58	+25 593	6.92	+25 703	7.58
23 362	7.58	25 497	8.07	24 527	6.98	24 643	8.37
24 368	8.15	24 437	8.24	24 533	7.42	24 642	8.47
24 381	8.18	24 451	8.57	24 537	7.57	25 700	8.71
24 369	8.29	25 496	8.67	24 534	7.89	25 692	8.97
23 350	8.88	24 449	8.72	24 523	8.01	24 641	9.04
23 349	8.92	24 450	9.06	24 520	8.77	25 698	9.13
23 347	9.02	24 443	9.21	24 528	8.87	25 708	9.32
23 351	9.03	25 507	9.40	24 532	9.01	25 702	9.60
23 354	9.16	24 440	9.55	25 583	9.07	24 650	9.65
23 346	9.28	24 439	9.68	24 526	9.11	25 701	9.68
24 380	9.40	25 502	9.78	24 521	9.20	24 651	9.73
23 345	9.45	25 508	9.82	25 588	9.29	25 694	9.83
24 378	9.73	24 445	9.87	24 524	9.38	25 704	9.88
23 352	9.93	25 506	9.88	24 525	9.71	24 648	10.14
24 373	9.94	25 509	10.05	24 522	10.09	24 653	10.24
+25.9		**+25.10**		**+25.11**		**+25.12**	
+24 709	6.46	+24 854	6.60	+25 1180	7.38	+24 1386	6.87
25 766	7.04	25 852	7.94	25 1153	7.84	25 1460	7.03
24 722	7.91	25 866	7.98	26 1117	7.94	25 1446	7.16
24 719	7.99	25 843	8.32	25 1174	8.21	24 1406	8.43
25 765	8.22	25 863	8.43	24 1148	8.33	25 1458	8.56
25 753	8.32	24 869	8.57	25 1133	8.53	25 1459	8.75
24 711	8.54	25 878	8.58	24 1153	8.67	24 1388	8.94
25 755	8.84	24 850	8.83	25 1163	8.68	25 1433	9.12
25 761	9.30	25 868	9.13	25 1125	8.68	24 1414	9.58
24 712	9.48	25 857	9.61	24 1156	9.10	25 1416	9.62
		24 872	9.70	25 1151	9.22	24 1401	9.65
		25 849	10.34	25 1152	9.73	25 1441	9.70
				25 1134	10.35	25 1442	10.03
						25 1430	10.21
						25 1437	10.28
						25 1424	10.33

TABLE 2 -- Continued

BD	Mag.	BD	Mag.	BD	Mag.	BD	Mag.
+25.13		**+25.14**		**+25.15**		**+25.16**	
+25 1677	8.42	+25 1816	6.47	+24 1955	6.88	+25 2065	6.87
25 1659	8.92	25 1860	7.11	25 1950	7.99	25 2084	7.19
24 1658	9.03	25 1864	7.33	24 1969	8.38	24 2054	7.56
25 1655	9.05	24 1840	7.83	25 1966	8.70	25 2083	7.81
25 1657	9.07	25 1854	8.00	25 1958	8.82	25 2081	8.26
25 1669	9.16	25 1844	8.01	25 1959	8.86	25 2073	8.62
24 1656	9.22	25 1826	8.03	25 1973	9.00	25 2062	8.63
24 1645	9.35	24 1843	8.30	24 1956	9.06	24 2059	8.99
25 1664	9.47	26 1718	8.43	25 1965	9.13	25 2064	9.22
25 1680	9.63	24 1847	8.46	25 1961	9.24	25 2080	9.30
24 1657	9.67	25 1839	9.40	24 1962	9.45	25 2069	9.34
24 1641	9.81	25 1848	9.92	25 1955	9.77	24 2070	9.60
25 1670	9.83	25 1846	9.95	24 1967	9.82	25 2067	9.90
25 1665	10.30	25 1847	10.29	25 1954	9.85	24 2067	9.95
25 1675	10.32			25 1957	10.01		
25 1668	10.45			25 1970	10.03		
+25.17		**+25.18**		**+25.19**		**+25.20**	
+25 2163	6.77	+25 2260	7.13	+26 2176	6.91	+26 2250	6.54
26 2021	7.04	25 2263	7.56	25 2352	8.21	24 2386	7.71
25 2078	7.20	25 2258	7.71	26 2175	8.34	26 2249	7.72
25 2170	7.81	24 2238	7.83	25 2338	8.43	25 2418	7.92
25 2186	8.41	25 2271	8.41	25 2346	8.83	25 2411	8.48
25 2185	8.67	25 2277	9.45	25 2340	8.89	25 2403	8.50
25 2165	8.95	25 2264	9.80	25 2345	9.37	25 2401	9.19
25 2184	9.04	25 2269	10.00	25 2350	9.46	25 2415	9.78
25 2180	9.05	25 2274	10.01	25 2337	9.60	25 2409	9.81
25 2164	9.40	26 2105	10.06	25 2336	9.67	25 2402	10.04
25 2168	9.57	25 2275	10.11	25 2342	9.82	25 2407	10.15
25 2173	10.02	25 2265	10.25	25 2347	9.82	25 2416	10.17
25 2172	10.08					25 2404	10.43
25 2176	10.13						
25 2166	10.37						
+25.21		**+25.22**		**+25.23**		**+25.24**	
+25 2495	7.39	+24 2531	6.86	+24 2612	7.71	+25 2733	6.55
25 2501	7.41	25 2583	7.73	26 2481	8.03	26 2530	7.78
25 2493	7.44	25 2598	8.48	24 2611	8.41	25 2744	7.92
25 2487	7.78	24 2530	8.98	25 2649	8.95	26 2529	8.54
25 2481	8.38	26 2416	9.03	24 2622	9.03	25 2732	9.59
25 2482	8.72	26 2415	9.16	25 2655	9.21	24 2697	9.74
25 2486	8.82	26 2418	9.35	25 2658	9.65	25 2739	9.93
25 2496	8.98	26 2421	9.43	26 2477	9.71	26 2535	9.99
25 2492	9.01	25 2591	9.45	25 2656	9.76	25 2740	10.01
25 2488	9.03	24 2536	9.71	26 2476	9.86	25 2741	10.12
24 2448	9.24	25 2595	9.72	25 2661	10.33		
25 2485	9.48	26 2417	9.90				
25 2483	9.91	24 2526	9.96				
24 2446	9.93	25 2582	10.16				
		25 2585	10.28				
		25 2584	10.38				

TABLE 2 -- Continued

BD	Mag.	BD	Mag.	BD	Mag.	BD	Mag.
+25.25		**+25.26**		**+25.27**		**+25.28**	
+25 2841	6.80	+25 2916	6.54	+25 3020	7.22	+24 3038	7.81
25 2839	6.91	25 2902	6.63	25 3009	7.71	23 2978	8.14
24 2776	7.52	26 2685	7.39	24 2954	7.94	25 3113	8.37
26 2603	8.29	25 2904	7.65	25 3003	8.01	24 3031	8.48
25 2835	8.77	25 2912	7.91	25 2994	8.22	25 3110	8.95
25 2826	9.01	25 2908	8.34	25 3005	8.62	24 3037	9.01
25 2842	9.11	25 2922	8.52	24 2957	8.65	25 3114	9.33
25 2838	9.31	26 2692	8.74	25 3000	8.77	24 3036	9.41
25 2832	9.40	25 2910	8.75	25 2997	8.94	24 3044	9.50
25 2831	9.47	25 2913	9.36	25 3012	9.53	24 3039	9.63
24 2782	9.84	26 2688	10.22	25 3006	9.64	25 3112	9.65
24 2781	9.95	25 2915	10.30	25 3007	9.68		
		25 2909	10.34	25 2996	9.72		
		25 2914	10.36	25 3008	9.94		
				25 3015	9.98		
				26 2766	10.50		
+25.29		**+25.30**		**+25.31**		**+25.32**	
+24 3127	6.80	+25 3357	6.45	+24 3425	6.83	+24 3650	6.53
24 3141	6.88	25 3344	6.72	26 3255	6.96	23 3572	6.80
25 3215	7.22	24 3271	6.88	26 3247	7.56	25 3735	7.42
24 3121	7.61	24 3264	6.97	25 3543	7.85	23 3584	7.91
23 3058	7.91	25 3364	7.10	25 3541	7.95	25 3745	8.03
24 3137	8.33	24 3275	7.42	25 3520	8.24	25 3737	8.07
24 3124	8.47	25 3368	7.79	25 3540	8.98	24 3655	8.28
25 3212	8.52	24 3270	8.38	25 3524	9.34	24 3659	8.49
24 3133	8.74	24 3252	9.11	25 3537	9.46	24 3668	8.68
24 3135	9.07	25 3360	9.17	25 3542	9.50	24 3666	8.90
24 3145	9.35	24 3274	9.22	24 3421	9.53	25 3747	9.32
24 3143	9.48	25 3342	9.28	25 3538	9.60	24 3660	9.42
24 3122	9.67	25 3354	9.48	25 3547	9.78	24 3667	9.45
24 3136	9.83	24 3255	9.52	25 3539	9.87	24 3664	9.51
24 3139	9.95	25 3358	9.93	25 3533	9.98		
24 3125	10.37	25 3362	10.22	24 3419	10.32		
+25.33		**+25.34**		**+25.35**		**+25.36**	
+24 3849	6.51	+23 4004	6.93	+25 4422	7.00	+24 4445	6.29
24 3832	6.82	24 4116	7.35	25 4443	7.08	23 4361	6.99
24 3838	7.63	23 3998	7.36	24 4276	8.26	25 4565	8.10
24 3825	8.56	23 3970	7.75	24 4299	8.52	24 4440	8.11
24 3844	8.61	23 3974	8.42	25 4418	8.68	23 4359	8.23
24 3856	8.67	23 3997	8.47	24 4303	8.75	25 4568	8.26
25 3913	8.77	23 3975	8.72	24 4295	8.98	24 4449	8.29
25 3940	8.82	24 4103	8.95	24 4274	9.27	24 4433	8.49
24 3828	9.03	24 4090	9.18	25 4430	9.46	25 4570	8.78
24 3834	9.08	23 3979	9.35	24 4294	9.57	24 4450	8.81
25 3922	9.22	24 4091	9.42	24 4284	9.73	25 4581	8.83
25 3915	9.27	24 4108	9.56	25 4427	9.89	24 4442	8.90
24 3827	9.31	24 4104	9.66	24 4283	9.91	24 4436	9.15
24 3842	9.37	24 4107	9.81	25 4421	10.04	24 4439	9.30
25 3931	9.53	24 4109	10.13	24 4285	10.08	23 4357	9.66
24 3835	10.06			25 4432	10.09	24 4441	10.01

TABLE 2 -- Continued

BD	Mag.	BD	Mag.	BD	Mag.	BD	Mag.
+25°.37		**+25°.38**		**+25°.39**		**+15°.1**	
+25 4691	6.54	+25 4828	6.89	+24 4773	7.04	+14 5074	6.47
23 4493	7.01	23 4600	7.24	24 4770	7.37	15 4925	7.28
23 4486	7.59	23 4633	7.42	24 4776	7.49	14 5077	7.36
23 4490	8.00	23 4612	7.58	24 4777	7.97	14 5094	7.45
24 4550	8.04	23 4606	7.89	24 4764	8.31	13 5196	8.02
24 4545	8.17	23 4616	8.48	25 4934	8.31	14 5084	8.13
24 4546	8.47	23 4624	8.66	24 4774	8.44	15 4916	8.86
24 4567	8.63	23 4628	8.71	24 4759	9.00	14 5088	9.01
23 4482	8.69	23 4618	8.83	24 4761	9.22	14 5082	9.36
23 4476	8.91	23 4621	9.20	24 4758	9.30	14 5078	9.44
24 4563	8.91	24 4668	9.25	24 4765	9.51	14 5080	9.82
24 4542	9.46	24 4678	9.62	24 4755	10.22		
24 4554	9.83	24 4677	9.81				
23 4479	9.92	23 4632	10.18				
		24 4672	10.38				
		24 4681	10.43				
+15°.2		**+15°.3**		**+15°.4**		**+15°.5**	
+15 69	6.84	+14 169	7.04	+15 244	6.77	+14 392	7.75
15 74	6.84	13 175	7.78	15 251	7.40	13 388	8.64
14 53	7.36	15 164	7.89	15 268	7.58	15 335	8.79
14 60	8.07	15 167	8.41	13 266	8.84	13 389	9.06
15 79	8.76	14 172	8.45	15 250	9.03	13 390	9.21
14 61	9.54	14 178	9.28	14 272	9.08	13 385	9.25
15 78	9.68	14 185	9.64	14 261	9.72	14 395	9.76
15 85	9.79	14 187	9.68	14 267	9.74	14 401	9.76
14 69	9.80	14 182	9.86	14 268	9.74	14 390	9.89
14 62	10.26	14 189	10.08	14 263	9.85	14 391	9.99
15 88	10.33					14 406	10.22
						14 394	10.52
+15°.6		**+15°.7**		**+15°.8**		**+15°.9**	
+15 430	6.31	+14 586	6.46	+15 592	7.11	+14 728	7.49
15 414	6.79	16 458	7.09	14 650	7.16	15 670	7.93
14 502	7.11	14 565	7.27	15 594	7.53	15 669	8.10
14 503	7.63	15 507	7.72	15 582	7.60	15 663	8.32
14 518	7.77	15 495	8.29	14 646	7.77	14 735	8.79
14 513	7.95	15 499	8.52	15 580	7.98	14 736	8.90
14 511	8.76	14 566	9.16	15 579	8.53	15 659	8.91
15 436	9.32	15 500	9.17	14 642	8.66	15 664	9.48
14 507	9.62	14 562	9.54	14 656	8.69	15 662	9.72
14 514	9.63	15 502	9.67	15 576	9.23	14 745	9.75
15 427	9.99	15 494	9.81	15 586	9.76	15 667	9.85
		14 572	9.97	14 655	9.87	14 731	10.21
		15 503	10.27	15 577	10.01	14 740	10.31
		15 496	10.29	15 584	10.22		
		15 492	10.33	14 653	10.36		
				14 647	10.44		

TABLE 2 -- Continued

BD	Mag.	BD	Mag.	BD	Mag.	BD	Mag.
+15.10		**+15.11**		**+15.12**		**+15.13**	
+14 857	7.33	+14 1047	6.39	+16 1178	6.31	+15 1416	6.30
14 843	7.91	14 1027	7.57	15 1233	7.11	15 1412	6.62
15 755	8.17	14 1054	7.77	15 1230	7.17	15 1461	6.79
15 779	8.26	14 1037	8.10	15 1223	7.44	14 1539	7.01
14 850	8.39	14 1056	8.62	14 1344	7.45	15 1444	7.31
15 766	9.03	14 1033	8.83	15 1224	7.63	14 1545	7.86
15 769	9.11	14 1036	8.87	14 1338	7.71	15 1427	8.08
15 762	9.13	15 949	8.87	14 1315	8.03	15 1435	8.51
14 854	9.19	15 947	9.46	15 1221	8.08	14 1535	8.56
15 758	9.47	15 934	9.68	15 1244	8.28	15 1410	8.74
15 778	9.62			14 1319	8.29	15 1438	9.03
14 849	10.01			15 1216	8.48	15 1437	9.18
15 760	10.11			15 1235	8.82	15 1417	9.36
14 856	10.20			15 1231	9.30	14 1533	9.53
				15 1214	9.32	15 1439	9.81
				15 1238	9.52	15 1432	10.50
+15.14		**+15.15**		**+15.16**		**+15.17**	
+14 1713	6.36	+14 1850	6.34	+15 1891	7.63	+15 2027	6.58
14 1712	6.46	16 1687	6.92	15 1901	7.69	14 2095	6.86
14 1699	7.61	16 1669	7.24	14 1962	7.81	15 2011	7.85
15 1605	8.03	16 1657	7.31	14 1971	7.83	16 1956	7.88
15 1601	8.55	14 1839	7.54	15 1889	7.99	15 2031	9.03
15 1616	8.62	16 1667	8.30	14 1967	8.46	16 1946	9.49
15 1611	8.69	15 1783	8.45	15 1886	8.57	14 2079	9.51
15 1606	9.13	15 1780	8.67	14 1974	8.90	15 2028	9.71
15 1609	9.13	16 1671	8.93	15 1880	8.93	15 2024	9.74
15 1608	9.43	15 1792	9.31	15 1878	9.04	14 2072	9.96
14 1710	9.51	14 1864	9.33	15 1884	9.33	15 2020	10.23
15 1610	9.73	16 1663	9.35	15 1889	9.33		
14 1707	9.83	15 1790	9.81	15 1907	9.62		
15 1614	9.99	15 1782	9.98	15 1894	9.74		
14 1708	10.20	15 1791	10.22	15 1888	9.78		
14 1709	10.30						
+15.18		**+15.19**		**+15.20**		**+15.21**	
+15 2136	7.48	+14 2251	7.07	+13 2348	7.12	+13 2436	7.36
15 2141	7.51	14 2244	7.18	15 2290	7.40	16 2280	8.61
15 2126	7.70	16 2116	7.22	14 2345	7.41	15 2357	8.90
16 2061	7.76	15 2205	7.42	15 2276	7.72	14 2422	9.14
16 2059	7.84	15 2197	8.42	15 2283	7.88	15 2358	9.27
15 2135	8.78	14 2243	8.89	15 2282	8.28	15 2365	9.37
15 2140	9.03	15 2203	9.43	15 2288	8.98	15 2364	9.52
15 2125	9.16	14 2249	9.52	15 2277	9.01	15 2361	9.59
14 2182	9.17	15 2199	9.71	14 2341	9.14	15 2366	9.80
14 2166	9.30			14 2332	9.22	14 2420	9.83
14 2171	9.48			14 2338	9.46	15 2370	9.94
16 2050	9.56			14 2331	9.67		
15 2147	9.84			15 2281	9.77		
15 2137	9.97			14 2342	9.80		
15 2138	10.06			14 2335	9.96		
14 2172	10.10						

TABLE 2 -- Continued

BD	Mag.	BD	Mag.	BD	Mag.	BD	Mag.
	+15.22		+15.23		+15.24		+15.25
+16 2360	8.01	+16 2420	6.78	+16 2508	6.72	+16 2598	7.94
15 2441	8.05	15 2515	7.78	16 2498	7.17	16 2593	8.00
15 2443	8.31	14 2548	8.47	16 2513	7.34	16 2603	8.59
16 2348	9.23	16 2427	8.53	14 2617	8.08	14 2691	8.75
15 2432	9.44	15 2517	9.58	15 2581	8.18	15 2654	8.92
15 2435	9.49	15 2508	9.73	15 2578	8.25	16 2601	8.95
15 2439	9.52	14 2551	9.80	15 2576	8.33	15 2647	9.22
14 2483	9.88	15 2514	9.91	15 2579	8.85	14 2688	9.74
15 2438	10.45	15 2510	9.96	15 2568	8.92	16 2592	9.86
		16 2421	10.00	16 2506	9.51	15 2655	9.94
				15 2575	9.65		
				14 2607	9.80		
				15 2573	9.85		
				15 2571	10.03		
				15 2569	10.38		
	+15.26		+15.27		+15.28		+15.29
+15 2714	7.31	+16 2725	6.95	+15 2923	7.22	+15 3000	7.18
16 2659	7.68	14 2837	8.60	14 2951	7.33	13 3126	7.42
14 2751	9.19	16 2745	8.67	14 2946	7.37	14 3042	8.04
15 2724	9.21	16 2737	8.69	15 2921	8.57	15 2994	8.54
16 2666	9.47	14 2843	8.79	14 2943	8.88	14 3056	8.58
16 2667	10.02	14 2845	9.04	14 2944	9.20	14 3047	8.93
15 2726	10.20	15 2819	9.12	15 2922	9.36	13 3128	9.08
15 2729	10.21	15 2821	9.47			14 3041	9.24
15 2722	10.26	14 2839	9.49			14 3046	9.35
16 2664	10.38	15 2825	9.84			14 3040	9.60
						14 3044	9.80
	+15.30		+15.31		+15.32		+15.33
+15 3066	6.34	+15 3179	6.44	+14 3427	6.28	+14 3603	6.62
15 3082	6.44	14 3279	6.46	15 3365	6.54	15 3518	6.63
15 3058	6.94	14 3270	7.04	15 3363	7.08	15 3537	6.80
15 3077	7.07	15 3182	7.75	15 3354	7.30	14 3615	7.14
16 3051	7.16	15 3190	8.48	15 3341	7.69	14 3606	7.36
15 3072	7.50	14 3262	8.50	15 3344	7.86	15 3525	7.86
15 3083	7.62	14 3261	8.55	14 3404	8.30	14 3602	7.88
15 3074	7.96	14 3248	8.82	15 3358	8.32	14 3596	7.98
15 3070	8.22	14 3247	9.38	15 3362	8.50	14 3587	8.36
15 3069	8.77	15 3185	9.63	14 3420	8.69	14 3599	8.44
15 3060	8.88	14 3252	10.02	14 3413	8.94	14 3595	9.15
15 3075	8.98			14 3419	10.34	14 3597	9.40
15 3068	9.08					15 3529	9.74
15 3078	9.08					14 3605	9.96
						14 3598	10.53

TABLE 2 -- Continued

BD	Mag.	BD	Mag.	BD	Mag.	BD	Mag.
+15°.34		**+15°.35**		**+15°.36**		**+15°.37**	
+14° 3829	6.56	+14° 4083	7.04	+15° 4227	6.75	+15° 4340	6.36
14 3802	6.71	14 4096	7.18	15 4181	6.83	14 4530	6.59
14 3830	7.22	14 4074	7.85	14 4343	7.66	15 4317	6.92
15 3721	7.44	14 4052	7.88	14 4355	7.77	14 4544	6.96
14 3831	7.60	13 4188	7.96	14 4367	8.12	14 4493	7.84
14 3822	8.12	14 4062	8.04	14 4341	8.47	13 4607	7.90
14 3818	8.31	15 3985	8.24	14 4345	8.50	14 4512	8.07
15 3704	8.44	15 3964	8.70	14 4331	8.56	14 4507	8.21
14 3811	8.92	14 4065	9.28	14 4334	8.76	13 4600	8.58
14 3809	9.37	14 4076	9.30	14 4349	8.76	14 4525	9.07
14 3817	9.54	14 4079	9.48	14 4338	9.15	14 4506	9.15
15 3724	9.97	14 4071	9.70	14 4357	9.86	14 4508	9.46
15 3717	10.49	14 4082	10.11			14 4511	9.63
		14 4064	10.37			14 4500	9.74
		14 4075	10.37			14 4519	9.84
		14 4073	10.46			14 4524	10.14
+15°.38		**+15°.39**		**+15°.40**		**+15°.41**	
+14° 4637	6.51	+14° 4753	8.12	+13° 4983	7.25	+14° 4952	7.44
14 4647	7.32	14 4764	8.38	14 4866	7.53	14 4974	7.52
15 4462	8.18	14 4761	8.43	14 4868	7.86	14 4990	7.84
14 4648	8.26	14 4763	8.64	13 4977	7.92	14 4967	8.10
14 4635	8.30	14 4749	9.17	14 4851	8.15	13 5086	8.17
14 4641	8.48	14 4748	9.28	14 4853	8.15	15 4815	8.58
13 4755	9.04	14 4756	9.38	13 4986	8.23	14 4979	8.63
13 4752	9.20	14 4758	9.55	13 4982	8.30	14 4966	8.78
14 4639	9.22	14 4750	9.71	14 4867	9.04	15 4814	9.51
14 4636	9.56	14 4755	9.83	14 4862	9.42	14 4968	9.65
14 4633	9.65	14 4760	9.99	14 4859	9.51	15 4801	9.70
14 4644	9.66	14 4757	10.01	13 4981	9.65	15 4810	9.81
14 4638	9.80	13 4875	10.03	14 4857	9.78	14 4977	10.04
14 4649	9.92			13 4987	9.88		
14 4642	10.32			14 4856	10.16		
+15°.42		**+5°.1**		**+5°.2**		**+5°.3**	
+14° 5074	6.34	+ 5° 5247	7.01	+ 3° 93	7.73	+ 4° 166	7.62
13 5201	6.89	6 5242	7.19	4 99	7.77	5 144	8.03
15 4925	6.94	5 0002	7.35	3 86	8.04	4 186	8.72
14 5094	7.13	5 5257	8.16	4 80	8.20	4 179	8.98
13 5196	7.93	4 5089	8.19	5 85	8.85	4 169	9.30
14 5084	7.96	5 5252	8.44	5 81	8.92	4 178	9.65
15 4916	8.86	5 5253	8.44	4 94	8.95	4 183	9.65
14 5088	8.92	4 5080	8.77	4 84	9.52	4 181	9.70
14 5087	8.97	3 4925	9.07	4 86	9.52	4 173	10.58
14 5082	9.49	4 5081	9.18	4 90	9.59		
		5 5258	9.33	5 83	9.81		
		5 5251	9.46				
		5 5254	9.67				
		5 5261	9.72				

TABLE 2 -- Continued

BD	Mag.	BD	Mag.	BD	Mag.	BD	Mag.
+5.4		**+5.5**		**+5.6**		**+5.7**	
+ 5 251	7.72	+ 5 338	6.78	+ 5 402	7.94	+ 4 544	7.17
3 257	7.92	5 336	7.91	4 439	8.00	4 548	7.29
4 316	8.26	4 386	8.20	4 453	8.11	5 503	7.64
5 252	8.51	4 392	8.27	3 393	8.72	3 481	7.67
4 320	8.73	4 388	8.67	4 454	9.32	3 478	8.13
4 327	9.18	5 321	9.10	5 394	9.69	5 501	8.63
5 259	9.28	5 316	9.28	5 395	9.75	3 476	9.07
4 324	9.60	4 382	9.55	4 448	10.11	4 551	9.09
4 323	9.64	4 390	9.68	5 396	10.39	3 488	9.11
4 317	9.67	5 325	10.15	3 388	10.39	4 540	9.16
5 256	9.82	4 393	10.33	5 398	10.43	3 475	9.52
4 322	10.18					4 541	9.64
5 244	10.18					4 542	9.82
						5 504	10.52
+5.8		**+5.9**		**+5.10**		**+5.11**	
+ 3 552	7.12	+ 4 723	7.56	+ 4 811	6.60	+ 4 1012	7.43
2 628	7.26	4 736	8.06	5 827	7.08	5 996	7.53
5 567	7.90	4 740	8.20	5 805	8.12	5 986	7.74
4 614	7.99	4 738	8.34	4 829	8.45	4 1003	7.92
4 602	8.24	5 688	8.65	5 820	8.48	5 998	8.05
4 619	8.63	5 690	9.21	5 821	8.75	4 1028	8.26
5 568	8.84	3 707	9.46	4 835	8.87	5 1010	8.52
4 603	9.02	6 733	10.02	5 799	8.87	5 997	8.90
3 540	9.12	5 704	10.08	5 798	9.00	4 1018	9.16
5 570	9.23			5 816	9.05	4 1005	9.18
3 542	9.68			5 825	9.32	5 999	9.42
4 607	9.77			4 841	9.33	5 1000	9.57
4 611	9.91			5 807	9.42	5 1005	9.88
4 610	10.05			4 833	9.46	5 992	10.06
4 613	10.13			5 822	9.50	4 1017	10.35
4 615	10.24			5 824	9.62	4 1019	10.47
+5.12		**+5.13**		**+5.14**		**+5.15**	
+ 4 1181	6.60	+ 5 1434	6.62	+ 5 1658	7.02	+ 5 1845	7.06
4 1174	7.14	5 1448	6.77	4 1695	7.15	5 1848	7.20
5 1156	7.22	4 1429	6.81	5 1652	7.81	4 1859	7.67
4 1198	7.45	6 1405	6.92	4 1647	8.18	4 1861	8.13
5 1149	8.56	4 1446	7.27	5 1657	8.37	4 1862	8.32
5 1146	8.63	5 1414	7.74	4 1693	8.53	5 1844	8.33
5 1128	8.89	5 1406	7.82	5 1644	8.62	4 1864	8.44
5 1167	8.97	5 1402	8.01	4 1684	8.77	4 1856	8.97
4 1183	9.00	5 1433	8.53	4 1699	8.80	5 1838	9.18
5 1183	9.22	5 1440	8.65	4 1689	8.90	4 1885	9.22
5 1144	9.25	5 1432	9.22	4 1686	9.01	4 1866	9.26
5 1137	9.47	5 1412	9.44	5 1642	9.02	4 1871	9.37
5 1138	9.51	5 1431	9.77	4 1680	9.26	4 1867	9.73
5 1143	9.91	5 1429	10.12	5 1645	9.68	4 1870	9.85
		5 1430	10.37	4 1679	9.90		
		4 1468	10.44				

TABLE 2 -- Continued

BD	Mag.	BD	Mag.	BD	Mag.	BD	Mag.
+5.16		**+5.17**		**+5.18**		**+5.19**	
+ 5 1950	7.40	+ 6 2109	8.14	+ 4 2236	7.20	+ 5 2296	7.28
5 1958	7.80	5 2131	8.36	4 2227	7.89	4 2283	7.30
4 1981	7.88	5 2115	8.53	5 2220	8.00	5 2290	7.43
5 1974	7.97	5 2120	8.79	5 2222	8.35	4 2291	8.04
4 1974	8.31	5 2111	9.18	5 2225	8.61	4 2292	8.86
5 1964	8.32	5 2121	9.33	5 2227	8.62	5 2298	9.18
5 1972	8.70	5 2129	9.67	6 2198	9.02	4 2293	9.41
5 1962	9.16	5 2124	9.71	5 2211	9.29	5 2291	9.43
5 1973	9.35	5 2122	9.78	5 2228	9.26	5 2294	9.51
5 1965	9.71	5 2126	9.85	5 2219	9.56	5 2295	9.55
5 1969	9.73	5 2133	10.35	6 2204	9.88	5 2287	9.69
5 1966	9.97			5 2223	10.02	4 2297	9.82
5 1961	10.15			5 2221	10.06		
+5.20		**+5.21**		**+5.22**		**+5.23**	
+ 4 2378	7.15	+ 4 2463	6.34	+ 5 2545	6.55	+ 5 2631	6.48
4 2388	7.61	7 2440	6.94	4 2553	6.81	5 2633	6.97
4 2385	7.70	7 2443	7.09	5 2555	7.85	4 2614	7.21
5 2385	7.74	5 2484	7.26	4 2541	8.29	5 2638	7.72
4 2379	7.82	6 2448	7.47	4 2549	8.46	5 2624	7.83
5 2394	7.90	4 2454	8.03	5 2556	8.96	6 2613	7.91
5 2386	8.16	4 2452	8.12	5 2547	8.99	5 2634	7.94
5 2388	8.49	5 2476	8.83	5 2546	9.14	5 2635	8.00
4 2377	8.72	5 2481	9.12	5 2554	9.48	5 2630	8.22
5 2408	9.01	5 2483	9.62	6 2522	9.82	5 2626	8.71
4 2382	9.24	5 2491	9.70	5 2553	9.98	5 2625	8.82
5 2395	9.42	6 2429	9.91			6 2617	8.96
5 2406	9.56	5 2478	10.02			5 2632	8.98
5 2392	9.59	5 2490	10.20			6 2619	9.77
		5 2488	10.23				
		5 2486	10.37				
+5.24		**+5.25**		**+5.26**		**+5.27**	
+ 5 2702	7.03	+ 5 2769	7.92	+ 4 2833	8.18	+ 6 2946	6.85
4 2690	7.97	6 2772	8.25	5 2852	8.35	4 2924	7.38
4 2693	8.02	6 2759	8.50	6 2846	8.51	4 2914	7.41
4 2692	8.23	5 2774	8.68	5 2847	8.67	4 2909	7.88
5 2709	8.48	6 2763	9.05	5 2854	8.91	4 2925	8.20
5 2710	8.86	4 2768	9.10	5 2840	9.29	5 2919	8.24
4 2687	9.33	5 2770	9.50	5 2846	9.36	3 2939	8.26
5 2707	9.53	5 2775	9.52	5 2850	9.72	5 2916	8.36
4 2685	9.63	5 2767	9.72	4 2832	9.92	5 2928	8.37
		6 2767	9.72	5 2834	10.05	5 2921	8.64
		5 2771	9.80	5 2849	10.29	4 2915	8.70
		5 2764	9.82			5 2915	8.81
						5 2925	8.95
						5 2920	9.05
						5 2928	9.31
						4 2917	10.25

TABLE 2 -- Continued

BD	Mag.	BD	Mag.	BD	Mag.	BD	Mag.
+5.28		**+5.29**		**+5.30**		**+5.31**	
+ 5 2981	7.65	+ 5 3090	7.85	+ 6 3236	6.86	+ 6 3322	6.46
5 2983	8.33	5 3088	8.37	5 3221	7.44	6 3318	7.14
5 2989	8.52	5 3100	8.47	4 3191	7.66	5 3282	7.32
5 2992	8.74	4 3065	8.85	5 3203	7.72	5 3284	7.89
5 2994	8.80	5 3097	9.15	6 3225	8.49	6 3329	8.03
6 3018	8.89	5 3095	9.47	5 3193	8.51	6 3315	8.80
5 2991	9.23	4 3068	9.54	5 3213	8.58	5 3293	8.85
4 2990	9.38	5 3084	9.72	5 3212	8.76	5 3285	9.00
5 2984	9.44	5 3087	9.82	5 3214	8.78	5 3294	9.23
5 2986	9.73	5 3103	9.99	5 3195	9.06		
4 2992	10.12	5 3085	10.31	4 3183	9.73		
5 2987	10.16			5 3196	9.73		
5 2988	10.28			4 3182	9.76		
5 2990	10.40			5 3197	9.86		
				5 3200	10.00		
+5.32		**+5.33**		**+5.34**		**+5.35**	
+ 4 3448	7.67	+ 5 3574	8.21	+ 4 3838	6.98	+ 5 4087	6.76
5 3428	8.02	5 3599	8.29	5 3926	7.53	4 4057	6.92
5 3419	8.71	4 3573	8.62	5 3934	7.82	4 4019	7.46
5 3407	8.81	4 3572	8.86	4 3860	8.23	5 4068	7.54
5 3414	8.95	4 3574	8.96	4 3844	8.54	5 4060	7.74
5 3399	8.98	4 3584	9.02	5 3929	8.68	4 4008	7.88
4 3445	9.02	4 3581	9.21	5 3930	8.74	4 4052	8.12
4 3437	9.10	4 3595	9.32	5 3927	8.78	4 4016	8.65
5 3405	9.23	5 3589	9.36	5 3942	8.96	4 4048	8.88
5 3409	9.32	5 3596	9.46	4 3843	9.19	4 4039	9.46
4 3436	9.76	5 3579	9.56	4 3865	9.43	4 4029	9.52
5 3416	9.80	5 3600	10.01	5 3924	9.45	5 4096	9.90
5 3424	9.94	4 3600	10.08	4 3850	9.60	5 4094	9.92
5 3410	10.14			5 3925	10.14		
5 3418	10.20			5 3923	10.18		
+5.36		**+5.37**		**+5.38**		**+5.39**	
+ 4 4264	6.34	+ 6 4522	6.87	+ 3 4466	6.86	+ 4 4706	6.53
3 4172	6.36	5 4503	7.22	4 4585	8.12	4 4675	6.73
3 4138	6.88	5 4484	8.44	4 4586	8.32	3 4568	7.06
4 4243	7.68	4 4419	8.62	4 4584	8.41	4 4695	7.11
5 4310	7.84	5 4494	8.93	5 4665	8.51	3 4575	7.13
4 4254	8.36	5 4483	9.06	5 4648	9.12	4 4697	7.21
4 4259	8.44	5 4505	9.41	4 4571	9.22	4 4694	8.18
4 4262	8.99	5 4500	9.62	5 4649	9.24	4 4701	8.71
4 4258	9.02	4 4435	9.68	5 4655	9.45	4 4690	8.79
5 4302	9.12	5 4507	9.84	5 4654	9.88	3 4570	9.05
4 4238	9.18	4 4443	9.87	4 4580	9.96	4 4700	9.09
4 4249	9.42	4 4433	9.92			4 4693	9.19
4 4271	9.66	4 4418	10.31			4 4692	9.57
4 4239	9.98					3 4581	9.71
4 4246	10.07					4 4698	9.80
4 4255	10.12					4 4689	10.13

TABLE 2 -- Continued

BD	Mag.	BD	Mag.	BD	Mag.	BD	Mag.
+5.40		**+5.41**		**+5.42**		**+5.43**	
+ 3 4689	6.89	+ 4 4896	6.58	+ 4 4985	7.05	+ 3 4896	7.53
5 4968	7.74	3 4751	6.66	4 4991	7.92	3 4895	7.81
4 4831	7.90	3 4745	6.72	5 5157	8.30	4 5055	8.01
5 4975	7.96	4 4894	7.33	4 4987	8.50	4 5046	8.02
5 4971	8.14	5 5063	8.51	4 4998	8.68	4 5054	8.46
5 4966	8.39	5 5053	8.76	4 4995	8.96	4 5049	8.58
4 4817	8.61	3 4752	8.84	4 4996	8.98	4 5059	9.02
4 4821	8.87	4 4895	8.86	4 4989	9.30	4 5056	9.39
4 4816	8.92	3 4756	9.02	4 4999	9.43	3 4894	9.42
4 4822	8.92	5 5046	9.04			4 5057	9.42
4 4823	9.22	4 4882	9.35			4 5048	9.62
4 4814	9.42	5 5052	9.59			4 5050	9.83
4 4820	9.50	4 4887	9.66			4 5061	9.85
4 4810	9.54	4 4885	9.70			4 5051	9.99
4 4813	9.54	4 4889	9.70			4 5053	10.08
		4 4886	9.94				
-5.1		**-5.2**		**-5.3**		**-5.4**	
- 4 5623	6.36	- 5 5843	6.76	- 4 5868	6.66	- 5 6048	7.63
6 5908	7.64	6 6075	8.42	5 5973	6.72	6 6297	7.82
6 5914	8.39	5 5855	8.75	5 5961	8.20	5 6081	7.84
5 5720	8.76	5 5848	8.93	5 5963	8.84	5 6083	8.04
4 5620	8.93	5 5847	9.00	5 5972	8.85	5 6056	8.12
4 5616	9.04	6 6068	9.09	5 5965	9.02	6 6293	8.48
5 5721	9.04	6 6064	9.12	5 5978	9.26	5 6075	8.96
5 5711	9.27	6 6056	9.41	5 5959	9.31	5 6055	9.21
5 5713	9.38	6 6063	9.45	4 5865	9.42	6 6309	9.32
4 5618	9.46	6 6058	9.55	5 5977	9.71	5 6070	9.43
4 5615	9.65	6 6071	9.55	5 5962	9.82	5 6064	9.61
5 5707	9.74	5 5849	10.06	4 5864	10.01	5 6066	9.87
5 5714	9.98	6 6067	10.08	5 5975	10.26	5 6065	10.08
5 5710	10.04	5 5858	10.10			5 6060	10.17
5 5709	10.04	5 5856	10.39				
4 5619	10.30						
-5.5		**-5.6**		**-5.7**		**-5.8**	
- 6 6335	6.54	- 6 96	6.73	- 5 210	7.10	- 5 309	6.38
4 6019	7.66	6 103	8.58	5 202	7.22	4 285	7.04
4 6013	8.15	4 69	8.70	5 215	7.48	4 269	8.12
5 6117	8.28	5 105	8.84	6 220	7.71	5 323	8.27
6 6346	8.61	5 95	9.23	5 195	7.82	5 327	8.95
5 6100	8.63	5 94	9.58	5 223	7.89	5 324	9.18
5 6097	8.76	6 110	9.60	5 221	8.18	6 351	9.38
5 6103	8.98	5 87	9.80	5 199	8.35	6 348	9.70
5 6088	9.02			5 198	8.53	5 325	9.78
6 6337	9.17			6 226	8.80	5 314	10.20
5 6105	9.71			5 207	8.94	6 340	10.23
4 6018	9.89			6 217	9.96	5 322	10.41

TABLE 2 -- Continued

BD	Mag.	BD	Mag.	BD	Mag.	BD	Mag.
-5.9°		**-5.10°**		**-5.11°**		**-5.12°**	
-5° 430	8.21	-4° 476	6.80	-5° 644	7.03	-5° 810	7.22
4° 373	8.49	5° 528	6.92	4° 586	7.18	6° 809	8.01
4° 378	8.69	5° 536	7.08	4° 609	7.38	6° 805	8.14
5° 429	8.82	5° 541	7.15	5° 642	7.89	5° 816	8.32
5° 425	8.90	4° 491	7.62	5° 668	8.06	4° 709	8.79
4° 382	9.32	5° 524	7.84	4° 593	8.59	5° 803	9.00
5° 422	9.46	6° 566	8.43	5° 660	8.75	5° 795	9.44
5° 447	9.73	5° 532	8.78	5° 671	8.79	5° 806	9.61
5° 443	10.18	5° 527	8.79	5° 664	8.83	5° 814	9.76
5° 442	10.39	5° 542	9.17	5° 646	9.08	5° 813	10.17
		5° 529	9.96	4° 601	9.32		
		6° 569	9.98	5° 669	9.86		
		5° 530	10.06	4° 606	9.88		
				5° 652	9.93		
-5.13°		**-5.14°**		**-5.15°**		**-5.16°**	
-5° 953	6.58	-4° 1042	8.13	-4° 1231	7.21	-4° 1405	6.80
6° 969	6.94	4° 1053	8.67	5° 1379	7.89	5° 1576	6.82
5° 963	7.90	4° 1049	8.91	4° 1227	7.92	6° 1475	7.43
5° 981	7.96	4° 1043	9.26	4° 1210	8.00	5° 1565	7.47
5° 957	7.97	5° 1168	9.43	4° 1233	8.39	6° 1482	8.12
4° 879	8.08	4° 1035	9.62	4° 1223	8.47	5° 1567	8.17
5° 984	8.46	4° 1050	10.02	5° 1370	8.96	6° 1477	8.53
4° 889	8.49	5° 1164	10.14	5° 1393	9.03	5° 1553	8.96
5° 978	8.55	4° 1046	10.18	5° 1373	9.23	5° 1560	9.13
4° 898	8.89	5° 1146	10.25	5° 1361	9.35	5° 1550	9.43
4° 895	8.96	4° 1048	10.41	4° 1224	9.41	5° 1550	9.64
5° 994	9.26			4° 1221	9.49	5° 1568	9.73
5° 986	9.77			4° 1232	9.59		
4° 902	9.92			4° 1226	9.70		
-5.17°		**-5.18°**		**-5.19°**		**-5.20°**	
-5° 1844	6.35	-5° 2080	6.50	-6° 2407	6.63	-4° 2379	6.63
5° 1839	7.04	5° 2118	7.26	3° 2151	6.93	5° 2566	6.86
5° 1815	7.29	5° 2086	7.28	6° 2367	7.97	4° 2377	7.14
4° 1665	7.31	4° 1930	7.82	4° 2158	8.06	4° 2380	7.17
4° 1667	7.46	4° 1939	8.00	6° 2378	8.12	5° 2544	7.36
5° 1820	7.83	5° 2095	8.11	4° 2143	8.52	5° 2545	8.40
4° 1669	8.06	4° 1926	8.12	5° 2297	8.61	5° 2573	8.44
4° 1676	8.12	5° 2092	8.62	5° 2301	8.91	5° 2572	8.72
5° 1797	8.13	5° 2109	9.16	5° 2296	9.11	5° 2563	8.92
4° 1683	8.17	5° 2093	9.39	4° 2149	9.18	5° 2547	8.92
5° 1800	8.48	4° 1938	9.52	4° 2145	9.51	5° 2565	9.42
5° 1796	8.78	4° 1929	9.68	5° 2307	9.57	4° 2370	9.50
4° 1687	8.89	5° 2101	9.85	5° 2300	9.76	4° 2363	9.52
5° 1809	9.32	5° 2090	10.00			5° 2577	9.71
		4° 1937	10.37			4° 2368	9.81
						5° 2556	9.99

TABLE 2 -- Continued

BD	Mag.	BD	Mag.	BD	Mag.	BD	Mag.
-5.21°		**-5.22°**		**-5.23°**		**-5.24°**	
- 3 2535	6.42	- 4 2667	7.16	- 4 2819	7.39	- 4 2952	7.42
4 2530	6.61	4 2666	7.37	4 2809	7.79	5 3133	7.87
3 2545	7.24	4 2681	7.86	4 2827	7.85	4 2946	7.89
3 2532	7.37	4 2660	8.65	4 2830	8.45	4 2941	8.19
4 2519	8.39	4 2671	8.78	4 2816	8.72	5 3125	9.16
5 2689	8.50	4 2662	8.92	4 2821	8.98	3 2991	9.20
5 2680	8.51	4 2670	9.22	4 2812	9.02	3 2984	9.36
4 2522	8.52	4 2683	9.71	4 2810	9.93	4 2942	9.43
5 2698	8.72	4 2673	9.74	5 3013	9.94	4 2936	9.46
5 2684	8.78	5 2846	9.75	5 3015	10.12	5 3128	9.50
4 2531	9.49	4 2668	10.06			4 2937	9.52
4 2538	9.54					4 2939	9.52
5 2692	10.00					3 2992	9.75
-5.25°		**-5.26°**		**-5.27°**		**-5.28°**	
- 5 3275	6.98	- 3 3213	7.00	- 4 3296	6.35	- 2 3622	7.11
4 3049	7.22	4 3162	7.06	3 3298	6.38	5 3605	7.31
4 3057	7.92	4 3155	8.22	3 3309	7.09	4 3408	7.69
5 3250	8.21	3 3200	9.07	5 3513	7.37	5 3634	8.09
4 3058	8.54	5 3382	9.35	4 3281	7.61	4 3418	8.12
4 3060	8.92	4 3158	9.50	4 3276	8.13	5 3625	8.17
4 3044	9.00	3 3198	9.69	3 3302	8.21	4 3419	8.24
4 3056	9.19	4 3164	9.78	5 3516	8.54	3 3396	8.70
4 3045	9.32	4 3169	9.89	4 3294	9.44	3 3395	9.18
5 3254	9.42	4 3171	10.12	3 3308	9.47	4 3405	9.36
3 3089	9.49			4 3288	9.51	4 3404	9.61
4 3052	9.64			3 3305	10.30	4 3395	9.88
4 3054	9.74			4 3293	10.33		
-5.29°		**-5.30°**		**-5.31°**		**-5.32°**	
- 5 3713	7.73	- 5 3837	6.52	- 4 3749	7.59	- 4 3855	7.13
5 3730	7.91	5 3824	7.37	5 3953	7.72	6 4181	7.38
5 3735	8.29	5 3825	7.38	5 3952	8.00	6 4193	7.46
4 3514	8.38	4 3645	7.71	3 3673	8.24	6 4183	7.52
4 3521	8.43	4 3643	7.86	4 3744	8.65	5 4060	8.08
3 3501	8.59	4 3633	8.37	4 3753	9.01	4 3881	8.76
3 3497	8.63	4 3628	8.73	3 3675	9.13	5 4063	9.18
4 3506	8.87	5 3835	8.82	4 3745	9.20	4 3857	9.22
3 3490	9.05	4 3644	9.21	5 3942	9.44	4 3858	9.26
4 3508	9.07	4 3640	9.32	3 3667	9.57	5 4061	9.72
4 3519	9.69	4 3638	9.44	4 3756	9.94		
4 3510	9.85	4 3647	9.48	5 3951	10.07		
4 3504	9.94	4 3641	10.12	4 3742	10.12		
4 3509	10.31	4 3642	10.29	4 3751	10.19		

TABLE 2 -- Continued

BD	Mag.	BD	Mag.	BD	Mag.	BD	Mag.
-5.33		**-5.34**		**-5.35**		**-5.36**	
- 4 4007	7.96	- 5 4292	8.36	- 3 4040	7.56	- 6 4618	6.63
3 3836	8.49	5 4304	8.61	4 4225	7.78	5 4465	8.01
4 3995	8.77	5 4307	8.74	4 4206	8.28	5 4475	8.06
4 3997	8.79	5 4293	9.23	4 4212	8.42	4 4308	8.09
4 4009	9.44	5 4294	9.60	4 4221	9.01	4 4301	8.99
5 4187	9.47	4 4118	9.63	5 4395	9.52	4 4321	9.32
4 3998	9.50	4 4107	9.77	5 4398	9.52	4 4315	9.44
5 4185	9.96	4 4106	9.94	4 4226	9.79	5 4467	9.63
4 3992	10.18	5 4298	10.14	4 4210	9.82	4 4307	9.94
4 3996	10.37	5 4306	10.15	4 4216	9.92	4 4314	10.10
				4 4224	10.16	4 4312	10.13
				4 4218	10.35		
				4 4220	10.44		
-5.37		**-5.38**		**-5.39**		**-5.40**	
- 5 4586	6.88	- 6 4869	6.88	- 6 5077	6.69	- 5 5096	7.26
5 4589	7.37	6 4897	6.98	4 4781	7.01	4 4960	8.43
4 4403	7.94	5 4736	7.66	5 4915	8.24	5 5091	8.43
4 4405	8.08	5 4744	8.00	4 4750	8.27	5 5099	8.53
5 4602	8.09	5 4738	8.25	4 4751	8.43	5 5120	8.55
4 4414	8.14	5 4745	8.26	4 4719	8.53	5 5114	9.08
5 4590	9.15	5 4721	9.33	5 4917	9.23	5 5093	9.34
5 4577	9.18	5 4741	9.50	4 4725	9.49	4 4968	9.53
4 4407	9.20	5 4747	9.57	5 4912	9.65	5 5100	9.61
5 4591	9.97	5 4751	9.68	4 4745	9.92	5 5097	10.00
5 4593	9.98	5 4742	9.92			4 4949	10.24
5 4578	10.08	5 4732	10.02			5 5101	10.37
5 4587	10.17	5 4743	10.11			5 5089	10.39
5 4576	10.30	5 4749	10.15			5 5090	10.39
-5.41		**-5.42**		**-5.43**		**-15.1**	
- 5 5253	6.52	- 4 5355	6.91	- 5 5584	6.58	-15 7	7.00
5 5299	6.54	6 5683	7.44	4 5504	6.85	15 6539	7.29
6 5487	6.92	5 5447	7.54	5 5592	7.05	16 6415	8.63
4 5154	7.53	5 5452	8.13	5 5613	7.99	16 6419	8.67
4 5147	7.63	6 5674	8.55	6 5790	8.11	15 6532	9.00
5 5291	7.70	6 5670	8.58	5 5593	8.13	15 6541	9.26
5 5275	7.72	5 5440	8.67	5 5597	8.32	16 6411	9.27
6 5479	7.99	5 5458	9.03	5 5587	8.52	15 6542	9.43
5 5262	8.14	5 5456	9.05	5 5586	8.82	15 6537	9.67
5 5278	8.75	5 5446	9.17	5 5589	9.72	15 6536	9.85
5 5272	9.43	5 5457	9.24	5 5600	9.77	15 6534	9.92
5 5276	9.58	5 5463	9.27	6 5799	9.85		
5 5271	9.64	6 5657	9.31	5 5591	10.07		
5 5269	9.78	5 5464	10.04	5 5594	10.11		
5 5279	9.93	6 5662	10.27	6 5795	10.21		
5 5283	10.35			6 5796	10.33		

TABLE 2 -- Continued

BD	Mag.	BD	Mag.	BD	Mag.	BD	Mag.
-15.2°		**-15.3°**		**-15.4°**		**-15.5°**	
-15 109	6.40	-14 235	6.96	-14 335	6.51	-14 434	7.34
14 110	8.40	14 225	7.19	15 307	6.62	14 435	7.34
15 105	8.62	15 211	8.19	15 321	7.18	15 416	7.66
16 109	8.98	15 210	8.41	14 339	7.20	15 414	8.26
15 116	9.06	15 217	8.45	14 337	8.24	14 463	8.93
16 102	9.18	15 233	8.69	15 336	8.24	15 412	9.02
14 113	9.32	14 228	8.94	15 328	8.52	15 430	9.05
15 118	9.39	15 217	8.98	15 334	8.56	14 453	9.29
14 96	9.65	15 222	8.98	15 331	9.04	14 455	9.45
16 106	9.72	15 232	9.20	14 346	9.09	14 444	9.66
15 107	9.87	15 229	9.93	15 326	9.14	15 423	9.76
15 111	10.36	15 221	10.24	15 324	9.22	15 431	9.83
		15 219	10.29	15 332	9.44		
				14 336	9.92		
-15.6°		**-15.7°**		**-15.8°**		**-15.9°**	
-14 557	6.95	-15 617	7.07	-16 807	6.99	-16 963	6.66
14 576	7.02	15 627	7.09	16 791	7.42	14 943	7.37
15 519	7.78	14 677	7.25	14 832	7.73	15 867	8.23
16 538	7.86	15 620	7.93	15 717	8.13	15 865	8.59
16 543	8.07	14 699	8.69	15 720	8.43	14 951	8.82
15 532	8.27	14 697	8.95	15 730	8.44	14 958	9.08
15 525	8.74	14 688	9.36	14 834	9.22	15 858	9.19
16 534	8.75	15 622	9.54	15 738	9.46	15 861	9.53
15 522	9.51	15 609	9.60	14 833	9.53	15 847	9.64
16 539	9.67	15 621	9.62	15 732	9.70	15 866	10.13
15 526	9.73	14 689	9.79	15 736	9.85		
15 521	9.85			15 722	10.06		
				15 734	10.23		
-15.10°		**-15.11°**		**-15.12°**		**-15.13°**	
-13 1135	6.57	-14 1243	6.73	-14 1450	6.32	-15 1599	6.99
14 1105	7.22	15 1193	6.92	14 1476	6.64	14 1710	7.74
15 1018	7.45	15 1212	7.08	15 1390	7.36	15 1608	7.75
14 1103	7.72	14 1272	7.26	14 1430	7.54	15 1629	8.43
14 1080	7.81	14 1267	7.83	15 1388	7.73	14 1688	8.57
14 1094	8.01	15 1199	8.00	14 1480	8.12	15 1620	9.11
15 1014	8.24	14 1266	8.08	14 1467	8.28	14 1684	9.14
14 1083	8.84	15 1200	8.41	14 1479	8.68	14 1687	9.18
15 1017	9.42	14 1262	9.01	14 1453	8.79	14 1685	9.79
15 1009	9.56	15 1175	9.08	15 1381	8.85	14 1703	9.98
15 1005	9.88	15 1201	9.23	14 1466	9.24	14 1686	10.04
14 1082	10.03	15 1203	9.30	14 1461	9.59	14 1697	10.15
14 1091	10.07	15 1208	9.44	14 1457	9.66		
15 1012	10.21	15 1207	9.63	14 1452	9.66		
15 1013	10.23	15 1195	10.23	14 1459	9.67		
				14 1468	9.93		

TABLE 2 -- Continued

BD	Mag.	BD	Mag.	BD	Mag.	BD	Mag.
-15.14		**-15.15**		**-15.16**		**-15.17**	
-13 2104	7.34	-15 2278	7.32	-15 2597	7.26	-14 2835	6.52
13 2109	7.45	14 2404	7.68	14 2611	7.44	15 2778	7.79
15 1941	8.14	14 2393	7.95	14 2608	7.79	14 2802	7.96
14 2065	8.33	13 2426	8.05	13 2644	7.83	14 2840	8.15
14 1970	8.79	14 2398	8.52	15 2569	8.06	14 2819	8.66
14 1973	9.04	14 2406	9.10	14 2637	8.09	14 2824	8.78
14 1977	9.32	14 2401	9.14	14 2629	8.16	14 2813	9.09
14 1980	9.35	14 2422	9.34	14 2631	8.31	14 2826	9.25
14 1982	9.42	14 2425	9.40	14 2610	8.32	14 2814	9.27
14 1984	9.56	14 2395	9.65	13 2670	8.50	14 2820	9.74
14 1979	9.56	14 2400	9.73	14 2614	8.52		
		14 2413	9.85	14 2630	8.79		
		15 2316	9.96	14 2633	9.43		
		14 2410	9.96	15 2565	9.44		
		14 2399	10.03	14 2623	9.67		
				14 2625	9.69		
-15.18		**-15.19**		**-15.20**		**-15.21**	
-15 2929	6.66	-14 3134	7.07	-14 3263	7.70	-14 3388	6.84
15 2949	7.62	15 3062	8.02	14 3245	7.77	14 3406	7.76
15 2925	8.60	14 3151	8.09	15 3206	7.94	15 3349	7.96
13 2988	8.82	14 3138	8.20	14 3262	8.11	14 3370	8.00
14 2980	9.08	13 3129	8.24	14 3255	8.31	14 3391	8.11
15 2936	9.22	13 3143	8.53	13 3300	8.32	14 3382	8.99
14 2987	9.25	13 3135	9.00	14 3266	8.37	14 3402	9.03
14 2975	9.55	14 3123	9.35	15 3194	8.79	14 3383	9.38
13 2980	9.56	15 3077	9.52	14 3260	9.26	14 3381	9.55
14 2978	9.62	15 3067	9.81	15 3190	9.53	14 3386	9.83
14 2979	9.83	14 3133	9.86	14 3261	9.72	14 3396	10.09
14 2983	10.08	14 3136	10.20				
-15.22		**-15.23**		**-15.24**		**-15.25**	
-14 3500	6.51	-15 3543	6.94	-14 3717	7.65	-14 3867	7.21
15 3450	7.28	14 3587	7.17	14 3709	7.79	14 3846	8.13
13 3514	7.62	14 3612	7.74	14 3713	8.21	14 3861	8.82
14 3493	7.91	14 3596	7.75	14 3733	8.83	13 3811	8.96
14 3488	7.98	14 3581	7.94	14 3727	8.96	15 3792	9.01
15 3452	7.99	14 3592	8.77	14 3721	9.46	14 3860	9.02
14 3489	8.57	14 3585	8.95	15 3665	9.76	14 3849	9.22
13 3512	8.62	14 3593	9.34	14 3719	9.83	14 3845	9.88
14 3494	8.64	13 3607	9.37	14 3726	10.28	14 3854	10.14
14 3484	8.74	14 3590	9.66			14 3857	10.23
14 3486	8.84	14 3594	9.79				
14 3479	9.57	14 3579	10.09				
13 3515	10.02	14 3583	10.24				
14 3483	10.25	14 3597	10.31				
14 3482	10.29						

TABLE 2 -- Continued

BD	Mag.	BD	Mag.	BD	Mag.	BD	Mag.
-15.26		**-15.27**		**-15.28**		**-15.29**	
-15 3924	7.18	-15 4050	7.75	-14 4266	6.34	-14 4389	7.54
15 3922	7.72	14 4147	8.10	15 4165	7.02	14 4401	8.35
14 4006	8.58	14 4160	8.13	14 4270	8.21	15 4300	8.54
14 3996	8.94	13 4102	8.44	14 4277	8.29	13 4417	9.17
14 4003	9.38	14 4145	8.78	15 4182	8.47	14 4411	9.31
14 4002	9.75	14 4155	9.03	15 4173	8.82	14 4417	9.49
14 3988	9.75	14 4140	9.12	15 4176	8.96	14 4410	9.75
13 3943	10.32	14 4161	9.52	15 4192	9.23	15 4301	9.79
14 3997	10.38	14 4139	9.71	15 4175	9.85	15 4293	9.87
14 3993	10.42	15 4052	9.99	15 4179	10.14		
		14 4144	10.12	14 4271	10.23		
		14 4148	10.24	14 4273	10.26		
-15.30		**-15.31**		**-15.32**		**-15.33**	
-14 4509	6.71	-15 4655	6.92	-15 4808	7.64	-15 5067	6.94
14 4507	7.27	14 4693	7.43	14 4880	7.75	15 5091	7.68
15 4420	8.33	15 4613	8.33	14 4884	7.77	15 5063	8.24
14 4510	8.69	14 4715	8.44	15 4803	7.91	15 5086	8.50
15 4409	8.85	15 4619	8.92	15 4834	8.48	15 5062	8.61
14 4512	9.06	15 4635	9.00	14 4887	8.79	15 5076	8.65
15 4425	9.35	15 4620	9.23	15 4806	8.81	15 5059	8.81
14 4508	9.47	15 4610	9.28	15 4822	8.99	14 5153	8.83
15 4422	9.61	15 4616	9.32	14 4872	9.11	15 5069	8.88
14 4506	9.93	15 4614	9.47	14 4885	9.20	14 5165	8.92
14 4518	10.35	15 4627	9.54	15 4821	9.30	15 5068	9.32
15 4423	10.43	15 4628	9.71	15 4812	9.48	15 5071	9.43
		14 4714	10.07	15 4820	9.56	15 5064	10.01
		14 4692	10.30	14 4879	9.61		
				15 4810	9.80		
				14 4898	9.83		
-15.34		**-15.35**		**-15.36**		**-15.37**	
-16 5272	6.98	-14 5578	6.54	-16 5609	6.54	-16 5769	7.84
14 5380	7.37	15 5484	6.77	15 5663	7.22	15 5884	7.99
16 5293	7.40	16 5454	8.13	15 5670	7.75	15 5881	8.01
14 5392	7.42	15 5481	8.26	16 5604	8.11	15 5864	8.32
15 5341	7.67	15 5504	8.71	15 5679	8.82	15 5872	8.50
15 5335	8.87	15 5479	8.90	15 5672	8.96	16 5780	8.78
15 5325	8.99	15 5492	8.96	15 5683	9.04	14 5915	8.96
15 5333	9.07	15 5483	9.38	15 5675	9.39	14 5925	9.16
15 5332	9.18	16 5455	9.63	16 5610	9.56	15 5874	9.27
15 5334	9.32	15 5497	10.02	15 5678	9.71	14 5917	9.47
15 5318	9.48	15 5501	10.11	16 5618	9.96	15 5878	9.86
15 5321	9.55			16 5620	10.03	15 5889	9.96
15 5338	9.61					15 5883	10.05
15 5337	9.85					16 5782	10.19
15 5336	10.25					15 5893	10.20
15 5330	10.34					14 5916	10.39

TABLE 2 -- Continued

BD	Mag.	BD	Mag.	BD	Mag.	BD	Mag.
			-15.38°				
-15 6037	7.04	-15 6169	7.04	-14 6355	7.89	-16 6293	6.80
15 6027	7.26	14 6233	7.51	14 6359	8.49	16 6291	6.88
14 6094	7.27	15 6174	7.77	15 6294	8.52	16 6259	7.32
14 6095	8.26	14 6242	8.13	15 6295	8.89	15 6400	8.08
14 6078	8.97	14 6228	8.18	15 6282	8.93	16 6265	8.67
15 6033	9.16	15 6168	9.43	15 6285	9.60	16 6286	9.16
14 6082	9.25	15 6164	9.50	15 6286	9.69	15 6408	9.21
14 6081	9.43	15 6173	10.11	14 6366	9.82	16 6282	9.25
14 6077	9.62	14 6236	10.18	15 6292	9.89	15 6395	9.64
15 6034	9.62	15 6171	10.18	15 6289	10.10	15 6413	9.64
15 6030	10.16	15 6167	10.18	14 6360	10.19	16 6272	9.70
		15 6162	10.23	15 6283	10.24	16 6257	9.82
				15 6290	10.32	15 6404	9.85

-15.42°

-16 6394	6.41
14 6588	7.08
15 6532	9.00
15 6528	9.04
15 6521	9.49
15 6527	10.03
15 6524	10.04
15 6529	10.09
16 6388	10.22
16 6389	10.24

STAR COUNTS IN THE ANDROMEDA NEBULA

CARL K. SEYFERT AND J. J. NASSAU
Warner and Swasey Observatory of the Case School of Applied Science
Received January 2, 1945

ABSTRACT

Counts of stars from magnitude 15.0 to magnitude 18.5 in and around the Andromeda nebula have been made on blue-sensitive plates taken with the 24–36-inch Schmidt telescope of the Case School of Applied Science. In order to calibrate the counts, magnitudes of a sequence of stars near M31 from 14.9 mag. to 18.3 mag. were determined by comparisons with Selected Area 20 and the North Polar Sequence. The counts, corrected for the foreground stars, show a total of 2564 stars belonging to M31 between the limits of absolute magnitude −3.8 and −6.3. Possible errors in the counts arising from the limited resolving power of the plates used, the variable nebulous background of M31, and the distance correction on the Schmidt plates were investigated and found to be negligibly small.

The apparent shape of M31 as outlined by the counts is roughly elliptical and agrees reasonably well with isophotal contours of the spiral.

The observed luminosity distribution of stars in M31 is compared with previously published data for M33, NGC 6822, the Magellanic Clouds, and the Milky Way. The shape of the luminosity curve of the main body of M31 (diameter 6000 parsecs) is very similar to the corresponding curve for the solar neighborhood within the observed range of absolute magnitudes. The border region of M31 (6,000–11,000 parsecs in diameter) reveals a statistical absence of stars brighter than −5.3 in absolute magnitude.

The thickness of M31 as shown by the high-luminosity stars is estimated to be of the order of 200 parsecs, a value comparable with the thickness of the Milky Way as estimated by Oort.

The present results indicate an absence of highly luminous stars in the outermost envelope of M31. This fact suggests that the outer shell of the Andromeda nebula may be composed of material similar to that found by Baade in the nucleus of M31 (i.e., lacking in highly luminous O- and B-type stars).

In recent years it has become increasingly evident that the Andromeda nebula is a stellar system similar to our own galaxy in size, probably similar in form and structure, and possibly so in stellar composition. The present investigation of star counts was initiated to study the distribution of the observable stars in M31 not only in order to increase our knowledge about the composition of that system but to give us additional clues by analogy about the structure of the Milky Way. In addition it was felt that a study of this nature would enlarge our scanty knowledge of the bright end of the luminosity function in a system similar to our own.

Counts of stars over a large area in and around M31 were made in 1906 by Götz[1] but are found to have limited significance, since, according to the author, the limiting magnitude is 16.0. Star counts have also been made in selected regions of NGC 6822 and M33 by Hubble,[2,3] in the Small and Large Magellanic Clouds by Shapley [4,5] and McCuskey,[6] and in IC 1613 by Baade.[7]

THE MAGNITUDE SEQUENCE

In order to calibrate the star counts, magnitudes of 12 stars near BD+41°119 were determined by means of photographic comparisons with Selected Area 20 and with the North Polar Sequence. The new sequence is 1° north of M31 and approximately 3.5° south of SA 20. The stars of the sequence are shown in Figure 1. Two plates on which

[1] *Pub. Obs. Königstuhl—Heidelburg*, **3**, 1, 1906.

[2] *Ap. J.*, **62**, 409, 1925; *Mt. W. Contr.*, No. 304.

[3] *Ap. J.*, **63**, 236, 1926; *Mt. W. Contr.*, No. 310.

[4] *Harvard Circ.*, No. 260, 1924.

[5] *Harvard Bull.*, No. 881, 1931; *Galaxies*, pp. 79–80, Blakiston Co., 1943.

[6] *Harvard Circ.*, No. 401, 1935.

[7] Unpublished data.

both SA 20 and the M31 star sequence appear were used, and the magnitudes of the M31 sequence estimated by means of a graduated scale of star images. In addition, the magnitudes of a second sequence of stars approximately midway between SA 20 and the M31 sequence were determined and used as intermediate standards to aid in determining the

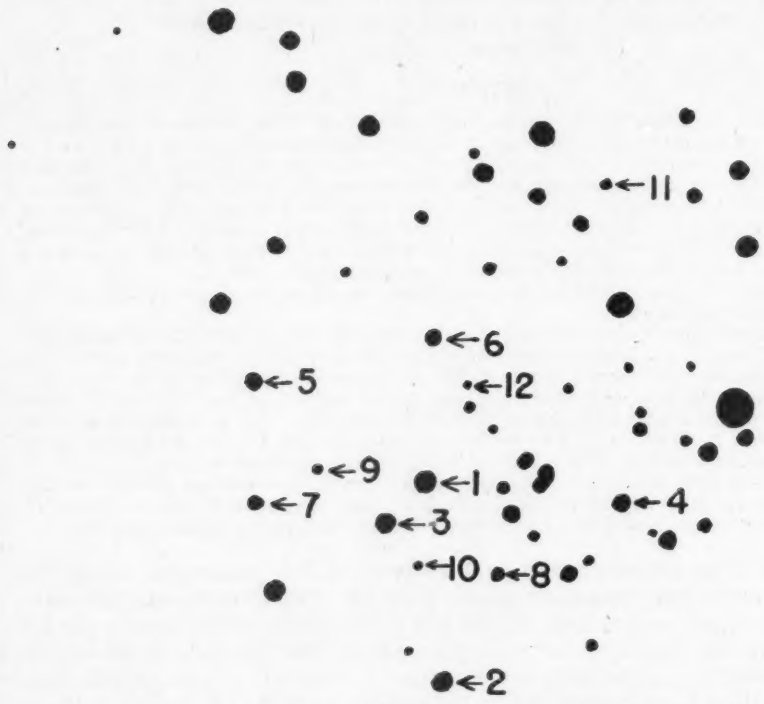

FIG. 1.—A map of the stars in the M31 sequence. The brightest star shown is BD+41°119, 8.8 vis. mag. North is up and west is to the right. The magnitudes of the sequence stars are given in Table 1. Scale of map: 1 mm equals 6″.

TABLE 1

PHOTOGRAPHIC MAGNITUDES OF THE M31 SEQUENCE
(Near BD +41°119)

Star No.	m_{pg}	Star No.	m_{pg}	Star No.	m_{pg}
1	14.93	5	16.24	9	17.47
2	15.30	6	16.70	10	17.85
3	15.54	7	17.06	11	17.92
4	15.54	8	17.16	12	18.30

magnitudes of the M31 star sequence from other plates. The final photographic magnitudes listed in Table 1 are means of determinations from four different plates. The accidental probable error of a final mean magnitude is ± 0.04.

Since all the measures contributing to the magnitudes were obtained by "transferring" star sequences from one part of a plate to another part of the same plate, we feel that the

PLATE VII

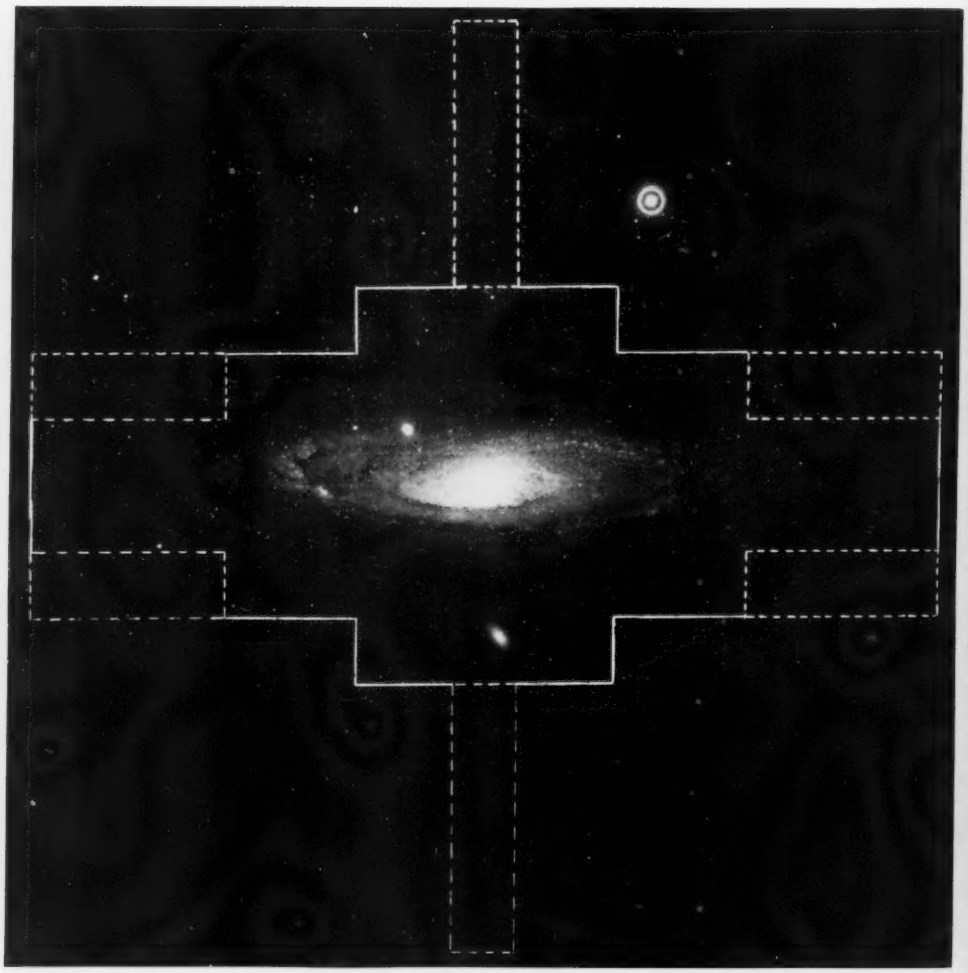

REPRODUCTION OF A SCHMIDT CAMERA PLATE OF M31 SHOWING THE AREA COUNTED

The squares bounded by dotted lines are "normal" regions or areas considered to be free of M31 stars.

M31 sequence has the same zero point and scale as SA 20. For a further test of the validity of our magnitudes, direct comparisons with the North Polar Sequence were made with four plates, two on the pole and two on the M31 sequence. Measures from these plates indicate that our results based on comparisons with SA 20 need no modification.

THE STAR COUNTS

The star counts were made on two plates; a reproduction of one of these plates with the area counted is shown in Plate VII. A reseau marked off in 5-mm squares was placed behind the plate to facilitate the counts. No attempt was made to count the two 5-mm squares which included the companion nebulae M32 and NGC 205. The central 1 sq. cm. around the nucleus of M31 was also omitted from the counts. A graduated scale of star images was kept in the field of view of the binocular microscope used for counting, and all stars as bright as, or brighter than, each of the scale images were counted. At the beginning and end of each of the counts the stars of the M31 magnitude sequence were compared with the graduated scale images in order to determine the magnitude limit corresponding to each of the counts. The counts on the first plate reached a limit of 18.00 mag., whereas the limit of the second plate counted was 18.40 mag. The exposure times of the two plates (Eastman 103 a-0) were 10 and 20 minutes, respectively.

With the combined data from the two plates, the counts were grouped into 72 squares, each 1 cm on a side; and for each of these squares a plot was made of m against $\log N_m$, the logarithm of the number of stars per square centimeter as bright as, or brighter than, m. (One square centimeter on the Schmidt plates is very nearly equal to one-fourteenth of a square degree.) A comparison of the results from the two plates showed a probable error of a single observation in $\log N_m$ varying from ± 0.04 at 15.5 mag. to ± 0.02 for 17.5 mag. or fainter.

Values of $\log N_m$ at $m = 15.0, 15.5, 16.0, \ldots, 18.5$ were read from each of the 72 curves. From these data for each square, values of A_m were calculated, where A_m is defined as the number of stars per square centimeter on the plate between $m - 0.25$ and $m + 0.25$.

In order to correct the counts for the effect of foreground stars, 20 of the counted squares judged to be essentially free of M31 stars were selected as shown in Plate VII. The average A_m values from these 20 "normal" regions were subtracted from the corresponding A_m values in each of the 72 squares. Since the total area counted covers an appreciable area of the sky, the counts corrected for the average normal background required a further correction depending on the galactic latitude of the individual square. This small second-order correction was computed with the aid of Seares's[8] tables of stellar distribution and applied to the counts.

The counts from the Schmidt plates were found to require no correction for distance from the center of the plate. However, since the general nebulous background of the spiral is appreciable and variable, it was thought possible that this fact might introduce systematic errors into the magnitudes used. In order to test this effect, special plates were taken on which an exposure of the region of the north celestial pole was superposed on an exposure of M31. Care was taken to insure that the Polar Sequence stars were placed in regions free of M31 nebulosity. The magnitudes of stars near the pole which fell by chance in the nebulosity of M31 were obtained by comparisons with the North Polar Sequence, which was free of the nebulosity. The magnitudes of these stars were again determined from single-exposure pole plates, and the two sets of measures were compared. The results from three double-exposure plates showed that the systematic effect of the nebulosity on the magnitudes was less than 0.1 mag. and could be neglected. It is worth while to note, however, that the nebulosity produces accidental errors of measurement somewhat larger than normally expected.

[8] *Ap. J.*, **67**, 1, 1928; *Mt. W. Contr.*, No. 346.

A plate taken with the 100-inch Mount Wilson telescope was examined in order to test the possible error introduced by the limited resolving power of the Schmidt plates. We are grateful to Dr. Walter Baade for lending us this photograph. The plate contains one of the most crowded portions of M31 and includes the star cloud NGC 206. Counts and direct comparisons, star for star, were made between the 100-inch plate and the Schmidt plates over a region which corresponds to three half-centimeter squares of the Schmidt plates. The results showed no significant discordances in the counts from our plates with the exception of the counts in NGC 206, where a 7 per cent deficiency in stars counted on the Schmidt plates was observed.

RESULTS

For each square centimeter of the counted area the excess (or deficiency) of stars fainter than 16.0 mag. over the normal foreground number was tabulated as shown in Plate VIII. An excess per square centimeter on the plate equal to or greater than 15 (approximately the square root of the counted number of stars) was considered significant. With this criterion, the outline of the nebula as detected from the star counts was drawn to include all squares with excesses of 15 or more (Pl. VIII). The distribution of stars in each apparent-magnitude interval is given in Table 2 for the whole nebula. The table shows that the stars belonging to the nebula begin to appear at approximately 16.0 mag.

TABLE 2

THE DISTRIBUTION OF STARS IN M31 ACCORDING TO APPARENT MAGNITUDE

	Apparent Magnitude							
	15.0 to 15.5	15.5 to 16.0	16.0 to 16.5	16.5 to 17.0	17.0 to 17.5	17.5 to 18.0	18.0 to 18.5	16.0 to 18.5
No. of stars.....	−2	−22	+13	+76	+353	+772	+1350	+2564

The star counts indicate a major axis of 11 cm, or 180′ of arc, and a minor axis of 5 cm, or 82′ of arc. Since visual inspection of photographs of M31 indicate axes of 160′ and 40′, it appears that the major axis of M31 as obtained from the star counts is increased only slightly, though the minor axis is approximately doubled.

It is of interest to note that star clouds are located close to each end of the major axis as defined by the star counts. The positions of these clusters are indicated by arrows in Plate IX. The cluster near the north-following end of the major axis is a large star cloud nearly 500 parsecs in diameter, located approximately 70′ from the nucleus. The group at the opposite end of the major axis is more compact, not more than 100 parsecs in diameter, and is located 97′, or about 6000 parsecs, from the nucleus.

The shape of the nebula as derived from star counts is not unlike that found from the isophotal contours of the nebula. Dr. R. C. Williams kindly furnished us with contours of M31 made from one of our Schmidt camera plates, and we wish to thank Dr. Williams for his generous co-operation in this matter. The new isophotes shown in Plate IX are in good agreement with the earlier results of Williams and Hiltner[9,10] obtained from a plate taken with the 18-inch Schmidt camera at Mount Palomar. In addition to the isophotes of M31, Plate IX shows the extent of the nebula as outlined by the star counts. Since the agreement between the two boundaries is reasonably satisfactory, we can conclude that the shape of M31 as defined by the luminous material is essentially the same

[9] *Pub. Univ. Michigan*, **8**, 45, 1940.

[10] *Ibid.*, p. 103.

PLATE VIII

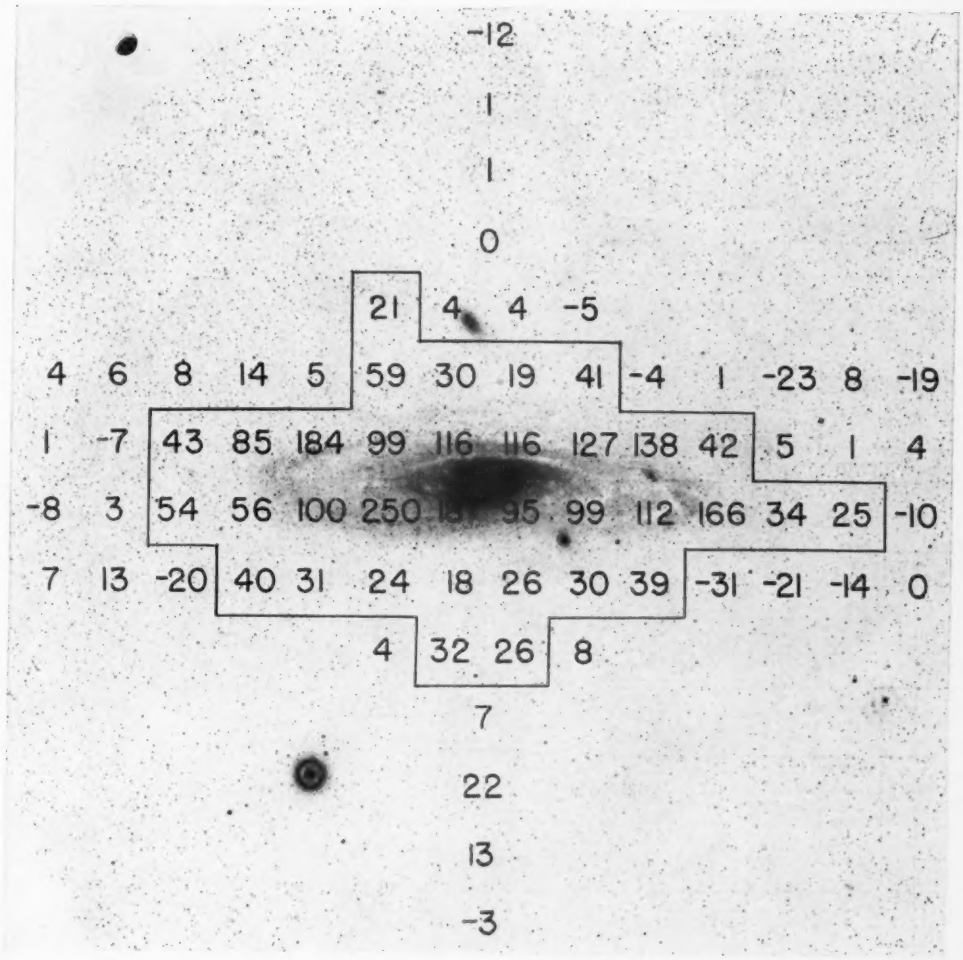

DISTRIBUTION OF M31 STARS

The numbers are excesses (or deficiencies) of stars fainter than 16.0 mag. over the normal foreground number. The outline of M31 as indicated by the star counts is shown.

PLATE IX

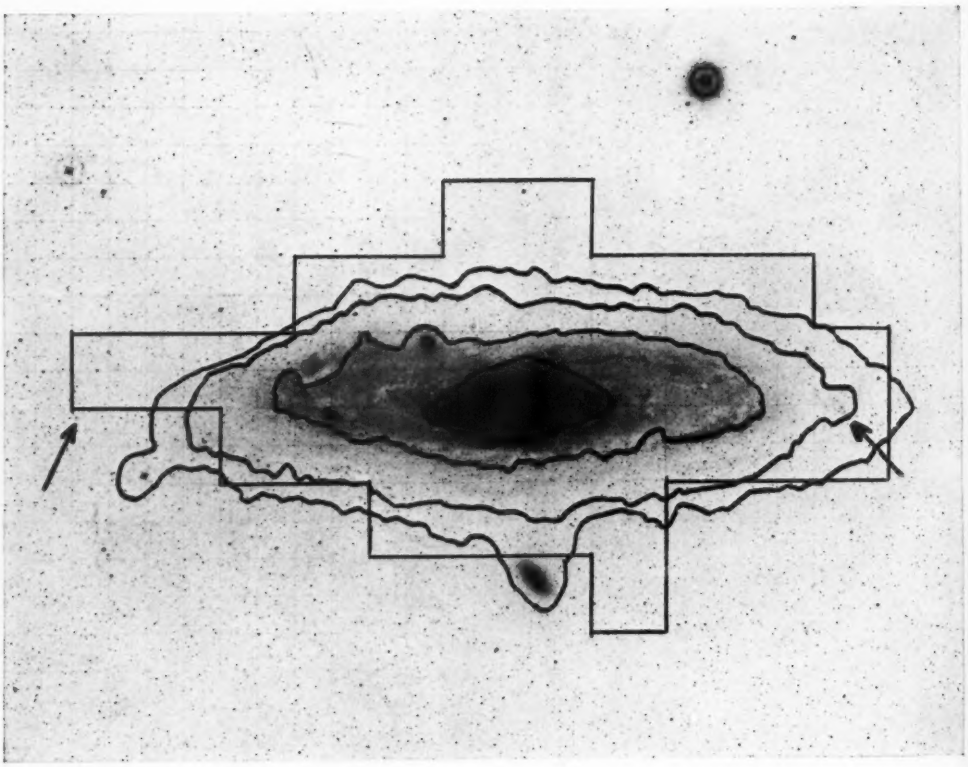

ISOPHOTAL CONTOURS OF M31

The straight lines show the extent of M31 as indicated by the star counts. The arrows mark the positions of two star clouds close to the extremities of the major axis.

as that outlined by star counts. It should be pointed out here that the extensive outermost envelope, observable by means of the photoelectric cell or with microphotometer tracings, contains too few high-luminosity stars to be detected by our counts.

THE MODULUS OF M31

The *true* photographic modulus of M31—21.6 mag.—was found by adopting Hubble's[11] value of the distance—210,000 parsecs. The *apparent* modulus was obtained by applying a reasonable amount of galactic absorption to the true modulus. The absolute magnitudes of stars in M31 were then derived by applying the apparent modulus to the apparent magnitudes. The galactic absorption, as indicated by counts of faint nebulae in the vicinity of M31, is uncertain, owing to the possible confusion of outlying knots of M31 nebulosity with field nebulae. Hence, probably the best estimate of the galactic absorption is obtained from the average absorption for the galactic latitude of M31 which is, according to Hubble,[12] 0.7 mag. The adopted apparent modulus of M31 is, therefore, 21.6 mag. +0.7 mag., or 22.3 mag. This agrees with Baade's[13] recently published value of the apparent modulus of M31—22.4 mag.—which he obtained from a complete rediscussion of Hubble's data.

STELLAR LUMINOSITY DISTRIBUTION IN M31

If we now use the data of Table 2 and apply our value of the apparent modulus (22.3 mag.) to the apparent magnitudes, we obtain the total number of stars in M31 within

TABLE 3

THE DISTRIBUTION OF STARS IN M31

Absolute Magnitude	No. of Stars in Main Body	No. of Stars in Boundary	Total No. of M31 Stars	Absolute Magnitude	No. of Stars in Main Body	No. of Stars in Boundary	Total No. of M31 Stars
−7.3 to −6.8.....	+ 1	− 3	− 2	−5.3 to −4.8.....	+ 234	+119	+ 353
−6.8 to −6.3.....	− 4	−18	−22	−4.8 to −4.3.....	+ 494	+278	+ 772
−6.3 to −5.8.....	+15	− 2	+13	−4.3 to −3.8.....	+ 799	+551	+1350
−5.8 to −5.3.....	+81	− 5	+76				
				−6.3 to −3.8.....	+1623	+941	+2564

specified limits of *absolute magnitude* (the luminosity distribution). The data thus derived are given in the last column of Table 3. It should be pointed out that the data obtained in this way are unaffected by the presence of any absorption within M31 itself, since any such absorption would affect the apparent magnitudes of the Cepheids used to establish the distance modulus in the same manner. The only exception to the above statement would arise in the unlikely event that the supergiant stars under consideration and the Cepheids have widely different distributions in the spiral.

From Table 3 we observe that, for the nebula as a whole, the counts reveal no stars brighter than −6.3 mag. Table 3 also gives the distribution according to absolute magnitude separately for the central 12 sq. cm. (3200 sq. min.) of the "main body" (2d col.) and for the 22 sq. cm. (5860 sq. min.) in the "boundary region" of M31 (3d col.). The "main body" of M31 comprises the region easily visible on our photographs. For our

[11] Edwin Hubble, *The Realm of the Nebulae*, p. 134, Yale University Press, 1936.

[12] *Ap. J.*, **79**, 8, 1934; *Mt. W. Contr.*, No. 485.

[13] *Ap. J.*, **100**, 137, 1944; *Mt. W. Contr.*, No. 696.

purpose we define it as the rectangle 33′ × 98′ centered on the nucleus and oriented with the long dimension parallel to the major axis. The "boundary region" includes all the nebula as outlined by the counts outside the "main body." It is perhaps significant that, although the star counts show 96 stars brighter than −5.3 mag. in the main body of M31, no stars brighter than −5.3 absolute mag. are found in the boundary region of the nebula.

KNOWN LUMINOSITY DISTRIBUTIONS IN STELLAR SYSTEMS

Luminosity distributions, or the material from which luminosity distributions may be derived, have been published for NGC 6822 and M33 by Hubble[2,3] and for the Small and Large Magellanic Clouds by Shapley.[4,5] The data collected from these various sources are presented in Table 4 and in Figure 2, together with the present data for M31.

TABLE 4

THE LOGARITHM OF THE NUMBER OF STARS BETWEEN SPECIFIED LIMITS OF ABSOLUTE MAGNITUDES IN STELLAR SYSTEMS

Abs. Mag.	S.M.C.	L.M.C.	N6822	M33	M31 (Total)	M31 (Main Body)	M31 (Boundary)	Milky Way (v.R.)
−6.5 to −6.0	.....	2.1:	.....	1.70	0.7:	0.7:	.....	1.4 –10
−6.0 to −5.5	.....	2.2:	.....	2.16	1.65	1.65	.....	2.0
−5.5 to −5.0	1.7:	2.4:	1.14	2.37	2.28	2.20	1.5:	2.50
−5.0 to −4.5	2.2:	2.97	1.34	2.95	2.75	2.57	2.30	2.93
−4.5 to −4.0	2.74	3.16	1.48	3.33	3.03	2.82	2.62	3.18
−4.0 to −3.5	3.05	3.38	1.84	3.50	3.25:	3.0:	2.9:	3.45
−3.5 to −3.0	3.18	3.51	2.42	3.96	.....	.....	.....	3.76
−3.0 to −2.5	3.06	3.83	2.84	.....	.....	.....	.....	4.08
−2.5 to −2.0	3.42	4.04	.....	.....	.....	.....	.....	4.30
−2.0 to −1.5	3.69	4.21	.....	.....	.....	.....	.....	4.56
−1.5 to −1.0	4.15	4.36	.....	.....	.....	.....	.....	4.66
−1.0 to −0.5	4.56	4.65	.....	.....	.....	.....	.....	4.85
−0.5 to 0.0	4.93	5.01	.....	.....	.....	.....	.....	5.15–10
Apparent modulus	17.3	17.1	21.6	22.3	22.3	22.3	22.3	.....

The luminosity function for the Milky Way in the solar neighborhood has been obtained by van Rhijn,[14] Schilt,[15] and others. The final column of Table 4 gives, for comparison purposes, the values published by van Rhijn, i.e., the logarithm of the number of stars per cubic parsec between M − 0.25 and M + 0.25 in the solar neighborhood. The other values given in the table represent, for each half-magnitude interval, the logarithms of the *total* numbers of stars in each system. The apparent moduli for the Magellanic Clouds were taken from Shapley's studies,[5] and the moduli for NGC 6822 and M33 were obtained from Baade's[16] recent paper.

Table 4 shows that the number of highly luminous stars in each half-magnitude interval for the whole of the Large Magellanic Cloud agrees very well with the corresponding number of stars in the whole of M33. M31, on the other hand, appears to have only two-thirds the total number of highly luminous stars found in the Large Cloud or in M33. The Small Cloud and NGC 6822 are poorly populated with these very bright stars. In particular, the star counts show that neither the Small Cloud nor NGC 6822 has any

[14] Gronigen Pub., No. 47, 1936.

[15] *Ann. New York Acad. Sci.*, **42**, 259, 1941.

[16] *Ap. J.*, **100**, 147, 1944; *Mt. W. Contr.*, No. 697.

detectable stars brighter than −5.5. Attention has already been called to the fact that the star counts show no stars brighter than −5.3 in the boundary region of M31.

As to the form of the luminosity distribution-curves, all except that for NGC 6822 agree reasonably well with the shape of the luminosity function as defined by van Rhijn. The luminosity distribution-curve for the rich main-body region of M31 parallels van Rhijn's curve with conspicuous closeness.

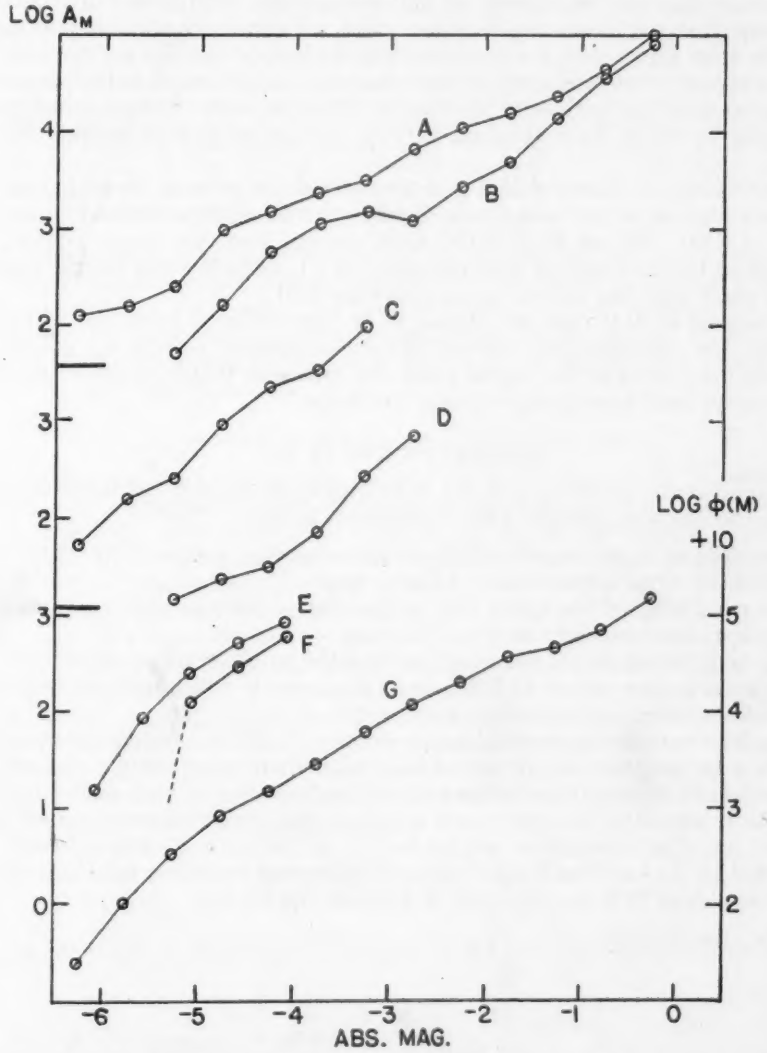

FIG. 2.—Luminosity distributions for the Large Magellanic Cloud (*A*), Small Magellanic Cloud (*B*), M33 (*C*), NGC 6822 (*D*), main body of M31 (*E*), and boundary region of M31 (*F*). Curve *G* is the luminosity function for the Milky Way according to van Rhijn. The ordinates for curve *G* (log of number of stars per cubic parsec between M−0.25 and M+0.25) are given at the right-hand side of the figure. The ordinates for curves *A*–*F* (at the left) are the logarithms of the total numbers of stars (within each system) between absolute magnitude M−0.25 and M+025.

THE PROBABLE THICKNESS OF M31

The *luminosity function* of M31, i.e., number of stars per cubic parsec within given intervals of absolute magnitude, cannot be obtained without a knowledge of the volume of space with which we are dealing. The volume is not known because we do not know the *thickness* of the nebula. If, however, we assume a value for the luminosity function of M31, we may calculate the volume and hence the thickness of the spiral.

If we assume that the "main body" of M31 is a cylinder, 6000 parsecs in diameter, and if we assume that the luminosity function which we obtain for these highly luminous Andromeda stars agrees with the corresponding luminosity function for the solar neighborhood as given by van Rhijn, we obtain a thickness of M31 equal to 160 parsecs. If we had chosen to make the luminosity function of M31 agree with other published luminosity functions, we would have obtained varying thicknesses of M31 ranging up to 300 parsecs.

If, therefore, the thickness of M31 is of the order of 200 parsecs, the main body of the nebula, seen edge-on, would have a ratio of major to minor axis, as defined by the brightest stars, of 6000 : 200, or 30 :1. NGC 4565, a spiral seen very nearly edge-on, has a ratio of major to minor axis of approximately 20 : 1, excluding the central bulge, or a value not much less than the one given above for M31.

The thickness of M31 does not appear to be very different from that of the Milky Way. Oort[17] has calculated that one-half of the photographic light in our galaxy is situated within 166 parsecs of the central plane. He concludes that "the denser parts of the galactic system must have an exceedingly flat shape."

PRESENT PICTURE OF M31

If we combine the present results for M31 with those recently published by Baade,[13] we obtain the following picture of the Andromeda nebula:

a) A nucleus of approximately 1000 parsecs diameter, composed of relatively low-luminosity stars fainter than −1.1 abs. mag.

b) The main body of the spiral with a diameter of 6000 parsecs, containing highly luminous stars as bright as −6.3 abs. mag.

c) The boundary region of the spiral, as detected by the star counts, extending from the main body to about 11,000 parsecs diameter, in which no stars brighter than −5.3 abs. mag. are found from the counts.

d) The faint outer envelope extending to perhaps 25,000 parsecs diameter, detectable only with the photoelectric cell or from microphotometer tracings of photographs. The fact that this shell contains no stars brighter than −3.8 in sufficient numbers to be detected by the star counts suggests that the envelope may very possibly have a stellar composition similar to that of the nucleus. This inference is supported by the fact that Baade[13] observed numerous extremely faint stars along the minor axis of M31 to a distance of 32′ from the center.

[17] *B.A.N.*, **238**, 249, 1932.

ON THE EXCITATION OF THE CORONAL LINES

KUN HUANG

Department of Physics, National University of Peking, Kunming, China

Received December 1, 1944

ABSTRACT

The transition probabilities of the coronal lines identified by Edlén are calculated with the help of the observed multiplet separations and the theory of intermediate couplings. On the basis of these transition probabilities and the observed intensities the concentrations of the ions responsible for their emission are estimated. These quantities make possible a discussion of the excitation mechanism, which leads to the conclusion that the ions are most probably excited by collisions with electrons that have energies corresponding to temperatures higher than 20,000° K. On this view a lower limit for the required magnitude of the cross-section of the collisional process is obtained.

In the present paper some quantities related to the coronal lines are calculated on the basis of Edlén's identifications,[1] and with these results the probable mode of their excitation is considered in some detail. Since the available intensity measurements are beset with uncertainties, our consideration may not be reliable in a quantitative sense. Yet the method promises to reveal the nature of the excitation mechanism completely when more accurate data are available.

CALCULATION OF THE TRANSITION PROBABILITIES

The coronal lines are forbidden by Laporte's rule, for they arise from transitions among states belonging to the same electronic configurations. Since the high effective charges acting on the valence electrons of the ions concerned cause considerable departures from the *LS* coupling, magnetic dipole radiations are allowed in all cases. As, ordinarily, electric quadrupole radiations are very much smaller than magnetic-dipole radiations, we need consider only the latter in calculating the transition probabilities.

In consequence of the works done by Shortley and others it is now a fairly simple matter to calculate the transition probabilities. It is known from the theory of intermediate couplings that for the various p^n-configurations a single coupling parameter, χ, may be introduced which completely describes the departure from *LS* coupling. Shortley and Robinson[2] have tabulated the relative multiplet separations against the coupling parameter for these configurations. With the help of their tables the coupling parameters for the various ions may be found by making use of the wave lengths of the coronal lines.

The transition probability is given explicitly by

$$A \overset{i}{\underset{j}{\downarrow}} = \frac{35{,}320}{2\omega_i + 1}\, \sigma^3 S(ij),$$

where S, the strength of the transition, is given in the case of magnetic-dipole radiation by

$$S(i,\ j) = \frac{1}{\hbar^2} \sum_{M_i,\ M_j} |\ (i, M_i | \vec{L} + 2\vec{S} |\ j, M_j)\ |^2 .$$

The terms M_i and M_j are the magnetic quantum numbers of the states i and j, respectively. Since the evaluation of S does not involve the use of the radial wave functions, S may be calculated generally when the coupling parameter is known. Such calculations

[1] *Ark. f. Mat. Astron. Fys.*, Vol. **28**, No. 1, 1941.

[2] *Phys. Rev.*, **52**, 713, 1937.

are made by Shortley and others[3] for the whole range of values of χ, and their results are tabulated. Their results enable us to obtain the transition probabilities directly with our knowledge of the coupling parameters. For the configurations p^1 and p^5 it is easy to verify that S has the definite value $\frac{4}{9}$.

A word may not be amiss as to the accuracy of the theory as applied to our problem. Robinson and Shortley have compared the theoretical and the experimental results for a large number of cases, including also some very highly ionized atoms.[2] The agreement is generally good, but it is particularly satisfactory for $3p^2$ and $3p^4$ with χ near 0.5. Most fortunately, the cases we meet all gather around this region, as we shall presently see. Thus:

1. *Fe* XIII $3p^2$:

$$\frac{(^3P_2 - {}^3P_1)}{(^3P_1 - {}^3P_0)} = \frac{9259}{9303} = 0.995 \qquad (\chi = 0.496).$$

2. *Ni* XV $3p^2$:

$$\frac{(^3P_2 - {}^3P_1)}{(^3P_1 - {}^3P_0)} = \frac{12{,}459}{14{,}917} = 0.835 \qquad (\chi = 0.653).$$

3. *Fe* XI $3p^4$: In this case $^3P_0$ is not known. However, since for $\chi \backsim 0.5$, $^3P_0 - {}^3P_1$ is small compared with $^1D_2 - {}^3P_1$, we may take as our initial approximation

$$(^1D_2 - {}^3P_0)_0 = (^1D_2 - {}^3P_1) = 25{,}075\,,$$

from which we find

$$\left(\frac{^3P_1 - {}^3P_2}{^1D_2 - {}^3P_c}\right)_0 = \frac{12{,}667}{32{,}112} = 0.395 \qquad [(\chi)_1 = 0.455].$$

For this value of χ the above approximation is seen to be justified. To make sure that the value is sufficiently accurate, we proceed to the next approximation. Corresponding to $(\chi)_1$, we have

$$\left(\frac{^3P_0 - {}^3P_1}{^3P_1 - {}^3P_2}\right)_1 = 0.1415\,; \qquad (^3P_0 - {}^3P_1)_1 = 1.79 \times 10^3.$$

Making use of this improved value, we find

$$\left(\frac{^3P_1 - {}^3P_2}{^1D_2 - {}^3P_c}\right)_1 = \frac{12{,}667}{31{,}913} = 0.397 \qquad [(\chi)_2 = 0.455].$$

This second approximation is but little different from the first one.

4. *Ni* XIII $3p^4$: This case is completely analogous to (3), and we proceed in the same manner:

$$(^1D_2 - {}^3P_0)_0 = (^1D_2 - {}^3P_1) = 27{,}443\,,$$

$$\left(\frac{^3P_1 - {}^3P_2}{^1D_2 - {}^3P_c}\right)_0 = \frac{19{,}541}{38{,}299} = 0.510 \qquad [(\chi)_1 = 0.606],$$

$$(^3P_0 - {}^3P_1)_1 = (^3P_1 - {}^3P_2)\left(\frac{^3P_0 - {}^3P_1}{^3P_1 - {}^3P_2}\right)_1 = 19{,}541 \times 0.0393 = 769\,,$$

$$\left(\frac{^3P_1 - {}^3P_2}{^1D_2 - {}^3P_c}\right)_1 = 0.512 \qquad [(\chi)_2 = 0.608].$$

[3] Shortley, Aller, Baker, and Menzel, *Ap. J.*, **93**, 718, 1941.

The magnetic-dipole radiation strengths corresponding to these values of χ and the transition probabilities calculated therefrom are given in Table 1. The data are not sufficient for the determination of χ in the case of *Ca* XIII $2p^4$; for this case we have assumed tentatively a value of 0.5 for χ.

TABLE 1

λ (A)	Intensity*		Identification	S	A (Sec^{-1})
3328.1.....	1.0	.....	*Ca* XII $2p^5$ $^2P_{1/2}-^2P_{3/2}$	1.3333	484
3388.10.....	16	.....	*Fe* XIII $3p^2$ $^1D_2-^3P_2$	0.6595	90.7
3600.97.....	2.1	.....	*Ni* XVI 3p $^2P_{3/2}-^2P_{1/2}$	1.3333	191
3642.87.....	.....	.....	*Ni* XIII $3p^4$ $^1D_2-^3P_1$	0.1648	18.3
3986.88.....	0.7	.....	*Fe* XI $3p^4$ $^1D_2-^3P_1$	0.1116	9.45
4086.29.....	1.0	.....	*Ca* XIII $2p^4$ $^3P_1-^3P_2$	2.2520	295
4231.4.....	2.6	.....	*Ni* XII $3p^5$ $^2P_{1/2}-^2P_{3/2}$	1.3333	237
5116.03.....	4.3	2.6	*Ni* XIII $3p^4$ $^3P_1-^3P_2$	2.3351	156
5302.86.....	100	120	*Fe* XIV 3p $^2P_{3/2}-^2P_{1/2}$	1.3333	60
6374.51.....	8.1	28	*Fe* X $3p^5$ $^2P_{1/2}-^2P_{3/2}$	1.3333	69
6701.83.....	5.4	3.3	*Ni* XV $3p^2$ $^3P_1-^3P_0$	1.8924	56.4
7891.94.....	.....	29	*Fe* XI $3p^4$ $^3P_1-^3P_2$	2.3885	43.3
8024.21.....	.....	1.3	*Ni* XV $3p^2$ $^3P_2-^3P_1$	2.1091	21.9
10746.80.....	.....	240	*Fe* XIII $3p^2$ $^3P_1-^3P_0$	1.9279	13.9
10797.95.....	.....	150	*Fe* XIII $3p^2$ $^3P_2-^3P_1$	2.2558	9.6

* First column under "Intensity": Grotrian's values (*Zs. f. Ap.*, **7**, 26, 1933); second column: Lyot's values (*M.N.*, **99**, 580, 1939); both taken from Edlén's paper (n. 1, above).

ESTIMATION OF THE DENSITIES OF THE IONS

Now that the transition probabilities are known, it is possible to find the number-densities of the ions in the respective excited states. According to the measurements of Waldmeier,[4] the intensity of the line λ 5303 at a distance of 42″ from the solar limb is equivalent to the continuous radiation emitted by the center of the solar disk and contained in a wave-length interval of 6.75×10^{-5} A at the same wave length. The rate of radiation in the interval from λ to $\lambda + \delta\lambda$, normal to the surface in unit solid angle by unit surface, is given by

$$\frac{2hc^2\delta\lambda}{\lambda^5(e^{h\nu/kT}-1)}.$$

The total number of λ 5303 photons emitted by a column of coronal material of unit cross-section at a distance of 42″ from the solar limb in unit time is obtained by dividing the quantity by $h\nu$

$$\frac{8\pi c \times 6.75 \times 10^{-13}}{\lambda^4(e^{h\nu/kT}-1)} = 7.1 \times 10^{14}.$$

The value of 6000° K has been used for the temperature T. Dividing it again by the transition probability 60, we get the numbers N of the ions *Fe* XIV in the state $^2P_{3/2}$ in the same column.

The intensity of the continuous radiation of the corona falls off with the distance from the center of the solar disk, p, approximately according to Turner's law:

$$\frac{\text{Constant}}{p^6}.$$

[4] In a series appearing in Vols. **20** and **21** of *Zs. f. Ap.*, 1942. The writer has seen only a mimeographed abstract of them.

But, according to Grotrian,[5] the intensities of the coronal lines vary proportionately with the continuous radiation; hence we may use Turner's law approximately for the coronal lines. If we assume the number-density of the ions of *Fe* XIV in the excited state $^2P_{3/2}$ to vary with an inverse power of the radial distance from the center of the sun,

$$\frac{I}{r^n},$$

then the number in an infinite column of unit cross-section at a perpendicular distance, p, from the center of the sun should be

$$N = \int_{-\infty}^{\infty} \frac{I}{p^n \sec^n \theta}\, d(p \tan \theta) = \left(2\int_0^{\pi/2} \sec^{2-n} \theta\, d\theta\right) \frac{1}{p^{n-1}}.$$

This shows that we should take $n = 7$, so that $N = 16I/15p^6$. Therefore, the number-density of the excited ions of *Fe* XIV at $r = 7.26 \times 10^{10}$ cm ($p = 7.26 \times 10^{10}$ corresponding to 42″ from the solar limb) is given by

$$\frac{I}{(7.26 \times 10^{10})^7} = \frac{15}{16} \frac{N}{7.26 \times 10^{10}} = 153/\text{cc}.$$

In Table 1 the intensities of the lines as determined by Grotrian and Lyot are separately given. Probably because of the fluctuations of the line intensities with time, their results do not agree. The intensities given by Grotrian are the relative measures of the energy radiated. The values given by Lyot are referred to the energy contained in 1 A of the continuous radiation at the same wave length. The intensities of the other lines, relative to λ 5303, enable us to obtain directly the number-densities of the other excited ions with the help of the transition probabilities. The results are given in the fifth column of Table 2. In the calculation we have used Lyot's values whenever available; for the rest, Grotrian's values are used. Hence the results, taken as a whole, can perhaps be used only in giving some idea of the magnitudes of these quantities. In the second column of Table 2 are given the values of the concentrations of the ions in ground states, as roughly estimated in a manner to be explained later.

DISCUSSION OF THE EXCITATION MECHANISM

The high stages of ionization of the ions suggest that they are produced within the sun and ejected into the corona. This is in line with the view of Waldmeier,[6] who explains the great line width of λ 5303 as caused by Doppler effect due to the radial motions of the emitters. There is, however, the difficulty with this view, as may easily be shown, that the decrease of line breadth with height should be much more rapid than that which is actually observed. In the present paper we shall, however, be concerned only with the problem of excitation. The magnitudes of the transition probabilities show clearly that the excitation must take place in the corona. We shall investigate the mechanism mainly responsible for such excitation processes.

One is somewhat tempted to adopt the process of electron capture as the mechanism of excitation. We may imagine that the outward-streaming ions capture electrons now and then, and drop to some excited state of the ion in the preceding stage of ionization. These excited ions will then, in their turn, emit the lines we observe. It is easy, however, to verify that, if the probability of capture is comparable with the photoexcitation, the ions would capture electrons far too rapidly to emit the lines at the great heights observed.

[5] *Zs. f. Ap.*, **7**, 26, 1933.

[6] *Zs. f. Ap.*, **15**, 44, 1938.

In fact, as we shall presently see, a rough estimate shows it to be otherwise: the probability of electron capture is quite negligible compared with the photoexcitation.

TABLE 2

Ion	No. in Ground State	Excited State	Line Utilized	No. in Excited State	$E-E^*$ (Cm^{-1})
Ca XII	1.3	$^2P_{1/2}$	3328.1	0.12	30,039
Ca XIII	11.6	$^3P_1$	4086.29	0.24	24,465
Ni XII	6.2	$^2P_{1/2}$	4231.4	1.23	23,626
Ni XIII	6.5	$^3P_1$	5116.03	1.28	19,541
		$^3P_2$	8024.21	4.11	27,376
Ni XV	3.2	$^3P_1$	6701.83	4.55	14,917
Ni XVI	1.7	$^2P_{3/2}$	3600.97	0.69	27,762
Fe X	160	$^2P_{1/2}$	6374.51	32	15,683
		$^1D_2$	3986.88	5.1	37,743
Fe XI	160	$^3P_1$	7891.94	47	12,668
		$^1D_2$	3388.10	10.3	46,068
Fe XIII	540	$^3P_2$	10797.95	750	18,561
		$^3P_1$	10746.80	840	9,303
Fe XIV	220	$^2P_{3/2}$	5302.86	150	18,853

* The last column contains the energy of the excited state above the ground state in wave-number units.

For an estimate of the capture cross-section we have to use the hydrogenic approximation. The asymptotic value of cross-section for infinite ionization potential given by Stueckelberg and Morse[7] is

$$Q_{i}^{\downarrow k}(V) = \frac{A(ik)}{V} Z^2 ,$$

where $A(ik)$ has definite values for definite pairs of states and V is the kinetic energy of the electron captured. It is known that the best results are obtained if, in choosing the proper $A(ik)$ to be used, the corresponding spectroscopic states are correlated. So, if we take the excitation of the $^2P_{3/2}$ of the ion *Fe* XIV for our example, the capture cross-section becomes

$$Q_{i}^{\downarrow k}(v) = \frac{4.1 \times 10^{-4}}{v^2} ,$$

where we have used the velocity v in place of the kinetic energy. If we use a value of 10^8/cc. for the concentration of the free electrons (corresponding to a value of about 1′ from the sun's surface, according to Minnaert[8]) and assume a Maxwellian distribution for the velocities of the electrons,

$$f(v)\,dv = 4\pi \left(\frac{m}{2\pi k T_e}\right)^{3/2} v^2 e^{-(1/2)(mv^2/kT_e)} dv ,$$

[7] *Phys. Rev.*, **36**, 16, 1930. [8] Cf., e.g., Unsöld, *Physik der Sternatmosphären*, p. 440, Berlin, 1938.

the probability for capture is given by

$$\int_0^\infty N_e v Q\downarrow_i^k (v)\, f(v)\, dv = \frac{8.5\times 10^{-2}}{\sqrt{T_e}} \cong 8.5\times 10^{-4},$$

if T_e has the order of magnitude of 10^4.

The probability of photoexcitation may be calculated quite exactly. In terms of the Einstein coefficients B (absorption) and A (spontaneous emission), it is given by

$$B\uparrow_i^j \rho_\nu = \frac{\omega_j}{\omega_i} A\downarrow_i^j \frac{c^3}{8\pi h\nu^3} \rho_\nu .$$

If we take ρ_ν roughly as that of the black-body radiation of about 6000° K diluted by a factor $\frac{1}{3}$, we find for the excitation of *Fe* XIV from $^2P_{1/2}$ to $^2P_{3/2}$,

$$B\uparrow_i^j \rho_\nu = \frac{1}{3}\frac{\omega_j}{\omega_i} A\downarrow_i^j (e^{h\nu/kT}-1)^{-1} = 0.44/\text{sec}.$$

The foregoing estimated values show that the capture process is unimportant as compared with the photoexcitation. This conclusion holds generally, as a look at the transition probabilities and the $A(ik)$ coefficients will serve to show. In the consideration of the removal of the excited states the process of capture is clearly even less important, for the spontaneous emissions occur with considerably greater probabilities than the corresponding photoexcitations for the present case.

The only other conceivable process that may play a role in the excitation is the inelastic collisions with free electrons. The nature of the results causes us to approach the problem from a different direction. From Table 2 it is seen that there are only two sets of values that can tell us something about the distributions of the ions over the excited states. They are the numbers of *Fe* XIII ions in $^3P_2$ and $^3P_1$ and the numbers of *Ni* XV ions in $^3P_2$ and $^3P_1$. Both sets are calculated from Lyot's data. Clearly, values based on Grotian's data, such as the number of *Fe* XIII ions in $^1D_2$ and the number of *Fe* XI ions in $^1D_2$, cannot be used, for the present purpose, in conjunction with the values based on Lyot's data. The amount of information, though meager, seems, however, to point to something definite. If we apply the idea of a Boltzmann distribution, the ratio of the numbers in $^3P_2$ and $^3P_1$ for the ions of *Fe* XIII and *Ni* XV will be found to correspond to the temperatures 29,000° K and 21,000° K, respectively. Though the distributions will not be actually those of Boltzmann, these values should, nevertheless, roughly indicate the "temperatures" of the agent of excitation. Since the solar radiation alone should give rise to distributions corresponding to temperatures lower than 6000° K, the inevitable conclusion seems to be that inelastic collisions with free electrons must play an essential role and that a great part of the free electrons must possess kinetic energies exceeding the thermal energy of 20,000° K.

On the assumption of a Boltzmann distribution the densities of the ions of *Fe* XIII and *Ni* XV in the ground state may be roughly estimated. Their values are given in the second column of Table 2. In the same column are also given the corresponding densities of the other ions, estimated similarly by assuming a temperature of 25,000° K. When results can be obtained both from Lyot's and Grotrian's data, the values based on Lyot's data are given in the table.

Assuming the process of inelastic collisions with free electrons to be responsible for the wide departure from a distribution corresponding to a temperature of about 6000° K, we can find out the required magnitude of the cross-section of the process and, along with it, the relative importances of the electron collisions and the emission and absorption. For both *Fe* XIII and *Ni* XV the configuration concerned is $3p^2$. We shall, for simplicity, take only the three ^3P states into account. Let it be supposed that $E_i < E_j < E_k$ for the three

states i, j, k. If we use symbols such as $\Sigma\overset{k}{\underset{j}{\downarrow}}$, $\Sigma\overset{k}{\underset{j}{\uparrow}}$, etc., to represent the total probability for the ion to go from one state to another, we must have, for a steady distribution,

$$N_k\left(\Sigma\overset{k}{\underset{j}{\downarrow}}+\Sigma\overset{k}{\underset{i}{\downarrow}}\right)=N_j\Sigma\overset{k}{\underset{j}{\uparrow}}+N_i\Sigma\overset{k}{\underset{i}{\uparrow}},$$

$$N_j\left(\Sigma\overset{k}{\underset{j}{\uparrow}}+\Sigma\overset{j}{\underset{i}{\downarrow}}\right)=N_k\Sigma\overset{k}{\underset{j}{\downarrow}}+N_i\Sigma\overset{j}{\underset{i}{\uparrow}},$$

which give, on eliminating N_i, the relation between N_k and N_j

$$N_k\left\{\Sigma\overset{j}{\underset{i}{\uparrow}}\left(\Sigma\overset{k}{\underset{j}{\downarrow}}+\Sigma\overset{k}{\underset{i}{\downarrow}}\right)+\Sigma\overset{k}{\underset{j}{\downarrow}}\Sigma\overset{k}{\underset{i}{\uparrow}}\right\}=N_j\left\{\Sigma\overset{k}{\underset{i}{\uparrow}}\left(\Sigma\overset{k}{\underset{j}{\uparrow}}+\Sigma\overset{j}{\underset{i}{\downarrow}}\right)+\Sigma\overset{k}{\underset{j}{\uparrow}}\Sigma\overset{j}{\underset{i}{\uparrow}}\right\}.$$

According to Hebb and Menzel,[9] the cross-section for the transition from a state k to a state j caused by collisions with free electrons is given by

$$\frac{4.17}{\omega_k}\frac{\Omega(kj)}{v^2}$$

for slow collisions, where $\Omega(kj)=\Omega(jk)$ and v is the velocity of the electron before collision. Take once more a Maxwellian distribution for the velocities of the electrons. The probabilities of the process between such a pair of states as k and j are then easily found to be given by

$$\sigma\overset{k}{\underset{j}{\downarrow}}=\frac{854}{\sqrt{T_e}}\frac{\Omega(kj)}{\omega_k}=\frac{\Pi(kj)}{\omega_k}$$

and

$$\sigma\overset{k}{\underset{j}{\uparrow}}=\frac{854}{\sqrt{T_e}}\frac{\Omega(jk)}{\omega_j}e^{-(E_{kj}/kT_e)}=\frac{\Pi(jk)}{\omega_j}e^{-(E_{kj}/kT_e)},$$

where

$$\Pi(kj)=\frac{854}{\sqrt{T_e}}\Omega(kj)=\frac{854}{\sqrt{T_e}}\Omega(jk)=\Pi(jk).$$

So we may write out the above relation between N_k and N_j as

$$N_k\left\{\left[\frac{1}{\omega_i}\Pi(ij)\,e^{-(E_{ij}/kT_e)}+\frac{1}{3}A\overset{j}{\underset{i}{\downarrow}}\frac{\omega_j}{\omega_i}(e^{E_{ij}/kT}-1)^{-1}\right]\left[\frac{1}{\omega_k}\Pi(kj)+A\overset{k}{\underset{j}{\downarrow}}(1+\tfrac{1}{3}\right.$$

$$\times(e^{E_{kj}/kT}-1)^{-1})+\frac{1}{\omega_k}\Pi(ki)\Big]+\left[\frac{1}{\omega_k}\Pi(kj)+A\overset{k}{\underset{j}{\downarrow}}(1+\tfrac{1}{3}(e^{E_{kj}/kT}-1)^{-1})\right]$$

$$\left.\times\frac{1}{\omega_i}\Pi(ik)\,e^{-(E_{ki}/kT_e)}\right\}=N_j\left\{\frac{1}{\omega_i}\Pi(ik)\,e^{-(E_{ik}/kT_e)}\left[\frac{1}{\omega_j}\Pi(jk)\,e^{-(E_{jk}/kT_e)}+\frac{1}{3}\frac{\omega_k}{\omega_j}\right.\right.$$

$$\times A\overset{k}{\underset{j}{\downarrow}}(e^{E_{kj}/kT}-1)^{-1}+\frac{1}{\omega_j}\Pi(ji)+A\overset{j}{\underset{i}{\downarrow}}(1+\tfrac{1}{3}(e^{E_{ji}/kT}-1)^{-1})\Big]+\left[\frac{1}{\omega_j}\Pi(jk)\right.$$

$$\times e^{-(E_{kj}/kT_e)}+\frac{1}{3}\frac{\omega_k}{\omega_j}A\overset{k}{\underset{j}{\downarrow}}(e^{E_{kj}/kT}-1)^{-1}\left]\left[\frac{1}{\omega_i}\Pi(ij)\,e^{-(E_{ji}/kT_e)}+\frac{1}{3}\frac{\omega_j}{\omega_i}A\overset{j}{\underset{i}{\downarrow}}\right.\right.$$

$$\left.\left.\times(e^{E_{ji}/kT}-1)^{-1}\right]\right\}.$$

[9] *Ap. J.*, **92**, 408, 1940.

Since $A\,{}^{k}_{i}$ corresponding to the transition ${}^3P_2 - {}^3P_0$ vanishes, all terms with $A\,{}^{k}_{i}$ as a factor have been omitted from the equation. We shall regard the quantities $\Pi(kj)$, $\Pi(ik)$, and $\Pi(ji)$ as the unknowns of the equation and seek to obtain an idea of their magnitudes as required by the known ratios of N_k and N_j. For our approximate estimate we may neglect 1, compared with $e^{E_{kj}/kT}$, etc. With the view of obtaining a lower limit for the Π's, we let the T_e, appearing explicitly in the equation, approach infinity, and we find

$$N_k\left\{\left[\frac{1}{\omega_i}\Pi(ij)+\frac{1}{3}\frac{\omega_j}{\omega_i}A\,{}^{j}_{i}e^{-(E_{ji}/kT)}\right]\left[\frac{1}{\omega_k}\Pi(kj)+A\,{}^{k}_{j}+\frac{1}{\omega_k}\Pi(ki)\right]+\frac{1}{\omega_i}\Pi(ik)\right.$$

$$\left.\times\left[\frac{1}{\omega_k}\Pi(kj)+A\,{}^{k}_{j}\right]\right\}=N_j\left\{\frac{1}{\omega_i}\Pi(ik)\left[\frac{1}{\omega_j}\Pi(jk)+\frac{1}{3}\frac{\omega_k}{\omega_j}A\,{}^{k}_{j}e^{-(E_{kj}/kT)}+\frac{1}{\omega_j}\Pi(ji)\right.\right.$$

$$\left.\left.+A\,{}^{j}_{i}\right]+\left[\frac{1}{\omega_j}\Pi(jk)+\frac{1}{3}\frac{\omega_k}{\omega_j}A\,{}^{k}_{j}e^{-(E_{kj}/kT)}\right]\left[\frac{1}{\omega_i}\Pi(ij)+\frac{1}{3}\frac{\omega_j}{\omega_i}A\,{}^{j}_{i}e^{-(E_{ji}/kT)}\right]\right\}.$$

Since the three Π's cannot all be determined and we are not particularly interested in their individual magnitudes, it is convenient to consider the quantity $[\Pi^2(kj)+\Pi^2(ik)+\Pi^2(ij)]^{1/2}$ and find its minimum value as allowed by the equation. Take first the case of *Fe* XIII. When numerical values are substituted, we obtain the equation of a quartic surface:

$$\Pi(kj)\Pi(ik)+\Pi(ik)\Pi(ji)+\Pi(ji)\Pi(kj)+1.53\Pi(kj)$$
$$+88.6\Pi(ik)-53.8\Pi(ji)-82.5=0.$$

It is not difficult to find that the orthogonal transformation

$$\begin{pmatrix}\Pi(kj)\\ \Pi(ik)\\ \Pi(ji)\end{pmatrix}=\begin{pmatrix}\frac{1}{\sqrt{3}} & 0.092 & -0.809\\ \frac{1}{\sqrt{3}} & 0.656 & 0.484\\ \frac{1}{\sqrt{3}} & -0.748 & 0.325\end{pmatrix}\begin{pmatrix}x\\ y\\ z\end{pmatrix}$$

will transform the co-ordinate axes into the principal directions of the surface. The resulting equation, in terms of x, y, and z, may be written in the familiar form

$$-\frac{(x-3.95)^2}{45.5^2}+\frac{(y-65.7)^2}{64.1^2}+\frac{z^2}{64.1^2}=1.$$

The surface is a symmetric hyperboloid of one sheet. Our particular orthogonal transformation has laid the equatorial plane through its axis of symmetry. Obviously, the radius vector of minimum length lies within the plane. The curve in which the plane cuts the surface is the hyperbola

$$-\frac{(x-3.95)^2}{45.5^2}+\frac{(y-65.7)^2}{64.1^2}=1,$$

from which the approximate value of 1.2 for the minimum of the radius vector may easily be obtained. This result leads to the approximate relation

$$\Omega>\frac{\sqrt{T_e}}{854}\frac{1.2}{\sqrt{3}}=0.00081\sqrt{T_e}\cong 0.115.$$

For *Ni* XV we obtain, by an identical treatment,

$$\Omega > 0.072 .$$

Although theoretical values of Ω's are lacking, it is of considerable interest to find that these values for the Ω's are in good accord with the values calculated by Hebb and Menzel[9] for *O* III $2p^2$, which cover the range 0.1–10. This seems to confirm our view of the mechanism of excitation. It will, indeed, be very desirable to have exact theoretical informations on the magnitudes of the Ω's; but, most unfortunately, such calculations involve the difficulty of the slow convergence of the series concerned, which makes even a rough estimate extremely difficult. It is easy to verify, in this limiting case, that the probability of excitation due to collision with electrons is somewhat larger than the average probability of photoexcitation, but spontaneous emissions are mainly responsible for the removal of the excited states.

The writer wishes to express his gratitude to Professor Ta-you Wu for suggesting this problem and for his constant guidance during the preparation of the present paper.

THE CONTINUOUS ABSORPTION OF LIGHT BY NEGATIVE SODIUM IONS

KUN HUANG
Department of Physics, National University of Peking, Kunming, China
Received December 1, 1944

ABSTRACT

The absorption coefficient of negative sodium ions for continuous radiation is calculated with an analytical expression for the wave function of the ion, which is obtained by fitting the numerical wave function given by Hartree and Hartree. For the wave function of the ejected electron the free electron solution is used. The errors committed are estimated by more elaborate calculations and are found to be unimportant. With the help of Milne's relation the cross-section for the reverse process—electron-capture by neutral sodium atoms—is also calculated.

Hartree and Hartree[1] showed that negative sodium ions probably exist and gave the numerical wave function for such ions. In view of possible astrophysical applications, we undertake the calculation of the continuous absorption coefficient of such ions for light as a function of frequency.

REDUCTION OF THE GENERAL FORMULA

The absorption coefficient for continuous radiation[2] is given by

$$Q = \frac{8\pi^3\nu}{3c}\, g\, |\vec{M}|^2, \tag{1}$$

where g is the statistical weight of the final-state wave function used, Φ, in energy units; ν is the frequency of the light absorbed; and $\vec{M}$ is the matrix element

$$e\Sigma \ldots . \Sigma \S \ldots . \S \Phi^* (\Sigma \vec{r}_i) \Psi d\tau_1 \ldots . d\tau_N ,$$

with Ψ standing for the initial-state wave function.

This Ψ is the wave function of the negative ion in the present case and may be expressed in terms of the individual electron wave functions $\psi_{1s}\sigma^+, \psi_{1s}\sigma^-, \ldots . \psi_{3s}\sigma^+, \psi_{3s}{}^-\sigma$, in the form

$$\Psi = \frac{1}{\sqrt{N!}} \begin{vmatrix} \psi_{3s}(1)\,\sigma^+(1)\,\psi_{3s}(2)\,\sigma^+(2) \ldots . \\ \psi_{3s}(1)\,\sigma^-(1) \ldots . \\ \ldots \ldots \ldots \\ \psi_{1s}(1)\,\sigma^-(1) \ldots . \end{vmatrix} .$$

If we neglect the effect of polarization of the sodium atom under the influence of the ejected electron, which has always been found to be less important than the effects we shall discuss later, Φ may also be written in the determinantal form

$$\Phi = \frac{1}{\sqrt{N!}} \begin{vmatrix} \chi(1)\,\sigma^+(1)\,\chi(2)\,\sigma^+(2) \ldots . \\ \phi_{3s}(1)\,\sigma^-(1) \ldots . \\ \ldots \ldots \ldots \\ \phi_{1s}(1)\,\sigma^-(1) \ldots . \end{vmatrix} ,$$

[1] *Proc. Cambridge Phil. Soc.*, **34**, 550, 1938.

[2] The formula may easily be verified if the wave function is normalized in the manner described by Shortley in *Ap. J.*, **89**, 295, 1939.

in which, besides the wave functions of the atomic electrons of the sodium atom, there enters also the function χ, which represents the ejected electron moving in the field of the neutral atom. We find it convenient to use spherical polar co-ordinates to describe the ejected electron. Since Σl_i for Φ and Ψ must differ by 1 for $\vec{M}$ not to vanish, χ must be a p-state wave function.

As equation (1) is for atoms oriented at random, and the negative ion is spherically symmetrical, Q will obviously be the same, irrespective of which one of the three p-states ($m = 1, 0, -1$) is used. Corresponding to a state with definite m, four different states arising from various spin orientations are possible. However, out of the four states, obviously only the two with oppositely oriented spins for the ejected electron and the atom give rise to nonvanishing $\vec{M}$; and, furthermore, their contributions are identical. With these facts taken into account, the total absorption coefficient corresponding to light of a definite frequency is therefore given by

$$Q = \frac{16\pi^3\nu}{c} g |\vec{M}|, \tag{2}$$

where

$$M = e\vec{i}_z \int \ldots \int \Sigma \ldots \Sigma \Phi^* (\Sigma z_i) \Psi d\tau_1 \ldots d\tau_N ,$$

where Φ involves only χ with $m = 0$.

In evaluating the quantity $\vec{M}$ the usual procedure has been to take account of the valence electrons only, while completely ignoring the core electrons. We have, however, taken pains to carry out the exact reductions and the necessary numerical integrations to justify the procedure. Since our result is of the nature of a confirmation, it is not necessary to make more than a brief mention of it. For the details of the reductions it suffices to mention that we have made use of an obvious adaptation of Slater's method[3] for orthogonalizing the atomic wave functions in an antisymmetric combination to our purpose of making wave functions in Φ orthogonal to some in Ψ. The calculated values of

$$(\phi_{1s}, \psi_{1s}) = (\phi_{2s}, \psi_{2s}) = (\phi_{2p}, \psi_{2p}) = 1$$

and

$$(\phi_{1s}, \psi_{2s}) = (\phi_{2s}, \psi_{1s}) = (\phi_{1s}, \psi_{3s}) = (\phi_{3s}, \psi_{1s}) = 0$$

are correct to within 0.001 and enable us to reduce $\vec{M}$ to

$$\left.\begin{aligned} \vec{M} = e \{ & \int \chi^* (\vec{r}) r \cos\theta \psi_{3s} (\vec{r}) d\tau - \int \chi^* \psi_{2p_0} d\tau' \int \phi^*_{2p_0} (\vec{r}) r \cos\theta \psi_{3s} (\vec{r}) d\tau \\ & - \int \phi^*_{2s} \psi_{3s} d\tau' \int \chi^* (\vec{r}) r \cos\theta \psi_{2s} (\vec{r}) d\tau + \int \chi^* \psi_{2p_0} d\tau' \int \phi^*_{2s} \psi_{3s} d\tau'' \\ & \times \int \phi^*_{2p_0} (\vec{r}) r \cos\theta \psi_{2s} (\vec{r}) d\tau \} \{ \int \phi^*_{3s} \psi_{3s} d\tau - \int \phi^*_{2s} \psi_{3s} d\tau \int \phi^*_{3s} \psi_{2s} d\tau' \} . \end{aligned}\right\} \tag{3}$$

The calculated values

$$\int \phi^*_{3s} (\vec{r}) d\tau \psi_{3s} (\vec{r}) = 0.91 ,$$

$$\int \phi^*_{2s} (\vec{r}) d\tau \psi_{3s} (\vec{r}) \cong 0.01 ; \qquad \int \phi^*_{3s} (\vec{r}) d\tau \psi_{2s} (\vec{r}) \cong 0.01 ,$$

and some integrations made with the help of the accurate χ to be obtained later (with $k_a^2 = 0.182$), show that the second term in the first bracket of expression (3) amounts to 1.6 per cent of the first term, while the last two terms fall safely below 1 per cent of the

[3] *Phys. Rev.*, **42**, 33, 1932.

first term. Hence we find the expression which would be obtained directly by following the usual procedure,

$$\vec{M} = 0.91\, e \int \chi^*(\vec{r})\, r \cos\theta \psi_{3s}(r)\, d\tau\,, \tag{4}$$

to be usable for the range of energy under consideration. Since the value of this expression decreases rapidly with increase of energy, whereas the second term in the first bracket of expression (3) is but little affected by energy changes, the error in using expression (4) will first become appreciable when its value decreases to a tenth of its value at $k^2 = 0.182$.

The radial factor $R_c(r)$ of χ has the asymptotic form at infinity given by

$$rR_c(r) = C \sin(kr + \delta)\,.$$

It is normalized to one state per unit energy range if we put[2]

$$C = \left(\frac{8\pi m}{h^2 k}\right)^{1/2}.$$

In the following we shall use $R_c(r)$ having unit amplitude at infinity, and atomic units will be employed. Therefore, making use of equation (4) and performing the integration over angular co-ordinates, we can reduce equation (2) to

$$Q = 4.06 \times 10^{-26} \frac{\nu}{k} \left| \int R_c(r)\, r^3 \psi_{3s}(r)\, d\tau \right|^2, \tag{5}$$

on which the following calculations will be based.

CALCULATION BASED UPON THE USE OF FIELD-FREE SOLUTIONS FOR THE EJECTED ELECTRON

In making a similar calculation for H^-, Massey and Bates[4] have considered the problem with the greatest care and have found that the use of a simple plane wave for the ejected electron gave completely satisfactory results. A similar conclusion was arrived at by Bates[5] in connection with some neutral atoms—the conclusion that in calculating their continuous absorption coefficients the hydrogen continuous wave functions may be used with advantage for the ejected electrons. The results of these authors suggest the use of the field-free solutions for χ in our problem. As we shall see, the correctness of this suggestion is, however, not at all obvious, though it may be verified by carrying out accurate calculations. Following the procedure adopted by Massey and Bates in their calculation for H^-, we shall present the calculation based on the use of the field-free solutions and shall then proceed to show that the results so obtained are essentially correct.

The radial wave equation for a free electron in the p-state is

$$\frac{d}{dr^2}[rR_c(r)] = \left\{-k_a^2 + \frac{2}{r^2}\right\} rR_c(r)\,. \tag{6}$$

The solution regular at the origin is

$$\left.\begin{aligned} rR_c(r) &\backsim \sqrt{r} J_{3/2}(k_a r) \\ &\backsim \cos k_a r - \frac{\sin k_a r}{k_a r}\,. \end{aligned}\right\} \tag{7}$$

The latter expression is also seen to be correctly normalized.

Since equation (7) is analytic, it is convenient to have an analytic expression for the wave function of the valence electron of the negative ion. Since the function has already been given numerically by Hartree and Hartree,[1] the method proposed by Slater[3] pro-

[4] *Ap. J.*, **91**, 202, 1940. [5] *M.N.*, **100**, 25, 1939.

vides the means for obtaining its analytic expression. Because of the extremely small effective charge acting on the valence electrons, the electron cloud spreads to an unusually large distance from the nucleus in the present case. As a consequence, it has been found necessary to use three exponential terms for the outer region instead of the two usually employed. The expression obtained is

$$rR_{3s}(r) = Are^{-ar} + Br^2e^{-\beta r} + r^3(Ce^{-\gamma r} + De^{-\delta r} + Ee^{-\epsilon r}), \qquad (8)$$

with

$$A = 1.75\,, \quad B = -3.60\,, \quad C = 0.168\,, \quad D = 1.48 \times 10^{-2}\,, \quad E = 8.13 \times 10^{-4}\,,$$

$$a = 8.41\,, \quad \beta = 3.75\,, \quad \gamma = 0.943\,, \quad \delta = 0.473\,, \quad \epsilon = 0.272\,.$$

In the course of the present investigation we have also obtained the analytic expression for the wave function of the 3s-electron of the neutral sodium atom.[6] Here equation (8) may be used, but with the following values for the parameters:

$$A = 3.00\,, \quad B = -4.87\,, \quad C = 0.259\,, \quad D = 0.0773\,, \quad E = 0\,,$$
$$a = 9.60\,, \quad \beta = 3.48\,, \quad \gamma = 1.103\,, \quad \delta = 0.707\,.$$

The work in obtaining equation (8) has been laborious; yet the result is satisfactory. The average error is probably less than 1 per cent, and the deviations seldom exceed 3 per cent.

The integration of the expression $\int_0^\infty R_c(r)\, r^3 R_{3s}(r)\, dr$ with $rR_c(r)$ and $rR_{3s}(r)$, as given respectively by equations (7) and (8), is elementary and leads to the result

$$k_a^2\left\{\frac{-117.7}{(70.73+k_a^2)^3} - \frac{28.8}{(14.06+k_a^2)^4}(k_a^2 - 70.3) + \frac{7.605}{(0.8892+k_a^2)^5}(3k_a^2 - 4.446)\right.$$
$$\left. + \frac{0.3362}{(0.2238+k_a^2)^5}(3k_a^2 - 1.119) + \frac{0.01062}{(0.074+k_a^2)^5}(3k_a^2 - 0.370)\right\}.$$

For the absorption of light of frequency ν, the value of k_a is connected with ν by the energy relation

$$h\nu = E_0 + \frac{2\pi^2 m e^4 k_a^2}{h^2},$$

where E_0 is the electron affinity of the negative ion. The value of E_0 is at present unknown; so we have to leave this point open. We have, however, calculated the absorption

TABLE 1

ATOMIC ABSORPTION COEFFICIENT Q OF Na^-

WAVE NUMBER (CM^{-1})	Q (CM^2)		WAVE NUMBER (CM^{-1})	Q (CM^2)	
	E_0=0 EV.	E_0=0.5 EV.		E_0=0 EV.	E_0=0.5 EV.
10,000.....	6.45×10^{-17}	14.6×10^{-17}	40,000.....	0.69×10^{-17}	0.98×10^{-17}
15,000.....	4.4	8.13	50,000.....	.39	.53
20,000.....	2.7	4.75	60,000.....	.22	.30
25,000.....	1.83	2.96	70,000.....	.121	.164
30,000.....	1.29	1.97	80,000.....	.063	.086
35,000.....	0.94	1.37	90,000.....	0.030	0.043

[6] *Phys. Zs. d. Sowjetunion*, **6**, 368, 1934.

coefficient over a range of frequencies for the two assumed values of E_0: 0 and 0.5 ev., for we expect the value of E_0 to lie somewhere between these values. The results are given in Table 1.

EFFECT OF DISTORTION BY ATOMIC FIELD

We proceed to show that the above results are sufficiently accurate even if the effect of the Coulomb interactions of the ejected electron with the atomic electrons and nucleus is taken into account (the distortion of the plane wave by the atomic field). The wave equation for the ejected electron, including this effect of distortion, is

$$\frac{d}{dr^2}[rR_c(r)] = \left\{-k_a^2 - \frac{22}{r} + 2V(r) + \frac{2}{r^2}\right\} rR_c(r), \tag{9}$$

where $V(r)$ is the potential energy due to the Coulomb interactions, given explicitly by

$$V(r) = 2V_{1s}(r) + 2V_{2s}(r) + 6V_{2p}(r) + V_{3s}(r)$$

where

$$V_{3s}(r_1) = \int \phi_{3s}^*(\vec{r}_2)\frac{1}{r_{12}}\phi_{3s}(\vec{r}_2)\,d\tau_2\,, \text{ etc.}$$

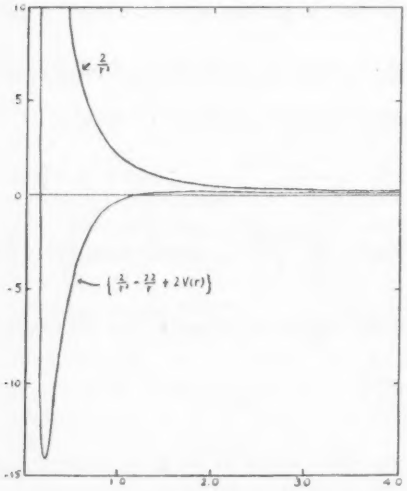

FIG. 1

The values of $V_{\text{core}}(r) = 2V_{1s} + 2V_{2s} + 6V_{2p}$ have been tabulated by Fock and Petrashen.[6] The term $V_{3s}(r)$ is here calculated with the numerical wave function given by these authors. In Figure 1 the functions $2/r^2$ and $2/r^2 - 22/r + 2V(r)$ are plotted. It is seen that the atomic field introduces great modifications, especially near the nucleus. It is hard to see how much it may affect the wave functions and consequently the absorption coefficients. Hence we have integrated equation (9) numerically for $k_a^2 = 0.091$, 0.182, and 0.273, corresponding to $\sigma = 1 \times 10^4$, 2×10^4, and 3×10^4 cm^{-1} for $E_0 = 0$ and $\sigma \cong 1.5 \times 10^4$, 2.5×10^4, and 3.5×10^4 cm^{-1} for $E = 0.5$ ev., respectively.

Beyond $r = 6.8$ the effect of the atomic field may be neglected. The numerical integrations have been carried out to $r = 7.6$, so that the slope at $r = 6.8$ may also be determined by interpolation. For $r > 6.8$ the general solution of equation (6) is

$$\begin{aligned} rR_c(r) &= \sqrt{r}\{A'J_{3/2}(k_a r) + B'J_{3/2}(k_a r)\} \\ &= A\left\{\cos k_a r - \frac{\sin k_a r}{k_a r}\right\} + B\left\{\sin k_a r + \frac{\cos k_a r}{k_a r}\right\} \\ &= C\left\{\sin(k_a r + \delta) + \frac{\cos(k_a r + \delta)}{k_a r}\right\}. \end{aligned}$$

Here C and δ are so determined that the curves will join smoothly at $r = 6.8$. The solution as a whole must then be divided by C to be properly normalized.

The integral $\int_0^\infty R_c(r)\, r^3 R_{3s}(r)\, dr$ is evaluated numerically for $r < 6.8$ and integrated analytically for the region beyond. The values so obtained are given in the accompanying table, side by side with the values obtained in the manner of deriving the values in Table 1. The two latter pairs of values do not show any actual difference if we take into ac-

R_c	k_a^2		
	0.091	0.182	0.273
Equation (6)	−11.2	−6.65	−4.31
Equation (9)	−12.3	−6.70	−4.25

count the deviations of equation (8) from the Hartree and Hartree values. Even for the case of the lowest energy, the difference amounts to only 10 per cent. For still higher energies the accuracy of the results based upon the free-electron equation (6) will increase; so there is no necessity for repeating the laborious task of numerical integration for other values of k.

EFFECT OF EXCHANGE

We go on to discuss the possible effects of the exchange phenomenon. Since the singlet combination of the zero-order states should be used for the present case, the proper wave function to be used for the final state—atom + ejected electron—is

$$\left.\begin{aligned}\frac{1}{\sqrt{2N}}\Big\{\sum_{\mu=1}^{N}\chi^+(\mu)\,(-1)^\mu X^-(1\ldots\mu-1\,\mu+1\ldots N)-\sum_{\mu=1}^{N}\chi^-(\mu)\\ \times(-1)^\mu X^+(1\ldots\mu-1\,\mu+1\ldots N)\Big\},\end{aligned}\right\}\quad(10)$$

where X stands for the antisymmetric wave function for the neutral atom, the signs plus (+) and minus (−) being put there to indicate the state of spin of the atom. The signs with χ have a similar significance for the ejected electron. It is easy to verify that each summation in equation (10) is antisymmetric by itself. The wave equation for χ is obtained by introducing equation (10) into the general wave equation and proceeding in the manner in which reductions for somewhat similar purposes are usually conducted. The equation obtained, after somewhat lengthy reductions, is

$$\left.\begin{aligned}&\nabla_1\chi^-(1)-\Big\{\frac{-2\,2}{r_1}+2\sum_{i\neq 1}V_i(r_1)-k_a^2\Big\}\chi^-(1)=\sum_{i}^{\text{core}}\phi_i(1)\Big[\lambda_i\textstyle\int\chi^-(\mu)\\ &\times\phi_i^*(\mu)\,d\tau_\mu-2\textstyle\int\chi^-(\mu)\dfrac{1}{r_{1\mu}}\phi_i^*(\mu)\,d\tau_\mu-2\int\chi^+(\mu)\,\phi_{3s+}^*(\mu)\,d\tau_\mu\int\phi_i(\nu)\dfrac{1}{r_{\mu\nu}}\\ &\times\phi_{3s-}^*(\nu)\,d\tau_\nu\Big]+\phi_{3s}^+(1)\Big[\lambda_{3s}\textstyle\int\chi^-(\mu)\,d\tau_\mu\phi_{3s+}^*(\mu)-2\int\chi^-(\mu)\dfrac{1}{r_{1\mu}}\phi_{3s+}^*(\mu)\,d\tau_\mu\Big]\\ &-\phi_{3s}^-(1)\Big[\lambda_{3s}\textstyle\int\chi^+(\mu)\,d\tau_\mu\phi_{3s+}^*(\mu)-2\int\chi^+(\mu)\dfrac{1}{r_{1\mu}}\phi_{3s+}^*(\mu)\,d\tau_\mu\Big],\end{aligned}\right\}\quad(11)$$

where $\int d\tau$ is used symbolically to include also summations over spin co-ordinates.

The terms representing the exchange with the core electrons may clearly be neglected, for their values fall off very rapidly with radial distance from the nucleus and are small compared with the terms representing the Coulomb interactions nearer to the nucleus. The latter point will be clear from the result of the calculation we shall make for the valence electron. So, on leaving out the insignificant contributions from the core electrons, we obtain, after multiplying with the proper spin and angular factors and summing (or integrating) over these co-ordinates:

$$\left.\begin{aligned}\frac{d}{dr_1^2}[r_1R_c(r_1)] - \left\{\frac{-22}{r_1} + 2V(r_1) - k_a^2 + \frac{2}{r_1^2}\right\} r_1R_c(r_1) \\ = \frac{2}{3} r_1R_{3s}(r_1) \int_0^\infty R_c(r_2)\left(\frac{r_<}{r_>^2}\right)_{12} R_{3s}(r_2)\, r_2^2 dr_2 .\end{aligned}\right\} \quad (12)$$

When equations (12) and (9) are compared, we see that the left-hand side alone of (12) would be equivalent to (9), so that the term on the right-hand side represents the effect

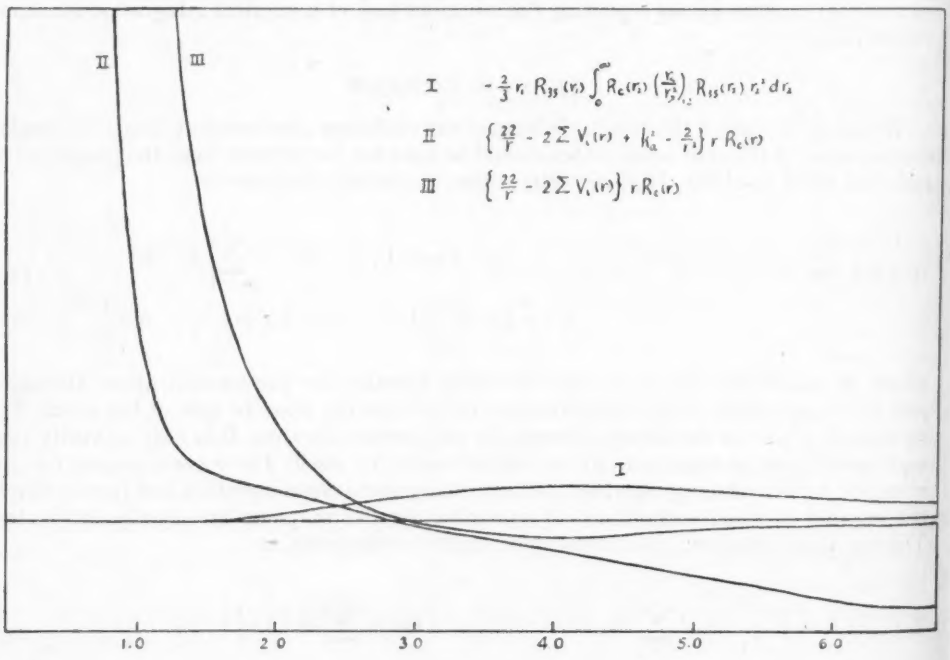

FIG. 2

of exchange with the valence electron. This term is evaluated for $k_a^2 = 0.182$, with $R_c(r)$ based on equation (9), obtained in connection with the discussion of the effect of distortion. The result is represented graphically in Figure 2. In the same figure the functions

$$\left\{\frac{22}{r} - 2V(r) + k_a^2 - \frac{2}{r^2}\right\} rR_c(r)$$

and

$$\left\{\frac{22}{r} - 2V(r)\right\} rR_c(r)$$

are also plotted for comparison. The exchange term is seen to be generally small, as compared with the former curve. As compared with the latter curve, which represents the effect of distortion, it dies away somewhat more slowly but has a very much smaller magnitude nearer to the nucleus. Therefore it is safe to suppose that its effect is, at most, comparable with the effect of distortion due to Coulomb interactions. It is further to be noticed that the two effects have opposite signs in the region where the exchange effect could have any importance; so a part of the error in neglecting both effects tends to cancel itself out, as was already pointed out by Massey and Bates in connection with the hydrogen problem.

CAPTURE CROSS-SECTIONS

The cross-section for the reverse process—capture of electrons by neutral sodium atoms—may easily be calculated. The cross-sections for the two processes Q_c (electron capture) and Q (absorption) are simply related by Milne's formula[7]

$$Q_c = \frac{2h^2\nu^2}{m^2v^2c^2}Q. \tag{13}$$

The term Q should, in the present case, be understood to include the factor 3, owing to the three different values for m possible for the ejected electron after the absorption of

TABLE 2

CAPTURE CROSS-SECTIONS

Electron Energy (Ev.)	$E_0=0$ $Q_c\times10^{23}$ (Cm^2)	Electron Energy (Ev.)	$E_0=0$ $Q_c\times10^{23}$ (Cm^2)	Electron Energy (Ev.)	$E_0=0.5$ $Q_c\times10^{23}$ (Cm^2)	Electron Energy (Ev.)	$E_0=0.5$ $Q_c\times10^{23}$ (Cm^2)
1.23.....	3.89	4.93.....	1.66	0.73.....	14.9	4.43.....	2.62
1.85.....	3.98	6.16.....	1.18	1.35.....	12.4	5.66.....	1.75
2.47.....	3.26	7.40.....	0.80	1.97.....	7.2	6.90.....	1.16
3.08.....	2.76	8.63.....	0.51	2.58.....	5.32	8.13.....	0.73
3.70.....	2.34	9.86.....	0.304	3.20.....	4.11	9.36.....	0.45
4.32.....	1.97	11.1.....	0.163	3.82.....	3.27	10.6.....	0.243

light. The reason for this is that the Q in equation (13) refers to the process of absorption, as a result of which the electron ejected may move in any direction. Because of the spin orientations, we should add an additional factor of $\frac{1}{2}$, instead of the factor 2 that we added in deriving the absorption coefficient; for the oncoming electron may equally likely have a spin the same as or different from that of the atom. Therefore, the capture cross-sections are to be obtained from the corresponding absorption coefficients, as given by equation (5), by the multiplication of the factor $h^2\nu^2/2m^2v^2c^2$. In Table 2 are given the capture cross-sections corresponding to the absorption coefficients given in Table 1.

In conclusion, we may say that the results given in Table 1 should be fairly reliable. For $k = 0.091$ the error probably does not exceed 10 per cent. The absorption coefficient is seen to decrease rapidly with the increase of frequency of the light absorbed. This conclusion is obviously true, even though the electron affinity of the ion is not known. The result of the present investigation tends also to indicate the general correctness of the suggestion mentioned in the paper as to the proper wave function to be used for the ejected electron.

The writer wishes to express his gratitude to Professor Ta-you Wu, who suggested this problem and under whose direction the work was done.

[7] *Phil. Mag.*, **47**, 209, 1924.

THE PERIOD-LUMINOSITY AND THE PERIOD-SPECTRUM RELATIONS OF CLUSTER-TYPE CEPHEIDS

PARIS PIŞMIŞ
National Astrophysical Observatory, Tonanzintla, Puebla, Mexico
Received December 14, 1944

ABSTRACT

The results of the present discussion are based on the material of M. Schwarzschild for 43 cluster-type variables of types a and b in the globular cluster M 3. It is pointed out that the color-magnitude diagram of these variables shows a descending branch resembling that of the main sequence. It is shown that this characteristic, combined with the theoretical period-density relation (satisfied by these variables), gives, as a consequence, the period-spectrum and the period-luminosity relations.

It is generally accepted that the cluster-type Cepheids fail to show the period luminosity and the period-spectrum relations, while the classical Cepheids do show them. It is therefore concluded that the short-period Cepheids also fail to satisfy the period-density relation predicted by theory and satisfied by the long-period Cepheids.[1] These conclusions are based on studies of cluster-type variables in the Galaxy and in several globular clusters.

In a recent study of the variables in Messier 3, M. Schwarzschild[2] has shown that the cluster-type Cepheids of this cluster, of Bailey's types a and b, fulfil the period-density relation. By making general assumptions—that the Stefan-Boltzmann law and the mass-luminosity relation hold for these stars—Schwarzschild transforms the $P^2\bar{\rho} = \text{Constant}$ relation (the theoretical period-density relation) into the following form, capable of being tested by observations:

$$\overline{CI}_H = +1.22 \times (\log P + 0.243 \times \bar{m}_b) + \text{Constant} . \qquad (1)$$

Here $\overline{CI}_H$ and $\bar{m}_b$ stand for the mean red index and the mean blue magnitude, respectively.

For 51 of the variables in M 3, Schwarzschild plots his values of $\overline{CI}_H$ against $\log P + 0.243 \times \bar{m}_b$. Whereas a straight line fitting all the points would result in a slope too small, as compared to that given by the equation, the a and b types alone (excluding the variables with periods less than 0.4 days) conform satisfactorily to the theoretical relation. A possible interpretation suggested by Schwarzschild is that the c-type variables are pulsating in a higher mode. In what follows we shall consider only the a- and b-type variables (43 in number).

In the color-magnitude diagram occupied by the 43 variables (Fig. 4, in *Harvard Circ.*, No. 437) one sees clearly that these variables form a descending branch resembling that of the main sequence. Such a relation between the colors and the magnitudes has not been obtained in previous studies of this cluster or of other clusters. Throughout the change of mean color the mean luminosity was found to be sensibly constant.[3]

It can easily be shown that the existence of relation (1) and the relation between mean colors and mean magnitudes ($\overline{CI}_H$ and $\bar{m}_b$) implies the existence of period-luminosity and period-spectrum (or period-color) relations. With the help of the color-magnitude relation written in the form

$$\bar{m}_b = F(\overline{CI}_H) , \qquad (2)$$

[1] Summarized in Shapley, *Star Clusters* (Harvard Monograph No. 2), 1930.

[2] *Harvard Circ.*, No. 437, 1940.

[3] See, e.g., ten Bruggencate, *Sternhaufen*, Berlin, 1927.

we can eliminate $\overline{CI}_H$ from equation (1) and obtain

$$P = \varphi(\overline{CI}_H), \tag{3}$$

which is the period-color relation. Now equation (2) can be written as

$$\overline{CI}_H = F_1(\bar{m}_b). \tag{4}$$

If from relation (1) we eliminate $\overline{CI}_H$ by means of equation (4), we obtain

$$P = \varphi_1(\bar{m}_b), \tag{5}$$

which is the period-luminosity relation.

In Figure 1 the mean colors of the 43 variables determined by Schwarzschild are plotted against their periods. It appears that the period-spectrum relation of these vari-

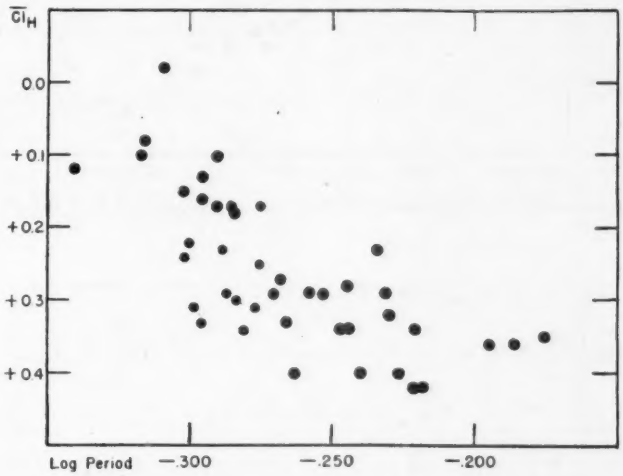

FIG. 1.—The period-color relations of 43 short-period Cepheids of Bailey's types a and b in M 3

ables is similar to that of the classical Cepheids; for both groups of Cepheids, the larger the period the later the spectral type. If one uses, instead of $\overline{CI}_H$, $\overline{CI}_{HC}$, namely, the mean colors calculated by Schwarzschild from P and $\bar{m}_b$ with the help of equation (1), the scatter of the period-spectrum diagram diminishes considerably (Fig. 2).

Figure 3 gives the period-luminosity diagram. Here the period is plotted against $\bar{m}_b$.[4] This relation is the reverse of that found for the classical Cepheids. The average dispersion is about one-half of that for classical Cepheids. The increase of period in Figure 3 is accompanied by a decrease in the luminosity. This tendency was to be expected, since in both short-period and classical Cepheids an increase of period is accompanied by an increase of color index; but to the increase of color index there corresponds a decrease of luminosity in short-period Cepheids and an increase of luminosity in the classical ones. In other words, the function φ is an increasing function for both types of Cepheids, while F is a decreasing function in classical Cepheids but an increasing one in short-period Cepheids.

[4] Corrections to the periods of some of the M 3 variables have recently been published by W. C. Martin (*Ap. J.*, **95**, 314, 1942), but none of those corrections is for the a and b types.

The magnitudes and the color indices determined by Schwarzschild are of excellent quality, relative to each other; therefore there is no room to doubt the reality of the period-spectrum and the period-luminosity relations shown by the a- and b-type variables in M 3.

The difference in the statistical behavior of these cluster-type Cepheids and the classical ones in general consists, then, in (1) the period-luminosity relation and (2) the color-

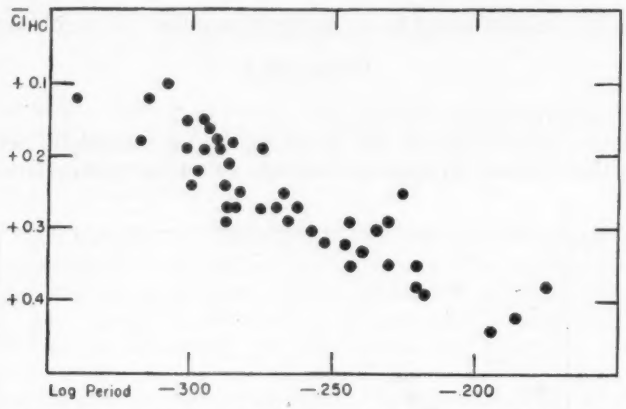

FIG. 2.—The period-spectrum relations of 43 short-period Cepheids in M 3, using colors corrected by Schwarzschild.

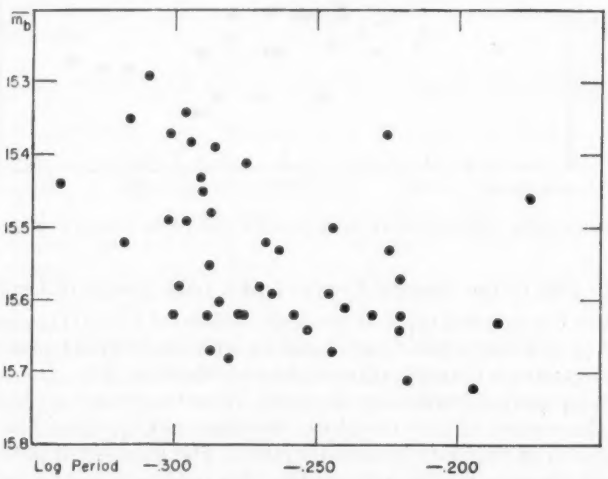

FIG. 3.—The period-luminosity relations of 43 short-period Cepheids of Bailey's types a and b

magnitude relation. It will be of considerable interest to investigate the significance of this difference. But, as can be inferred from what has been said above, given the period-spectrum relation, (1) follows from (2), and vice versa. Recent attempts to interpret the Hertzsprung-Russell diagram for stars in general have been successful (Strömgren), and the energy sources in at least the main-sequence stars are satisfactorily accounted for (Bethe). It would, therefore, be preferable to consider the interpretation of the HR diagram of the cluster-type variables first.

It seems rather certain that the a- and b-type Cepheids in M 3 form a branch running along the main sequence (perhaps with a slightly different inclination), shifted somewhat toward brighter magnitudes. The problem which suggests itself is, then, that of accounting for the dependence of the mean colors on the mean magnitudes of these short-period variables. It is, however, necessary, before one can proceed further, to know the exact position of the cluster-type variables in the HR diagram[5]—in other words, to know the variation of the mean effective temperature with the mean luminosity (Schwarzschild's magnitudes and colors are on a relative scale and hence cannot provide the desired information). With this knowledge at hand it will be possible to explain the HR diagram of the cluster variables by an adequate process of energy production.

Summarizing, we may say that the period-density relation given by the theory of pulsation and a knowledge of the sources of energy for the a- and b-type variables (also for Cepheids in general) will be sufficient to explain the period-spectrum and the period-luminosity relations (the mass-luminosity law will be assumed to hold for these stars).

It is, of course, open to question whether all a- and b-type variables will show the same statistical tendencies as the variables in M 3.[6] Determinations of magnitudes and colors of high accuracy for variables in clusters rich in these objects will decide the question.

[5] It is certainly preferable to obtain a complete HR diagram for the cluster stars with material of high accuracy.

[6] The writer has noticed that the median magnitudes and the periods of variables in NGC 3201 determined by F. W. Wright (*Harvard Bull.*, No. 915, p. 2, 1941) satisfy a period luminosity relation of the same character as that for M 3. However, probably owing to the provisional character of the magnitudes, the dispersion of the diagram is considerable.

THE SPECTRUM OF W SERPENTIS*

CARL AUGUST BAUER
Yerkes and McDonald Observatories
Received November 27, 1944

ABSTRACT

The radial velocities and spectral variations of W Serpentis were determined from 31 spectrograms taken at the McDonald Observatory in 1943. All absorption lines give similar velocity-curves, with the exception of *Ca* II K, which may be blended with an interstellar component. The velocity-curves give $\gamma = -10$ km/sec, $K = 28$ km/sec, and $P = 14.153$ days. The minimum of radial velocity occurs about one day after minimum light, instead of several days later. The conclusion is that the velocity-curve does not represent the motion of the brighter component of the binary but is probably a picture of complicated motions within an extended shell surrounding the system. All spectral lines vary with the phase. The hydrogen emission lines have strong red components at minimum light and strong violet components in the vicinity of phase 5 days. The absorption lines at maximum light suggest a composite character containing A-type features together with features of class G. However, all features originate in the same source and cannot be attributed to two different stars. Lines of *Fe* II, [*Fe* II], *Ti* II, *Ca* II, and other elements occur in emission at minimum light. The absorption lines of *Fe* I are relatively strong at minimum and are unsymmetrical, changing in character at zero phase. Some lines of *Ti* II and certain other absorption features become broad and diffuse at principal minimum.

I. INTRODUCTION

W Serpentis[1] (BD−15°4842) was discovered to be a variable star by Miss A. Cannon[2] in 1907. Its spectrum was described by A. H. Joy[3] as "distinctly Cepheid in character, that is, the lines of ionized elements, especially *Ti* II, *Fe* II, and *Cr* II, predominate." In addition, he described the spectrum and the changes in it with phase. He listed 17 emission features, other than the bright hydrogen edges, to the red of λ 4233, and he gave the probable identifications of 9 of these as being due to *Fe* II with the additional statement that most of the unidentified lines had been previously observed in the spectrum of η Carinae and stars of the W Cephei type. These lines have since been identified with forbidden [*Fe* II]. He noted that the hydrogen absorption lines fall nearly in their normal places and that the emission edges vary greatly in strength—the red components showing the greater range of variation. The red component of $H\beta$ is somewhat weaker than the violet component at maximum light, while at minimum light it is far stronger. Finally, Joy gave the results of his radial-velocity determinations from 19 spectrograms. The range of his velocity-curve was 38 km/sec, with $\gamma = -24$ km/sec, and the curve (which was not published) could be represented by elliptical elements with a small eccentricity. D. B. McLaughlin[4] reported that, in addition to the regular variations with a period of 14.15 days, W Ser showed irregular light-variations with a period of two or three months and with an amplitude of 0.2–0.5 mag. S. Gaposchkin[5] has made a thorough study of the light-curve of W Ser based upon more than 900 observations from photographic plates. He found that the light-curve was peculiar but that it strongly resembled the eclipsing type. His curve showed a narrow minimum with a depth of about 1 mag., and, in addition, the curve showed variation between principal minima. At maximum

* *Contributions from the McDonald Observatory, University of Texas*, No. 102.

[1] HD 166126; $\alpha = 18^h4^m1$; $\delta = -15°34'$ (1900); Sp. Pec., Gaposchkin (*Variable Stars*, p. 76, Cambridge, 1938) gives sp. br. = G1 sp. ft. G4.

[2] *A.N.*, **175**, 169, 1907. [3] *Pub. A.S.P.*, **39**, 234, 1927. [4] *Pub. A.A.S.*, **8**, 117, 1934.

[5] *Harvard Ann.*, **105**, 509, 1937. I am indebted to Professor A. H. Joy for calling my attention to an excellent series of observations by D. J. K. O'Connell (*Ann. Bossha Obs. Lembang*, **8**, 22, 1937).

light the star had a photographic magnitude of 9.47. The time of minimum light could be predicted by the following elements:

$$\text{Minimum} = \text{JD } 2426625.241 + 14^{d}.15326 \cdot E .$$

In addition to the deep minima (m_1), the light-curve shows two shallow minima (designated m_2 and m_3) and consequently three maxima (M_1, M_2, and M_3), of which M_2 seems to be the principal. The period of the long-term fluctuations was determined with considerable uncertainty as about 270 days, but probably these changes in brightness shoud not be regarded as truly periodic. The characteristic features of the light-curve are displayed at all times; but they are perhaps less pronounced near the minimum of the long-term fluctuations. It is noteworthy that the deep minimum partakes of the long-term fluctuations. He suggests that the light-curve is compounded of two kinds, one of the eclipsing type and the other of an undetermined type. Gaposchkin believed that the large loss of light at minimum (more than 1 mag.) pointed to an almost central eclipse. On the basis of the depth of the eclipse he determined the spectral class of the secondary component to be gK2.

A determination of the spectroscopic parallax by Mount Wilson investigators[6] gives an absolute visual magnitude of -3.7, based on an observed spectral class of cG5e.

The importance of a spectrographic study of W Ser lies in the information which can be obtained relative to the unusual conditions existing in its atmosphere. Recent studies of the two peculiar eclipsing variables, SX Cassiopeiae[7] and RX Cassiopeiae,[8] by O. Struve have led to the astrophysically important conclusion that in both of these stars an important contribution to the formation of the observed absorption lines comes from the gases above the normal reversing layer. W Ser shows some important similarities to and differences from either of these two stars, and its spectrum presents so many remarkable peculiarities as to warrant a thorough investigation.

II. THE OBSERVATIONS

The present study of W Ser is based upon 31 spectrograms obtained at the McDonald Observatory from June 22 through September 4, 1943, with the 82-inch reflector, using a Cassegrain quartz spectrograph, and a 500-mm camera. This combination gives a dispersion of 40 A/mm at λ 3933. The plates were all taken during five consecutive cycles. They were secured in the shortest possible interval in order to reduce any long-term variations which might be expected. The observations were favored by unusually fine observing weather, and the plates are almost all of excellent quality. Owing to the faintness of the star and the relatively high dispersion used, the exposure times were necessarily long. On average nights they were between $1\frac{1}{2}$ and 2 hours at normal light and as long as 3 hours at minimum light. The slit width was varied from 0.05 to 0.075 mm. This width is reduced by a factor of 2 in the camera. The spectra obtained usually have a usable range of, from about λ 3700 to λ 5020. I am indebted to Messrs. O. Struve and G. Münch for obtaining a number of the exposures for me.

III. THE VISUAL LIGHT-CURVE

In addition to the spectrographic observations, visual estimates of the magnitude were made by comparing the brightness of W Ser to three standard stars. The 4-inch finder of the 82-inch telescope was used in making these observations. The data for the three comparison stars are listed in Table 1. The individual estimates of relative brightness made by the three observers were used without adjustment in deriving the magni-

[6] Adams, Joy, Humason, and Brayton, *Ap. J.*, **81**, 265, 1935.

[7] *Ap. J.*, **99**, 89, 1944.

[8] *Ibid.*, p. 295.

tudes. The resulting visual light-curve (Fig. 1) shows all the principal features exhibited by Gaposchkin's photographic light-curve; however, there are differences in the phases of the secondary minima and maxima and the range is slightly less. Moreover, the principal minimum does not occur at the time predicted by Gaposchkin's elements. According to his elements, minimum should occur June 24.026 U.T., 1943, while according to the observations discussed here, principal minimum occurred June 25.19 U.T., 1943. Thus we have:

$$\text{Observed} - \text{Predicted} = +1.16 \text{ days} .$$

The observations of the light were made principally for the purpose of fixing as accurately as possible the phase relationship between the light-curve and the velocity-curve. All

TABLE 1

DATA FOR THE COMPARISON STARS

Designation	HD Number	m_{ptm}*	m_{ptg}†
a	166539	8.9	9.20
b	165945	9.2	10.10
c	166523	9.7	10.46

* Photometric magnitude from the *Henry Draper Catalogue*.

† Photographic magnitude after Gaposchkin (*Harvard Ann.*, **105**, 509, 1937).

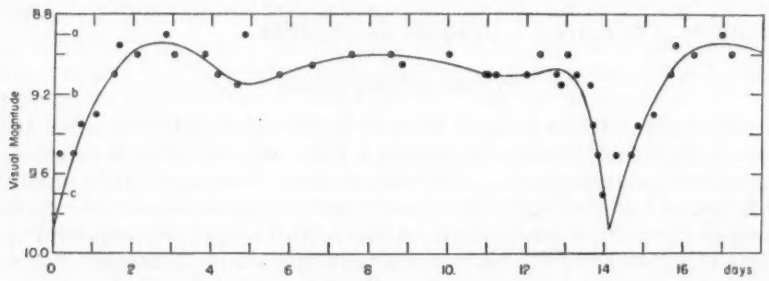

FIG. 1.—The visual light-curve of W Serpentis

the phases given in this paper are reckoned from the observed time of principal minimum, namely, June 25.19 U.T., 1943, and using the period $P = 14.15326$ days, given by Gaposchkin. I wish to acknowledge a very helpful letter and a chart of the comparison stars that Dr. Gaposchkin kindly sent to me.

IV. THE RADIAL VELOCITIES

The 28 stellar lines of Table 2 were selected for the determination of the radial velocities. These lines cover a wide range of the spectrum and represent a variety of elements. A total of 29 comparison lines was selected from the iron-arc comparison spectrum. With few exceptions, all these stellar and comparison lines were measured on each plate. The spectrograms were measured on a Gaertner measuring engine, and the measurements were reduced with the aid of a dispersion table. While many of the absorption lines selected become quite weak near the time of minimum light, the lines of Table 2 include a large proportion of the strongest lines at this phase. Some of the absorption

TABLE 2

LIST OF STELLAR LINES USED TO DETERMINE THE RADIAL VELOCITY

H		*Fe* I	*Ti* II	*Ca* I
H 10	3797.90	3820.44	3913.47	4226.74
H 9	3835.39	3849.98	4012.39	
H 8	3889.05	4005.25*	4395.04	
Hδ	4101.75	4045.83	4399.78	*Ca* II
Hγ	4340.48	4063.61	4443.81	3933.68
		4071.75	4533.97	
	Fe II	4325.62	4571.98	*Mg* II
	4178.86	4404.76		4481.24
	4233.17			
	4583.84			*Sr* II
				4077.73
				4215.54

* *Fe* I 4005.25 gave a good velocity-curve, which was very similar to that of the other *Fe* I lines except that it was systematically too high. This displacement was attributed to a blending with the strong line *V* II 4005.71. Consequently, a correction of −24.7 km/sec was applied to this line to bring it into agreement with the mean velocity-curve for all *Fe* I lines. This correction corresponds to a wave length of 4005.58 A for the blend.

TABLE 3

RADIAL VELOCITIES OF W SER

PLATE	DATE 1943	U.T. MID-EXP.	PHASE (DAYS)	RADIAL VELOCITY IN KM/SEC				
				Mean *Fe* I, *Fe* II, *Ti* II, *H*, *Sr* II, *Ca* I	Mean *Fe* I, *Ca* I	Mean *Fe* II, *Ti* II, *Sr* II	*H*	*Ca* II K
CQ 2162	June 22	5:54	11.21	+11.7	+14.7	+10.6	+ 7.2	.....
2170	23	8:41	12.32	− 3.2	− 5.8	+ 1.2	− 9.0	− 8.9
2175	24	7:43	13.28	+ 0.3	+ 5.1	+ 2.6	−12.2	−30.7
2183	25	8:12	0.15	−27.6	−20.7	−31.0	−31.0	−19.1
2189	27	7:17	2.11	−27.7	−20.8	−26.1	−44.0	−35.1
2194	28	5:55	3.06	−13.0	− 8.7	− 9.5	−28.9	−41.6
2200	29	8:27	4.16	−38.4	−34.1	−43.1	−34.7	−66.9
2205	July 5	4:43	10.01	+ 4.3	+ 2.1	+ 6.8	− 0.4	−14.5
2209	6	5:08	11.02	− 0.1	+ 3.1	+ 0.2	− 6.9	−18.0
2219	7	4:34	12.00	+ 6.8	+10.1	+10.0	− 6.4	−15.4
2226	8	5:28	13.04	−14.1	−11.5	−14.2	−21.6	.....
2232	9	4:11	13.98	−22.1	−14.4	−20.1	−40.6	− 7.3
2248	12	4:18	2.83	− 3.5	− 4.0	+ 0.2	−11.5	−11.6
2256	13	4:00	6.55	−25.4	−21.2	−28.8	−24.5	−30.4
2265	14	4:22	4.83	−23.3	−24.7	−21.8	−24.6	−30.8
2276	18	4:12	8.83	+15.1	+14.0	+15.8	+15.3	−11.5
2283	20	6:38	10.93	− 9.5	− 6.2	−10.0	−14.3	− 9.6
2286	22	5:41	12.89	−27.2	−19.9	−26.1	−43.1	−13.3
2294	23	4:25	13.83	−22.8	−22.2	−19.0	−33.0	−19.9
2299	24	4:21	0.68	−40.1	−36.9	−41.7	−42.2	−29.5
2303	25	3:23	1.64	−24.6	−18.9	−24.6	−34.9	−57.2
2306	28	3:31	4.65	−27.1	−23.1	−31.6	−23.6	−21.8
2315	29	5:24	5.72	−31.9	−26.5	−34.0	−36.3	−43.9
2327	Aug. 6	4:24	13.68	−16.0	−13.8	−12.6	−28.2	−22.5
2334	7	4:26	0.53	−27.9	−32.1	−27.1	−22.7	− 7.6
2343	8	4:24	1.53	−20.2	−18.9	−19.5	−24.4	−17.2
2356	13	4:43	6.55	− 9.9	− 9.8	− 9.1	−11.9	−25.0
2364	14	4:54	7.55	+23.2	+21.8	+24.3	+23.1	+ 2.1
2370	15	4:37	8.54	+21.4	+17.5	+25.6	+18.1	− 1.3
2378	20	6:08	13.61	+ 2.9	− 9.2	+16.0	−19.7	.....
2424	Sept. 4	3:38	0.19	−45.2	−31.4	−53.7	−49.6	− 6.4

lines measured show complex structure. In these instances the position measured corresponds to the core, if present, or to the strongest component if the line appeared double. This procedure seldom led to any difficulty and evidently is justified by the resulting velocity-curves. At certain phases there was some uncertainty in setting on the narrow core of *Ca* II K, owing to the difficulty in distinguishing a core in the very broad absorption underlying it. The radial velocity of each line was reduced to the sun by the graphical method described by G. Van Biesbroeck.[9] The radial velocities are given in Table 3.

V. THE VELOCITY-CURVES AND THE ELEMENTS

The radial velocities as determined from the individual lines were averaged for small groups of similar lines lying in the same region of the spectrum, and preliminary velocity-

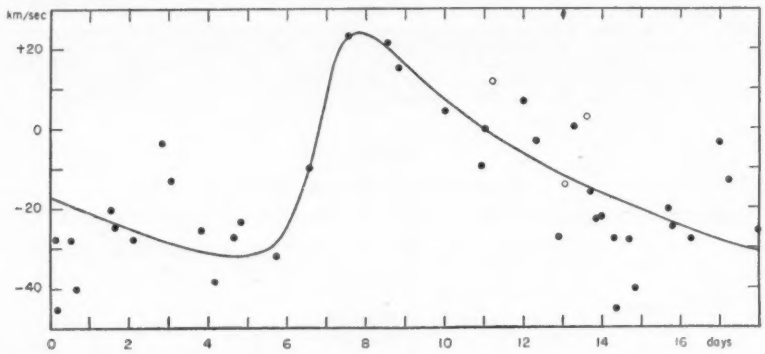

FIG. 2.—The velocity-curve of W Ser obtained from all lines measured except *Ca* II K

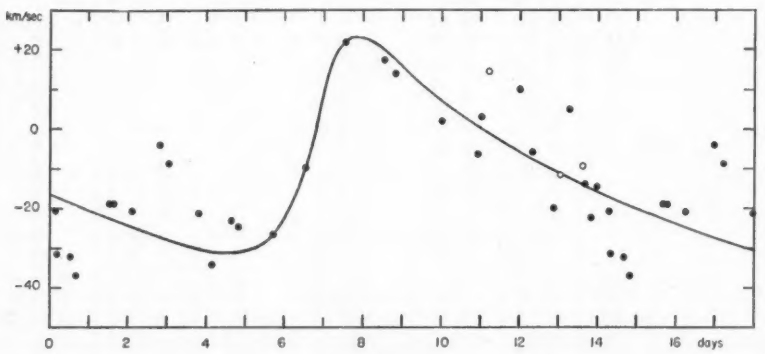

FIG. 3.—The velocity-curve of W Ser obtained from lines of *Fe* I and *Ca* I 4226.7

curves were plotted from these data. The velocity-curves of all of these groups of lines showed a remarkable similarity, making it possible to combine them into larger homogeneous groups for which the mean velocities are given in Table 3. The velocity-curves are shown in Figures 2–6. A quick inspection of these curves reveals that they all agree in showing a steep rise and a gradual fall of the velocity. With the exception of the curve for *Ca* II K the curves all have very nearly the same amplitude and γ-axis. The differences in the amplitude and γ-velocity for *Ca* II K may be due to a blending of the stellar line with a stationary interstellar component of *Ca* II K or to a blending with the emis-

[9] *Ap. J.*, **64**, 258, 1926.

sion features which are conspicuous near this line. The ordinates of the points plotted in Figure 2 are the means of the velocities of all lines except *Ca* II K. The velocity-curve of Figure 2 was determined by adjusting the elements found by the method of Lehmann-Filhés until a good fit to the points was obtained. The curves drawn in Figures 3, 4, and 5 were obtained by making small adjustments to the curve determined for Figure 2. The

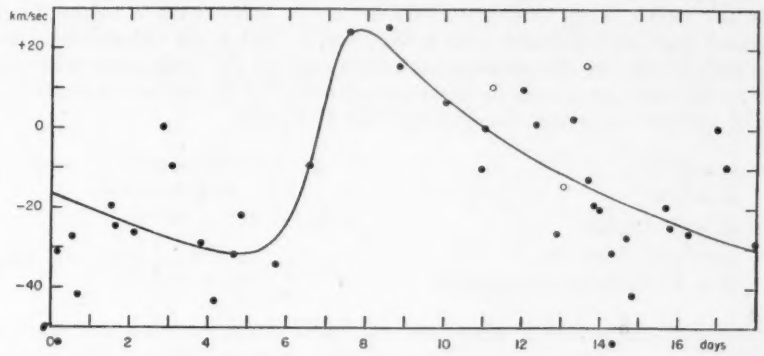

FIG. 4.—The velocity-curve of W Ser obtained from lines of *Fe* II, *Ti* II, and *Sr* II

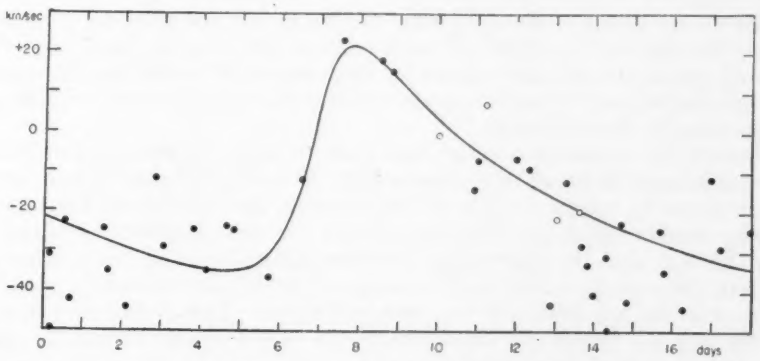

FIG. 5.—The velocity-curve of W Ser obtained from the lines of hydrogen

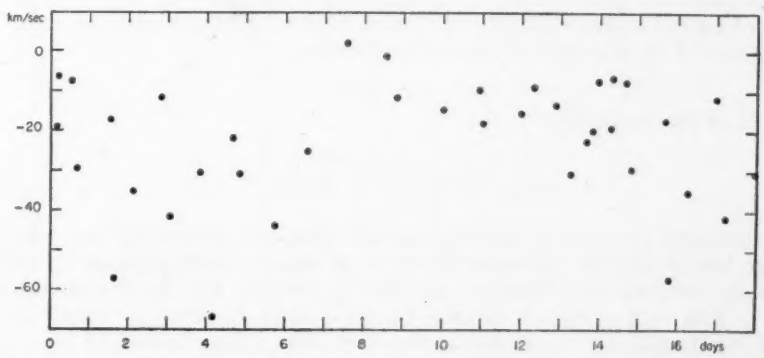

FIG. 6.—Radial velocities obtained from the line *Ca* II *K*. Note that the γ-axis and amplitude differ from those of the curve in Figure 2.

points show a considerable amount of scatter, the largest deviations from the curve being about 25 km/sec. These departures do not show any relation to the cycle during which the corresponding plates were obtained, and in this sense they are not systematic. There is considerable evidence that between the approximate phases 0–4 days the measured radial velocities for the *Fe* I lines depart considerably from the velocity-curve drawn in Figure 3. The points in this interval fall along an arc which appears to rise about 10 km/sec above the curve. This tendency is more clearly defined for a velocity-curve (not shown) based upon only the iron lines λ 3820 and λ 3849 in the ultraviolet. Part of this deviation may be due to the peculiar asymmetry of the *Fe* I lines near minimum; however, this asymmetry is apparently more pronounced before eclipse than afterward. The elements of the curve adopted for Figure 2 are as follows:

$e = 0.50$ — $T = 6.9$ days after observed light-minimum

$\omega = 296°$

$K = 28$ km/sec — $a \sin i = 4.7 \times 10^6$ km

$\gamma = -10.2$ km/sec — $f(m) = \dfrac{m_2^3}{(m_1 + m_2)^2} \sin^3 i = 0.021\odot$

$P = 14.15326$ days (assumed)

These elements introduce at least one important difficulty: they are not compatible with the light-curve. According to these elements, the velocity is −4.1 km/sec at the time of superior conjunction, when $(v + \omega) = 90°$. On the curve of Figure 2 this velocity indicates the phase of the conjunction as about 11.3 days. This gives a difference of 2.9 days between the phase of observed light-minimum and the phase of conjunction derived from the observed velocities. It can be seen at once that the light-curve cannot be shifted with respect to the observations by this amount. It would also be impossible to remove this discrepancy by adjusting the velocity elements without seriously violating the radial-velocity determinations.

In adjusting the elements an effort was made to place the minimum of the curve as far as possible after the epoch of minimum light. This required placing some strain upon the observations. In reality, despite the large scatter, one would be inclined to make the eccentricity smaller and to place the minimum of the curve between the phases zero and one day. In that case the discrepancy between mid-eclipse and conjunction as determined from the velocity-curve would correspond to 90°, and minimum radial velocity would be observed less than one day after mid-eclipse. This discrepancy is so striking that if the star is a binary (as seems likely) the velocity-curve cannot be regarded as giving a true picture of the orbital motion.

In addition to this discrepancy, the small value of $(1 - e)\ a \sin i$ (or the mass function) raises another difficulty when it is considered together with the spectrum. For the condition that the separation of the centers of the two stars at periastron must be larger than the sum of their radii, we have the expression

$$a(1 - e) > r_1 + r_2 .$$

This leads to the inequality

$$\frac{m_1}{m_2} > \frac{(r_1 + r_2) \sin i}{(1 - e)\ (a_1 \sin i)} - 1 ,$$

in which we have the value of the denominator from the elements of the velocity-curve. The large loss of light at minimum points to an almost central eclipse by a star of approximately the same size. Thus we can write $(r_1 + r_2) \sin i \simeq 2r_1$. Numerically we have $(m_1/m_2) > 0.6r - 1$, where r is expressed in solar radii. As described later, the spectrum is that of a supergiant of approximate class G0. Thus a large value of r is expected, and this leads to a large mass ratio. While there is considerable uncertainty present, it appears that this inequality leads to an excessive mass ratio; however, the only alternative

PLATE Xa

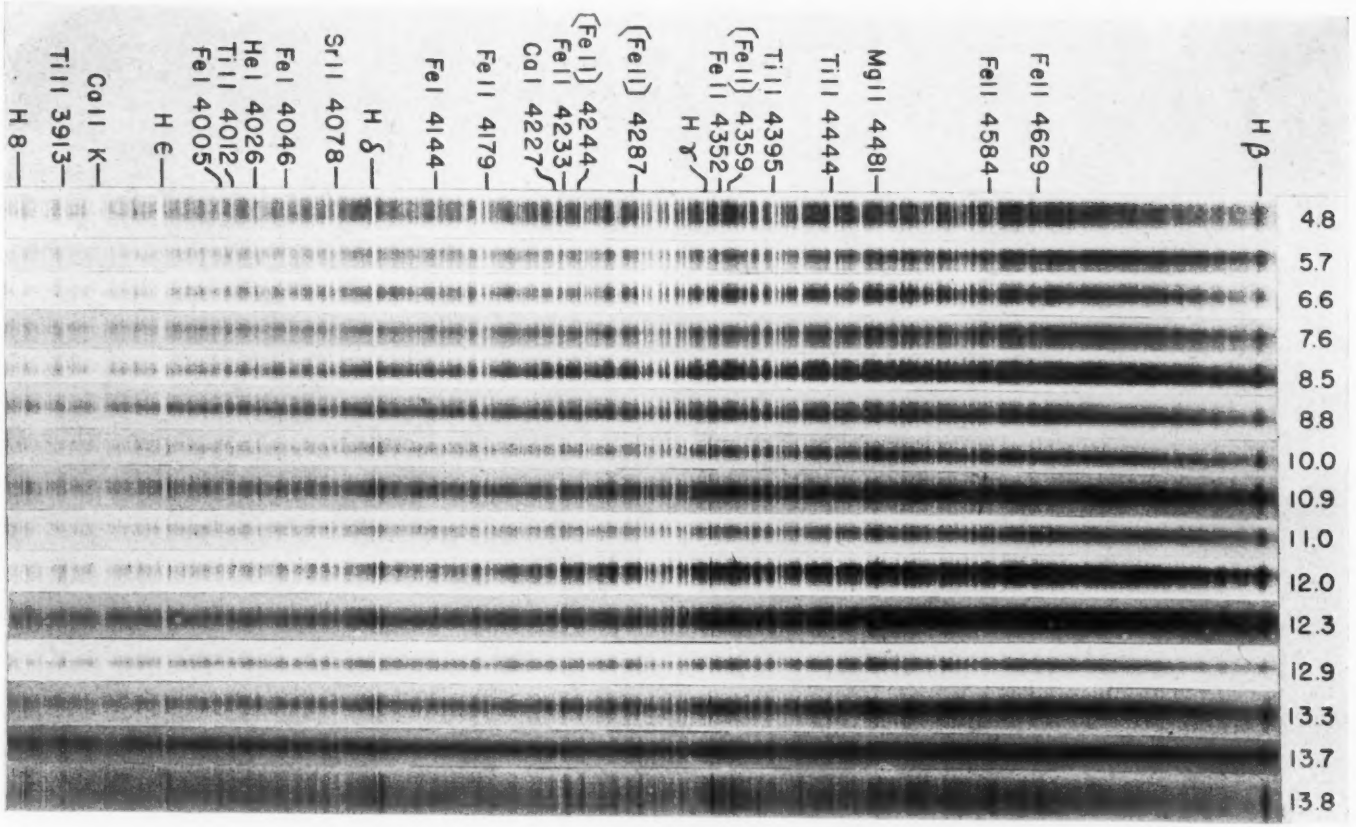

SPECTRA OF W SER

Notice the marked weakening of all emission lines at phase 12.9 days and again at phase 1.5 days

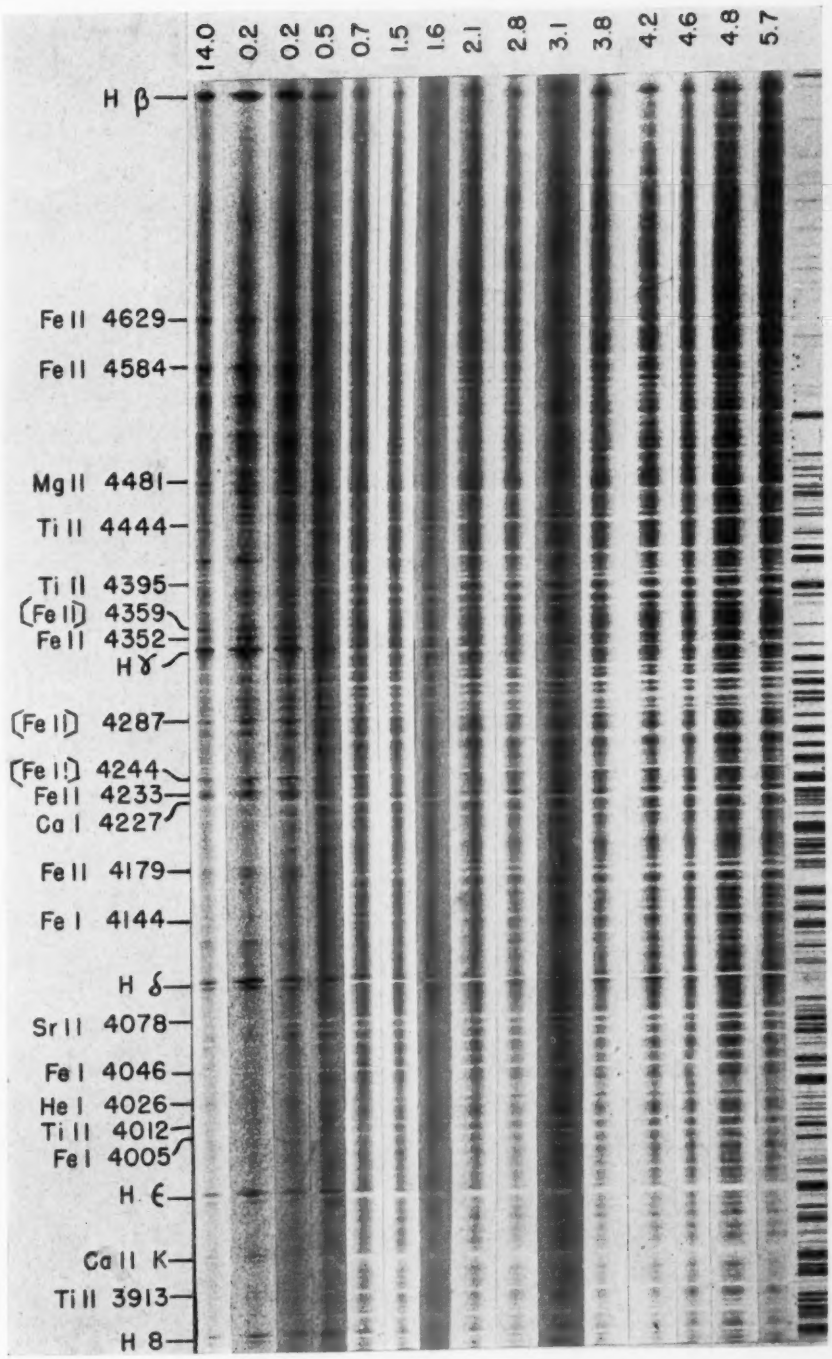

PLATE Xb

Notice the marked weakening of

is to reject either the spectroscopic value of $(1 - e)\ (a_1 \sin i)$ or the spectral type. In consequence of the first discrepancy, and possibly also the second, we are led to suspect that the velocity-curves do not represent the true motion of the star. This conclusion is not unique, for Struve has arrived at a similar result for the two somewhat similar systems of SX Cas and RX Cas. Here, again, we find that we should not trust a peculiar spectrum to give us the radial velocity of the center of mass of the star.

VI. A DESCRIPTION OF THE SPECTRUM AND ITS CHANGES WITH PHASE

The spectrum of W Ser is peculiar, and, like the light-curve, it is subject to continual changes even outside of primary minimum. A number of the spectrograms covering the complete cycle are reproduced in Plate X*a*, *b*. Although the spectrum is peculiar, no difficulties were encountered in identifying the lines by comparison with the spectra of stars having published lists of identifications. It was impossible to classify the spectrum rigorously as to type and luminosity. In most respects the spectrum and the light are most nearly normal on the 2 plates taken at phases 7.55 and 8.54 days after minimum light. Near phase 8 days the spectrum is characterized by many very narrow and very deep absorption lines. The lines of the ionized elements, especially *Fe* II and *Ti* II, are very prominent. $H\beta$ shows moderately strong emission components, of which the violet is slightly stronger than the red, and the central absorption reversal is only barely detectable. The higher members of the Balmer absorption lines are narrow and quite strong, though they are even stronger at some other phases, making it appear that they are partly covered by emission at this phase. At 8 days $H\gamma$ and $H\delta$ show inconspicuous emission wings, while for $H\epsilon$ and *H* 8 there is, perhaps, just a trace of emission.

The very narrow and deep absorption lines appearing outside of eclipse and the great relative strength of the lines of the ionized element are well-known characteristics of high luminosity. A direct comparison between W Ser and normal supergiants in regard to strength and width of lines shows that W Ser belongs to a luminosity class between I and II on Morgan's scale.[10] The actual luminosity class obtained by the use of line ratios varies a great deal according to the pair of lines selected.[11] For example, the two ratios shown in the accompanying tabulation give a very different luminosity class when applied to W Ser and emphasize the pecularities of its spectrum.

Ratio	W Ser	G2 I	G2 III	G0 V
Ca I 4226 : *Sr* II 4077	3:2	1:2	.....	3:2
Fe I 4383 : *Fe* II 4172	1+:1	1+:1	2:1	.....

It is even more difficult to ascribe a definite spectral class to W Ser. The general appearance of the spectrum has in the past led to its classification as a G star. The use of specific line ratios again gives contradictory results, as shown in the accompanying tabulation.

Near phase 8 days the spectrum of W Ser differs from a normal G0 I supergiant spectrum in at least the following respects: (1) the strength of Hδ relative to the metallic lines indicates an earlier spectral type; (2) the appearance of *Ca* II K resenbles that of a spectral type near A and the slight resolution of *Ca* II H from $H\epsilon$ indicates a spectral type earlier than F 8, but this is in contradiction to the appearance of the lines of *Fe* I, *Ca* I, and *Mg* I, which are too strong for such an early type; (3) the high degree of resolu-

[10] *Atlas of Stellar Spectra*, Chicago, 1943.

[11] The comparison of W Ser with normal stars was made with the help of a series of standard spectra secured by Mr. Stewart Sharpless.

tion of the G-band indicates an earlier spectral type; (4) $H\beta$, $H\gamma$, and $H\delta$ show emission; and (5) there are large discrepancies between the classifications determined from different line ratios.

Ratio	W Ser	F8 I b	G0 I	G2 I	Others
Ca I 4226 : $H\delta$ 4101	2:3	2^-:3	**2:3**	.....	.....
Fe I 4045 : $H\delta$ 4101	1:2	**1:2**	2:3	.....	.....
Ca I 4226 : $H\gamma$ 4340	3:2	3:4	2:2	2^+:2	(G5 I—**3:2**)
Fe I 4325 : $H\gamma$ 4340	3:2	$1:2^+$	$1:2^-$	1:1	(G5 I—**3:2**)
Sr II 4077 : $H\delta$ 4101	1:2	$3:2^+$	3:2	.....	(F6 I—**1:2**)
Sr II 4215 : *Fe* I 4143	1:1	2:3	**1:1**	.....	.....
Sr II 4215 : *Fe* I 4045	1:2	**1:2**	1^+:2	.....	.....
Ti II 4399 : *Fe* I 4404	3:1	4:1	5:1	.....	.....
Fe I 4005 : *Ti* II 4053	2:1	3:1	4:1	.....	(F4 I—about 2:1)

It is of particular interest to determine whether there is any dilution of the radiation producing the absorption spectrum. Of the lines sensitive to dilution, the best two which are available in the spectral region examined are *Mg* II 4481 and *Fe* I 4260. The latter appears as a very broad and diffuse line; and, since it is involved with emission features at minimum, it is probably blended with *Fe* II 4258.2. *Mg* II 4481 should be very weak in a normal G0 supergiant. For example, in δ Cephei[12] the *Mg* II line predominates at maximum (sp. F 8 I) but is equal to *Fe* I 4482 at minimum (sp. G 3 I). But the strong A-type lines—*Ca* II, *Fe* II, *Ti* II, etc.—lead us to expect a strong line of *Mg* II. For *Mg* II 4481 and *Fe* I 4260 the ratios in W Ser and a standard G0 I star are shown in the accompanying tabulation. While the existence of dilution is only indicated by the line *Fe* I

Ratio	W Ser	G0 I
Fe I 4260 : *Fe* I 4071	1:2	1:1
Mg II 4481 : *Fe* I 4404	1:3	3:1

4260, it is quite definitely present for the line at λ 4481. If *Fe* I 4404 is abnormally weak, as is indicated later, the effect would be to make the dilution factor even smaller. In addition, the line λ 4481 is broader and more diffuse than the neighboring lines of *Ti* II and *Fe* II.

In the absence of a reliable identification of λ 4481 it is difficult to state definitely whether dilution is present or whether the feature at λ 4481 is abnormal for other reasons, but it is not unreasonable to suppose that the dilution may be quite large.

We can conclude that at maximum light the absorption-line spectrum is entirely abnormal: it combines features of a supergiant—a spectrum (weak, narrow *Ca* II; very strong, sharp *Fe* II, *Ti* II, etc.; absence of broad *H* wings), possibly of the shell type (suspected dilution effect in *Fe* I 4260 and *Mg* II 4481) with features normally associated with a later type (strong *Fe* I, *Ca* I) and of no great luminosity (relative weakness of *Sr* II). Yet there is little indication of any true superposition of two continuous spectra: at *Ca* II K and H the late component is almost absent; on the other hand, the strong *Fe* I lines λλ 4045, 4063, 4071, and *Ca* I 4226 are deep; they fail to show the characteristic shallow appearance of lines which are produced in the composite spectrum of a double star. We infer that the continuous spectrum at maximum light is that of one star of undetermined type and that many absorption features are produced in an extended nebu-

[12] Krieger, *Ap. J.*, **79**, 98, 1934.

lous shell surrounding the principal component (because all absorption lines show the same periodic oscillations in velocity). These features are related to the central absorptions of *H* and to the emissions of *H*, *Fe* II, *Ti* II, *Ca* II, etc., observed at minimum.

The spectrum of W Ser undergoes a continual change with phase which is especially striking near the time of minimum light. The absorption lines become greatly weakened at minimum, and some of them appear broadened or even double. The lines of the ionized elements, notably *Fe* II and *Ti* II, lose their c characteristics and either appear in emission or approach an emission condition.

The variation of the hydrogen lines is particularly significant. The appearances of the various lines of the Balmer series are very different from each other. $H\beta$ and $H\delta$ and probably $H\gamma$ and $H\epsilon$ show emission wings at all phases, while the higher members of the Balmer series show emission only near the time of minimum. At all phases the strength of the emission wings decreases progressively for the higher members of the Balmer series. The ratio of the strength of the violet to the red emission wing is also subject to

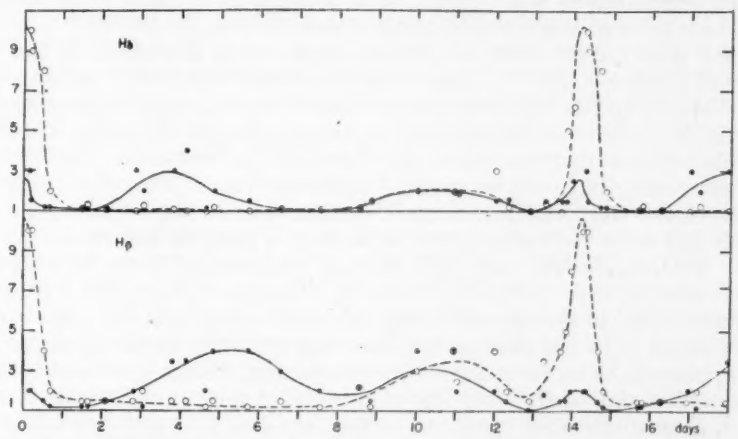

FIG. 7.—The variation in the strength of the emission edges of $H\beta$ and $H\delta$. The solid curve represents the ratio: strength of violet component to continuum. The broken curve represents a similar ratio for the red component. The ratios were estimated from enlarged prints of the spectra. There is considerable evidence of variation in the strength of the *H* emission wings from one cycle to another.

continual change, as is shown graphically in Figure 7, in which the ratio of the strength of the emission of each component to the surrounding continuum is plotted against the phase for the lines $H\beta$ and $H\delta$. The other hydrogen lines are disturbed by neighboring absorption lines and do not give accurate information; however, there is no evidence that any of the lines depart appreciably from the trend shown in Figure 7. It is important to notice how the changes in the total amount of emission appear to be closely related to the changes in the total light at the corresponding phase. The strength of the emission reaches maxima at phases which correspond very closely to the minima, m_1, m_2, and m_3, of the light-curve; and the emission has minima at nearly the same phases as the maxima, M_1, M_2, and M_3, of the light-curve. This reciprocal relation indicates that a large part of the apparent change in the strength of the emission is due simply to the changes in the total light. It is especially interesting to find that the change in the ratios of the strength of the violet to the red emission edges does not show the effect of an eclipse of an approaching stream of gas just prior to mid-eclipse and of a receding stream of gas just after mid-eclipse, as was found for SX Cas and RX Cas. The central hydrogen absorption lines become considerably narrower at minimum. The central absorption of $H\beta$ is absent from phase 13.7–0.5 days, and at the same time the central absorption of the

other hydrogen lines is greatly weakened. Again, between 7.6 and 8.8 days the central absorption of the hydrogen lines is considerably weakened. Some of the hydrogen lines show complexity of structure because of blending with strong absorption lines. At $H\gamma$ the violet emission component is suppressed by the strong absorption line *Ti* II 4337.9, which shows as a distinct line close to $H\gamma$ at all phases outside of eclipse. It is absent only on the plates taken at 14.0 and 0.2 days, and on the latter plate the bright violet edge of $H\gamma$ appears nearly normal, as judged from $H\delta$. This appearance of the *Ti* II absorption line outside of minimum is normal and indicates that the suppression of the bright edge cannot be due to the photographic superposition of an absorption line and is probably caused by absorption in or above the emitting shell. The bright violet wing of $H\epsilon$ is suppressed by the strong *Ca* II H line at all phases. The violet wing of *H* 8 is also weakened by an absorption line probably due to *Fe* I 3886.3, which appears as a distinct line at most phases outside of eclipse. Similarly, the bright violet edge of *H* 9 is weakened by absorption, probably due to *Mg* I; and this absorption line shows at all phases. The bright violet component of *H* 11 appears to be abnormally strong, but no other line was found to which some of this emission might reasonably be attributed.

At phase 8 days the *Fe* I lines are narrow, deep, and symmetrical. As the light falls off sharply at minimum, the *Fe* I lines, while becoming considerably weakened, remain relatively distinct; and at minimum some of them are among the strongest absorption lines present. In addition to their change in strength, the *Fe* I lines also change noticeably in width and symmetry. At phase 13.8 days the *Fe* I lines are distinctly asymmetrical in the sense that they have sharp violet edges and broad, shallow red edges. At this phase some of the strongest lines actually appear double: the broad wings appearing more nearly like weak red components. This effect is most noticeable for the lines *Fe* I 4045, 4063, 4071, 4143, 4307, and 4325. Just at minimum all these lines again appear narrow and symmetrical. Following minimum, at phases 0.2 and 0.5 days these lines appear asymmetrical in the opposite sense, the violet edges now being shaded; but this asymmetry seems to be less pronounced than that occurring before minimum. The line *Fe* I 4404 appears to be an exception to this broadening, though there is some uncertainty on this point owing to the weakness of this line at minimum. Outside of minimum, *Fe* I 4404 is abnormally weak compared to the lines *Fe* I 4383 and *Fe* I 4415, which belong to the same multiplet ($a^3F_4 - z^5G^\circ$). However, both *Fe* I 4383 and 4415 are quite seriously blended, and this may account for their strength. Nevertheless, the lines *Fe* I 4045, 4063, and 4071, which are not blended, are exceptionally strong. It is important to notice that *Fe* I 4404, while partaking in the general weakening of the absorption lines at minimum, gains in strength relative to the near-by lines as shown by the accompanying ratios. The abnormal weakness of *Fe* I 4404 was also present in RX Cas, where its

Ratio	8 Days	Min.
Fe I 4383 : *Fe* I 4404.....	5:1	1:3
Ti II 4395 : *Fe* I 4404.....	5:1	3:2⁻

suppression was thought possibly due to overlying emission. However, in W Ser, it would be difficult to explain the relative increase in the strength of *Fe* I 4404 at minimum, if its abnormal weakness were due to involved emission.

Ca I 4227 is a strong narrow line with only inconspicuous wings. It varies in width, depth, and symmetry in a manner very similar to that previously described for the majority of *Fe* I lines. *Ca* I 4227 exhibits a weak red absorption component from 13.3 to 13.8 days. The lines *Sr* II 4078 and 4215 also show marked variations similar to *Fe* I.

At phase 8 days the lines of *Fe* II are very deep and narrow. As the phase increases, there is a great weakening of these lines, and they change gradually into a broad emission

feature which is usually divided into two nearly equal components by a central absorption. The phase at which the emission is first detectable varies greatly from line to line; but, at least roughly, the stronger the line in absorption, the longer it shows emission components and the stronger these components are at minimum. For *Fe* II 4233, which appears to be one of the strongest and least disturbed *Fe* II lines, emission components are just detectable at 9.0 days; and with increasing phase their strength relative to the neighboring continuum varies in nearly the same peculiar way as is shown implicitly in Figure 7 for the total strength of both bright hydrogen components. The bright violet component of *Fe* II 4233 appears slightly stronger than the red at all phases except possibly at 0.2 and 0.5 days.

At 8 days the lines of *Ti* II are narrow, deep, and symmetrical. The strongest lines of *Ti* II show emission at minimum, but these are much weaker than the emissions of *Fe* II lines of similar strength in absorption. The absorption centers of the *Ti* II lines cut deeper into the continuum at minimum light than do the absorption centers of *Fe* II lines of similar strength. From the most distinct lines it appears that the *Ti* II absorption lines remain symmetrical at all phases and that the violet emission component is usually the strongest. At minimum light the absorption lines *Ti* II 4443, 4468, 4563, and 4571 are broad compared to most of the other *Ti* II lines of similar strength. Many of the fainter absorption lines also present a washed-out appearance at minimum light.

At 8 days the line *Ca* II K is composed of a narrow, moderately deep core which can just be distinguished at the center of very broad, shallow absorption wings that can be followed out as far as 6–8 A on either side of the core. The wings gradually fill in and become less conspicuous as the phase of minimum light is approached. For about ½ day on both sides of minimum, the sharp core of *Ca* II K shows emission components of which the red is always the stronger. Since these emission lines are quite broad, they overlie the broad absorption wings seen at 8 days and make it difficult to determine the variation in them. However, this line does not appear to give any evidence of a late-type component. The line *Ca* II H is closely involved with $H\epsilon$, making it difficult to trace its development; however, it certainly does not show any broad absorption wings like *Ca* II K. Although the appearance of *Ca* II H does change, yet this change cannot be separated from the changes taking place in $H\epsilon$. The best plates show these two lines distinctly separated. The absence of a very strong *Ca* II absorption line at minimum suggests again that we are not observing the composite spectrum of two stars but that of a star and a surrounding shell.

The line which agrees in wave length with *Mg* II 4481 presents an extremely interesting and unusual sequence of changes. Starting at phase 6 days when the absorption line has its minimum width, it broadens, becoming shallower at the same time. Already at 7.6 days it is a shallow absorption feature with a width of about 5 A. At 8.5 days this broad feature appears to be just resolved into two components having a separation of about 4 A. This general appearance continues up to 10 days, at which time the two components are definitely separated by an emission line having a total width of about 5 A. At this phase it is difficult to decide whether the emission of *Mg* II 4481 is actually bordered on each side by real absorption lines. The same general appearance continues, except that the strength of the emission varies similarly to that already described for the other emission lines, i.e., showing a reciprocal relation to the light-curve. Between 13 and 14 days the two absorption components appear to cut below the continuum, and this appearance indicates that they are real absorption lines. By 3.1 days the width of the emission line has decreased again, and this decrease continues until the two absorption lines merge at about 4.6 days. Throughout these changes the red absorption component appears stronger than the violet, and at no phase does the complex line of *Mg* II 4481 appear as narrow as the surrounding absorption lines of similar strength.

All the strong predicted lines of forbidden [*Fe* II] appear in the spectrum of W Ser as single emission lines having a width of about 3 A. The strongest of these lines, such as

TABLE 4

IDENTIFICATION OF THE EMISSION LINES IN THE SPECTRUM OF W SER

IDENTIFICATION		OBSERVED INTENSITY OF EMISSION FEATURE	IDENTIFICATION		OBSERVED INTENSITY OF EMISSION FEATURE
Element	Lab. Wave Length and Intensity		Element	Lab. Wave Length and Intensity	
H 20	3682.8	1	*He* I	3964.7 (50)	1?
H 19	3686.8	1	*Ca* II H	3968.5 (500)	7
H 18	3691.6	1	*He*	3970.1 (80)	
H 17	3697.2	2	*Fe* II	3974.2 (3)	2
H 16	3703.9	2	*Fe* II	3975.0 (2)	
Ca II	3706.0 (10)	1?	*Fe* II	3981.6 (pr.)	1?
H 15	3712.0	2	*Fe* II	4002.1 (2)	2
H 14	3721.9	2	*Fe* II	4002.6 (3)	
Fe II	3725.3 (3)	1	*V* II	4005.7 (800)	1?
H 13	3734.4	2	*He* I	4009.3 (10)	2?
Ca II	3736.9 (11)	1?	*Ti* II	4012.4 (50)	
Ti II	3741.6 (50)	1	*Fe* II	4012.5 (1)	
Fe II	3745.4 (pr.)	1	*Fe* II	4024.6 (5)	3
Fe II	3746.6 (pr.)	1	*He* I	4026.2 (5)	
H 12	3750.2	3	*Ti* II	4028.3 (80)	1?
Fe II	3755.6 (4)	1	*Fe* II	4031.5 (1)	1?
Ti II	3759.3 (200)	3	*Fe* II	4033.0 (3)	
Fe II	3759.5 (6)		*V* II	4035.6 (400)	1?
Fe II	3762.9 (5)	1?	*Fe* II	4044.0 (pr.)	1?
H 11	3770.6	3	*Fe* II	4046.8 (pr.)	1?
Fe II	3779.6 (pr.)	1?	*Fe* II	4048.8 (3)	1?
Fe II	3781.5 (1)	1?	*Ti* II	4053.8 (8)	1
Fe II	3783.4 (4)	2	*Fe* II	4057.5 (2)	1?
H 10	3797.9	4	*Ni* II	4067.0 (30)	2
He I	3819.6 (4)	1?	*Fe* II	4069.9 (1)	
He I	3819.8 (1)		*Fe* II	4076.0 (pr.)	2
Fe II	3824.9 (4)	1?	*Fe* II	4077.2 (3)	
Fe II	3827.1 (4)	1	*Fe* II	4082.6 (1)	1?
Fe II	3827.7 (pr.)		*Hδ*	4101.7 (100)	8
H 9	3835.4	4	*Fe* II	4111.9 (1)	1?
Mg II	3848.2 (7)	2?	*He* I	4120.8 (3)	2
Si II	3853.7 (3)	4	*Fe* II	4122.6 (4)	
Si II	3856.0 (8)		*Fe* II	4124.8 (1)	
Si II	3862.6 (6)	3	*Si* II	4128.0 (8)	4
Fe II	3863.4 (1)		*Fe* II	4128.7 (3)	
Fe II	3863.9 (1)		*Fe* II	4138.2 (pr.)	1
He I	3867.5 (15)	1?	*He* I	4143.8 (15)	1?
V II	3878.7 (300)	2?	*Ti* II	4161.5 (30)	2
Fe II	3880.8 (1)	1	*Ti* II	4163.6 (150)	
He I	3888.6 (10)	6	*Ti* II	4171.9 (70)	1?
H 8	3889.0 (60)		*Fe* II	4173.4 (8)	2
V II	3899.1 (200)	1?	*Fe* II	4178.8 (8)	3
Ti II	3900.5 (70)	2	*V* II	4183.4 (250)	1?
V II	3903.3 (250)	1?	*Ti* II	4184.3 (20)	
Fe II	3906.0 (5)	1	*V* II	4202.3 (150)	1?
Ti II	3913.5 (60)	3	*Fe* II	4233.2 (11)	7
Fe II	3914.5 (2)		[*Fe* II]	4244.0	6
Fe II	3918.5 (pr.)	1?	[*Fe* II]	4244.8	
Ca II K	3933.7 (400)	4	*Sc* II	4246.8 (500)	1?
Fe II	3935.9 (6)	2	*Fe* II	4258.2 (3)	2
Fe II	3938.3 (2)	2	*Fe* II	4263.9 (1)	1?
Fe II	3939.0 (4)		*Fe* II	4273.3 (3)	5
Fe II	3945.2 (pr.)	1?	[*Fe* II]	4276.8	
V II	3952.0 (500)	1?	*Fe* II	4278.1 (1)	1?
Fe II	3960.9 (3)	1			

PLATE XI

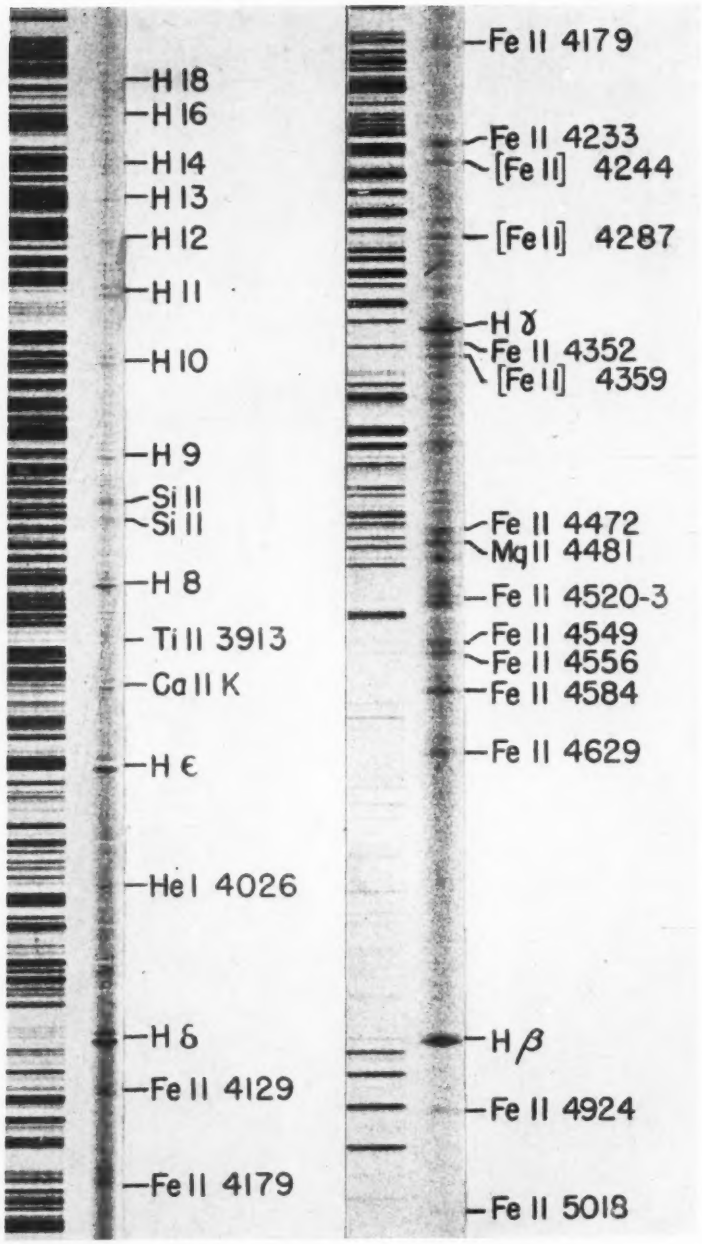

THE SPECTRUM OF W SERPENTIS AT MINIMUM LIGHT

TABLE 4—*Continued*

Identification		Observed Intensity of Emission Feature	Identification		Observed Intensity of Emission Feature
Element	Lab. Wave Length and Intensity		Element	Lab. Wave Length and Intensity	
Fe II	4286.3 (1)	6	*Ti* II	4468.5 (150)	
[*Fe* II]	4287.4		*He* I	4471.5 (100)	5
Ti II	4289.9 (30)	1?	*Fe* II	4472.9 (2)	
Ti II	4290.2 (60)		[*Fe* II]	4474.9	
Fe II	4296.6 (6)	3	*Mg* II	4481.3 (100)	5
Fe II	4303.2 (15)	3	*Fe* II	4489.2 (4)	6
[*Fe* II]	4305.9	3	*Fe* II	4491.4 (5)	
Fe II	4313.0 (1)	1?	*Fe* II	4495.5 (pr.)	1?
Fe II	4314.3 (4)		*Fe* II	4508.3 (8)	6
Sc II	4314.1 (150)		*Fe* II	4515.3 (7)	5
[*Fe* II]	4319.6	3	*Fe* II	4520.2 (7)	7
Fe II	4319.7 (1)		*Fe* II	4522.6 (9)	
Ti II	4337.9 (125)	2?	*Fe* II	4534.2 (2)	2
Fe II	4338.7 (pr.)		*Fe* II	4541.5 (4)	2
Hγ	4340.5 (200)	9	*Fe* II	4549.5 (10)	6
Fe II	4351.8 (9)	6	*Ti* II	4549.6 (200)	
Fe II	4354.4 (2)		*Fe* II	4555.9 (8)	6
Fe II	4357.6 (4)		*Ti* II	4572.0 (300)	2
[*Fe* II]	4358.4	5	*Fe* II	4576.3 (4)	3
[*Fe* II]	4359.3		*Fe* II	4582.8 (3)	8
Fe II	4361.2 (2)	1?	*Fe* II	4583.8 (11)	
Fe II	4368.3 (1)	2?	*Fe* II	4595.7 (pr.)	1?
Fe II	4369.4 (2)		*Fe* II	4598.5 (1)	1?
Mg II	4384.6 (8)	2	*Fe* II	4620.5 (3)	3
Fe II	4384.3 (pr.)		*Fe* II	4629.3 (7)	6
Fe II	4385.4 (7)		*Fe* II	4635.3 (5)	2?
He I	4387.9 (30)	1?	[*Fe* II]	4639.7	2?
Fe II	4389.4 (1)		*Fe* II	4657.0 (1)	2
Ti II	4395.0 (150)	1	*Fe* II	4666.8 (2)	2
Ti II	4399.8 (100)	1	*Sc* II	4670.4 (300)	
Fe II	4402.9 (2)		*He* I	4713.1 (3)	1?
[*Fe* II]	4413.8	3	*He* I	4713.4 (1)	
Fe II	4413.6 (10)		*Fe* II	4731.4 (3)	3
[*Fe* II]	4416.3	3	*Fe* II?	4734.1 (3)	
Fe II	4416.8 (7)		[*Fe* II]	4774.7	2
Fe II	4431.6 (1)	1?	[*Fe* II]	4814.6	2
Ti II	4443.8 (125)	2	*Hβ*	4861.3 (500)	10
Fe II	4446.2 (1)		[*Fe* II]	4874.5	1?
Fe II	4449.7 (1)	3	[*Fe* II]	4905.4	2?
Fe II	4451.5 (4)		*He* I	4921.9 (4)	5
[*Fe* II]	4452.1		*Fe* II	4923.9 (12)	
Fe II	4455.3 (3)	2	*He* I	5015.7 (100)	3?
[*Fe* II]	4457.0		*Fe* II	5018.4 (12)	

λλ 4244, 4287, 4359, and 4414, appear as emission lines at nearly all phases, while the weaker lines appear only near minimum. The strength of these lines relative to the surrounding continuum shows the same reciprocal relation to the light-curve as was previously described for the other emission lines.

At the time of minimum light the most conspicuous features of the spectrum of W Ser are the numerous emission lines. These are shown in Plate XI. It has been possible to account for all of these lines in a very satisfactory manner. No features of even moder-

ate strength are left unidentified, and no lines which might reasonably be expected to appear are absent (Table 4). The presence of helium is indicated by the coincidence of several emission lines with the strongest predicted lines of *He* I. *He* I 4026 probably accounts for a moderately strong emission line appearing at this position at almost all phases. Attention is also called to the peculiar emission features identified with the lines *Si* II 3853.7 and 3856.0 and with *Si* II 3862.6 and *Fe* II 3863.4 and 3863.9. Both of these emission features appear as broad hazy lines with no central absorption.

Of exceptional interest is the behavior at minimum of [*Fe* II] 4277. Before minimum it is abnormally faint, when compared to [*Fe* II] 4244 and [*Fe* II] 4287. After minimum it gains in intensity, and at phase 0.5 day it is equal to [*Fe* II] 4287. This is undoubtedly caused by a relative velocity shift of [*Fe* II] and the neighboring absorption line, which is probably *Cr* I + *Cr* II 4275. Before minimum the emission lines tend, in general, to be shifted a little more to the violet than do the absorption lines. For example, this renders the space between [*Fe* II] 4287 and the strong absorption line on its red side greater at phase 13.3 days than at phase 0.2 day. The suspicion is strong that the absorption line λ 4275 cuts into the emission of [*Fe* II] 4277, because the former is not weakened by the superposition.

VII. DISCUSSION

It is interesting to compare W Ser with the two peculiar eclipsing systems—SX Cas and RX Cas. Both of these are systems of supergiants having an A star and a G star. In SX Cas the light of the gA6 star predominates in the spectrum at all times outside of the principal eclipse. In RX Cas the light of the gG3 star predominates to the red of λ 4000, and the light of the gA5e star predominates to the violet of this position. The spectrum of both systems shows emission lines which become greatly enhanced at the time of minimum. The emission lines reveal the effects of an eclipse of an approaching stream of gas just prior to mid-eclipse and of a receding stream just after mid-eclipse. From the phases at which the eclipses of these gaseous streams take place and from the amount of dilution, Struve concludes that the streams extend to a height above the surface of the A star of the order of one or two radii of the star. In both systems a distortion of the velocity-curve of the A star is attributed to the projection of these streams upon the disk of the A star with a consequent blending of the absorption lines of star and shell. In both systems the principal minimum occurs when the A star is being eclipsed by the G star. In the system of W Ser it is the star whose spectrum we observe which is being eclipsed at the time of principal minimum; however, the interpretation of the spectrographic behavior is complicated by several factors: (1) The presence of a secondary component is not revealed by the spectrum at minimum or by the behavior of any of the wide variety of absorption lines investigated. (2) The light-curve is so peculiar that it does not reveal the presence of a secondary minimum, and thus we cannot check $e \cos \omega$ by an independent method as was found so useful in the study of SX Cas. (3) The gaseous shell involved in W Ser is probably at a considerably greater height than in either SX Cas or RX Cas. This is indicated by (*a*) the presence of emission lines of [*Fe* II], which were not in emission in the other two stars; (*b*) the behavior in W Ser of the bright H edges, which do not reveal the eclipse of gaseous streams moving relatively close to the surfaces of the two stars; and (*c*) the possible effect of dilution. We have seen that there are reasons to suspect that the velocity-curve does not represent the actual motion of the center of mass of the star. The very close agreement between the velocity-curves derived from lines of very different behavior is difficult to account for on the picture that the lines are blends of star and shell lines. The bright hydrogen edges do reveal that from 12 to 2 days the emission comes principally from a part of the shell which is receding with respect to the absorption lines and from 3 to 8 days from a part of the shell which is approaching. In SX Cas and RX Cas the central absorption of the *H* lines is weakened at both or at one elongation, respectively. This behavior was interpreted as

due to the emission from gas moving at right angles to the line of sight. In W Ser the central absorption is weakened at principal minimum and at about 8 days.

It is probable that W Ser is a peculiar binary whose principal component is surrounded by a shell (or thick atmosphere). The measured velocities represent the motions of those parts of the shell which lie in front of the bright star at the time of observation. They cannot be interpreted in the usual manner as representing the motion of the center of gravity of one component. The outstanding fact is that at minimum light the absorption shows a large velocity of approach, with respect to the emission lines of *H*. The emission lines probably come from different levels in the shell. Thus the permitted *Fe* II lines are broader than the forbidden [*Fe* II] lines, and the former are centrally reversed, while the latter are not. The components of the permitted *Fe* II lines show much less asymmetry than those of the *H* lines. Some features observed in W Ser resemble those of VV Cephei.

I am greatly indebted to Dr. O. Struve, who suggested this interesting problem and who has given me very valuable advice during its progress. I also wish to express my thanks to the other members of the Yerkes staff for helpful discussions and to Mrs. M. Carlson, Miss A. Johnson, Miss G. Peterson, and to my wife, Grace, for aid in the computations.

SPECTROGRAPHIC OBSERVATIONS OF PECULIAR STARS. VII*

P. SWINGS‡ AND O. STRUVE
McDonald Observatory
Received December 23, 1944

ABSTRACT

A list of emission lines is given for VV Cephei in the region λλ 3100–3370 and for BF Cygni in the region λλ 3114–3889. The spectrum of the Be star MWC 56 has strong emission lines of *H* and *Fe* II. Forbidden [*Fe* II] is weakly present. Table 3 lists the radial velocities of Z Andromedae from September, 1939, until October, 1944. The spectra of the components of the double star MWC 451 have been obtained separately. One component has a typical shell-absorption spectrum.

THE ULTRAVIOLET SPECTRUM OF VV CEPHEI

Measures of wave lengths in the ultraviolet region, down to λ 3277, were recently published by Struve.[1] Because of the wealth of emission lines in the ultraviolet region, we have measured a spectrogram of small dispersion secured on January 19, 1942. The results are given in Table 1.

In the identification work considerable importance was attached to the excitation level. This is especially important for *Fe* II,[2] in which lines of low excitation which are weak in the laboratory (arc or spark) are strong in VV Cep, while strong arc or spark lines corresponding to higher excitation are absent in VV Cep (see also next section on BF Cyg). Especially strong in this region are *Fe* II, $a^4P-z^4D^o$, $a^4D-z^6D^o$. Similar considerations apply to other atoms, such as *Cr* II.

In the table the elements are given in the order of their importance. The table overlaps a little with Struve's table.

The identification of [*Ni* II] 3223.3, a^2D-a^2G, as a contributor to the stellar line is trustworthy; [*Cr* II] would require sharper lines (or higher resolution) to be sure. There is no evidence of [*Mn* II] or [*V* II]. The difficulty of finding new forbidden lines arises from the numerous permitted metallic lines.

THE ULTRAVIOLET SPECTRUM OF BF CYGNI

The spectrum of this star, from λ 3722 to λ 6678, has been recently described by Merrill.[3] We have measured several spectrograms taken at the McDonald Observatory, which extend the ultraviolet limit to λ 3114. Table 2 contains the results. Our spectrograms were taken in the summer of 1942, when, according to Merrill, *Fe* II and [*Fe* III] were of intermediate intensity; [*Fe* II] was relatively weak. We have already given some of our results for *Fe* I, II, [II], and [III] in an earlier paper.[4] On our spectrograms [*Ne* III] is absent. The following notes summarize the essential points derived from the new measurements. The suggested identifications of [*Fe* II], [*Cr* II], [*V* II], etc., are based upon our unpublished tables of forbidden lines of metals.

[*Fe II*].—In addition to the new [*Fe* II] lines published earlier,[4] there are other [*Fe* II] lines contributing to blends in the UV region. But [*Fe* II] was relatively weak in 1942, and the contributions to blends are difficult to ascertain. It would be useful to take spectrograms of this star at other times in the UV region, to supplement the data obtained from the series collected by Merrill in the region λ > 3722. At stages of strong [*Fe* II] it would

* *Contributions from the McDonald Observatory, University of Texas*, No. 103.

‡ Now engaged in war research in Pasadena, California.

[1] *Ap. J.*, **99**, 70, 1944.

[2] See our paper, *Ap. J.*, **97**, 208, 1943.

[3] *Ap. J.*, **98**, 334, 1943.

[4] *Op. cit.*, p. 194.

TABLE 1

EMISSION LINES IN THE REGION λλ 3100–3370 OF VV CEPHEI

λ	Int.	Identification
3102.7	1	*V* II 2.30 (2000)
3104.9	1	*Ti* II 5.08 (100), *Mg* II 4.75 (30), *Ti* II 4.59 (15), *Fe* II 5.17 (5)
3108.8	0	*Cr* II 8.65 (35), *Ti* II 8.93 (15)
3116.5	1n	*Cr* II 6.74 (35), *Cr* II 5.65 (40), *Fe* II 6.59 (6)
3123.8	1	[*Fe* II] 4.18, (*Fe* II 3.71 (1))
3133.0	1	*Cr* II 2.06 (125), *Fe* II 3.05 (4)
3135.3	0	*Cr* II 5.74 (30), *Cr* II 5.34 (25), *Fe* II 5.36 (9)
3144.8	2	*Cr* II 5.10 (35), *Ti* II 4.73 (20), *Fe* II 4.76 (5)
3147.1	0	*Cr* II 7.23 (150), *Fe* II 6.75 (2)
3153.4	3	*Cr* II 3.35 (20), *Fe* II 4.21 (12), *Fe* II 3.06 (2)
3162.2	8	*Fe* II 1.94 (5), *Ti* II 2.57 (200), *Fe* II 3.09 (5), *Ti* II 1.77 (150), *Cr* II 2.44 (10), *Fe* II 2.80 (8), [*Fe* II] 2.21
3166.8	7	*Fe* II 6.70 (4), *Fe* II 7.85 (11)
3176.9	0	*Fe* II 7.53 (10), *Fe* II 7.26 (1), *Fe* II 6.73 (0)
3178.8	1	*Ti* II 8.63 (25), *Fe* II 9.50 (8), *Fe* II 7.53 (10)
3182.7	3	*Fe* II 3.11 (8), *Cr* II 3.32 (150), *Ti* II 2.57 (40)
3185.5	5	*Fe* II 6.74 (11), *Fe* II 5.32 (5)
3192.6	8	*Fe* II 2.93 (9), *Fe* II 3.81 (11), (*Fe* II 2.06 (3))
3195.9	10	*Fe* II 6.08 (10), (*Ti* II 5.72 (20))
3202.4	1	*Ti* II 2.54 (200), *Cr* II 2.51 (15), ([*Cr* II] 2.0)
3209.6	5	*Fe* II 0.45 (10), *Cr* II 9.18 (125), [*Fe* II] 9.94, *Fe* II 9.60 (1)
3212.6	10	*Fe* II 3.31 (13), (*Ti* II 13.14 (25)), ([*Cr* II] 12.5)
3217.4	2	*Ti* II 7.06 (150), *Cr* II 7.40 (20), [*Fe* II] 7.51
3223.9	1	[*Ni* II] 3.3, *Ti* II 4.24 (150), [*Fe* II] 2.58, [*Fe* II] 4.54, *Fe* II 3.44 (1)
3227.2	10	*Fe* II 7.75 (13), ([*Fe* II] 7.0)
3232.6	2	*Ti* II 2.28 (100), *Fe* II 2.79 (7)
3237.9	1	*Fe* II 7.82 (8), *Fe* II 7.40 (5), ([*Cr* II] 8.8)
3243.5	0	*Fe* II 3.72 (8), [*Fe* II] 4.2
3246.9	1	*Fe* II 7.17 (9), *Fe* II 7.39 (3), *Cr* II 7.33 (8)
3255.6	9	*Fe* II 5.89 (8)
3258.4	2	*Cr* II 8.77 (50), *Fe* II 8.77 (10), *Fe* II 9.05 (10), (*Fe* II 7.89 (3))
3271.4	0	*V* II 1.12 (1200), *Ti* II 1.65 (125)
3277.2	15	*Fe* II 7.35 (9), ([*Fe* II] 7.08), ([*Fe* II] 7.5)
3281.1	10	*Fe* II 1.30 (7)
3289.2	3	*Fe* II 9.35 (7), ([*Fe* II] 9.5), ([*Fe* II] 9.76)
3296.0	7	*Fe* II 5.82 (6), *Cr* II 5.43 (200)
3303.4	3	*Fe* II 3.47 (4), *Fe* II 2.86 (4), [*Fe* II] 3.8
3307.5	0	*Cr* II 7.04 (30), *Ti* II 7.72 (12)
3322.5	3	*Ti* II 2.94 (300), *Fe* II 3.07 (8)
3340.1	1	*Cr* II 9.80 (150), *Ti* II 0.34 (100), ([*V* II] 0.37)
3347.6	3	*Cr* II 7.84 (125)
3353.2	2	*Cr* II 3.13 (50)
3358.8	3	*Cr* II 8.50 (200), *Fe* II 8.78 (pred.), *Fe* II 8.25 (3)
3366.4	1	*Ti* II 6.18 (50), *Fe* II 6.96 (3)

TABLE 2

EMISSION LINES IN BF CYGNI

λ	Int.	Identification
	Spectrogram QQ f/2 3120 (July 21, 1942)	
3114.3	0	*Fe* II 4.29 (7)
3125.8	0	*Cr* II 4.98 (100), (*Cr* II 5.02 (15)), (*Cr* II 5.46 (7)), (*Fe* I 5.65 (400)), (*V* II 5.28 (600))
3128.8	0	*Cr* II 8.70 (40), *Ti* II 8.64 (70), (*Fe* II 9.01 (1))
3149.8	1n?	(*Cr* II 9.83 (20)), (*Cr* II 0.11 (20))
3162.6	1	*Fe* II 3.09 (5), *Fe* II 1.94 (5), *Ti* II 1.77 (150), *Ti* II 2.57 (200), [*Fe* II] 2.21, (*Cr* II 2.44 (10)), (*Fe* II 2.80 (8))
3179.2	1–0	*Fe* II 9.50 (8), (*Ti* II 8.63 (25))
3183.1	2	*Fe* II 3.11 (8), (*Ti* II 2.57 (40)), (*Cr* II 3.32 (40), (*Zr* II 2.86 (35))
3185.5	1–0	*Fe* II 5.31 (5), (*Si* III 5.16 (3)), (*Si* III 6.01 (2))
3187.8	1	*He* I 7.74 (200), *Fe* II 6.74 (11), (*Fe* II 7.29 (8)), (*V* II 7.72 (200))
3190.6	1?	*Ti* II 0.87 (200), *V* II 0.69 (500), (*Fe* II 1.37 (1)), (*Fe* II 0.84 (pred.))
3193.2	3	*Fe* II 2.93 (9), *Fe* II 3.81 (11)
3196.3	4	*Fe* II 6.07 (10), (*Fe* I 6.93 (500)), (*Cr* II 6.96 (20)), (*Si* III 6.50 (3))
3198.9	0	(*Cr* II 8.00 (15))
3203.5	0	*Cr* II 3.53 (15), (*Fe* II 3.51 (1)), (*Fe* II 3.74 (0)), (*Si* II 3.89 (2))
3210.7	3n	*Fe* II 0.45 (10), (*Si* II 0.04 (3)), (*Si* III 0.52 (3)), [*Fe* II] 9.94, [*Fe* II] 0.74
3213.7	4	*Fe* II 3.31 (13)
3217.4	0	*Cr* II 7.44 (50), *Ti* II 7.06 (150), *V* II 7.12 (400), (*Cr* II 6.55 (20)), ([*Fe* II] 7.51)
3227.8	4	*Fe* II 7.73 (13)
3233.5	1	*Cr* II 4.06 (50), (*Fe* II 2.79 (7)), (*Si* III 4.00 (5)), (*Fe* I 3.97 (300)), (*Fe* II 4.92 (0))
3239.3	0	*Ti* II 9.04 (300), *Cr* II 8.77 (50), *Fe* I 9.44 (400), ([*Cr* II] 8.8), ([*Fe* III] 9.7)
3247.8	0	*Cr* II 7.33 (8), (*Fe* II 7.17 (9)), (*Fe* I 8.21 (200)), (*Fe* II 7.39 (3))
3256.0	4	*Fe* II 5.89 (8), ([*Fe* II] 6.3), ([*Fe* II] 6.7)
3259.2	1	*Fe* II 8.77 (10), *Fe* II 9.05 (10), *Cr* II 8.77 (30), ([*V* II] 9.25)
3273.5	0	(*Fe* II 3.50 (3)), (*Zr* II 3.04 (75)), ([*V* II]3.98)
3277.6	10	*Fe* II 7.35 (9), ([*Fe* II] 7.08), ([*Fe* II] 7.5)
3281.6	3	*Fe* II 1.30 (7), (*Ti* II 2.33 (150)), ([*V* II] 1.59)
3285.1	1	*Fe* II 5.42 (3), (*Fe* II 5.00 (0)), ([*V* II] 4.98).
3295.6	1	*Fe* II 5.82 (6), (*Cr* II 5.43 (50)), ([*V* II] 5.69)
3303.3	1	*Fe* II 2.86 (4), *Fe* II 3.47 (4), ([*Fe* II] 3.8), ([*V* II] 2.13), ([*V* II] 2.93), ([*V* II] 2.61)
3312.9	0	*Fe* II 2.71 (1), *Cr* II 2.18 (40), *Cr* II 1.93 (40), *Cr* II 3.08 (20)
	Spectrograms CQ 1517 and 1584 (July 6 and 18, 1942)	
3443.1	1n	*Ti* II 3.39 (35), *Ti* II 4.31 (150), *O* III 4.10 (5), (*Fe* II 2.24 (3)), (*Fe* II 3.83 (pred.))
3454.1	1	*Ni* II 4.16 (5), (*Fe* II 3.59 (2)), (*Cr* II 4.98 (35))

TABLE 2—*Continued*

λ	Int.	Identification
	Spectrograms CQ 1517 and 1584 (July 6 and 18, 1942)—*Continued*	
3459.7	0	*Mn* II 0.31 (75), *Mn* II 0.04 (8), (*Cr* II 9.29 (25)), ([*Fe* II] 0.2)
3471.0	0	*Ni* II 1.35 (2), (*Fe* II 0.24 (1))
3475.4	0	*Cr* II 5.13 (20), *Fe* I 5.45 (400), *Fe* II 5.74 (pred.), *Fe* II 5.25 (pred.)
3482.6	2	*Mn* II 2.90 (40), *Cr* II 2.58 (12), (*Fe* II 2.43 (2))
3484.0	0	*Cr* II 4.15 (20), *Ti* II 3.80 (70), (*Fe* II 4.35 (1)), ([*Fe* II] 4.0)
3488.8	0	*Mn* II 8.68 (40), *Fe* II 7.99 (3)
3494.7	3nn	*Fe* II 3.47 (10), *Fe* II 4.67 (5), *Fe* II 5.62 (4), *Cr* II 5.37 (25), *Cr* II 5.56 (20), *Mn* II 5.83 (40), (*Ni* II 5.6 (pred.))
3501.4	1	(*Co* II 1.73 (200)), ([*Fe* II] 1.6)
3507.9	1	*Fe* II 7.39 (3), *Fe* II 8.21 (1)
3511.5	0	*Cr* II 1.84 (35), *Ti* II 0.84 (125), (*Fe* II 1.25 (pred.))
3513.9	1	*Ni* II 3.93 (8), *Fe* I 3.82 (400)
3576.4	0	([*V* II] 6.20), ([*Fe* II] 5.7), (*Ni* II 6.76 (3)), (*Zr* II 6.88 (20))
3585.3	1	*Cr* II 5.31 (60), *Cr* II 5.54 (40)
3589.9	0	*V* II 9.74 (1000), (*Si* III 0.46 (8))
3601.0	0	(*Y* II 0.73 (300))
3614.3	0	*He* I 3.64 (30), *Fe* II 4.87 (5), *Sc* II 3.84 (70), (*Cr* II 3.21 (20)), (*Cr* II 3.26 (15)), ([*V* II] 3.84), (*Zr* II 4.79 (18))
3664.8	1	*H* 28 4.68, (*Cr* II 4.95 (30)), ([*Fe* II] 4.7)
3665.8	1	*H* 27 6.10
3667.6	3	*H* 26 7.68
3669.4	3	*H* 25 9.47
3671.2	4	*H* 24 1.48
3673.6	6	*H* 23 3.76
3676.2	7	*H* 22 6.36
3677.5	3	*Cr* II 7.69 (40), *Cr* II 7.93 (30), *Cr* II 7.86 (50)
3679.3	8	*H* 21 9.35
3682.5	10	*H* 20 2.81
3685.2	0–1	*Ti* II 5.19 (700), (*Cr* II 4.25 (25))
3686.6	12	*H* 19 6.83
3688.5	1	.....
3691.4	15	*H* 18 1.56 (2)
3694.9	2	(*Cr* II 4.97 (4)), (*Fe* I 5.05 (200))
3697.0	15	*H* 17 7.15 (3)
3699.6	1	.....
3701.5	1	(*Fe* I 1.09 (300)), (*V* II 0.34 (200))
3703.6	15	*H* 16 3.85 (4)
3705.4	3nn	*Fe* I 5.57 (700), *He* I 5.00 (30), (*Ti* II 6.23 (125))
3709.6	1	[*Fe* II] 9.1, *Fe* I 9.25 (600), (*Zr* II 9.27 (60)), (*V* II 0.29 (150))
3711.9	18	*H* 15 1.97 (5)
3715.1	2	*Cr* II 5.19 (20), *V* II 5.48 (1200), *Cr* II 5.45 (20)
3719.6	1	*Fe* I 9.93 (1000), (*Fe* II 0.17 (pred.))
3721.8	20	*H* 14 1.94 (6)
3725.5	1n	*Fe* II 5.30 (3)
3727.3	1–2	*Cr* II 7.37 (40), *Fe* II 7.04 (4), *V* II 7.35 (1000), (*Fe* I 7.62 (200))
3729.7	0	.....
3733.6	1	*Fe* I 3.32 (400), *He* I 2.86 (10), (*V* II 2.76 (800))
3734.3	20	*H* 13 4.37 (8)

TABLE 2—*Continued*

λ	Int.	Identification
	Spectrograms CQ 1517 and 1584 (July 6 and 18, 1942) —*Continued*	
3736.8	(3)	*Fe* I 7.13 (1000), [*Fe* II] 6.2, (*Cr* II 6.56 (1))
3741.6	1	*Ti* II 1.65 (200), (*Fe* II 1.56 (pred.))
3743.1	1	(*Fe* I 3.36 (200))
3745.6	2n	*Fe* I 5.56 (500), *V* II 5.81 (800), (*Fe* I 5.90 (150))
3748.4	3	*Fe* I 8.26 (500), *Fe* II 8.49 (8), (*Cr* II 8.68 (7)), (*Ti* II 8.00 (25))
3750.0	20	*H* 12 0.15 (10)
3754.4	0–1	*Cr* II 4.57 (20), (*Fe* II 5.56 (4)), (*Cr* II 5.13 (2))
3757.9	1	*Fe* I 8.23 (700), *Ti* II 7.69 (100)
3759.9	1	*Ti* II 9.30 (400), *Fe* II 9.46 (6), *O* III 9.87 (9), (*Fe* I 0.05 (150))
3761.5	2n	*Ti* II 1.32 (300), (*Cr* II 1.90 (8)), (*Cr* II 1.69 (7))
3764.1	2	*Fe* II 4.09 (pred.), *Fe* I 3.79 (500)
3766.9	0	*Fe* I 7.19 (500), *Fe* II 6.05 (2), (*Zr* II 6.83 (25)), (*Cr* II 6.65 (4))
3770.5	20	*H* 11 0.63 (15)
3773.6	2	Unidentified; also present in Z And
3777.6	0	.....
3779.7	1	[*Fe* II] 9.3, (*Fe* II 9.58 (pred.)), (*Fe* I 9.45 (100))
3783.3	3	*Fe* II 3.35 (4)
3785.7	1–2	(*Fe* II 6.37 (pred.)), (*Fe* I 5.95 (125))
3788.2	0–1	*Fe* I 7.88 (500), (*Y* II 8.70 (30))
3791.7	1	*Si* III 1.41 (3)
3795.7	2	*Si* III 6.11 (4), *Fe* I 5.00 (500)
3797.8	20	*H* 10 7.90 (20)
3805.4	3	*Fe* I 5.34 (400), (*He* I 5.76 (3))
3806.6	4	*Si* III 6.56 (5), *Fe* I 6.70 (200), ([*Fe* II] 6.3), (*Fe* II 6.82 (pred.))
3812.9	1–2	*Fe* I 2.96 (400), (*Ti* II 3.39 (20))
3814.3	1–2	*Fe* II 4.12 (4), *Ti* II 4.58 (35), *Cr* II 4.00 (12)
3815.8	1–2	*Fe* I 5.84 (700)
3818.6 3819.9	2A} 4E}	*He* I 9.61 (50), (*Fe* I 0.43 (800))
3822.0	1–0	*Fe* II 1.92 (pred.), *Fe* II 2.74 (3)
3824.8	3	*Fe* II 4.91 (3), (*Fe* I 4.44 (150))
3826.9	0	*Fe* II 7.08 (4)
3829.5	1	*Mg* I 9.35 (100)
3832.2	3	*Mg* I 2.31 (250), (*Fe* II 2.96 (2))
3835.3	30	*H* 9 5.39 (40)
3838.2	3	*Mg* I 8.26 (300)
3843.0	1	(*Mn* II 2.98 (1)), (*Zr* II 3.03 (30)), (*Fe* I 3.26 (125))
3848.3	2–3	*Mg* II 8.24 (10)
3850.2	3	*Fe* I 9.97 (500), *Mg* II 0.40 (5)
3853.1	1	*Si* II 3.67 (3), (*Fe* I 2.57 (150))
3856.0	6	*Si* II 6.03 (8), *Fe* I 6.37 (500)
3859.4	0	*Fe* I 9.92 (1000), *Fe* I 9.22 (100)
3862.5	4	*Si* II 2.59 (6)
3865.5	1–2	*Cr* II 5.59 (75), *Fe* I 5.5 (600)
3867.5	0	*He* I 7.48 (15), (*Fe* I 7.22 (150))
3872.3	3	*Fe* I 2.50 (300), *Fe* II 2.76 (pred.), (*Fe* I 1.75 (100)), (*He* I 1.82 (5))
3878.6	1	*Fe* I 8.02 (400), *Fe* I 8.57 (300), *V* II 8.71 (300)
3882.0	0n	*Ni* II 1.92 (1), ([*Fe* II] 2.7)
3886.5	1	*Fe* I 6.28 (600)
3887.4 3888.7	5A} 35E}	*H* 8 9.05 (60), *He* I 8.65 (1000)

become a source of interesting results, since [*Ni* II], [*Cr* II], etc., would probably also reach their maximum intensity at the same time.

Fe II.—The enhancement of the lines of low excitation potential is such that identifications must proceed very cautiously. Sometimes a weak laboratory line, or even a predicted one, of low excitation potential plays a greater role than a very strong laboratory line of higher excitation potential.

Si II.—As usual, λλ 4128-4131 are weak compared with λλ 3856-3863.

Fe III.—No permitted line observed (excitation level in the star is too low).

[*Fe III*].—Since the $3d^5D-3d^3F$, ^3P transitions are very intense,[5] the absence of $3d^5D-3d^3D$ (λ 3239, λ 3368, etc.) may at first appear strange. For a full discussion of the problem it would be essential to know the transition probabilities of the three multiplets $^5D-^3F$, ^3D, ^3P of [*Fe* III]. Such numerical data would also be of help in spectroscopic studies of novae or nebulae. But it may well be that a low transition probability is not required for the $^5D-^3D$ multiplet relative to $^5D-^3F$, ^3P to explain its absence in the spectra of shell stars. The excitation potential of $3d^3D$ is 3.8 volts, while those of ^3P and ^3F are 2.5 and 2.7 volts, respectively. An increase in excitation potential by 1.1 volts will probably correspond to a considerable decrease in population on the excited level. There is every reason to believe that the excitation of the [*Fe* III] lines is mainly due to collisions, as is that of the *Fe* II lines. In the case of *Fe* II the enhancement of the lines of low excitation potential suggests a reduction in line intensities by a factor of at least 10, relative to laboratory intensities, when the excitation potential increases by 1 volt. A similar reduction is brought about in the Boltzmann populations corresponding to an electron temperature of the order of 6000° when the excitation potential increases by 1 volt. (Such an electron temperature seems logical to adopt for shells of Be stars.)

It is true that forbidden lines of higher excitation are observed in BF Cyg, as, for example, the strong [*O* III] line at λ 4363, e.p. 5.33 volts; but this is probably due to the high abundance of oxygen as compared to iron.

[*Ni II*].—This was weak in 1942. But it must be strong at times (probably together with [*Fe* II]). In Merrill's paper there is an unidentified line at λ 4326.6 which is almost certainly the leading transition $\frac{5}{2}-\frac{5}{2}$ in the a^2D-b^2D forbidden multiplet of *Ni* II.[6] An unidentified line is also present in η Carinae at λ 4326.72. The line measured by Merrill at λ 4314 is, at least partly, due to the $\frac{7}{2}-\frac{9}{2}$ transition (λ 4314.9) in the a^4F-a^2G multiplet of [*Ni* II]. [*Ni* II] may also contribute to λλ 4200, 4314, and 4629 in Merrill's list (there is also a weak line at λ 4200.9 in η Car).

[*Mn II*].—The strongest multiplet to be expected, $4s^7S-a^5P$, falls in the region of λ 3340, which could not be measured on our plates. [*Mn* II] may be expected in [*Fe* II] stars or novae.

[*V II*].—A number of coincidences with predicted [*V* II] lines are found, but they are not convincing. One of the strongest forbidden lines of *V* II should be $a^5D_4-c^3F_4$ at λ 3334.66. An otherwise unidentified line has recently been found at λ 3334.69 in HD 45677.[7]

[*Cr II*].—The strongest line predicted at λ 3238.8; may participate in a blend at λ 3239.3, but this is not certain.

[*Ti II*], [*Co II*], [*Zr II*].—No lines are found in BF Cyg.

MWC 56

The star MWC 56 = MW 128[8] was discovered by Merrill, Humason, and Burwell[9] to have strong bright lines of *Hα*, *Hβ*, *Hγ*, and *Hδ*. These authors also state that "several indistinct maxima in the continuous spectrum may be additional bright lines." The spec-

[5] See Pl. XXII in Merrill's paper (*op. cit.*, opp. p. 337).

[6] Swings, *Pub. A.S.P.*, **55**, 276, 1943.

[7] *Ap. J.*, **98**, 90, 1943.

[8] $\alpha = 2^h35^m0$, $\delta = +60°\ 50'$, mag. 11.6, sp. Bep.

[9] *Ap. J.*, **76**, 178, 1932.

trum has apparently not been observed since 1932. Two spectrograms were obtained at the McDonald Observatory on October 15 and 17, 1944, with the Cassegrain quartz spectrograph giving a dispersion of 40 A/mm at λ 3933. The spectrum (Pl. XII) contains strong emission lines of *H*, which can be seen to *H* 19 or *H* 20. The emission lines of $H\gamma$, $H\delta$, $H\epsilon$, $H\zeta$, and perhaps one or two other members of the Balmer series are superposed centrally over very weak, broad absorption lines, which suggest that the underlying star may be a main-sequence object of type B. There are, however, no other absorption lines which can be identified with certainty; *He* I 4472 and 4026 may be present in absorption, but the lines are very indistinct. There are, however, numerous other emission lines. Most of them belong to *Fe* II. But forbidden [*Fe* II] is represented by λλ 4244, 4287, and 4359; other faint emission lines have been identified with *Ca* II K, *Si* II 3856 and 3863, *Ti* II 3761 and 4301, *Ni* II 4067, and *Mg* II 4481. The spectrum is intermediate between that of an ordinary Be star with bright *H* and *Fe* II and that of a peculiar star like Z Andromedae, where the forbidden lines are very strong. The radial velocity from the mean of all emission lines is −58 km/sec.

Z ANDROMEDAE

The increase in excitation reported in November, 1943,[10] has continued. The lines of [*Fe* VII] and [*Ne* V] were very strong on May 14 and October 5, 1944, while *Fe* I was extremely weak and *Fe* II somewhat weaker than on June 28, 1943. Of interest is the fact that, while the permitted lines of *Fe* II have decreased in intensity since June, 1943, the forbidden lines of [*Fe* II] have become stronger. We are therefore concerned not solely with changes in the conditions affecting the relative intensities of permitted and forbidden lines. The illustration in Plate XIII should be compared with that of Plate VIII in Volume 99 of this *Journal* to appreciate the significance of the spectral changes. As was recently pointed out by Merrill,[11] the radial velocities suggest changes with a recurrence of about 680 days. These changes are probably closely correlated with the changes in the relative intensities of the emission lines and with the observed changes in the brightness of the star. Prager[12] has given a period of 650 days for the variations in brightness. In order to supplement Merrill's velocity data, we have assembled in Table 3 his results and our recent measures. The scatter is very large: Merrill had already remarked that the "radial velocities derived from various groups of bright lines present a baffling complexity." But the general trend of his measurements is supported by the additional material. The tendency of *Ca* II K to give a more positive velocity than the other lines, at least since 1941, when the expanding-shell features had disappeared, may be caused by interstellar absorption. Incidentally, it is rather striking that when the *Ca* II K emission line was weak, as, for example, in October, 1944, there was no visible trace of an interstellar absorption line. It is probable that the distance of Z And is not very great and that its luminosity is considerably lower than that of an average star of class B0. Another point of interest consists in the systematic difference between *O* III and [*O* III]:

$$\text{Vel. of } O \text{ III} - \text{Vel. of } [O \text{ III}] = -28 \text{ km/sec}.$$

The wave lengths used for these lines were:

O III. . . . λ 3312.30	*O* III . . . . λ 3444.10
O III. . . . λ 3340.74	[*O* III]. . . . λ 4363.21

It is probable that the *O* III velocities and not those of [*O* III] are vitiated. The effect may be of instrumental origin and should perhaps not be regarded as physically significant.

MWC 451 = HDE 236970 = ADS 1934

Bidelman observed this double star in 1942 and found a composite spectrum similar to that of α Cygni, with helium lines, and suggested that the brighter component may be

[10] *Ap. J.*, 99, 209, 1944. [11] *Ap. J.*, 99, 23, 1944. [12] *Pop. Astr.*, 47, 335, 1939.

PLATE XII

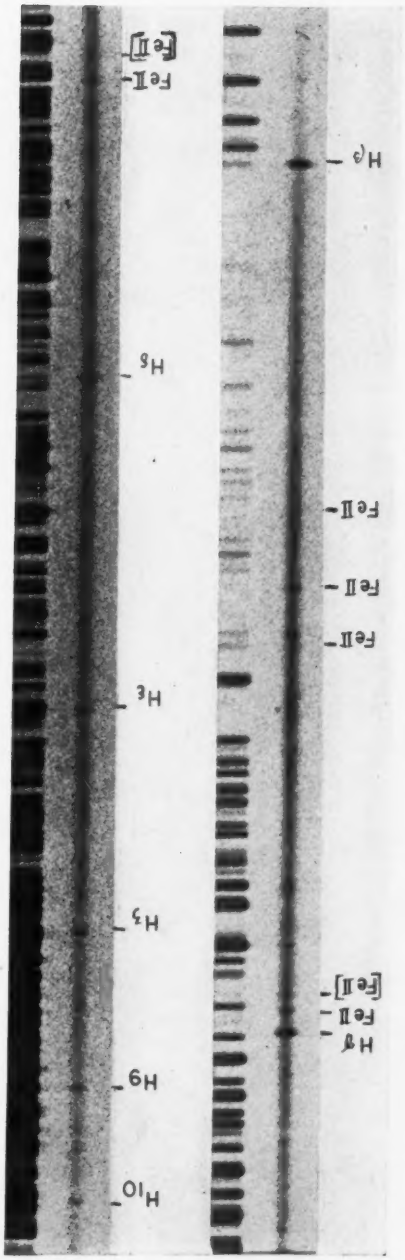

THE SPECTRUM OF MWC 56

PLATE XIII

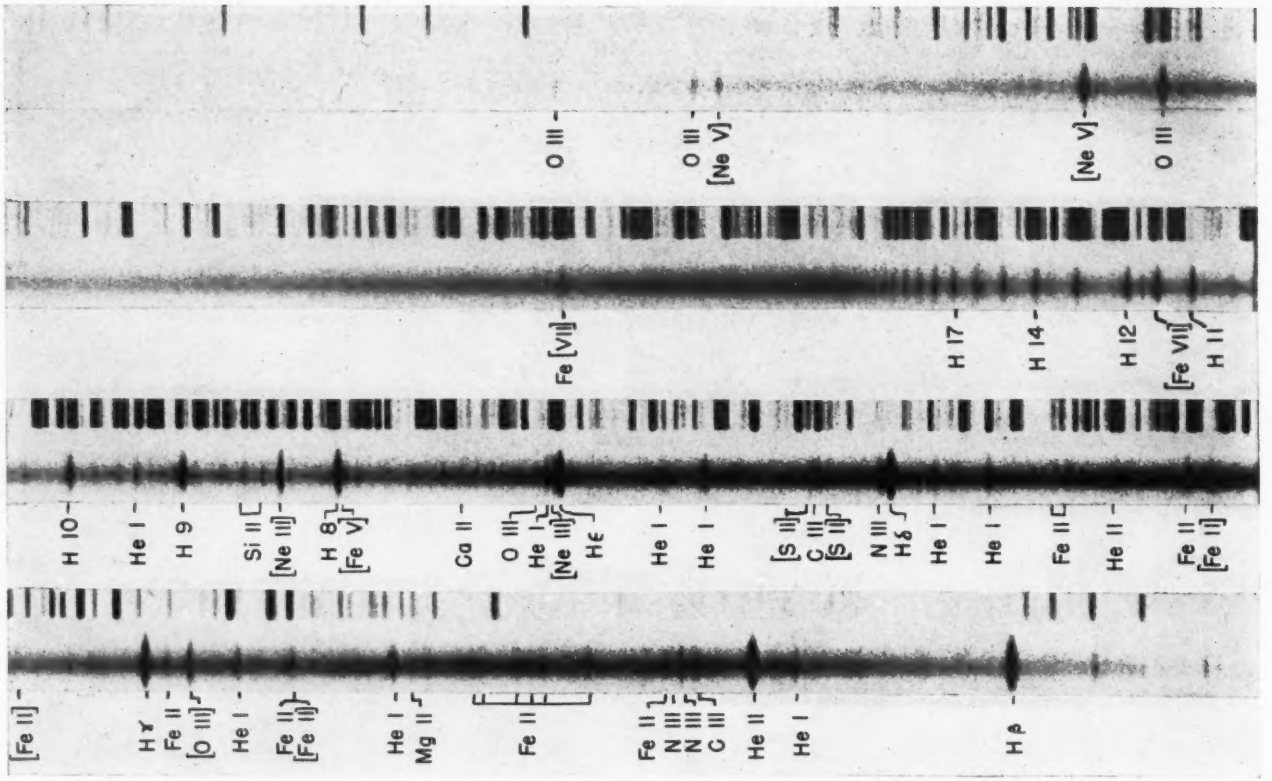

THE SPECTRUM OF Z ANDROMEDAE ON OCTOBER 5, 1944

a shell star, while the fainter might also be of type B. The separation is 0.8″, and the difference in magnitude is 0.5 mag., according to Van Biesbroeck, who also noted that the star appeared about as red as a G star. Bright *Hα* was discovered at Mount Wilson, and Bidelman noted that *Hβ* was abnormally weak on his spectrograms. On a night of good seeing (October 14, 1944) Dr. C. U. Cesco and one of the authors (Struve) obtained separate spectrograms of the two components. The visually fainter, blue star, which is the brighter of the two photographically, shows a typical shell spectrum with very sharp

TABLE 3

RADIAL VELOCITIES OF Z ANDROMEDAE

Obs.	Date	Mag.	Disp. at $H\gamma$ (A/mm)	*H*	*He* I	*Fe* II	*Ti* II	*Si* II	*Mg* II	*Ca* II	*O* III	[*O* III] λ 4363	[*Ne* III]	[*Ne* V]	[*Fe* VII]
	1939														
McD.	Sept. 16	8.1	60	+23	.....	+ 3	− 8	+ 8	.....	− 3	.....	.....	.....	.....	.....
Mt.W.	Oct. 3	7.8	75	(+38)	.....	.....	.....	.....	.....	.....	.....	.....	.....	.....	.....
Mt.W.	4	7.8	40	+40	.....	+10	+10	.....	.....	+23	.....	.....	.....	.....	.....
McD.	18	7.8	60	+60	.....	+35	+28	.....	.....	+36	.....	.....	.....	.....	.....
Mt.W.	23	7.9	40	+37	.....	+18	+28	.....	.....	+31	.....	.....	.....	.....	.....
McD.	Dec. 5	8.0	60	+59	.....	+42	+50	+62	.....	+28	.....	.....	.....	.....	.....
	1940														
Mt.W.	Jan. 20	8.3	40	+44	.....	+21	+18	+17	.....	+33	.....	.....	.....	.....	.....
Mt.W.	May 29	9.2	75	+42	(+ 5)	(+19)	.....	(+16)	.....	.....	.....	− 3	+12	.....	.....
Mt.W.	July 20	9.5	40	+28	+17	+ 1	+12	+ 6	.....	.....	.....	+ 6	+ 2	.....	.....
McD.	Aug. 15	?	60	+35	+21	−13	.....	+ 2	−16	.....	−50	+23	−10	− 2	+29
Mt.W.	Sept. 17	9.6	40	+ 7	+ 4	− 7	− 2	− 6	.....	+10	.....	− 2	+ 4	.....	.....
Mt.W.	Oct. 19	9.6	40	+ 5	+ 5	− 2	− 3	− 3	.....	+17	.....	− 6	+ 6	.....	.....
	1941														
Mt.W.	Jan. 15	9.6	75	− 3	− 9	−21	.....	−14	.....	− 6	.....	− 3	+ 2	.....	.....
Mt.W.	July 13	8.8	65	+ 2	+ 4	(−14)	−10	−13	.....	−14	.....	.....	−22	.....	.....
Mt.W.	14	8.8	40	+ 9	+ 5	− 6	− 8	.....	.....	.....	.....	−12	.....	.....	.....
McD.	25	?	60	+ 6	+28	−15	.....	−13	−25	+20	.....	−17	+11	.....	.....
McD.	Aug. 6	?	60	+14	+15	−11	.....	−13	−22	+19	−34	− 6	+ 5	.....	.....
Mt.W.	7	8.6	40	+ 7	+ 8	+ 1	− 2	+ 3	.....	+20	.....	− 7	− 7	.....	.....
McD.	Oct. 29	?	60	+23	+33	+ 2	.....	+25	.....	.....	.....	− 4	+ 4	.....	.....
McD.	Nov. 6	?	60	+ 8	.....	−13	.....	.....	.....	.....	.....	.....	.....	.....	.....
McD.	7	?	60	+21	+24	+ 7	+ 1	+19	.....	+34	−31	+ 4	− 4	+18	−14
Mt.W.	10	9.0	75	+19	+20	+ 9	.....	+14	.....	+28	.....	.....	−12	.....	.....
Mt.W.	Dec. 6	9.1	65	+16	+19	+ 9	.....	+11	.....	+45	.....	− 4	+ 2	.....	.....
	1942														
McD.	Jan. 14	?	60	+16	+30	0	.....	+ 3	.....	− 6	.....	− 7	+ 3	.....	.....
McD.	Feb. 1	?	60	+10	+ 1	−20	.....	+ 5	.....	+21	−21	−25	+11	−31	−24
McD.	July 15	?	60	+31	+28	+ 2	.....	− 1	.....	+48	− 6	+15	+ 9	+ 6	+ 1
Mt.W.	Oct. 23	10.2	65	−14	− 9	− 9	.....	+ 2	.....	+24	.....	− 5	− 2	.....	.....
McD.	Nov. 23	?	60	+ 6	0	0	.....	.....	.....	+28	−10	+36	+10	+ 2	−25
Mt.W.	Dec. 2	10.0	75	−16	+ 2	− 5	.....	(− 3)	.....	(+ 9)	.....	− 2	+ 8	.....	.....
	1943														
McD.	Jan. 21	?	60	−10	− 7	−12	.....	+ 2	+26	+12	−23	− 5	+ 5	+ 8	.....
McD.	June 28	?	60	−12	− 1	−10	−14	−20	−14	+10	−43	−10	−15	0	−56
Mt.W.	Aug. 11	9.1	65	− 9	− 2	− 9	−15	− 8	.....	+23	.....	−23	− 1	.....	.....
McD.	Nov. 14	?	60	+ 4	+ 4	− 1	0	0	.....	− 6	.....	− 6	+10	.....	.....
	1944														
McD.	May 14	?	60	− 2	+ 4	+ 1	.....	−27	.....	+16	− 6	+ 6	+10	+ 5	−23
McD.	Oct. 5	?	60	+ 1	− 3	− 6	.....	− 2	+17	+22	−10	+ 6	+14	+ 4	+ 1

and narrow absorption lines of *H* extending to *H* 28, with strong, sharp *Ca* II K and with narrow and weak lines of *Fe* II. In addition, there are broad lines of *He* I and *Mg* II. The visually brighter star has a normal spectrum of type around G5, or a little earlier. Since the photographic magnitude of this star must be considerably fainter than 10, our spectrogram is somewhat underexposed. There is, however, no indication that the luminosity is great: the *Sr* II lines are not conspicuous. Combined spectra of both components obtained without trailing, but with the slit placed along the line joining the two stars, confirm this result. Spectrograms obtained without trying to separate the components show very striking changes from night to night. We attribute these changes entirely to the effect of seeing combined with the tendency of the observer to guide on the visually bright G-type component.

SPECTROGRAPHIC OBSERVATIONS OF THE ECLIPSING VARIABLE AB PERSEI*

OTTO STRUVE
Yerkes and McDonald Observatories
Received January 11, 1944

ABSTRACT

The velocity-curve, derived from 25 spectrograms, is not consistent with the light-curve; and the orbital elements are probably affected by unknown causes: $P = 7.16$ days, $\gamma = -5$ km/sec, $K = 27$ km/sec, $e = 0.21$, $\omega = 226°$, and $T =$ phase 4.7 days after principal minimum. The spectrum changes in character: the *Ti* II lines are strong and sharp between phases 1 and 3 days, but they are weak and diffuse between phases 4.5 and 6.5 days. The range in the velocity-curve is small for an A5 star whose period is 7.16 days; and the mass function, $f(m) = 0.013\ \odot$, combined with the known inclination, suggests that the total mass is very small or that the mass ratio is very different from unity.

The eclipsing variable AB Persei = BD + 40°798 was discovered by A. S. Williams[1] and was extensively observed by him. The most recent photometric observations are by K. Lassovszky,[2] by F. Lause,[3] and by Mrs. C. Payne-Gaposchkin.[4] Lassovszky gave the following light-elements:

$$\text{Minimum} = \text{JD } 2422987.250 + 7.16025\ E\ .$$

Mrs. Payne-Gaposchkin computes the phases with the formula

$$\text{Phase} = 0.139660\,(\text{JD} - 2400000)$$

and finds that on JD 24000 the principal minimum occurred at phase 0.406 P. She notes that the period is variable. At the present time the phase of minimum should be about 0.385 P. Her instantaneous light-elements for JD 24,000 are

$$\text{Minimum} = \text{JD } 2424004.053 + 7.16025\ E\ .$$

All observers agree that there is a weak secondary minimum. The magnitude at maximum is[3] 9.4; at principal minimum, 10.2; at secondary minimum, 9.6. The total duration of eclipse is 0.75 day, and the duration of totality, 0.35 day. The principal elements of the system, as derived by Lassovszky, are

$k = 0.44$	$L_1 = 0.60$	$m_1 = 10.4$	$J_1/J_2 = 1/3.46$
$r_1 = 0.267$	$L_2 = 0.40$	$m_2 = 10.8$	$\rho_1 = 0.007\ \odot$
$r_2 = 0.117$			$\rho_2 = 0.082\ \odot$
$i = 87°$			

A set of elements by S. Gaposchkin[5] differs in the value of $k = 0.68$. The spectral type is given as F0 by R. S. Dugan[6] and as A4 by Gaposchkin;[5] A. B. Wyse[7] found A8.

Twenty-five spectrograms of AB Persei were obtained at the McDonald Observatory in 1943 and 1944 with the Cassegrain quartz spectrograph equipped with a 500-mm camera. The linear dispersion was 40 A/mm at λ 3930. The exposure time was about one hour. The spectrum is approximately of type A5, with strong and broad *H* lines. The lines of *Fe* II are present but are somewhat weak for this type; *Ti* II is strong, while *Fe* I and *Ca* I are relatively pronounced; *Mg* II and *Si* II are weak; *Ca* II is very strong. The spectrum belongs to the main sequence and is not peculiar at any time. But there seem

* *Contributions from the McDonald Observatory, University of Texas*, No. 105.

[1] *M.N.*, **84**, 442, 1924.

[2] *A.N.*, **252**, 221, 1934.

[3] *A.N.*, **260**, 289, 1936.

[4] Unpublished.

[5] *Variable Stars* ("Harvard Obs.," No. 5), p. 75, Cambridge, 1938.

[6] *Contr. Princeton U. Obs.*, No. 15, p. 12, 1934.

[7] Addenda to Dugan's "Finding List," *Contr. Princeton U. Obs.*, No. 15, 1936.

PLATE XIV

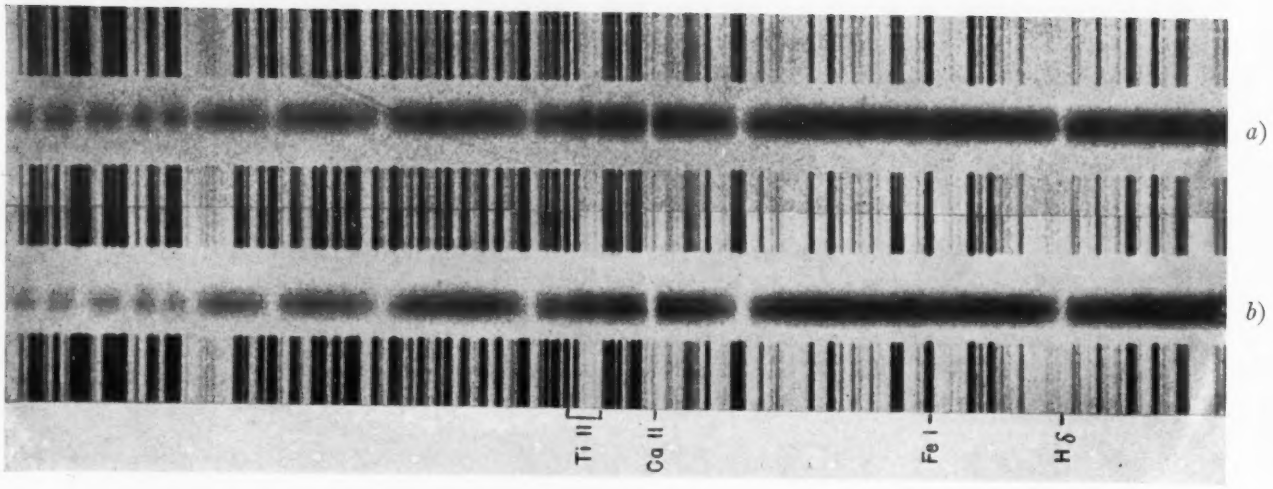

THE SPECTRUM OF AB PERSEI

a) Phase 2.115 days; *b*) phase 6.328 days after principal minimum

to be fairly conspicuous changes in the intensities and contours of some of the lines, and there is good evidence that these changes are periodic. Attention may be called to the great intensity and the sharpness of the lines of *Ti* II 3900 and 3913 at phases between 1 day and 3 days and to the weak and diffuse character of the same lines between phases 4.5 and 6.5 days. This is illustrated in Plate XIV. There is no simple explanation of this phenomenon, but it seems to affect all lines of *Ti* II and perhaps of other elements. It is impossible to decide whether the strong lines of *Ca* II and *H* are variable, but the available evidence favors the suspicion.

TABLE 1

RADIAL VELOCITIES OF AB PERSEI

Plate	Date	U.T.	JD	Phase in Days	Vel. (Km/Sec)
			2,431,+		
CQ 2537	1943 Nov. 6	9:05	034.878	6.667	−10
2598	9	9:59	037.916	2.545	−25
2638	11	9:23	039.891	4.520	−27
2639	11	10:41	039.945	4.574	−42
3891	1944 Oct. 7	6:57	370.790	6.047	+ 2
3917	10	6:22	373.775	1.872	± 0
3931	11	5:32	374.731	2.828	−15
3939	12	9:35	375.899	3.996	−35
3950	13	5:29	376.729	4.826	+10
3966	14	7:05	377.795	5.892	+14
3980	15	7:18	378.804	6.901	− 9
3991	16	7:17	379.803	0.740	+18
4006	17	7:33	380.815	1.752	+19
4019	18	4:58	381.707	2.644	−12
4075	Dec. 9	7:13	433.801	4.616	−21
4083	11	9:27	435.894	6.709	+ 1
4089	13	2:31	437.605	1.260	+13
4101	14	2:09	438.590	2.245	−20
4112	15	2:07	439.588	3.243	−26
4124	16	2:31	440.605	4.260	−34
4138	17	2:45	441.615	5.270	+ 1
4169	18	4:09	442.673	6.328	+33
4177	19	1:20	443.556	0.051	+10
4190	20	1:48	444.575	1.070	+23
4205	21	2:53	445.620	2.115	+ 7

The radial velocities are listed in Table 1. The phases were computed with Lassovszky's light-elements. The velocity-curve in Figure 1 shows a well-defined minimum at phase 4.0 days after principal minimum and a peculiar double maximum at 6.0 and 1.0 days. The scatter is reasonably small between phases 0.0 and 4.5 days but is very large between 4.5 and 6.5 days. This is probably due to the diffuseness of the absorption lines in the latter interval.

The velocity-curve presents some strange and as yet unexplained properties:

1. Principal minimum of light falls near the mid-point between two neighboring maxima or near the secondary minimum of the velocity-curve. The existence of this secondary minimum appears to me to be fairly certain, since it is based upon measurements of 4 accordant spectrograms. But if we should disregard it, we would have to conclude that principal light-minimum coincides with maximum radial velocity.

2. The total range of the velocity-curve is 54 km/sec, with a velocity of the center of mass at about −5 km/sec. This range is extraordinarily small for an eclipsing system of type A5 whose period is 7 days. It would presumably mean that the mass is small or that

the mass ratio is very different from unity. But, in view of the uncertainty as to the interpretation to be placed upon the variation in spectrum, it is not safe to draw definite conclusions.

3. If the secondary minimum of the velocity-curve is disregarded, the following orbital elements would satisfy the radial velocity measurements:

$\gamma = -5$ km/sec	T = phase 4.7 days
$K = 27$ km/sec	$a \sin i = 2.6 \times 10^6$ km
$e = 0.21$	$\frac{m_2^3 \sin^3 i}{(m_1 + m_2)^2} = 0.013\odot$
$\omega = 226°$	

It is again emphasized that these elements are not in accordance with the light-curve; and, since the latter is unquestionably that of a normal eclipsing variable, we must conclude that the velocity-curve is distorted by unknown causes.

4. The character of the distortion of the velocity-curve does not resemble the distortions previously found in U Cephei and SX Cassiopeiae. It is also at variance with all

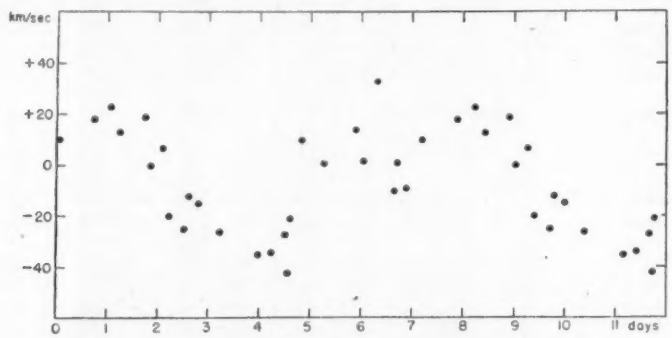

FIG. 1.—Radial velocities of AB Persei. The period is 7.16025 days

other velocity-curves of eclipsing variables investigated by us previously. The star is probably sufficiently important to deserve further attention from stellar spectroscopists.

5. The distortion of the velocity-curve is probably related to the peculiar variation in the appearance of the *Ti* II lines and perhaps of other lines. The diffuse character of the lines might conceivably be caused by the blending of two components of not too different spectral types. But at minimum radial velocity the lines are quite narrow and sharp, so that the explanation cannot be as simple as this.

6. One spectrogram, No. 4177, phase 0.051 day, was obtained when the star was visually observed through the finder of the 82-inch telescope and was recorded to have been very faint throughout the exposure. The spectral type on this plate is definitely later than A5: the lines of *H* are weaker, those of *Ca* I and *Ca* II much stronger than at maximum light. I estimate the type of the secondary component to be about F5. This is probably consistent with the values of Δm_1 and Δm_2. If the values of L_1 and L_2 are as close to each other as those given by Gaposchkin, namely, $L_1 = 0.55$ and $L_2 = 0.45$ (presumably in visual light), then there could well be some blending of the lines of the two components, and the puzzle would be why there is no such blending near minimum radial velocity.

I am indebted to Professor Richard Prager, who furnished important references; to Mrs. C. Payne-Gaposchkin, who sent me her unpublished photometric results; and to Drs. Carlos U. Cesco, Jorge Sahade, and S. Gaposchkin, who have taken part in the observations at the telescope.

PLATE XV

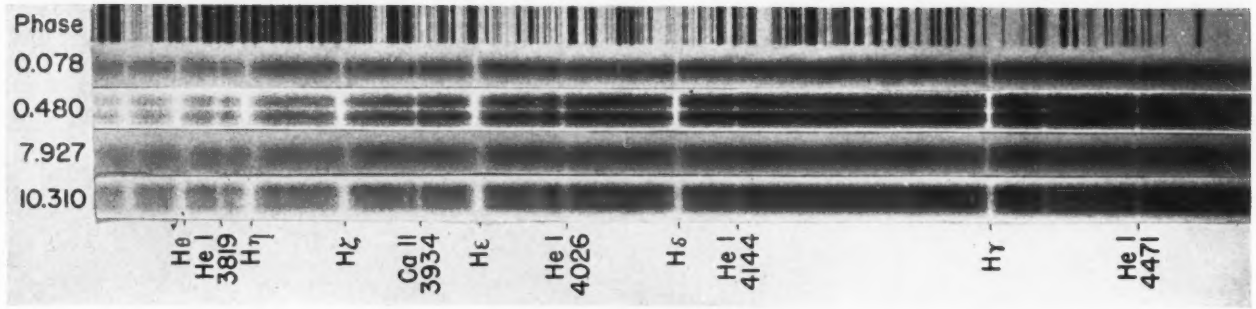

SPECTRA OF AU MONOCEROTIS

THE SPECTROSCOPIC ORBIT OF AU MONOCEROTIS*

JORGE SAHADE AND CARLOS U. CESCO
Yerkes and McDonald Observatories
Received January 11, 1945

ABSTRACT

The system of AU Monocerotis is formed by a B5 star, which is partially eclipsed at the principal minimum, and a star of type near F0 whose spectrum is observed only during eclipse. The orbital elements derived from the *He* I lines are the following: $K = 32.2$ km/sec; $\omega = 340°$; $e = 0.13$; $\gamma = +11.8$ km/sec; $a \sin i = 4.9 \times 10^6$, km; and $f(m) = 0.04 \odot$. The velocity-curve which corresponds to these elements, drawn through the measurements from the *H* lines and the appearance of the spectrograms between phases 8.776 and 10.505 days, suggests the existence of a flow of relatively cool gas from the atmosphere of the secondary star toward the B5 component—a phenomenon which is similar to the one described by Struve for SX Cassiopeiae.

The star BD−1°1449 (8.5 mag.) = AG Nic 1909 (8.8 mag.) = HD 50846 (Sp. B5) was announced in 1931 by Hoffmeister[1] to be an eclipsing variable of the Algol type and was provisionally designated as 41.1931. Its variability in light was confirmed afterward by Rügemer.[2] The first light-elements of AU Monocerotis were derived by Florja[3] and are as follows:

Time of minimum.....	JD 2426743.12	*D*.....	25.1	hours
Maximum.....	8.28 mag.	*d*.....	0	hours
Principal minimum.....	9.35 mag.			

No secondary minimum was found.

In order to determine the spectroscopic orbit of AU Monocerotis, the star was included in the observing program of the 82-inch reflecting telescope of the McDonald Observatory and was observed through the months of January, February, and March, 1944. Additional observations were made in September and December of the same year.

The spectrograms—45 in number—were taken on Eastman 103a-O emulsion with the quartz Cassegrain spectrograph, which gives a dispersion of 40 A/mm at λ 3393. At maximum light the exposure time was about 30 minutes in fair seeing.

The spectrum of AU Monocerotis, taken at maximum light, corresponds to one of the components which is of type B5 and shows the interstellar line of *Ca* II K. Two plates, taken during the eclipse, show the secondary component. The classification of both spectra was made with the kind assistance of Dr. W. W. Morgan, who described the spectrogram taken at phase 5.841 (CQ 3013) as follows:

B5, from *He* I and *Mg* II. The lines are broad. *N* II 3995 is weak and the star is definitely not a supergiant. The *H* lines are narrower than in the B5 V star τ Ari; on the other hand, they are of the same order of intensity as in the B5 IV star τ Her, but have a different appearance (the wings at $H\delta$ and $H\epsilon$ are less pronounced in AU Monocerotis). While the spectrum is probably abnormal with respect to the *H* lines, AU Monocerotis can best be described at maximum as a main sequence B5 star ($M \sim -1.5$). From the intensity of the interstellar K line a distance of between 400 and 800 pc is estimated; this factor also rules out the probability of the primary star's being a supergiant.

Dr. Morgan classified the secondary component as being a star of type near F0.

The *H* lines show changes in the different phases (Pl. XV). The spectrograms taken

* *Contributions from the McDonald Observatory, University of Texas*, No. 106.

[1] *A.N.*, **242**, 129, 1931. [2] *A.N.*, **247**, 325, 1933.

[3] *Veränderliche Sterne*, **5**, 106, Gorki, U.S.S.R., 1937; *Sternberg Astr. Int. Pub.*, Vol. **8**, Part II, 1937.

during eclipse show a deep core. After eclipse the *H* lines become stronger and shallower; and, beginning with the plate taken at phase 8.776 and ending with the one at phase 10.505, they are broad and seem to have flat bottoms. On some of the plates taken during this interval the *H* lines look double. The plate taken at phase 8.776 gave a very high positive velocity, both for the *He* I and *H* lines; on this plate the *H* lines seem to have a sharp red component, while the *He* I lines do not show anything unusual.

In Table 1 are listed the lines measured for radial velocity. The plotting of the measurements was made separately for each element, namely, *He* I and *H*, because of the changes noted in the *H* lines. The period adopted for this purpose was 11.1126 days, which was determined by Lause[4] and which agrees better with the spectroscopic observations than the one previously found by Florja[3] (11.1107 days). Table 2 gives the measured radial velocities.

TABLE 1

LINES MEASURED FOR RADIAL VELOCITIES

H	*He* I	*Ca* II
3797.90	3819.64	3933.67
3835.39	4026.22	
3889.05	4143.76	
3970.08	4471.51	
4101.74		
4340.47		

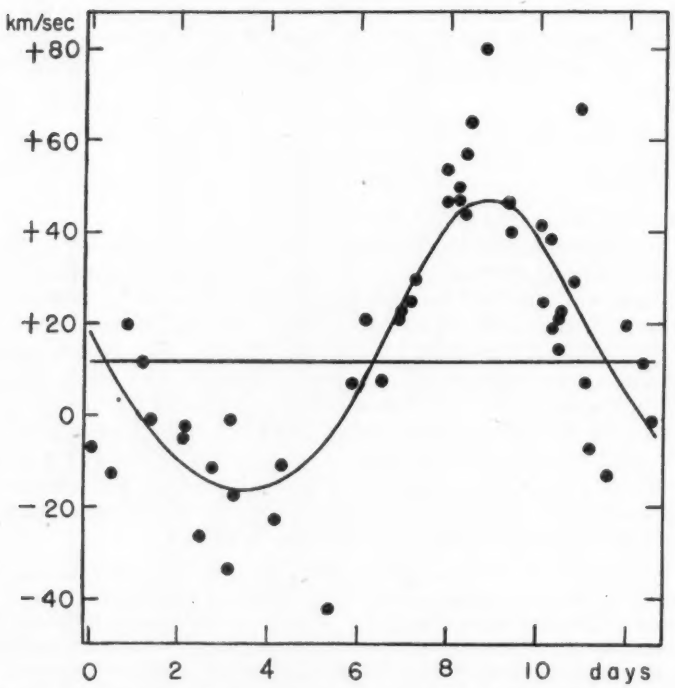

FIG. 1.—Radial velocities from the *He* I lines

Figure 1, which corresponds to the measurements of the *He* I lines, suggests a velocity-

[4] *Krakow Obs. International Suppl.*, No. 16, p. 59, 1938.

TABLE 2

MEASURED RADIAL VELOCITIES

PLATE	DATE 1944	U.T.	PHASE (IN DAYS)	RADIAL VELOCITIES IN KM/SEC FROM—		
				He I*	*H*	*Ca* II K
CQ 2865	Feb. 12	4:12	0.078	− 7.0	+ 10.8	+ 16.1
2764	Jan. 21	8:27	0.480	−15.1	+ 8.5	+ 22.0
3057	Mar. 17	6:19	0.828	+19.9	+ 36.4	+ 34.7
2875	Feb. 13	7:01	1.195	+11.4	+ 8.6	+ 33.6
2769	Jan. 22	5:46	1.368	+ 1.1	+ 17.3	+ 31.8
4210	Dec. 21	8:42	2.113	− 5.0	− 14.5	+ 4.7
2883	Feb. 14	6:37	2.179	−12.1	+ 11.6	+ 32.6
2776	Jan. 23	8:09	2.468	−26.1	− 16.3	+ 57.7
2999	Mar. 8	2:52	2.797	−10.0	− 12.2	+ 10.9
2940	Feb. 26	7:28	3.102	−33.8	− 4.4	+ 23.2
2829	Feb. 4	3:26	3.159	− 2.7	− 19.6	+ 27.5
2891	Feb. 15	7:24	3.211	−17.6	− 11.2	− 9.0
2897	Feb. 16	6:12	4.161	−22.6	+ 3.5	+ 54.0
2783	Jan. 25	4:14	4.305	−11.2	+ 0.1	+ 71.7
3005	Mar. 10	6:20	4.942	−26.9	− 10.1	.....
2791	Jan. 26	5:47	5.369	−42.1	− 17.4	+ 44.5
3013	Mar. 11	3:55	5.841	+ 7.1	− 3.7	− 21.1
2909	Feb. 18	6:33	6.176	+20.8	+ 1.3	+ 35.8
2793	Jan. 27	8:29	6.482	+ 2.7	+ 12.4	.....
3022	Mar. 12	4:48	6.878	+21.1	+ 27.1	+ 25.1
2956	Mar. 1	3:30	6.936	+22.7	+ 13.0	+ 37.6
2916	Feb. 19	6:16	7.164	+24.8	+ 34.8	.....
2796	Jan. 28	3:02	7.255	+29.8	+ 27.9	+ 31.6
3033	Mar. 13	5:59	7.927	+53.5	+ 44.7	+ 3.5
2964	Mar. 2	3:28	7.935	+46.2	+ 42.4	+ 31.3
2921	Feb. 20	7:20	8.209	+49.8	+ 43.6	+ 37.2
2802	Jan. 29	4:45	8.326	+43.8	+ 46.6	+ 27.8
2838	Feb. 9	7:28	8.327	+56.8	+ 33.2	.....
2804	Jan. 29	7:38	8.446	+64.5	+ 40.1	+ 9.4
3042	Mar. 14	2:21	8.776	+80.0	+ 95.6	+ 88.9
4144	Dec. 17	7:02	9.156	.....	+101.2	+ 43.2
2853	Feb. 10	6:41	9.294	+46.2	+ 52.1	+ 28.8
2809	Jan. 30	6:20	9.392	+40.0	+ 48.9	+ 27.2
2811	Jan. 30	9:29	9.523	+14.9	+ 64.8	+ 69.7
2861	Feb. 11	1:35	10.082	+41.7	+ 52.3	+101.4
2973	Mar. 4	7:21	10.097	+24.7	+ 63.6	+ 45.6
3776	Sept. 20	11:51	10.257	+38.8	+ 70.4	+ 31.6
2814	Jan. 31	4:22	10.310	+18.6	+ 60.9	+ 79.7
2816	Jan. 31	6:39	10.405	+14.4	+ 68.6	+ 14.4
2756	Jan. 20	4:34	10.431	+21.2	+ 71.5	+ 99.9
2817	Jan. 31	7:21	10.434	+34.8	+ 66.0	.....
2818	Jan. 31	9:03	10.505	+22.8	+ 63.0	.....
3053	Mar. 16	1:46	10.751	+29.4	+ 76.3	+113.8
2977	Mar. 5	1:56	10.871	+66.8	+ 29.4	+ 27.6
2980	Mar. 5	5:55	11.037	+ 7.1	+ 15.7	+ 40.5

* We have taken into account only the plates on which it was possible to measure at least two lines.

curve much more symmetrical than the one indicated by the points in Figure 2. Owing to the fact that the *He* I lines do not show any change with phase, except that they are stronger at eclipse, we tried to derive approximate orbital elements of the B5 component of AU Monocerotis, applying the Wilsing-Russell method to values read off from a curve

TABLE 3

ORBITAL ELEMENTS OF AU MONOCEROTIS FROM THE *He* I LINES

$P = 11.1126$ days (assumed)
$K = 32.2$ km/sec
$\omega = 340°$
$e = 0.13$
$T =$ phase 8.29 days
$\gamma = +11.8$ km/sec
$a \sin i = 4.9 \times 10^6$ km
$\frac{m_2^3 \sin^3 i}{(m_1 + m_2)^2} = 0.04 \odot$

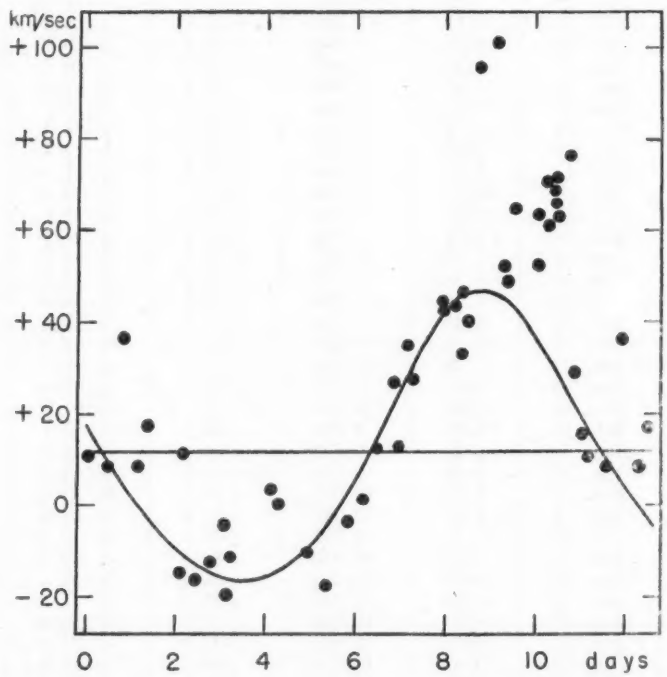

FIG. 2.—Radial velocities from the *H* lines and the velocity-curve derived from the *He* I lines

drawn in order to satisfy, in the best way, the plotted measurements. The elements obtained are listed in Table 3. The velocity-curve shows that the B5 star is eclipsed at principal minimum; the eclipse is not total, as we observe both components near mid-eclipse—a fact which agrees with Florja's light-curve.

When we drew the velocity-curve, which corresponds to the orbital elements, through the measurements from the *H* lines (Fig. 2), a group of points immediately after maxi-

mum positive velocity remains above the curve. This fact, together with the appearance of the *H* lines between phases 8.776 and 10.505, would suggest the existence of a mass of relatively cool gas (because the effect is absent in the *He* I lines) which would flow from the atmosphere of the F star toward the B5 star, a phenomenon which is similar to the one described by Struve[5] in the system SX Cassiopeiae.

The sharp interstellar *Ca* II K line suggests a velocity of about +30 km/sec. On a few plates at about phase 10.0 days the line is broader, and the measurements give values of the order of the velocity of the B5 star. In the principal minimum the *Ca* II K line is sharp and approximately as strong as in class A0.

We are indebted to Dr. O. Struve for suggesting the problem, to him and Dr. Helen Steel for taking a number of the spectrograms, and to Dr. W. W. Morgan for helping us in the classification of the spectra.

[5] *Ap. J.*, 99, 89, 1944.

THE SPECTRUM OF RZ SCUTI*

F. J. NEUBAUER AND OTTO STRUVE
Lick Observatory and McDonald Observatory
Received February 6, 1945

ABSTRACT

The velocity-curve of RZ Scuti has been derived from 128 spectrograms secured at the Lick and McDonald observatories. The orbital elements are $P = 15.19016$ days, $T = 2419643.07$, $K = 23.5$ km/sec, $\gamma = -28.3$ km/sec, $e = 0.05$, $\omega = 138°$, $a \sin i = 4{,}900{,}000$ km, $f(m) = 0.02\odot$. The mass function is very small for a B2 star whose period is 15 days. There is a very large rotational disturbance in the partial phases of the eclipse. The *He* I lines have a range of 250 km/sec; those of *H*, a range of only 100 km/sec. This shows that *H* forms a slowly rotating outer shell around a rapidly rotating reversing layer. At mid-eclipse the lines of *He* I and *Mg* II become so weak that they cannot be measured; *H* is also weakened but remains sharp and narrow. The spectrum of the secondary component of the system has not been observed.

The photometric orbit of the eclipsing variable RZ Scuti[1] was determined by Shapley in 1915[2] on the basis of a series of visual observations by Baker and Wylie.[3] Shapley remarked that "the scarcity of observations during principal minimum makes this solution quite uncertain." However, the photometric orbit suggests that "the star is remarkable because of the low density for a B-type spectrum." The magnitude of the star at maximum is 7.47. The observed primary range is 1.38 mag., and the secondary range is 0.025 mag. The eclipse is partial, the semiduration of the eclipse being 1.0 day and the parameter α_0 being 0.8. The luminosity of the brighter component is 0.9, and the semimajor axes are $a_b = 0.15$, $a_f = 0.22$. The inclination is $i = 77°$. Upon the basis of the same photometric orbit, S. Gaposchkin[4] has recently concluded that if the components obey the mass-luminosity relation the masses are $m_b = 21\ \odot$, $m_f = 8\ \odot$; the radii are $r_b = 13\ \odot$, $r_f = 25\ \odot$; the computed spectrum of the fainter component should be $Sp_f = G0$; the visual luminosity of the brighter component is 2.23 mag. greater than that of the fainter component; and the densities are given by $\log \rho_b = -1.98$, $\log \rho_f = -3.33$. The density of the fainter component rather definitely places it among the giants, but the density of the B-type component is only about ten times less than the average for its spectral class and is not exceptional.

A new light-curve based upon 1061 estimates on Harvard patrol plates has recently been published by S. Gaposchkin.[5] The photometric elements by Parenago,[6]

$$\text{Principal minimum} = \text{JD } 2419640.90 + 15.19016\ E\,,$$

satisfy the observations. The duration of the entire eclipse is 1.898 days = 0.125 P. The primary minimum gives $\Delta m_1 = 1.17$ mag., and the secondary minimum gives $\Delta m_2 = 0.05$ mag.

A somewhat different period ($P = 15.190201$ days) was observed by A. Soloviev;[7] but

* *Contributions from the Lick Observatory*, Ser. II, No. 10; also, *Contributions from the McDonald Observatory, University of Texas*, No. 107.

[1] HD 169753, $\alpha = 18^h21^m1$, $\delta = -9°15'$ [1900], Sp. B2k.

[2] *Contr. Princeton U. Obs.*, No. 3, 1915.

[3] *Laws Obs. Bull.*, No. 20, 1913.

[4] *Proc. Amer. Phil. Soc.*, **82**, 291, 1940; *Harvard Reprints*, No. 201.

[5] *Harvard Bull.*, No. 917, p. 15, 1943, and private information.

[6] *A.N.*, **238**, 212, 1930.

[7] *Astr. Circ. Acad. Sci. U.S.S.R.*, No. 29, April 10, 1944.

PLATE XVI

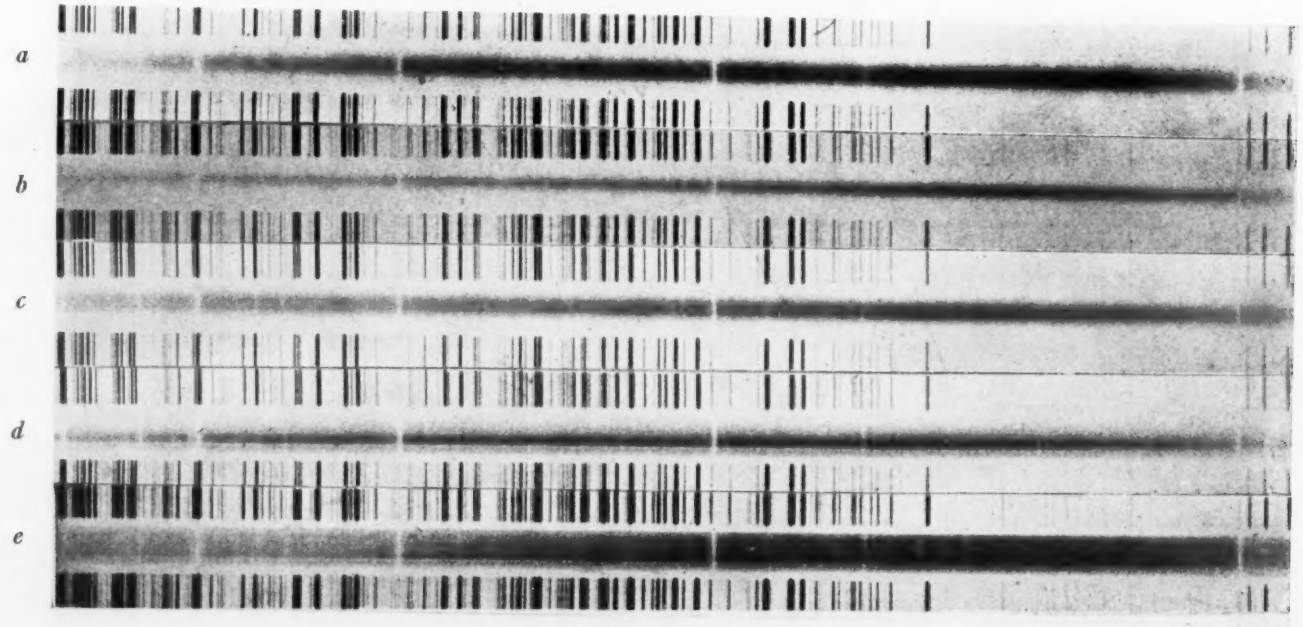

THE SPECTRUM OF RZ SCUTI

(*a*) Phase 11.366; (*b*) phase 15.158; (*c*) phase 0.047; (*d*) phase 0.151

TABLE 1

THE OBSERVATIONS

DATE*	PHASE	VELOCITY			*Ca* II	JD 2430000+
		H	*He* I	Mean		
44 July 20	0.034	− 64.1	−125.1	− 94.6	.....	1291.781
44 May 5s	0.047	29.6	190.2	140.6	−16.4	1215.849
44 May 5s	0.151	52.9	166.6	144.9	−13.2	1215.953
44 July 5s	0.179	73.6	158.9	130.0	− 5.4	1276.736
37 July 10	0.234	100.7	176.7	138.7	.....	8724.844†
44 July 5s	0.247	68.4	150.5	109.4	− 2.9	1276.804
44 July 5	0.251	56.9	157.7	107.3	.....	1276.808
38 July 25	0.360	79.9	111.0	95.4	.....	9104.725†
38 July 25	0.374	110.7	109.3	110.0	.....	9104.739†
44 Sept. 19	0.381	96.2	153.4	124.8	.....	1352.692
44 Aug. 5s	0.730	47.6	79.9	67.0	+ 1.8	1307.658
44 Aug. 5	0.752	52.5	46.4	49.4	.....	1307.690
44 May 6s	0.976	32.5	61.0	51.6	−10.6	1216.778
44 July 21s	0.994	46.3	62.9	54.6	.....	1292.742
44 May 6s	1.146	34.8	66.7	54.0	−24.3	1216.948
44 July 6s	1.173	35.6	41.4	38.5	− 0.2	1277.731
44 July 6s	1.206	37.7	59.3	48.5	−12.5	1277.764
39 June 10	1.459	41.9	24.6	33.2	.....	9424.818†
39 June 10	1.477	65.9	42.3	54.1	.....	9424.836†
44 July 22	1.939	43.3	102.2	72.8	−29.6	1293.687
44 May 7s	2.052	36.2	39.9	38.4	−18.4	1217.854
44 May 7s	2.076	44.0	33.4	37.6	−19.9	1217.878
39 June 26	2.150	32.4	72.7	52.6	.....	9440.698†
39 June 26	2.163	50.2	52.6	51.4	.....	9440.711†
44 July 7s	2.204	48.6	64.4	56.5	− 3.8	1278.762
44 July 7s	2.231	43.7	46.5	45.1	−10.0	1278.789
44 May 8s	2.985	35.9	58.2	49.2	− 7.7	1218.787
44 May 8s	3.005	19.1	68.0	50.4	−14.0	1218.807
39 June 27	3.146	72.7	81.5	77.1	.....	9441.694†
39 June 27	3.160	85.7	30.0	57.8	.....	9441.708†
44 Aug. 8	3.736	26.1	48.6	37.4	−21.6	1310.674
44 May 9s	3.988	64.2	61.8	62.8	−25.1	1219.790
44 May 9s	4.095	56.6	34.8	43.6	−14.6	1219.897
44 July 9	4.145	45.4	37.6	41.5	.....	1280.702
39 June 28	4.149	39.5	.....	39.5	.....	9442.697†
39 June 28	4.163	40.5	.....	40.5	.....	9442.711†
44 July 9	4.185	31.7	38.9	35.3	−42.1	1280.742
44 July 9	4.211	34.2	38.6	36.4	−27.5	1280.768
39 June 13	4.407	89.1	81.5	85.3	.....	9427.766†
39 June 13	4.419	24.5	82.9	53.7	.....	9427.778†
44 Aug. 9s	4.698	65.2	50.8	57.2	−17.9	1311.636
44 Aug. 9	4.735	40.5	33.0	36.8	−59.2	1311.673
44 July 25s	4.924	39.7	55.6	49.3	−21.1	1296.677
44 July 25s	4.939	65.0	59.1	63.0	.....	1296.692
44 May 10s	5.121	34.2	83.8	63.9	− 8.7	1220.923
44 July 10	5.142	38.3	65.5	51.9	.....	1281.699
44 July 26	5.950	31.1	33.9	32.5	.....	1297.698
44 May 11s	6.079	47.0	42.4	44.2	− 3.0	1221.881
44 May 11s	6.159	34.4	34.2	32.2	−18.4	1221.961
44 Aug. 11s	6.695	21.2	55.1	41.6	+ 5.8	1313.634
44 Aug. 11s	6.728	− 21.4	− 43.1	− 34.5	− 6.5	1313.663

* An "s" denotes Struve's measures of the McDonald plates. † Denotes 2,420,000+ recorded number of the Julian day.

TABLE 1—*Continued*

Date*	Phase	Velocity			*Ca* II	JD 2430000+
		H	*He* I	Mean		
44 May 12s.....	7.096	−28.1	−38.2	−34.1	−15.6	1222.898
44 May 12s.....	7.119	28.8	10.4	17.7	− 1.8	1222.921
44 July 12.....	7.139	37.7	51.1	44.4	.....	1283.696
44 July 12.....	7.171	52.5	47.6	45.0	.....	1283.728
44 Aug. 12.....	7.727	44.4	55.6	50.0	−39.1	1314.666
44 Aug. 12.....	7.750	39.2	34.5	36.8	−40.0	1314.689
44 Aug. 12.....	7.817	21.0	31.9	26.4	−26.8	1314.756
44 Aug. 12.....	7.838	37.9	43.3	40.6	−37.4	1314.777
44 Aug. 12.....	7.902	23.8	56.3	40.0	−48.3	1314.841
44 July 28s.....	7.924	18.3	24.2	21.8	+ 5.0	1299.672
44 Aug. 12.....	7.930	27.5	25.3	26.4	.....	1314.869
44 July 28s.....	7.942	− 20.6	− 21.6	− 21.1	+ 4.9	1299.690
44 May 13s.....	8.134	− 24.6	− 31.3	− 28.6	−11.2	1223.936
44 May 13s.....	8.152	− 31.7	− 11.6	− 19.6	−15.9	1223.954
44 Aug. 13s.....	8.694	+ 4.1	− 21.6	− 8.8	− 1.0	1315.633
44 July 29s.....	8.957	− 20.3	+ 23.4	+ 5.9	−13.7	1300.705
44 July 29s.....	8.976	+ 5.2	− 17.2	− 12.6	− 4.6	1300.724
44 July 29.....	8.997	− 20.4	− 7.8	− 14.1	−27.0	1300.745
44 May 14s.....	9.004	− 19.2	+ 24.0	+ 5.0	− 2.3	1224.806
44 May 14s.....	9.018	− 9.4	+ 3.4	− 3.7	− 0.8	1224.820
44 July 30.....	9.901	− 28.3	− 25.3	− 26.8	−26.2	1301.649
44 July 30s.....	9.930	+ 4.8	− 16.2	− 6.6	− 0.4	1301.678
44 July 30s.....	9.954	− 15.6	− 35.5	− 14.6	− 4.2	1301.702
44 May 15s.....	10.119	+ 5.4	+ 36.8	+ 24.8	− 4.4	1225.921
44 July 15.....	10.131	− 26.0	+ 14.0	− 6.0	.....	1286.688
44 May 15s.....	10.136	+ 13.8	+ 37.0	+ 27.1	− 4.6	1225.938
44 Apr. 30s.....	10.372	+ 15.2	− 49.8	− 0.8	+ 1.7	1210.984
44 Aug. 15.....	10.723	− 28.6	− 18.0	− 23.3	+31.0	1317.622
44 July 31s.....	10.896	− 18.6	− 5.6	− 13.8	+16.0	1302.644
44 July 31s.....	10.924	+ 1.2	− 12.2	− 7.2	+ 3.9	1302.672
44 July 31.....	10.942	− 67.4	+ 75.4	+ 4.0	.....	1302.690
44 May 1s.....	11.366	− 9.4	− 6.8	− 7.6	− 9.3	1211.978
44 Aug. 1s.....	11.900	− 32.6	− 15.5	− 22.5	− 2.5	1303.648
44 Aug. 1s.....	11.929	− 16.3	− 22.8	− 19.7	− 5.7	1303.677
44 Aug. 1.....	11.994	− 8.4	− 82.1	− 45.2	.....	1303.742
38 Aug. 6.....	12.310	− 6.1	− 26.2	− 16.2	.....	9116.675†
38 Aug. 6.....	12.324	− 2.0	− 14.4	− 8.1	.....	9116.689†
44 July 2s.....	12.364	− 5.7	− 22.3	− 15.7	− 4.4	1273.731
44 May 2s.....	12.364	+ 7.5	− 4.5	+ 2.0	−18.6	1212.976
44 July 2s.....	12.395	+ 24.1	− 10.9	+ 3.1	+ 4.2	1273.762
44 Sept. 16.....	12.514	+ 12.7	+ 16.4	+ 14.6	.....	1349.645
39 June 6.....	12.656	+ 20.3	+ 36.2	+ 28.2	.....	9420.825†
39 June 6.....	12.681	+ 31.1	+ 44.5	+ 37.8	.....	9420.840†
44 Aug. 2s.....	12.888	+ 11.4	+ 44.3	+ 31.1	+ 3.1	1304.636
44 Aug. 2s.....	12.913	+ 20.4	+ 15.1	+ 17.2	− 6.1	1304.661
44 Aug. 2s.....	12.936	+ 21.7	− 7.9	+ 6.9	+ 6.0	1304.684
44 July 18.....	13.141	+ 5.7	+ 28.7	+ 17.2	−16.2	1289.698
44 May 3s.....	13.341	+ 5.7	+ 55.3	+ 31.8	− 8.2	1213.953
44 July 3s.....	13.368	+ 45.9	+ 36.6	+ 41.3	+13.5	1274.735
44 July 3s.....	13.407	+ 35.7	+ 24.6	+ 31.7	− 1.8	1274.774

TABLE 1—*Continued*

Date*	Phase	Velocity			Ca II	JD 2430000+
		H	*He* I	Mean		
44 Aug. 18.....	13.747	+ 23.4	+ 45.4	+ 34.4	.....	1320.686
44 Aug. 18.....	13.768	+ 40.4	− 31.9	+ 4.2	.....	1320.707
44 Aug. 3s.....	13.890	+ 37.0	+ 30.9	+ 34.0	.....	1305.638
44 Aug. 3s.....	13.918	+ 45.4	+ 66.3	+ 52.0	.....	1305.666
44 Aug. 3.....	13.932	+ 13.6	+ 2.5	+ 8.0	.....	1305.680
44 July 19.....	14.132	+ 30.8	− 13.6	+ 8.6	−37.8	1290.689
39 June 23.....	14.342	− 7.2	+ 3.6	− 1.8	.....	9437.700†
44 July 4.....	14.351	− 4.8	+ 65.9	+ 30.6	.....	1275.718
44 July 4s.....	14.353	+ 40.6	+ 36.8	+ 38.7	− 5.3	1275.720
39 June 23.....	14.357	− 11.3	+ 14.7	+ 1.7	.....	9437.715†
44 July 4s.....	14.400	+ 32.9	+ 30.9	+ 31.9	+ 0.7	1275.767
44 July 4.....	14.411	+ 25.1	+ 78.1	+ 51.6	.....	1275.778
44 Sept. 18.....	14.502	+ 19.7	− 21.8	− 1.0	.....	1351.633
44 Sept. 3.....	14.520	+ 43.6	+ 44.7	+ 44.2	.....	1336.650
44 Sept. 3.....	14.545	+ 49.0	+ 24.2	+ 36.6	.....	1336.675
39 June 8.....	14.645	+ 66.7	+ 17.7	+ 42.2	.....	9422.814†
39 June 8.....	14.666	+ 61.7	+ 95.2	+ 78.4	.....	9422.835†
44 Aug. 4s.....	14.899	+ 51.6	+130.4	+108.8	+14.4	1306.647
44 Aug. 4s.....	14.941	+ 32.2	+136.4	+ 94.7	− 7.0	1306.689
44 Aug. 4.....	14.951	+ 49.8	+100.6	+ 75.2	.....	1306.699
44 Aug. 4s.....	14.983	+ 30.0	+135.2	+108.7	−13.2	1306.731
44 Aug. 4.....	15.014	+ 28.9	+101.3	+ 65.1	.....	1306.762
44 July 20s.....	15.112	− 7.8	+133.6	+ 39.4	.....	1291.672
44 July 20.....	15.138	− 21.9	−122.4	− 72.2	.....	1291.698
(44 May 5s.....	15.158	− 20.2	.....	− 20.2	− 0.7	1215.770) ‡
44 July 20s.....	15.164	− 52.1	−134.1	− 93.1	.....	1291.724
44 July 20.....	15.184	− 40.2	−102.4	− 71.3	.....	1291.744

‡ Mid-eclipse.

since it does not accord well with the spectrographic observations, we have not used it in this paper.

The radial velocity of RZ Scuti has been observed by Neubauer at the Lick Observatory.[8] From 21 spectrograms he derived a mean velocity of −29.0 km/sec and a range of 170 km/sec.

In his "Finding List for Observers of Eclipsing Variables"[9] Dugan gave the total duration of eclipse as 80? hours and listed this duration as a "point of interest."

Because of its relatively long period and possible giant characteristics, RZ Scuti was placed upon the spectrographic program of the McDonald Observatory, and a total of 66 spectrograms was obtained by Struve during the summer season of 1944. All plates, on Eastman 103aO emulsion, were taken with the Cassegrain quartz spectrograph and the 500-mm camera, giving a linear dispersion of 55 A/mm at $H\gamma$. The slit was kept at 0.05 mm, and the exposure times ranged from 10 to about 15 minutes, at maximum light.

After the first observations at McDonald Observatory had disclosed an unusually large rotational disturbance in the velocity-curve, these results were communicated to Neubauer at the Lick Observatory. The latter accepted an invitation to secure additional plates during the summer of 1944 and obtained 41 plates from July to September,

[8] *Ap. J.*, **97**, 308, 1943; *Contr. Lick Obs.*, Ser. II, No. 6.

[9] *Contr. Princeton U. Obs.*, No. 15, 1934.

1944. The spectrograph employed was the one-prism 12-inch camera attached to the 36-inch refractor, which gives a linear dispersion of 75 A/mm at $H\gamma$. Cramer High-Speed emulsion was used exclusively. Thus, the Lick material comprises a total of 62 plates, which, with the 66 radial velocities derived at the McDonald Observatory, makes a total of 128 spectrograms.

On the assumption that the spectroscopic period is the same as the photometric period given by Parenago, the determination of the spectroscopic elements is based upon the radial velocities given in Table 1. The observations in this table are arranged according

TABLE 2

NORMAL VELOCITIES

No.	Phases Included	Mean Phase	Number of Plates	*H* Lines	*He* I Lines	Mean Velocity Combined with *Mg* II and *He* I 4470.05	*Ca* II Velocity
1.....	15.138– 0.381	0.167	13	−66.7	−142.9	−110.2±6.8	− 7.7±2.0
2.....	0.730– 2.231	1.546	16	−43.3	− 56.0	− 50.3±1.8	−12.8±2.2
3.....	2.958– 4.939	4.061	18	−48.6	− 53.8	− 50.9±2.3	−25.1±3.2
4.....	5.121– 6.728	5.982	7	−32.5	− 51.1	− 43.0±3.0	− 6.2±3.4
5.....	7.096– 7.942	7.613	12	−31.6	− 36.7	− 33.5±2.1	−22.1±4.7
6.....	8.134– 9.954	9.064	11	−14.1	− 10.5	− 11.3±2.0	− 9.7±2.0
7.....	10.119–11.994	10.953	12	−14.3	− 4.1	− 7.5±3.9	− 2.7±3.2
8.....	12.310–12.395	12.351	5	+ 3.6	− 15.6	− 7.0±2.8	− 6.3±4.5
9.....	12.514–13.407	12.984	10	+21.1	+ 29.4	+ 25.8±2.5	− 1.4±2.5
10.....	13.747–14.545	14.211	15	+25.2	+ 25.1	+ 24.9±3.4	−14.1±8.1
11.....	14.645–15.112	14.901	8	+39.1	+106.3	+ 76.6±6.4	− 1.9±5.6

TABLE 3

SPECTROSCOPIC ELEMENTS

$$P \text{ (photometric)} = 15.19016 \text{ days}$$
$$T = \text{JD } 2419643.07 \text{ or } 2.170 \text{ days of phase of radial velocity-curve}$$
$$K = 23.5 \text{ km/sec}$$
$$\gamma = -28.3 \text{ km/sec}$$
$$e = 0.05$$
$$\omega = 138°$$
$$a \sin i = 4{,}900{,}000 \text{ km}$$
$$\frac{m_2^3}{(m_1 + m_2)^2} \sin^3 i = 0.020$$

to phase, in order to compare the radial velocities derived from the McDonald measures with the Lick radial velocities. The table also indicates the manner in which the observations were grouped in order to form normal places. In the first column is entered the Greenwich Civil date of the observation, and in the second column the corresponding phase for the period of 15.19016 days. The third and fourth columns give the velocity as derived from the hydrogen lines and the helium lines, respectively. The fifth column contains the mean weighted radial velocity. In the sixth column the interstellar *Ca* II velocity is listed. The last column gives the Julian day of the observation.

Table 2 shows the grouping of the data for normal places and is followed, in Table 3, by the orbital elements, which have been derived in the usual way. Little or nothing would be gained by a least-squares solution, in view of the few normal places upon which the curve is based—namely, six—with the addition of three radial velocities near mini-

mum light. These latter velocities are fairly certain, since Struve's measure of May 5, 1944, and the mean of the helium velocities shortly before and immediately after the minimum check. Also, the mean of the hydrogen lines shows a radial velocity which is almost the same for that epoch.

The spectrum[10] is variable. The Lick plates confirm this variability and show the usual lines that are found in an early class B star. The class is certainly not later than B3—perhaps a peculiar class B2, since there are traces of *Si* IV, too faint, however, to measure. No trace of a secondary spectrum can be detected on any of the plates. Struve's line, 4470.046,[11] is rather strong on some of the Lick spectrograms. Its displacement follows closely that of *He* I 4472. Although the scatter of the individual lines is large, the mean velocity is entitled to some weight. From the appearance of the spectrum one would expect a closer agreement, but the plates were measured with more than usual care and the scatter still remains. The spectrograms obtained at Lick before 1944 were measured by four different observers—Neubauer, Miss Roosen-Raad, Miss Blanche White, and Mrs. Delia M. Herbig—and the mean of the four measures was taken as the radial velocity. For the plates secured during the summer of 1944 there are at least two distinct

TABLE 4

RESIDUALS OF NORMAL VELOCITIES

Phase	Number of Plates	Residuals (O−C)
15.158	1	+4.5*
4.061	18	+0.7
5.982	7	−1.0
7.613	12	−5.8
9.064	11	+4.2
10.953	12	−1.8
12.351	5	−1.5
Total	66	.....

* Struve's one plate near mid-eclipse of May 5, 1944.

measures for each plate, one by Neubauer and one by Mrs. Herbig. The McDonald plates were all measured by Struve. From the radial velocities in Table 1 it is readily seen that the scatter of the McDonald measures is of the same order as that of the Lick measures.

Since the spectroscopic elements were based on only a partial velocity-curve, as shown in Figure 1, the elements are to some degree uncertain, but they are not inconsistent with the photometric data. The period of 15.19016 days is satisfied by the radial-velocity observations, and the small eccentricity is in line with the indication of the light-curve. It is possible that the orbit may be circular. The value of K is smaller than one might have expected for an eclipsing variable with this period and spectral class.

The spectrum is of type B2 or B3, with rotationally broadened lines of *He* I and *Mg* II and with fairly deep and well-defined lines of *H*. The lines of *Ca* II are sharp and strong; they are of interstellar origin. The *Mg* II line is usually quite weak and is difficult to measure. Hence the measurements are based mostly upon the lines of *H* and *He* I.

It is apparent from the velocity-curve that the B-type component is the one that undergoes eclipse at primary minimum of light. During the partial phases of the eclipse there is a very large rotational disturbance. This is especially well shown by the measure-

[10] Briefly described by Struve in *A.J.*, Vol. **51**, No. 3, 1944.

[11] *Ap. J.*, **42**, 198, 1925.

ments on May 5, July 20, and August 4, 1944. It is of great significance that this disturbance is different for the lines of *He* I and *Mg* II on one side and of *H* on the other. For *H* the total range of the disturbance is about 100 km/sec, while for *He* I and *Mg* II it is of the order of 250 km/sec. The latter range is only slightly smaller than that observed in U Cephei.[12] But with respect to the range of the rest of the velocity-curve, RZ Scuti shows by far the largest rotational disturbance yet observed.

It will be seen that the radius of the orbit of the B-type star, relative to the center of mass of the system, is about seven times the radius of the sun; and this is almost one-half of the radius of this component as computed by Gaposchkin. It will also be seen that the mass function is exceptionally small for a B-type spectroscopic binary. Since the spectrum of the secondary has not been observed, the mass ratio is not known from our data. If we make use of Gaposchkin's mass ratio $a = m_f/m_b = 0.38$, we find $m_1 = 0.7\ \odot$. This is incompatible with Gaposchkin's value for the mass, namely $m_1 = 21\ \odot$. It is

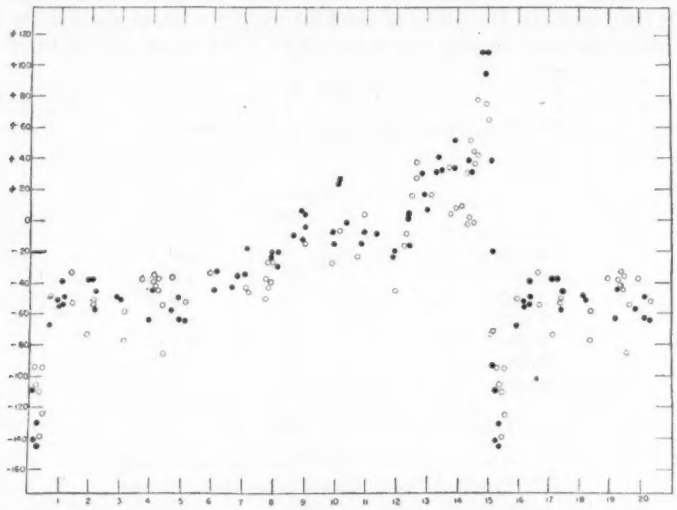

FIG. 1.—Individual radial velocities of RZ Scuti, using the means of all lines. ○ Lick Observatory; ● McDonald Observatory.

clear that only a much greater disparity in the masses of the two components will give for the B star a mass of the order of 20 ⊙. This discrepancy cannot be removed by any reasonable adjustment in the spectroscopic elements; the important thing is that the range in velocity (except during the rotational disturbance) is small, while the period is relatively long.

Between phases 12 and 14 days the velocity-curve is quite anomalous. The scatter is large, and the suspicion arises that the curve may not repeat itself exactly in this region. From the material under discussion we believe that there is no reason to suspect that the *H*-velocities differ appreciably from those of *He* I except during the partial phases of the eclipse. The latter does not exceed ±1.5 days from mid-eclipse (see Fig. 2) and should be only ±1.0 days, according to the light-curve. Hence the pronounced rise of the velocity-curve, beginning at about phase 12.5 days, can be explained only in terms of an additional disturbance—such as the one which is believed to vitiate the velocity-curves of SX Cassiopeiae and U Cephei. There is, however, no indication in the spectrum of RZ Scuti that the lines are modified in intensity or structure, prior to the beginning of the partial phase.

[12] *Ap. J.*, 99, 229, 1944.

The extraordinary behavior of the spectrum during the eclipse needs further examination. The small amplitude of the rotational disturbance derived from the *H* lines, as compared to that derived from the *He* I lines, presents a remarkable and, we believe, unique situation. The rotational displacement of a spectral line is usually written in the form

$$V = V_e F \sin i ,$$

where V_e is the equatorial velocity of rotation and F is the geometrical factor that depends upon the circumstances of the eclipse. This factor is independent of the profile of the undisturbed line. Hence the actual rotational velocities of the *H* layer and the *He* I layer must be very different. Hydrogen apparently forms a slowly rotating shell around the rapidly rotating layer which gives rise to the lines of *He* I and *Mg* II. This result is similar to that found from direct observations of line profiles in such stars as ζ Tauri and ϕ Persei. But RZ Scuti presents the first case of an eclipsing variable in which the rotational disturbance suggests the existence of layers having different rotational velocities.

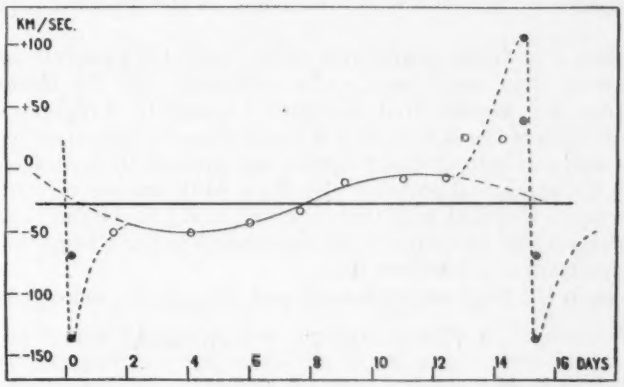

FIG. 2.—Velocity curve of RZ Scuti with normal points. ○ Means of all lines; ● Helium lines; ⊕ Hydrogen lines.

As judged by the appearance of the lines, the spectrogram at phase 15.158 = −0.032 day was taken when the star was closest to mid-eclipse.[13] This was verified by direct observation of the light of the variable in the finder of the 82-inch telescope. At this phase the *He* I lines and *Mg* II 4481 are absent or exceedingly weak, while on the following spectrograms taken the same night at phase +0.047 the lines of *He* I are present but are still considerably weaker than is normal. At phases 0.151 and 0.179 day these lines are fairly sharp and deep. In fact, on these two plates all lines are more conspicuous than they are outside of the eclipse. The *H* lines are shaded toward the violet, and there is no certainty about the shading in *He* I, while *Mg* II may be shaded toward the red. The shading of the *H* lines is opposite in sense to that expected in the case of a partial eclipse of a small bright star by a large faint star. The shading to be expected in this case[14] is toward the red after mid-eclipse and toward violet before mid-eclipse. However, these predictions all depend upon the assumption—not verifiable at present—that the axis of rotation of the bright star is parallel to the axis of the orbit.

[13] The large negative velocity obtained from the *He* I lines at phase 15.138 days might suggest that principal minimum occurred between phases 15.112 and 15.138. But there is no certainty that the rotational disturbance changes sign precisely at mid-eclipse: the axis of the star's rotation may be inclined to the axis of the orbit; this, together with the inclination of the orbit, may produce an asymmetry.

[14] *Ap. J.*, 99, 235, 1944.

On July 20 three spectrograms taken at the Lick Observatory, at phases 15.138, 15.184, and 0.034 days, show, respectively, the line *He* I 4472: (1) hazy but readily measurable, (2) extremely faint but still measurable, and (3) distinct.

The absence or extreme weakness of the lines of *He* I and *Mg* II at phase −0.032, which persists to some extent at phases 15.184 and +0.047 days, is accompanied by a marked weakening and sharpening of the *H* lines. The problem is to explain why all lines become weak at mid-eclipse, with *H* becoming, in addition, quite narrow. Since there are no traces of the absorption lines of the fainter component, which, according to S. Gaposchkin, should be of type G0, we infer that even at mid-eclipse the light of the B star dominates the spectrum. Accordingly, the changes in the line intensities must be intrinsic. There is a possibility that the rotationally distorted lines become very shallow at mid-eclipse if the latter is partial and if the eclipsing star is the larger.[15] This does not explain why the *H* lines remain narrow. But we have already seen that the rotational disturbance for *H* is less than for *He* I and *Mg* II. It is, therefore, possible that the weak, narrow *H* lines at mid-eclipse come from a tenuous shell with slow rotation, while the lines of *He* I and *Mg* II are rendered invisible by the rotational broadening on the apparent polar cap of the B star.

This explanation is probably not entirely satisfactory: the weakening of the *He* I lines is more conspicuous than would seem to be consistent with the theory of rotational broadening. Hence, it is possible that the effect is caused by a real physical weakening of the lines at the limb of the B star. Such a weakening was measured by Redman in the *H* lines of U Cephei; and independent evidence was adduced from McDonald plates that the *He* I lines of U Cephei, and probably also *Mg* II 4481, become very weak at the limb. If this phenomenon is identical with that observed in RZ Scuti, the weakening of *Mg* II would tend to suggest that radiative transfer according to the scheme "pure absorption" is playing an important role for these lines.

The *Ca* II lines in RZ Scuti are stationary and give a mean velocity of

$$V_{Ca\,II} = -10.7 \pm 1.2 \text{ km/sec} .$$

[15] *Ibid.*, Fig. 3, first column.

RECENT PROGRESS IN ASTROPHYSICS

A NEW THEORY BY C. F. VON WEIZSÄCKER OF THE ORIGIN OF THE PLANETARY SYSTEM

A significant new paper on the origin of the solar system has recently been published by C. F. von Weizsäcker.[1] In essence, Weizsäcker has freed the "one-star" hypothesis of its classical difficulties and has allowed an interpretation of the Bode-Titius law of planetary distances. A reprint of Weizsäcker's paper has become available to the writers, and this opportunity is taken to present a summary and a brief discussion so that Weizsäcker's theory may be made available to American astronomers for discussion now while war conditions continue to disrupt the normal flow of scientific literature between Germany and America.

Weizsäcker reviews, first, the time-honored objections to theories calling for planet formation by a contracting nebular shell surrounding a primitive sun. The primary (and fatal) objection is that, had the mass of the sun been spread out to beyond the orbit of Pluto, the major portion of the angular momentum of the nebular shell would today reside in the sun rather than in the planets, which possess 98 per cent of the angular momentum of the solar system; on the other hand, had the original shell contained only the mass of the present-day planets, the primitive sun already containing the major portion of the solar mass, condensation of separate planetary bodies would have been impossible because of the strong perturbing influence of the central mass of the sun (Roche condition).

Weizsäcker does not specifically deal with the objections to the hypotheses calling for planet formation by the ejection of material from an already developed sun, since this is not germane to his argument; but, of course, the same objection applies, so to speak, in reverse. Ejection of sufficient material to insure condensation into planets requires an extremely close approach of the disturbing star, while the possession by the planets of an inordinately large share per unit mass of the angular momentum of the system requires a large minimum separation of the two stars, or else exceedingly special conditions of high improbability. Thus the new theory enters a completely barren field, and the discussion which it is sure to provoke should be welcome and stimulating.

Weizsäcker considers an already well-developed primitive sun surrounded by a rotating shell of roughly one-tenth the mass of the central sun, in which each particle is assumed to describe a simple Kepler ellipse about the sun. He shows in considerable detail that such a shell will, in time, assume the form of an equatorial disk, in which the density in a direction perpendicular to the principal plane falls off exponentially, according to the usual barometric formula. He considers it sufficient, because of this property, to treat the nebular shell as essentially two-dimensional.

It is assumed that the nebula had the same composition as the present sun, not that of the present planets. Therein lies one of the crucial points of the Weizsäcker theory; and examination in some detail is demanded. Weizsäcker refers to a recent paper of Biermann,[2] which is not available to the writers, in which the hydrogen and helium content of the sun is found to be much higher than heretofore supposed, accounting for nearly 99 per cent of the solar mass. The work of Unsöld on the hydrogen and helium content of B stars[3] supports this high value, as does the work of Menzel, who[4] finds 54 per

[1] *Zs. f. Ap.*, **22**, 319, 1944.

[2] *Zs. f. Ap.*, **22**, 4, 1943.

[3] *Ap. J.*, **100**, 110, 1944.

[4] Goldberg and Aller, *Atoms, Stars, and Nebulae*, p. 114, 1944.

cent hydrogen, 45 per cent helium, and 1 per cent for all heavier elements; and Unsöld finds 57 per cent hydrogen, 40 per cent helium, and 3 per cent for the rest. It must be noticed here that the foregoing proportions, found from the analysis of stellar and solar atmospheres, are in no way contradictory to the results obtained from the study of stellar models. In fact, the usually accepted values of 35 per cent hydrogen and 65 per cent heavier elements are based on an arbitrary assumption of vanishing helium content. It was, however, shown by Strömgren[5] that the introduction of a finite helium content changes the concentrations of both hydrogen and heavier elements; in fact, one of the possible solutions corresponds to 55 per cent hydrogen, 40 per cent helium, and 5 per cent of the rest. Also, this change in the constitution of stellar matter will help to improve the agreement between the calculated rate of energy production in the carbon cycle and the observed stellar luminosities.

Thus the recent investigations imply that if today we were to build the planets of solar material we should have to discard 99 per cent of the matter taken from the sun to get the necessary residue of the heavier planetary material. And, indeed, Weizsäcker proposes that the greater part of the discoidal nebula, being composed of hydrogen and helium, did dissipate into space, carrying away with it the troublesome angular momentum that otherwise would have to be accounted for had the material "contracted" or fallen into the sun. Thus the high relative angular momentum of the planets is ascribed to the motion of the original nebula, which was dense enough to satisfy the Roche condition for the condensation of the planets.

Weizsäcker looks upon the material as a continuous, rotating stream of gas, intermingled with a much smaller quantity of solid particles of heavier elements condensed out of the nebula. He neglects opacity effects (screening effects) and assumes that the nebular material is in simple equilibrium with respect to the energy received from the sun ($\sim 1/r^2$) and emitted by the nebula ($\sim T^4$); in this event, temperatures not greatly different from present planetary temperatures would prevail, and the heavier elements could exist as solid particles.

At this point, the theory bears a striking resemblance to the planetesimal hypothesis, except, of course, that the planetesimals are regarded as condensed from the same nebula that was responsible for the sun rather than from a nebular filament for which the sun (with the aid of a highly improbably passing star) was responsible. The planetesimals, however, are "afloat" in a sea of hydrogen and helium, which is necessary to supply sufficient mass to satisfy the Roche condition and which might be thought of as a "matrix" for the formation of planets from the planetesimals.

One might now proceed in the manner of Chamberlain and Moulton and consider that the planetary system resulted from a "sweeping-up" process, through the mutual collision of particles. Weizsäcker, however, proposes a definite mechanism for planet formation, that of interference of "allowed" streams of material. A rough analogy to quantized Bohr orbits is suggested but, of course, only from the standpoint of illustration. This treatment indicates that the Bode-Titius law can be regarded as the result of this quantization on a macroscopic scale. The Bode relation, $r_n = a + b \cdot 2^n$, is shown to follow from logical assumptions. The constant 2 represents a particular case. Other constants are possible, and it is tempting to suppose that, if the planets were formed in this manner, other stars have planetary systems in which similar Bode relations obtain. In any event, if the Weizsäcker theory holds, planetary systems of a wide variety of types must be the rule rather than the exception.

Before discussing the details of the formation mechanism, Weizsäcker examines in considerable detail the form, density, and stability of the original nebula.

Assuming that the primordial shell was one hundred times as heavy as the planets, thus forming about one-tenth of the solar mass, Weizsäcker calculates (within the framework of his original assumptions) that it must have had the shape of a disk about 8×10^{14}

[5] *Ap. J.*, **87**, 520, 1938.

cm in diameter and 6×10^{12} cm in thickness, corresponding to the average density 10^{-9} gm/cm^3. Considering the interaction between the fast-rotating inner and the slowly rotating outer parts of the envelope, he estimates that the dissipation of material into interstellar space caused the density of the envelope to decrease with time proportionally to $e^{-(t/7\times10^6)\text{yrs.}}$ To reduce its original density of 10^{-9} gm/cm^3 to the present density, 10^{-22} gm/cm^3 of interplanetary space, requires a time of 2×10^8 years, which is in good agreement with the fact that (except for possible remaining traces) such an envelope is not in existence today.

In considering the collisions between the solid particles in the rotating nebula, Weizsäcker indicates that the collisions between two equal particles will probably lead to further fragmentation, whereas a small particle hitting a larger one will be captured, provided the second particle is sufficiently large to absorb the shock and to prevent the escape of flying splinters. Thus, in an assembly of particles of various sizes, the bigger ones should grow at the expense of the smaller ones, the process being accelerated as the over-all size of the bodies increases. Discussing this process in detail, Weizsäcker concludes that the time needed for a particle to grow from any small to any large size (how small and how large does not matter here because the radius diverges in finite time) must be of the order of magnitude of

$$t \cong \frac{\sqrt{\rho_0/G}}{\rho},$$

where ρ_0 is the density of condensed particles ($\cong$ 1 gm per cm^3), ρ the average density of particles in the space, and G the gravitational constant.

Assuming, as above, that the condensed material formed about 1 per cent of the total mass and that the average density of the nebula was about 10^{-9}, we get $\rho \cong 10^{-11}$ and $t \cong 10^{15}$ sec $\cong 10^8$ years. Thus the growth of planets, up to the limit at which no small particles were left to support further accumulation, must have taken place within a time comparable to the dissipation period of the gaseous envelope, and the number and relative positions of condensation centers of solid particles must have been influenced largely by interaction of currents existing in this envelope.

The central portion of Weizsäcker's paper considers possible steady currents or "steady states" in the material around the sun that could occur under the influence of gravity alone and would require no additional energy for their maintenance. It is obviously impossible, in a brief review, to give all the details that Weizsäcker presents; these are, however, essential to a real understanding of his paper. The most essential points are herein sketched.

Consider a group of particles possessing the same revolution period, identical semi-major axes (a) but different eccentricities. Set up a system of co-ordinates with the origin located on the circular orbit of radius a and allow the co-ordinate system to revolve about the sun in the period common to all the particles in the group under consideration. In the moving co-ordinate system a member-particle that traverses a circular orbit about the sun will remain stationary at the origin of co-ordinates; particles on orbits of small eccentricity will describe small ellipses about the origin of moving co-ordinates; and the greater the original eccentricity, the larger the secondary ellipse. It is easily shown that for small eccentricities the secondary ellipses (which might be called elliptical epicycles) differ only in size, having a constant ratio (2 : 1) of major axis to minor axis, the minor axes pointing to the sun. If this group of particles were the only group, one would observe in the system of moving co-ordinates a steady stream of particles moving about the origin in a direction opposite to that of the moving co-ordinates. Since all particles have the same major axes in the solar co-ordinate system, the total energy of the particles is the same; the angular momentum of the particles varies, however, since in orbits of fixed a the angular momentum is proportional to $(1 - e^2)^{1/2}$ and hence the outer particles in

this "vortex" have less angular momentum than the inner ones. This fact becomes important when considering the manner in which adjacent vortices can combine.

Viewed from the sun, the vortex subtends an angle χ which can be shown to be twice the maximum value of $(v - M)$, where v is the true anomaly and M is the mean anomaly. For values of e up to $\frac{1}{3}$, an error of less than 1 per cent is incurred by the approximation

$$e = \sin \frac{\chi}{4}.$$

Weizsäcker shows that a vortex may, in general, adopt a particle not originally belonging to it only if the angular momentum of the intruder lies below a certain threshold value, and he concludes from this and other considerations that an upper limit to the size of individual vortices must exist. The particles of a very small vortex must move in practically circular orbits about the sun; almost every particle from the outside that can meet such a vortex has greater orbital eccentricity (and hence less angular momentum) and can be captured. The greater the limiting eccentricity of the vortex, the greater the proportion of particles that cannot be captured on encounter. These particles will tend to disrupt the vortex. From these arguments Weiszäcker deduces that $e_{\max} = \frac{1}{3}$ is a logical limit, which, of course, leads to a limiting value of χ. The "quantum condition" now imposed is that only such stable vortices will exist for which 2π is an integral multiple of the angle χ. With $e_{\max} = \frac{1}{3}$, this calls for five vortices on each orbit about the sun. Further, the radii of "allowed" orbits will be in the ratio of

$$\frac{r_n}{r_{n-1}} = \frac{1 + e_{\max}}{1 - e_{\max}} = \epsilon.$$

If this arrangement of vortices is repeated in successive circular rings and if $e_{\max}$ is independent of distance from the sun, $r_n = r_0 \epsilon^n$.

With $e_{\max} = \frac{1}{3}$, $\epsilon = 2$ and $r_n \sim 2^n$, which is a sufficient approximation to the Bode law.

The planets are not formed, however, from the vortices but from "whirlpools" built up between them. Consider two adjacent vortices. At their point of contact the material of the outer one moves counterclockwise, while that of the inner one moves clockwise. The interaction will obviously produce whirlpools rotating in the same sense as do the planets. The whirlpools can be thought of as rotating balls in a ball bearing—if the outer bearing moves clockwise and the inner counterclockwise, the balls will rotate "directly," as do the planets.

Weizsäcker states that these "ball-bearing" whirlpools will have no tendency to grow without the application of external forces. They will come together, however, "in a manner difficult to visualize" but probably involving interaction with the material lying in the "wedge-shaped" regions between the vortices: It is not certain without further dynamical analysis whether the growth of planets can occur in the manner suggested by Weizsäcker, given the starting conditions. Weizsäcker argues that the existence of the Bode relation is strong evidence that the process must have occurred, even though the details are obscure.

The formation of satellites is but another step. Weizsäcker visualizes the whirlpools as fed by the vortices, the material entering through the polar regions and swirling outward in the equatorial regions. He computes the radius of the region around a growing planet at the limits of which the gravitational potential of the planet balances the kinetic energy of the swirling equatorial particles. This corresponds to the region in which satellites can be formed. Good agreement with observed present distances of nonretrograde moons from their parent bodies is found.

Formation of comets is not dealt with directly, but one may suppose that they resulted from "subwhirlpools," representing what one might term "abortive" planets. Meteors are considered either as the products of disintegrating comets or as of interstel-

lar origin, for Weizsäcker shows that the lifetime of a meteoritic particle in the solar system would be too small. He computes that interstellar meteorites could be built up to the size of 0.4 cm in 5×10^9 years. He does not refer to the work of Corlin[6] in this specific connection, nor does he, for that matter, consider at any point the particle-gathering mechanism suggested by Corlin in the general problem of the building of larger bodies from smaller particles.

Weizsäcker's theory offers an explanation of all the principal features of the solar system: the existence of an essentially common plane of revolution of the planets and the equator of the sun, the small eccentricities of planetary orbits, the sense of the revolution of the planets and satellites and the equators of the planets, and the lower densities of the larger planets (as a consequence of the ability of larger masses to accrete the lighter particles and gases). In connection with the latter point, the scarcity of the inert gases on the earth is a necessary consequence of the hypothesis of escape into space of the majority of the gases in the original nebula.

Weizsäcker next briefly extends his theory to include the formation of double stars but does not carry it very far. He points out that if the original nebular mass is sufficient, the largest "incipient" planet will rapidly sweep up the lion's share of the available material, whereupon it would, of necessity, become self-luminous, probably as a dwarf M star. He does not point out the tempting conclusion that can be drawn from this process: stars so built up would be hydrogen-poor and could therefore arrive at the white-dwarf stage without a long evolutionary process. Further, this method of star-building would allow the companion star in a binary system to show a great disparity in spectral class and density that would not imply a difference in age.

This corollary of the Weizsäcker theory is similar to an idea advanced by MacMillan,[7] by which double-star companions could arise by the accretion, by a large planet, of additional solid material. MacMillan advanced the idea that if the sun should encounter a dark nebula in its travels, Jupiter would sweep up material at a far greater rate than the other planets and would eventually form a companion star to the sun, the remaining planets in the meantime having been disrupted and swept up by the growing sun and major planet.

Such, then, is a brief picture of the new theory of Weizsäcker. Obviously, the dynamical process of planet formation must be considered at length and in much greater detail than Weizsäcker has done, before considered judgment can be passed. Assuming for the moment that the dynamical process suggested was responsible for the formation of the solar system, it at once becomes pertinent to inquire whether the process might not be going on somewhere in the galaxy at the present time. Stars with nebular shells are not uncommon. In these cases, however, the density is invariably much lower than that of the Weizsäcker nebula, and, further, radial velocities indicate in general that the shell is expanding and hence is not in simple rotation as called for here. If, indeed, a star did have such a discoidal shell extending outward, say, 50 astronomical units, the shell would extend only a few seconds of arc on either side of the parent-star even in the case of very near stars and would undoubtedly be invisible in the glare of the central star. There does not appear to be much greater chance of observing such a shell spectroscopically. Weizsäcker tentatively suggests, but does not pursue the point, that the rapid rotation observed in early B stars (which he states might be regarded as young stars since their rate of energy expenditure could not long have been supported by the carbon-nitrogen cycle) might be evidence of such a shell. Most spectroscopic evidence, however, indicates that this rotation must be identified with the region close to the photosphere, e.g., the absence of effects of "dilute radiation" and the fact that the lines of all elements are equally affected. Further, only a very small portion of such an extended shell would be projected

[6] *Zs. f. Ap.*, **15**, 239, 1938.

[7] *Ap. J.*, **48**, 35, 1918.

upon the main stellar body, in the line of sight to the earth, and the absorption lines would thus be sharp and not exceedingly broad, as is the case in the n stars of classes B and A. Indeed, an extended shell of 99 per cent hydrogen and helium and cool enough to contain solid particles of the heavier elements would be difficult to detect spectroscopically. Faint molecular lines sharing the radial velocity of the stellar lines would perhaps be the most promising indication from an observational viewpoint.

It does not seem likely, however, that the stars in the galactic neighborhood of the sun which can be observed in detail spectroscopically would still today be in the process of condensation, and Weizsäcker's contribution will have to be judged on other than observational grounds. His contribution, moreover, will probably be adjudged to lie mainly in the qualitative ideas he has advanced rather than in the details of planet and satellite formation. Of these, the principal ones are that much more mass was probably concerned in the formation of the planets than the planets now possess; that the angular-momentum difficulty that has proved fatal to all previous major theories can be resolved by the escape into space of the great majority of the primitive extrasolar material; and that the Bode-Titius law is capable of a physical explanation. More broadly, Weizsäcker has directed a fresh stream of thought into the long-stagnant pool of theories of planetary origin.

The writers have available for circulation a limited number of photostatic copies of the original Weizsäcker paper.

G. Gamow
J. A. Hynek

George Washington University
and
Perkins Observatory

REPORTS FROM FRENCH ASTRONOMERS

We are fortunate in having received two manuscripts from our French colleagues as well as a number of photographs by Dr. D. Chalonge, of the new observatory in the Haute Provence. The manuscripts are printed below, translated from their French originals by Professor Van Biesbroeck. Dr. Lyot's manuscript was accompanied by samples of his excellent solar and planetary photographs taken at Pic du Midi. These have been added to his manuscript at the appropriate places. A few of his unusually fine lunar photographs will be published elsewhere.

The observatory in the Haute Provence is situated near St. Michel, some 60 miles northeast of Marseille. The elevation is 600 meters, or 2000 feet. The observatory comprises the 120-cm (48-inch) reflector, shown on Plate XVII, *a;* the 80-cm (32-inch) reflector formerly used at Forcalquier (about 3 miles northeast of the present site); a nebular spectrograph (Pl. XVII, *b*); and a number of buildings, the principal one of which is shown on Plate XVIII, *b*. The dome of the 48-inch reflector is also shown on Plate XVIII, *a*.

The observatory operates under the auspices of the French Centre national de la Recherche scientifique. Dr. Dufay is the director; but at present, with the project not entirely completed, Mr. Charles Fehrenbach, formerly of Strasbourg, is in charge of actual operations.

Gerard P. Kuiper

Yerkes Observatory
January 18, 1945

PLATE XVII

a)

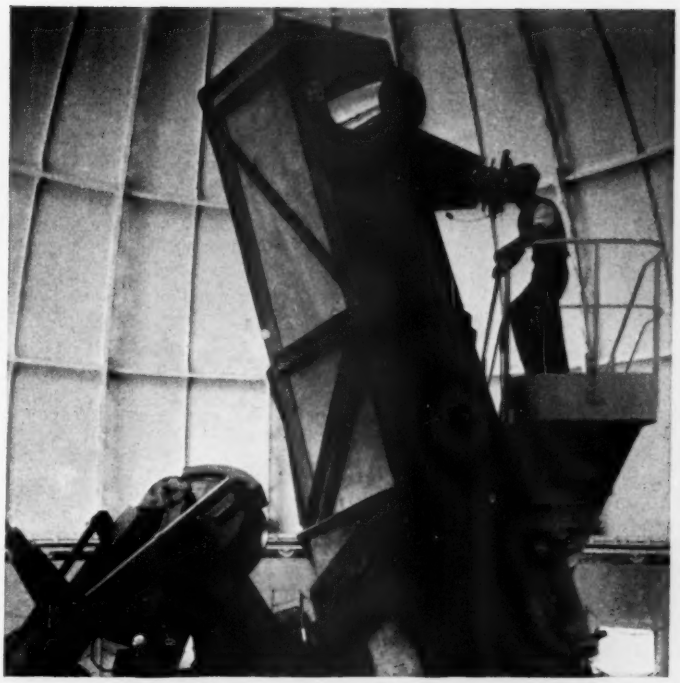

b)

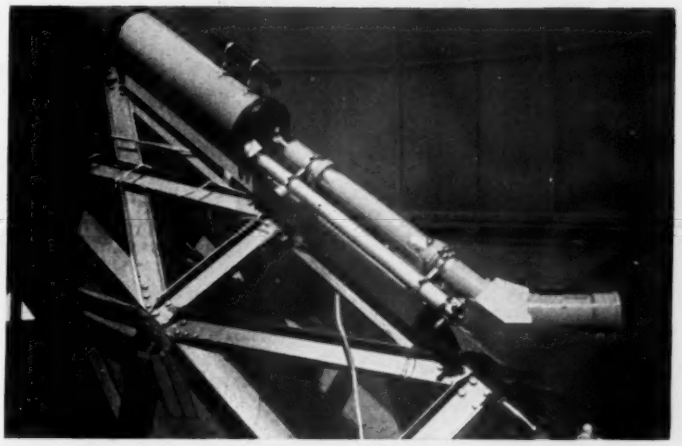

a) The 120-Cm Telescope, Newtonian Focus (More Recently the Wooden Casings Have Been Removed from the Frame)

b) Nebular Spectrograph (Quartz $f/2$) and Its 10-Inch Telescope

PLATE XVIII

a)

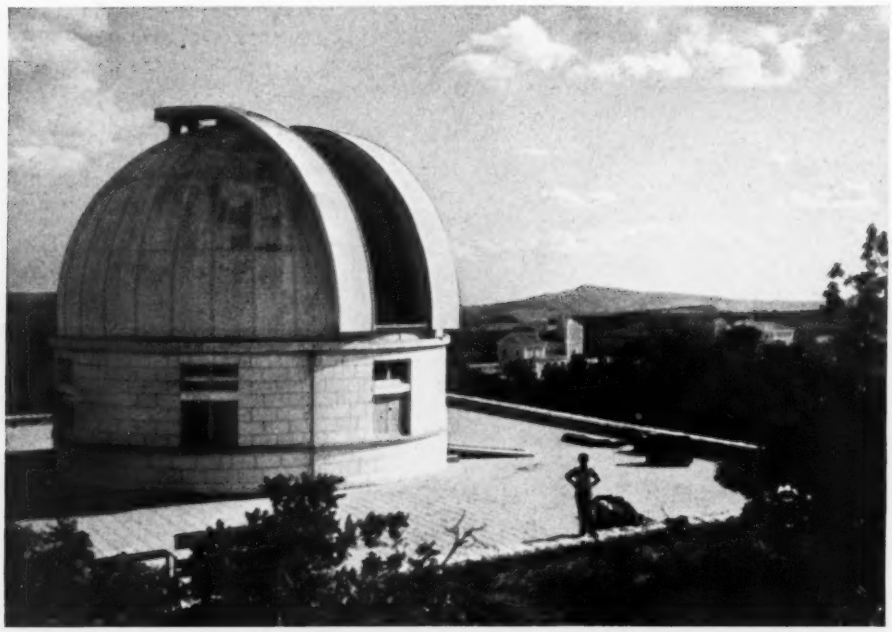

b)

a) Dome of the 120-Cm Reflector (Astronomer's Residence in Background)

b) Offices and Laboratory, West Side

PLANETARY AND SOLAR OBSERVATIONS ON THE PIC DU MIDI IN 1941, 1942, AND 1943

1. *Observations of the corona in monochromatic light.*[1]—B. Lyot has used the coronograph, of 0.20-meter aperture and 4-meter focal length, installed on the Pic du Midi in 1935[2] and a polarizing monochromatic filter added in 1939. The principle of this filter and its characteristics were described by him in 1933.[3] It was provisionally used with polaroid films in 1939.[4]

The filter is comprised of a set of 6 quartz plates and 7 polarizers, transmitting between 6600 and 4800 A—thirteen bands 2 A wide in the green, 3 A in the red—and situated near the principal chromospheric radiations $H\alpha$, D_3, b_1, and $H\beta$ and the principal coronal radiations 6374.5 and 5302.8. The 6 quartz plates are kept in a very small thermostat, which can maintain their temperature to within 0.1° between 0° and 60° C, in order to keep one of the transmitted bands in precise coincidence with the radiation to be isolated.

Another set of 3 quartz plates and 3 polarizers, followed by colored filters, eliminates the nonutilized radiations. The two coronal radiations can be isolated simultaneously.

With this filter the first monochromatic images were obtained in August, 1939, as well as cinematographic records of prominences. These can be obtained under very poor atmospheric conditions.

In 1941 the first 6 polaroids were replaced by spar polarizers of a suitable type. This has increased the transparency of the filter, especially in the green, and has further removed strong stray radiations in the red and reduced the diffuse light and enhanced the definition of the images.

The filter brings out many details in the corona. Thus the color, changing from green to red from one region to another, indicates the varying distribution of the two coronal radiations. Plates on which the sun has a diameter of 0.06 meter require an exposure of 7 minutes in the green and 4 minutes in the red. They bring out much finer structure and more contrast than can be obtained when total light is used.

Behind the 6 plates forming the main part of the filter can be placed a radiation-separator, producing four images, 24 × 36 mm, corresponding to different radiations. Three of these are received on a moving film, which registers simultaneously (*a*) the prominences with the line $H\alpha$, (*b*) the corona in the red, and (*c*) the corona in the green. The fourth image falls on an eyepiece, for guiding purposes.

These films, some of which were continued over more than 12 hours, cover a total duration of 92 hours. They confirm the difference between the green and the red corona and the nearly total independence of the corona and the prominences. On the other hand, they are far from confirming the motions in the corona mentioned by some observers: even when speeded up 2400 times, the corona remains stationary. The arches and jets appear and fade progressively along invisible trajectories, and the corona thus modifies its shape and aspect without perceptible motions.

2. *Observations of the chromosphere.*[1]—In 1942 Lyot added a spar plate to the filter so as to reduce to 1.5 A the width of the $H\alpha$ band being transmitted. This was mounted on the refractor of 0.38-meter aperture. Under these conditions the chromosphere became visible at the edge of the sun as a bright streaked band (Pl. XIX) of height varying between 3″ and 7″, surmounted by a darker region of 1″–2″ thickness and a series of fine jets.

Over the disk the chromosphere appeared to have a structure similar to that which the spectroheliograph shows, but with less contrast. The filaments were strongly visible;

[1] *Ann. d'ap.*, premier semestre, 1944.

[2] *L'Astronomie*, May, 1937, p. 203; May, 1938, p. 193.

[3] *C.R.*, **197**, 1593, 1933.

[4] *C.R.*, **212**, 1013, 1941.

near groups of active spots there were a great number of chromospheric eruptions, often brighter than the continuous spectrum around $H\alpha$ and sometimes less than 1″ in diameter. As many as 17 of these eruptions were seen in 1 hour (Pls. XX and XXI). At their first appearance they had large radial velocities, which could be studied by rapidly changing the wave length of the filter through the use of an elliptically polarized compensator.

In the month of August, 1942, Lyot took 130 meters of film of the chromosphere, using a fine, contrasty emulsion, at the rate of 2 exposures per minute. The great transparency of the filter made it possible to increase the solar image to 0.18 meter and to reduce the exposures to one-fortieth of a second. These films show the continuous boiling of the chromosphere at the sun's edge, the movements of the filaments, and the rapid changes in brightness of the eruptions.

3. *Solar eclipse, September 11, 1942.*—Gentili and Lyot intended to record with the coronograph the moon's motion across the corona during this partial eclipse. However, the sky remained mostly cloudy, with only a 4-minute break; even then the transparency was poor, the brightness of the sky amounting to thirty-five-millionth of the sun in the red. Four images, exposed through light cirrus clouds, nevertheless show the moon's rim projected on the corona up to a distance of 8′ from the sun's edge. Under favorable conditions the moon could probably be seen over twice that distance (Pl. XXII, *a*).

4. *The solar granulation.*—In May, 1943, the solar images at the 0.24-meter refractor often remained remarkably sharp and steady for about 3 hours in the morning, when the east wind blew directly on the objective. Lyot took advantage of this circumstance and secured 7 films, covering an average duration of 3 hours, at the rate of 6 images per minute, on a positive emulsion. The solar images average 0.25 meter in diameter. Three of these films illustrate the various shapes and the evolution of the grains which are born and die on the spot in the course of a few minutes. These observations will be published later.

5. *Photometry of the corona.*—The visual estimations of brightness of the coronal lines around the sun which were obtained in 1934[5] made it seem probable that there would be great differences in the distribution of the green and the red liner at the following solar minimum. In order to check on this, Lyot installed a photometer on the grating spectrograph attached to the coronograph, in May, 1943. The radially placed slit gave an image of the coronal line which was compared with the image of a second slit, illuminated by a near-by region of the continuous spectrum of the sun. Values not affected by atmospheric conditions in various position-angles and at a constant distance from the sun's edge were obtained, both in the green and the red, by turning the whole instrument around the axis of the coronograph.

In December, 1943, Lyot adapted to the coronograph his fringe-polarimeter,[6] modified so as to give at each point quantitatively the exact amount of polarized light of the corona, uninfluenced by atmospheric diffusion. The three series of observations on the green line, the red line, and the polarized light, requiring 4 hours of pure sky, were obtained by Gentili and Lyot in the course of 13 days between December 28, 1943, and January 20, 1944. The graphs drawn by Gentili in polar co-ordinates show a great range in the coronal lines from one spot to another. Their brightness is less than two-millionth of the continuous spectrum of the sun in certain regions near the poles, while in other regions that brightness reaches eighty-millionth. Sometimes both lines have a sharp maximum in the same spot; but generally their maxima are in very different positions. Often the red line is intense on the equator, while the green line, invisible at the equator, shows maxima on either side.

Polarized light, presumably with an intensity proportional to that of the continuous

[5] *C.R.*, **200**, 21 and 219, 1935.

[6] *Ann. de l'Obs. Meudon*, **8**, Part I, 10, 1929.

PLATE XIX

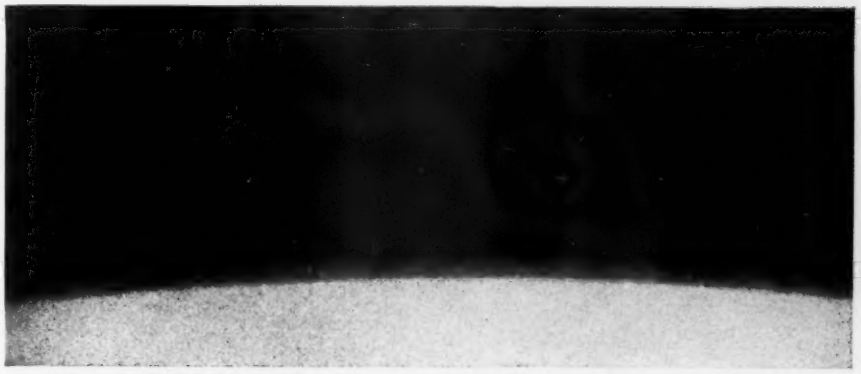

Top: The chromosphere on the eastern edge of the sun through the monochromatic filter centered on $H\alpha$ in a band 1.5 A wide. August 21, 1942, at 8^h57^m U.T.; exposure, $\frac{1}{40}$ second; solar diameter, 1 meter.

Bottom: Similar exposure on northeastern edge of the sun. August 22, 1942, at 13^h51^m U.T.

PLATE XX

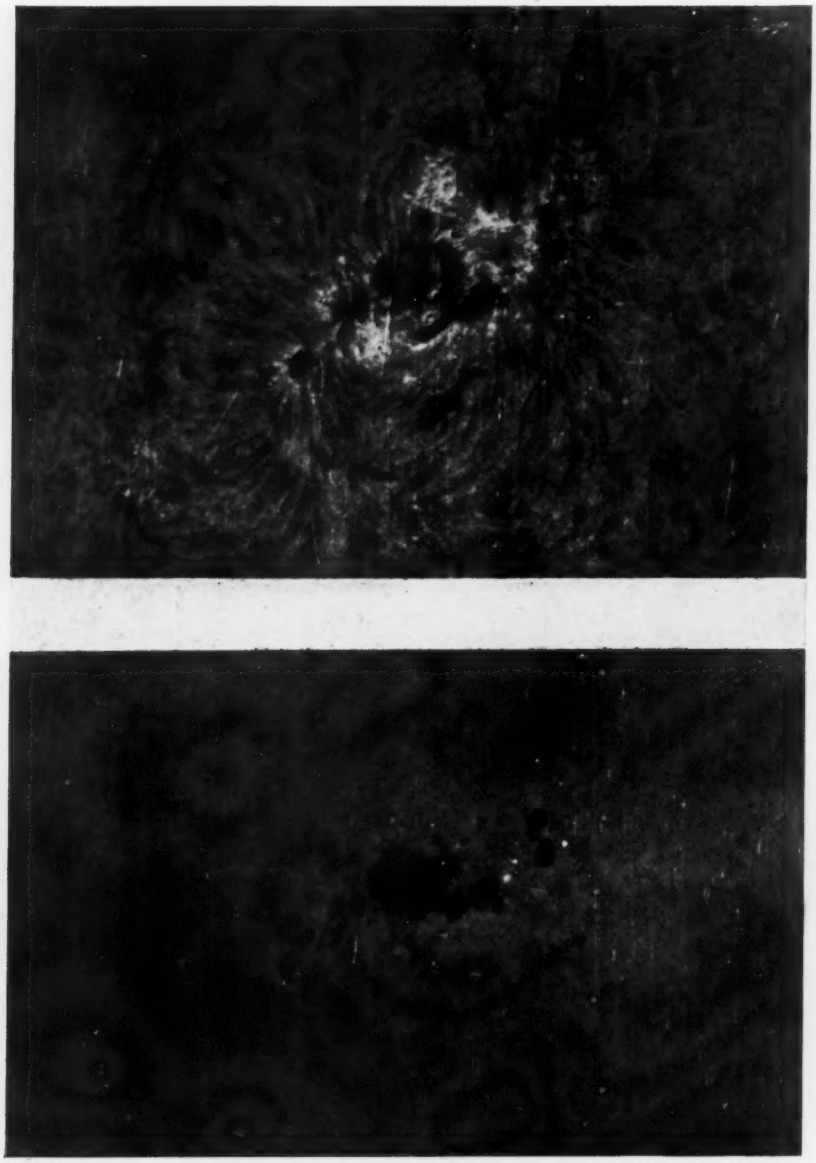

Top: Small group of sunspots photographed in a 1.5 A band centered on *Hα*. August 25, 1942, 7^h34^m U.T.; exposure, $\frac{1}{40}$ second; solar diameter, 57 cm.

Bottom: Same group with central wave length 1 A to the violet of *Hα*. Small eruption in *Hα* shown because of radial velocity shift. August 25, 1942, 13^h03^m U.T.; exposure, $\frac{1}{40}$ second; diameter, 57 cm.

PLATE XXI

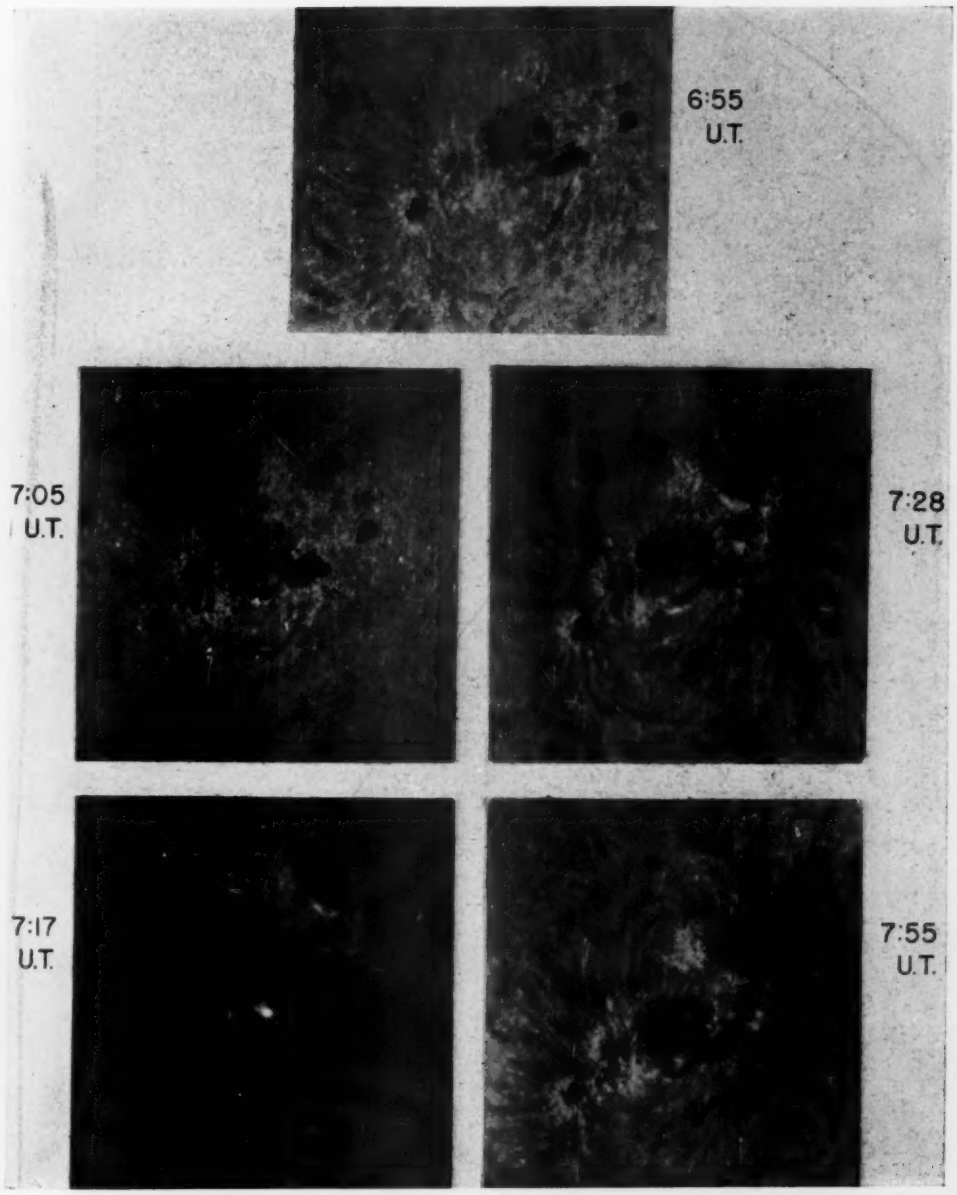

SMALL CHROMOSPHERIC ERUPTION IN *Hα*

The rate of rise and fall is indicated by times. Filter 1.5 A centered on *Hα*. August 25, 1942

PLATE XXII

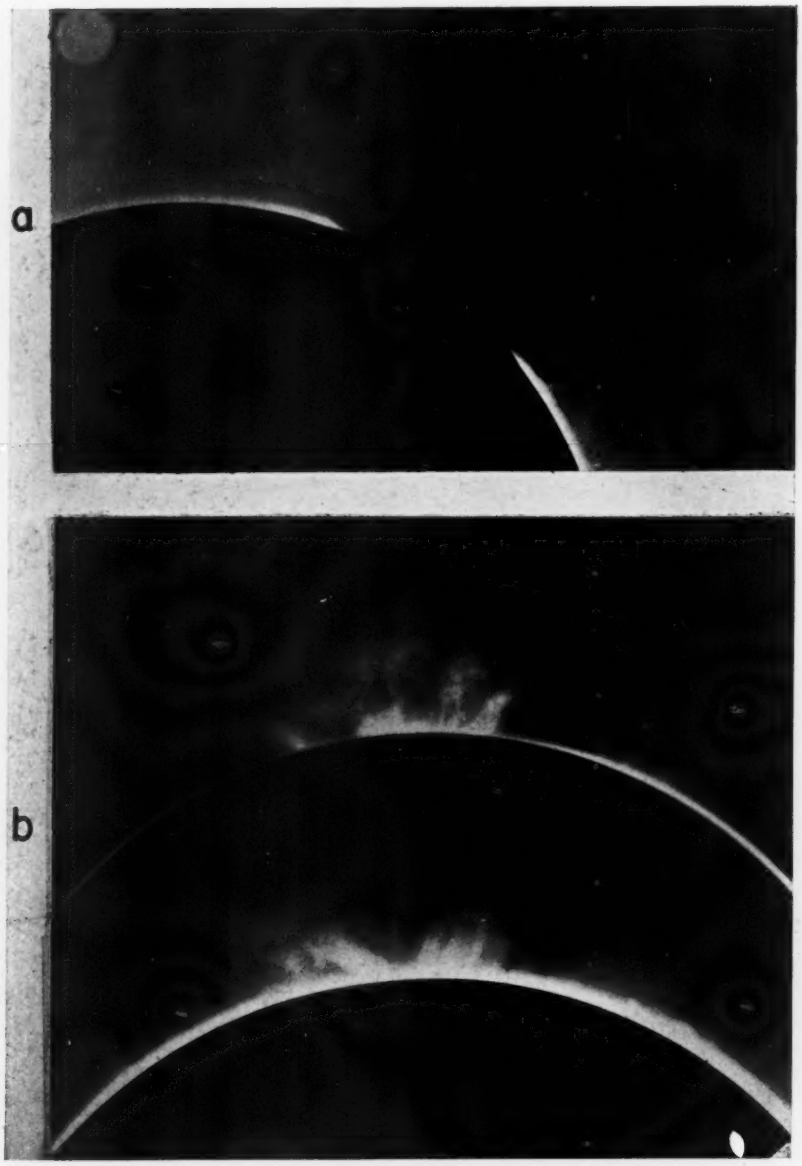

a) Partial eclipse of the sun, September 11, 1942, taken with the coronograph at 15^h55^m U.T., showing the moon's disk projected on the corona. Light cirrus clouds responsible for streaks. Bright edge due to diffraction around occulting disk.

b) Monochromatic images of the corona on September 3, 1941. *Top:* West rim in the green, 8^h5^m U.T.; exposure, 7 minutes. *Bottom:* West rim in the red, 8^h15^m; exposure, 4 minutes.

PLATE XXIII

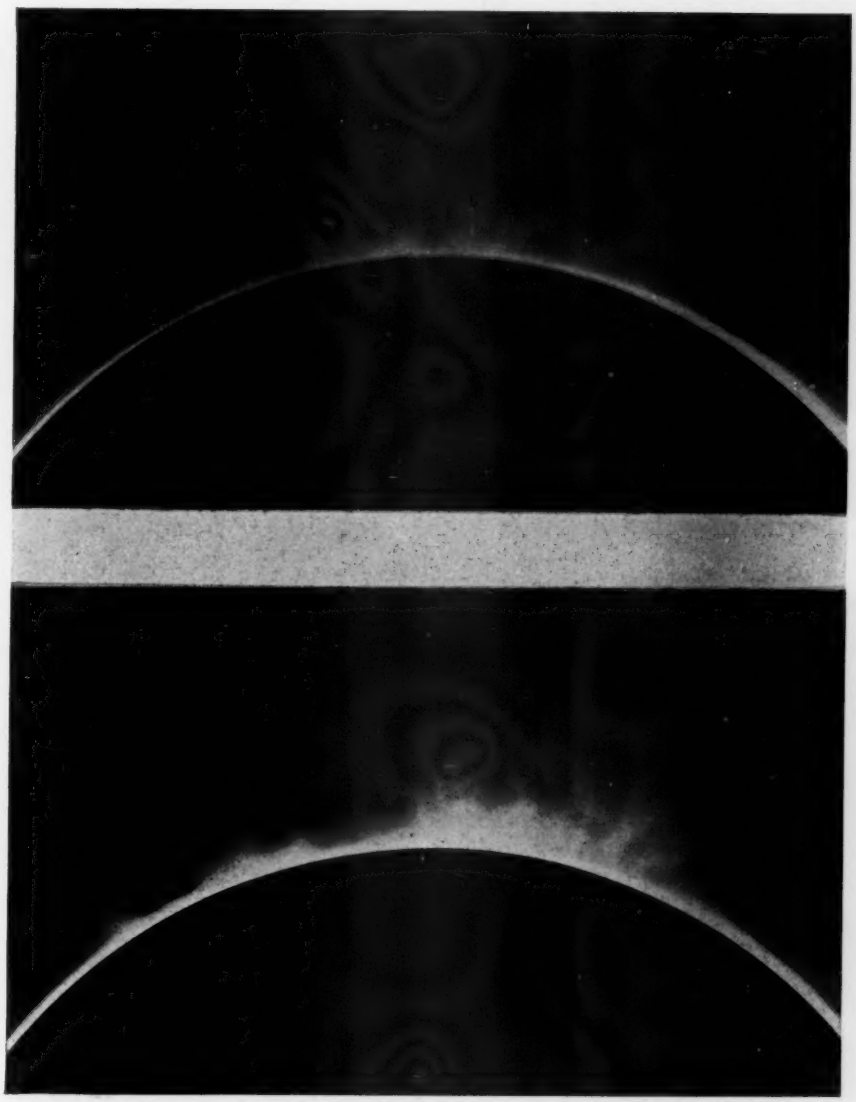

MONOCHROMATIC IMAGE OF THE CORONA IN THE GREEN; EXPOSURE, 7 MINUTES
Top: West rim, September 14, 1941. *Bottom:* East rim, September 15, 1941

PLATE XXIV

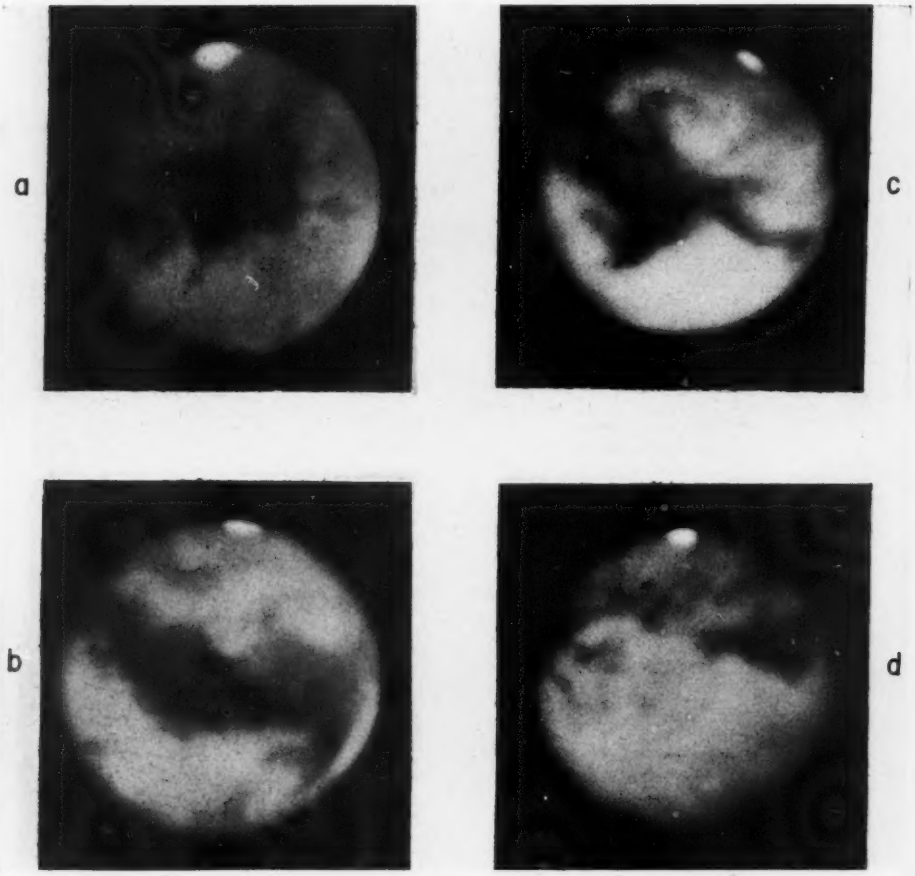

COMPOSITE PHOTOGRAPHS OF MARS (EACH BASED ON 10 EXPOSURES)

a) September 23, 1941, 0^h55^m U.T.; longitude of center, 28°

b) October 8, 1941, 0^h25^m; longitude of center, 247°

c) October 8, 1941, 3^h58^m; longitude of center, 300°

d) October 19, 1941, 23^h32^m; longitude of center, 129°

PLATE XXV

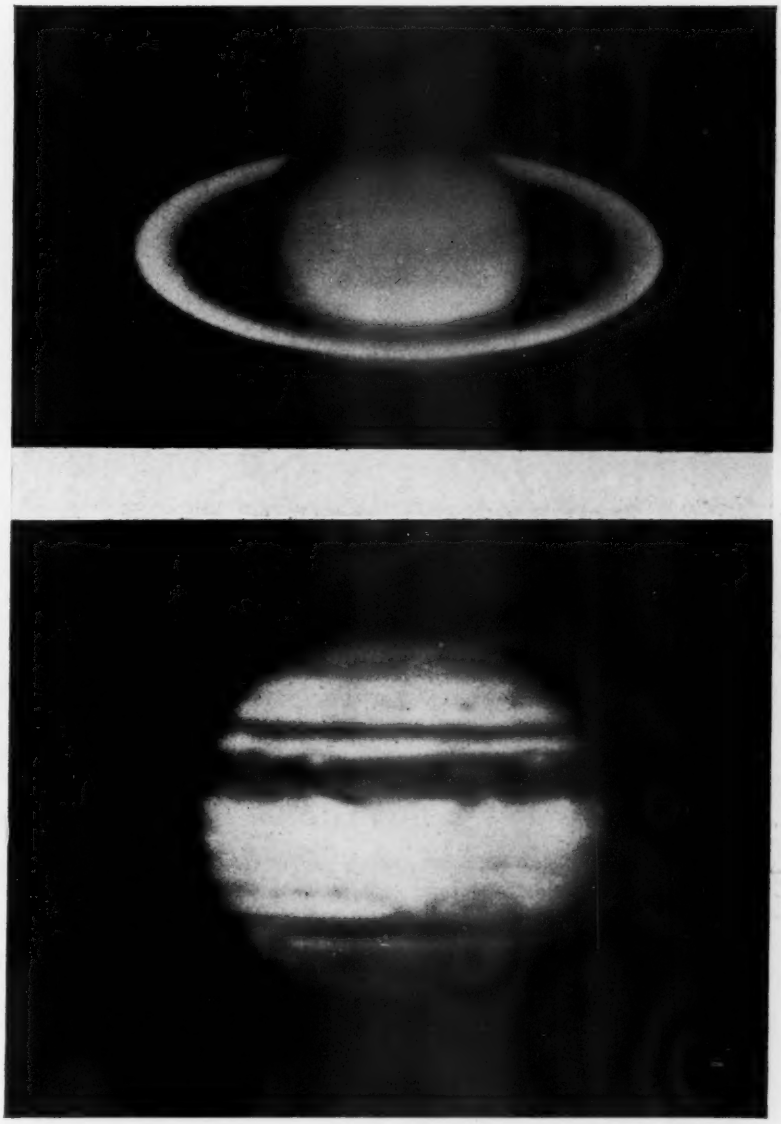

Top: Composite picture of Saturn on October 21, 1941, at 0^h
Bottom: Composite picture of Jupiter on October 11, 1941, at 2^h

spectrum, shows much more uniformity in distribution than the lines. This explains why the filter increases the contrast so much in the coronal details.

These observations will be published in the *Annales d'astrophysique*. Provisional results are given in Figure 1 and Plates XXII and XXIII.

6. *Planetary observations in 1941.*[7]—On the Pic du Midi the only instrument available for the physical observations of planets was the refractor of 0.24-meter aperture and 6-meter focal length. In spite of its moderate size, that instrument brought out the unusual

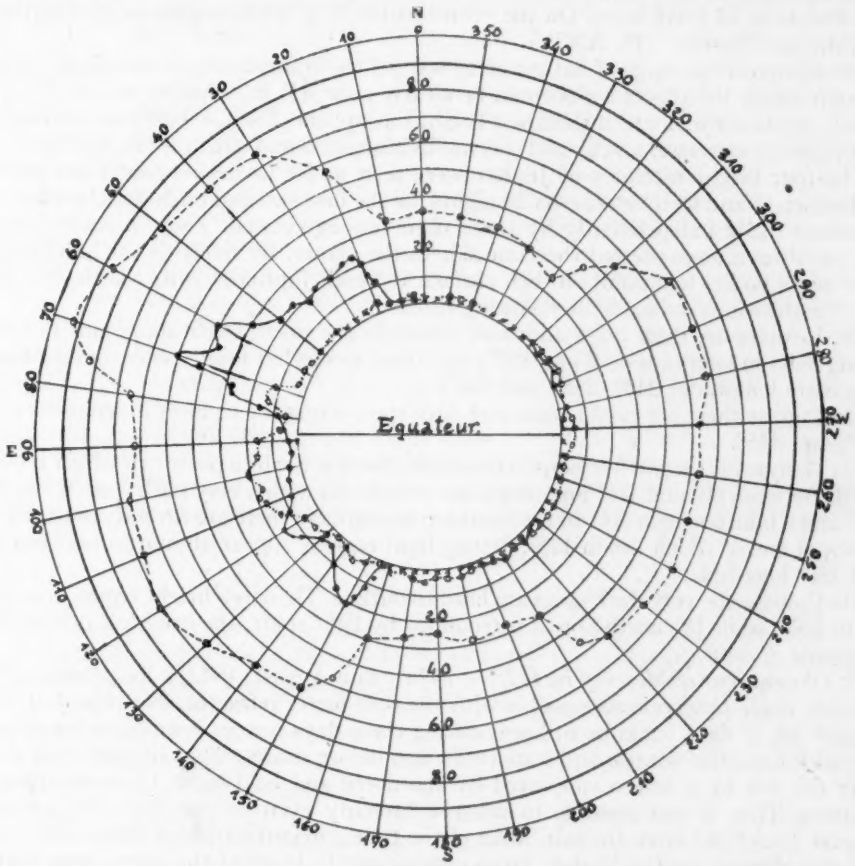

FIG. 1.—●—●—●: Intensity of the green coronal ray in millionths of the solar intensity; o···o···o: intensity of the red coronal ray in millionths of the solar intensity; o---o---o: intensity of the polarized light in hundred-millionths of the solar intensity.

sharpness and steadiness of the images on the mountain. Hence Camichel, Gentili, and Lyot decided to instal on the same mounting an excellent 0.38-meter-aperture objective of 6-meter focal length, made by the brothers Henry and belonging to the Toulouse Observatory. The new instrument, installed in August, 1941—thanks to the initiative of J. Baillaud—showed much finer structure on the planets than had the previous lens, in proportion to the aperture ratios. A magnification of 500 was required to bring out the details, and during the second half of the night they were visible most of the time.

[7] *L'Astronomie*, April, 1943, p. 49; May, 1943, p. 67.

On Mars, about the time of opposition, Gentili and Lyot observed new details, such as a "lake" and a "canal," similar to Juventae Fons and Baethys and situated between these and Jamunae Sinus; also, two twin lakes in Chryse and the doubling of the eastern tip of Meridian Bay, etc. Many exposures were secured by Camichel on contrasty, fine-grain panchromatic plates in a focus corresponding to about 35 meters. Positive images have been obtained by superposition of some 10 negatives.

On Mars these plates confirm the visual observations and bring out new configurations, especially in the "seas." For instance, Mare Chronium and Aonius Sinus break up in a mosaic of 22 small lakes. On the "continents" faint trails appear in the location of the principal "canals" (Pl. XXIV).

The composite pictures of Saturn bring out (*a*) the transparency of the outer ring, *A*, through which the planet's globe can be clearly seen; (*b*) the shadow of ring *B* on the planet, on the edge of which shadow a bright line appears that probably comes from the light passing between *B* and *C*; and (*c*) two divisions in *B* and one in *A* (Pl. XXV).

The four bright satellites of Jupiter were seen under favorable conditions between September 13 and October 22—on 20 nights for the first two and on 26 for the other two. Drawings made independently by three observers agree well. They indicate that the four satellites always present the same side to the planet. By referring the longitudes on these small bodies to a point on their surface at which Jupiter is at its zenith, it is found that the drawings indicate the following features:

On Io there are dark poles and dark bands in the north-south direction; two fairly strong belts in longitudes 80° and 152°; and three somewhat fainter ones, having the approximate longitudes 240°, 285°, and 340°.

On Europa there are bright poles and dark spots along the equator in longitudes 180°, 260°, and 345°.

On Ganymede, in the northern hemisphere, there is a white polar cap which is clearly visible between 60° and 180° and which has a dark rim with a very dark spot in longitude 135° and a fainter one in 50°. In the southern hemisphere there are several dark spots, the principal one of which lies in 145°. Strong light regions appear at sunrise between 300° and 350° longitude.

On Callisto the very dark spots are hard to outline. There is a bright region around the south pole, while the north pole is surrounded by light spots, the brightest of which is in longitude $\pm$ 140°.

7. *Observations of Mercury in 1942.*— In July and August, 1942, a long stretch of fine weather made observations possible with the 0.38-meter refractor. Between July 8 and August 13, 27 days could be utilized; during these days images were often excellent for several hours after sunrise and sometimes also before sunset. The objective was shaded from the sun by a screen supported by the dome and held some 12 meters from the shutters. Thus it was possible to observe Mercury even on the day of conjunction, August 2, at 1° 40′ from the sun. Most of the time a magnification of 500 could be used; and this showed, on the 5″ disk, spots comparable to those of the moon, seen with the naked eye. The drawings of Gentili and Lyot all show the same configurations, which turn from day to day simultaneously with the terminator.

A series of plates taken by Camichel, combined in composite positives, confirms the principal details.

These observations are not yet reduced but will be published in *L'Astronomie.*

8. *Planetary observations in 1943.*—In view of the results obtained with the 0.38-meter refractor, there was hope that a still larger instrument would have yielded even better results in proportion to its aperture. Thanks to the help of J. Baillaud, the visual objective of 0.60-meter aperture and 18.20-meter focal length, made by the brothers Henry for the large coude telescope of the Paris Observatory, was adapted to the mounting on the Pic du Midi. Since the tube was only 6 meters long, it was necessary to bend the light-beam by two flat mirrors of 0.50 and 0.30-meter aperture. When first tried, in

April, 1943, the instrument performed poorly. The objective was tested by the Foucault method and proved excellent, but the flats showed appreciable zones. They were returned at once to the Paris Observatory and refigured by Couder, who secured perfect surfaces. Reinstalled in November, the stellar disks appeared sharp; but the first diffraction ring was too bright, and relatively brighter than in the 0.38-meter lens. This was due to inequalities in the silvering of the mirrors.

In December, 1943, and January, 1944, the instrument showed a somewhat finer structure than did the 0.38-meter instrument, and especially it revealed numerous black small spots in the dark regions, mostly near the edges; only a few of these could be detected with the 0.38-meter refractor. On the other hand, the faintest details were less visible.

On Saturn the larger lens proved quite superior. It showed a division between the rings *B* and *C;* in 1944 one of the divisions in ring *B* was seen to be split up in two, while three divisions could be detected in ring *A*. On the satellites of Jupiter, also, new details could be detected, such as the splitting-up in two unequally bright parts of the polar cap of Ganymede and three dark spots in the polar caps of Io. The four satellites were followed under excellent conditions during 25 nights between December 8, 1943, and January 23, 1944. The drawings obtained by the three observers confirm and extend those of 1941.[7]

Camichel has perfected a method for measuring the diameter of the satellites of Jupiter. In the focal plane is produced an artificial disk having the same brightness and color as the satellite. The diameter of this disk is varied until both satellite and disk appear identical. The beams forming the two images must be parallel and have the same aperture ratio. Under the best circumstances, the eye will detect differences of 1 per cent in the diameter.[8]

Often the images given by the 0.60-meter refractor were sufficiently steady for making the two disks identical in appearance. The measures seemed free of systematic errors, and the mean of 30 settings gave diameters with a probable error less than 1 per cent. The diameters were found as follows, referred to a distance of 5 astronomical units:

Io.....	0".914	Ganymede....	1".380
Europa....	0.804	Callisto.....	1.288

And for Titan, the sixth satellite of Saturn, the diameter comes out 0".750.[9]

The measures on Io refer to the equatorial diameter; the very dark polar caps give the appearance of the polar diameter, being 0".05 smaller.

A long series of photographs of Mars has been obtained by Camichel, who used both refractors between August 8, 1943, and the beginning of February, 1944. The details are not so fine as those of 1941, the planet being farther away; but the "canals" are more numerous and darker, especially near the north pole.

In January, 1944, Gentili took a series of exposures on the moon at the 18.20-meter focus of the 0.60-meter refractor, using fast panchromatic plates. While they do not show so good a definition as the images of Mars, in several regions the plates show, nevertheless, small craters and rifts, of less than 0".7 in width, in which light and shadow is still recognizable.

Of the observations obtained in 1943, only the measures of the diameter of the satellites of Jupiter have been reduced and presented to the Academie des Sciences. The other results will appear in *L'Astronomie.*

BERNARD LYOT

PARIS, FRANCE

[8] *C.R.* (in press).

[9] Reduced in kilometers, the diameters would be: Io, 3310; Europa, 2910; Ganymede, 4990; and Callisto, 4660 km. If the diameter given for Titan is referred to the mean distance of Saturn, it would correspond to 5180 km.

THE ACTIVITIES OF THE MEUDON OBSERVATORY SINCE 1940

Since the beginning of the war the optical parts of the various telescopes in the domes have been dismounted and placed in safety. Only the spectroheliograph, located in a building with a strong roof, remained in service.

Solar observations and synoptic charts of the chromosphere.—The "routine work" with the spectroheliograph has been continued except for two months at about the time of the armistice in 1940. The yearly mean number of days of observations has been 210, which is about normal. The synoptic charts of the chromosphere established under the auspices of the I.A.U. have been published as far as rotation No. 1127 (end of 1937). The work was then stopped, since the plates from Kodaikanal and Mount Wilson for filling in the gaps in the Meudon series were no longer being received.

Solar research.—Mr. and Mrs. L. d'Azambuja have made a general study of the evolution of prominences and their movements. They have utilized the published synoptic charts (1919–1937) and the corresponding collection of spectroheliograms K_3 and H_α, on which the prominences visible as *filaments* can be followed from day to day as they cross the solar disk. Their principal conclusions are summarized below.

1. In one out of every two cases, prominences originate in the *faculae region* accompanying the spots and drift from these toward the higher latitudes. When they first appear they look like small filaments oriented nearly the way a meridian would look after traveling 15 or 20 days with the angular velocity, varying with the latitude as observed in the spots. The delay in the formation of filaments after the formation of the spot is of about the same order. It is conceivable that the filaments associated with the faculae are formed simultaneously with the spots in the direction of the meridian but do not appear at the surface of the chromosphere until about three-fourths of a solar rotation later.

2. Whether they are associated with faculae or not, the filaments usually reach their greatest development when passing the third time across the disk. After that they break up and disperse, generally during their fifth passage. They move slowly and regularly toward the pole of the hemisphere in which they are situated, at an average rate of 1.3° per rotation. Sometimes a long-lived filament can thus reach the zone where polar filaments are circulating along parallels. For some time they remain there as individual elements, but gradually they merge with the polar filaments so that the latter, often considered as independent from the equatorial prominences, appear as the ultimate stage of these filaments. The motion of the filaments toward the pole seems to slow down as the latitude increases and seems to be faster during the phase of increasing activity of the 11-year cycle.

3. At their successive transits over the disk the filaments, at first only slightly inclined to the meridian, gradually make a larger angle with the latter as a result of the polar slowing-down of the angular velocity of rotation. However, their trajectory always remains more open than that of a meridian, curving according to the law of rotation of the spots. This indicates that in their motion toward the pole the filaments are only partially swept along by the slower-moving chromospheric layers on which they penetrate.

4. The mean initial latitude of the prominences not connected with faculae is also nearly identical with the latitude of the spots in the same phase of the 11-year cycle. It reflects clearly the sudden increase which characterizes the change in cycle. Spörer's law therefore applies to the starting-points of the prominences.

Mr. H. Greenat, a prisoner of war since 1940, had just finished a paper about his work of the previous years. This paper, published during his imprisonment, treats various problems relating to the sun.

M. Pan-Puh, a Chinese astronomer who studied at Meudon from 1936 to 1940, has made a detailed study of internal movements in prominences. He has utilized the fine images of prominences obtained by Lyot's chronograph at the Pic du Midi for a cinematographic reproduction of the phenomena. The plates secured by himself at Meudon

were also utilized for this purpose. The measures on sharp points identified on the films or on successive spectroheliograms do not confirm E. Petit's laws. He finds that the ascending motions are as well represented by a curve of continuously varying velocity as by a broken line corresponding to a series of constant velocities, increasing suddenly by impulses at a series of points.

Research on planets, comets, and stars: laboratory work.—F. Baldet made numerous observations of Mars in 1941 with the 16-meter refractor. He has discussed the photometric and spectral observations of Comet Cunningham (1940c). He has compared 168 observations with the $1/r^2\Delta^2$ and $1/r^4\Delta^2$ laws of intensity and has written monographs on Comets Friend (1941a), Encke (1941b), and Paraskevopoulos (1941c). Baldet has assembled a microphotometer with a photoelectric cell for the measure of photometric plates of stars and comets. The measures are made on the projected image of the plate enlarged nine times linearly. Bertaud applied Bergstrand's method (*Uppsala Medd.*, No. 59), to the stars that are common to the catalogue of Cecilia H. Payne-Gaposchkin and H. Shapley (*Harvard Obs. Mimeo.*, Ser. 1, No. 2) and the *Göttinger Aktinometrie*, in order to reduce the magnitudes in the latter catalogue to the international system. He concludes with a list of 3308 stars, with color indices for 3294 of them. He has made a table giving the distribution of color indices with spectral type for the zone between 0° and +20° declination.

Bertaud has determined the photographic magnitude of the supernova in IC 4182 from a plate obtained at Meudon. His determination occurs, like that of Leutenegger, on the ascending branch of the light-curve. He has used Baade's method, but with two standard light-curves, in order to secure the extrapolated maxima for some novae where that phase had not been observed. One of the curves is made for the supernovae in NGC 1003 and IC 4182, the other for the supernovae in NGC 4157 and 4273. The result for five supernovae has given the absolute magnitude at maximum for two of them. Finally, Bertaud has discussed his spectral observations of Nova Herculis at Meudon and studied the velocities of the various absorption systems in six bright novae. He has confirmed and extended D. B. McLaughlin's empirical relation between these velocities and the duration of the decline. He has examined the spectral evolution of these novae and assumed the probable existence of emission jets analogous to the solar eruptions. He has also established a visual light-curve of Nova Lacertae 1936 from 3829 observations, studied the color index, made distance determinations from expansion nebulae, and produced a catalogue of 36 supernovae with their principal characteristics. For the maximum absolute magnitude of 18 galactic novae he has established the value $M = -6.6 \pm 0.6$; for a selection of 13 of them he finds $M = -7.1 \pm 0.5$.

L. D'AZAMBUJA

MEUDON OBSERVATORY
December 1944

REVIEWS

The Velocity of Light. By N. E. DORSEY. ("Transactions of the American Philosophical Society," Vol. **34**, Part I [1944].) Pp. 110. $2.25.

Among the constants of nature which underlie the whole superstructure of the physical sciences, the velocity of light, V in Dr. Dorsey's notation, is one of the most fundamental. Because of its importance and the technical difficulty of measurement, large resources of effort and money have been devoted to the determination of V, culminating in close agreement among the later values.

Among the distinguished observers who have measured V an implicit faith in its constancy seems to have prevailed. But other writers, comparing the published observations, have interpreted the apparent differences as secular and periodic variations.

Moved by far-reaching implications, which would be associated with a variability in V, Dr. Dorsey has carried out a critical study of all the useful direct determinations of the velocity of light, seeking an answer to the question: "Is V constant?" During the progress of his work it appeared that a relatively small additional effort would yield a definitive value of V derived from all the useful independent determinations. Dorsey thus arrived at two important conclusions, which will doubtless be given high weight: (1) ". . . . the data give no indication of any secular change in the velocity of light"; (2) "The best value that can be derived from the data now available is: Velocity of light in a vacuum = 299,773 km/sec $\pm$ 10 km/sec." The appended quantity, which he calls the "dubiety of the result," is not the probable error, in the technical sense of that term, but represents his best judgment of the actual uncertainty.

After a short Introduction, Dorsey sets forth about eight pages of cogent "Remarks," dealing with the theory of errors, least squares, and definitions of technical terms. These are more than a summary from textbooks on the adjustment of observations. The treatment is skilful, and the emphasis well placed. Many researches could be improved by observance of the principles expounded here.

Fizeau's determination of V in 1849 and that of Foucault in 1862 are briefly discussed but are set aside as having insufficient weight to justify their combination with later values or their use for testing the constancy of V.

Beginning with the investigations of Cornu in 1872 and closing with those of Huttel in 1941, fourteen researches on the velocity of light are arranged in three groups, according to the method of observation. Cornu's three papers and one by Perrotin and Prim form the first group, in which Fizeau's method of a toothed wheel was used for modulating the light. Dorsey devotes thirty-three pages to a scrutiny of this group. Finding Cornu's definitive value of V untrustworthy, he readjusts the observations and obtains a result appreciably nearer to those found by later observers. The work of Perrotin and Prim is found to contain systematic errors, and their reductions are said to involve erroneous equations. Dorsey recomputes their result with modified equations.

The second group brings together all the work in which Foucault's method of the rotating mirror was used, including Newcomb's researches, to which Dorsey devotes eight pages, and the various investigations of Michelson, ending with that of Michelson, Pease, and Pearson. For the discussion of the second group about thirty pages are used.

The third group of papers studied by Dorsey includes one by Karolus and Mittelstaedt, two by Anderson, and one by Huttel, all of whom used the electro-optical method of modulating the light, in which stationary Kerr cells replaced the rotating mechanical devices of Fizeau and Foucault. In marked contrast with his work on the preceding groups, Dorsey treats this entire third group of investigations in a few paragraphs, accepting, almost without comment and apparently without serious effort to test their validity, the authors' fundamental data as given.

For example, the only mention by Dorsey of precautions taken by the observers to maintain at constant frequency the alternating field on their Kerr cells is a casual reference to the use of quartz oscillators by one of them. One observer is reported to have known the frequency to 1 part in 10^6, while another is said to have had an uncertainty of 7 parts in 10^6 in his frequency; yet no comment is offered, nor is any indication given of methods used to measure the frequency. Dorsey leaves the reader to pursue such details for himself in the original papers.

The difference in treatment accorded the Kerr-cell work and that involving mechanical modulation extends to Dorsey's comments on the reports themselves. The Kerr-cell observers are commended for the excellence of their reports, but the others are severely criticized for omitting to publish details which would have made easier the appraisal of their results.

Near the close of his paper Dorsey assembles the fourteen values of V, covering the interval 1872–1941, in a table which is the basis of his conclusion that there is no indication of secular variation in V. For his conclusion as to the best value of V, Dorsey relies on the average of the Michelson, Pease, and Pearson result with the four derived by the Kerr-cell method. In the column of remarks in the table of final values he writes for each Kerr-cell result, "Apparatus studied"; but for the Michelson, Pease, and Pearson result, "Little study of apparatus."

To the reviewer this last remark, by such a careful writer, appears inexplicable. Certainly no physicist, past or present, ever made so exhaustive a study of apparatus for measuring V by the Foucault method as did Michelson. If he felt in the last years of his life that his greatest contribution to this problem could be made by overcoming the serious difficulties that hindered the fundamental observations, rather than by recording extensive secondary data, it would seem that his judgment should be respected. Since Dorsey assigns to the result of Michelson, Pease, and Pearson the same weight as to each of the four Kerr-cell values, perhaps the comments just quoted on the study of apparatus need not be taken too seriously.

The paper closes with two appendixes, containing, first, the theory of the various methods of measuring V and, second, a study of motion maintained by periodic impulses. The first appendix describes the Fizeau and Foucault methods in much detail but gives only a quarter of a page to a few notes on the electro-optical method.

The short second appendix in all probability contains the clue to hitherto unexplained variations in V as observed by the Foucault method. In a penetrating analysis Dorsey shows that rotary motion maintained by periodic impulses exhibits slight oscillatory departures from strict uniformity.

It is interesting to compare Dorsey's conclusions with those of Birge,[1] who studied the same original researches and, in addition, considered two indirect determinations of V, thus including a somewhat wider scope of data, which he treated in a manner distinctly different from Dorsey's. Birge concluded that there is no secular variation in V and also remarked that Edmondson's proposed periodic variation had been completely disproved.

One of the two indirect determinations of V discussed by Birge is the work of Rosa and Dorsey on the ratio of an electrical charge measured in electrostatic units to the same charge measured in electromagnetic units. Although Dorsey does not mention this investigation, in which he himself had participated, Birge praises it and shows that, when the published result is revised to allow for necessary corrections to the units used in 1906, a value of V having high weight is obtained.

Birge reached a definitive value of $V = 299{,}776$ km/sec, with an estimated uncertainty of ± 4 km/sec. The 3 km/sec by which Birge's result differs from Dorsey's is exactly accounted for by the difference in their procedures with regard to the small correction required for changing observed "group velocity" to true "wave velocity." Birge first called attention to the need of such a correction; and in the process of obtaining his final value, he applied it in each case where the author had not already done so. Dorsey omitted the correction from the results of Karolus and Mittelstaedt and of Huttel but allowed it to remain in Anderson's two values, giving no convincing reason for his procedure. Obviously, no physical significance can be attached to the slight difference between the two final results, but a certain intellectual satisfaction would have followed a complete agreement on this minor detail. To most scientists, however, satisfaction of a higher order is found in the conclusion, to which Dr. Dorsey has given so much toil, that to our best knowledge the velocity of light is a constant.

HAROLD D. BABCOCK

Mount Wilson Observatory

[1] *Reports on Progress in Physics*, **8**, 90, London, 1941.

PARABOLIZING MIRRORS WITHOUT A FLAT

In a paper entitled "Parabolizing Mirrors without a Flat,"[1] I overlooked two important articles on this subject. Dr. R. O. Redman has called my attention to a paper by Dr. C. R. Burch, "On Reflection Compensators for Testing Paraboloids."[2] In addition, Dr. Burch has called my attention to a paper by A. Couder, "Procédé d'examen d'un miroir concave non sphérique."[3]

FRANK E. ROSS

PASADENA, CALIFORNIA
February 6, 1945

[1] *Ap.J.*, **98**, 341–46, 1943.

[2] *M.N.*, **96**, 38–61, 1936.

[3] *Rev. d'optique*, **6**, 49–55, 1927.